DEPARTAMENT OF
ENVIRONMENTAL SCIENCES AND ENGINEERING

Carcinogenic toxicants and emerging pollutants. A comprehensive case-study on toxicant interactions *in vivo* and *in vitro*: from Molecular Toxicology to Environmental Risk Assessment

CARLA MARIA ALVES MARTINS

Master in Environmental Engineering

DOCTORATE IN ENVIRONMENT AND SUSTAINABILLITY

NOVA University Lisbon
September, 2023

DEPARTAMENT OF
ENVIRONMENTAL SCIENCES AND ENGINEERING

Carcinogenic toxicants and emerging pollutants. A comprehensive case-study on toxicant interactions *in vivo* and *in vitro*: from Molecular Toxicology to Environmental Risk Assessment

CARLA MARIA ALVES MARTINS

Master in Environmental Engineering

Adviser: Pedro Manuel Broa Costa
Auxiliary Professor, NOVA University Lisbon

Co-advisers: Kristian Dreij
Associate Professor, Karolinska Institutet, Sweden

Maria Helena Costa
Full Professor, NOVA University Lisbon

Examination Committee:

Chair: Maria Paula Baptista da Costa Antunes
Full Professor, NOVA University Lisbon

Rapporteurs: José Alhama Carmona,
Full Professor, Universidad de Córdoba, Spain
Maria João Aleixo Silva,
Researcher, Instituto Nacional de Saúde Dr. Ricardo Jorge

Adviser: Pedro Manuel Broa Costa,
Auxiliary Professor, NOVA University Lisbon

Members: Mário Emanuel Campos de Sousa Diniz,
Associate Professor, NOVA University Lisbon
Michiel Adriaan Daam,
Auxiliary Professor, NOVA University Lisbon

DOCTORATE IN ENVIRONMENT AND SUSTAINABILLITY

NOVA University Lisbon
September, 2023

Carcinogenic toxicants and emerging pollutants. A comprehensive case-study on toxicant interactions *in vivo* and *in vitro*: from Molecular Toxicology to Environmental

To my beautiful daughter and my husband

ACKNOWLEDGMENTS

This thesis was only possible with the invaluable collaborations and contribution of several people/institutions who supported me during these years. Thus, I would like to show my deepest gratitude:

To my supervisor Pedro Costa. Thank you for accepting in your team over these years and for everything you have done for me. For your guidance, motivation, friendship, patience and productive scientific discussions. I think that you deserve an award for all the patience and for survive to so many “heart attack” because of me! Above all thank you for giving me new challenges and the opportunity to try different things.

To all my laboratory colleagues for their support both at work and personally, for their friendship and for the moments of relaxation, which always result in undoubtedly interesting ideas and theories. Thank you for putting up with my daydreams, joys, sadness, stress... a little bit of everything! Especially to Ana and Cátia who have been with me on this journey of research for so long. Always a joy to work with you guys.

To my husband, my forever boyfriend, for his patience even on the most difficult days of this adventure. It was always with love and THAT hug that you reminded me that we need to fight until the end, and that even in the worst moments there will always be a way out and that in the end we will be better than now.

To my beautiful daughter, the giant love that lives in my heart.

To the girls, Sofia, Neuza and Maria, who despite my outbursts were always there for me. Always ready to find a good excuse for good times outing and good food!

To my parents, who from the beginning taught me that in life we should keep our values and never give up on dreams.

To my co-supervisor Kristian Dreij from Karolinska Institutet (Sweden) for accepting me in your laboratory and for always being available to teach me so much in such a short time. Thanks to all colleagues there who help me in my work and always made me feel welcome to Stockholm.

To Leonor and all girls from Zebrafish Facility of Instituto de Medicina Molecular João Lobo Antunes (Lisboa), for accepting me in your facility and for always being available to teach me and help through the bioassays. Lara and Aida it was always a joy to work with you.

“Always looking for the "why" in everything.”

ABSTRACT

Noxious chemicals have serious repercussions for wildlife and human health, not just due to incidental pollution, but also to chronic exposure to mixed pollutants. To the span of legacy toxicants such as aromatic hydrocarbons we persistently add new, like pharmaceuticals, that become reclassified as 'of emerging concern'. Taking diclofenac (DFC), one of the most toxic non-steroid anti-inflammatory drugs (NSAIDs) to wildlife, and the carcinogenic PAH benzo[*a*]pyrene (B[*a*]P) as model compounds, we disclosed that binary combinations cause interaction effects *in vivo* and *in vitro* even at realistically low concentrations. Comparing both, DFC caused high zebrafish embryo mortality and more acute morphoanatomical lesions and B[a]P was more cytotoxic for human hepatoma HepG2 cells, however all this effects seemed to be diminished or delayed by co-exposure. The observed genotoxicity *in vivo* and *in vitro* indicated antagonism in short exposures. Bioinformatics and RNAseq yielded about 300 genes differentially expressed only in co-exposed zebrafish embryos and indicated that pathways related to cell cycle control may partly explain antagonism. The findings indicate serious chronic effects even when toxicopathological and genotoxicity-related responses seem to be reduced by co-exposure, which was confirmed by carryover of effects from parental generations (exposed to toxicants during embryonic development) to their offspring, even though individual exposures continue to have higher implications than mixtures. The overall complexity of effects and mechanisms was dependent of dose and duration of exposure. Altogether, mechanistic aspects and toxicopathology of co-exposure indicate significant risk of chronic disease along the life cycle of organisms. *In vitro* assays, in turn, were paramount to test multiple binary mixtures and enabled refining research towards potential adverse outcomes and molecular pathways, which is nowadays acknowledged as paramount to quantify risk under realistic scenarios and associate environment health and human occupational exposure.

Keywords: Benzo[*a*]pyrene, Diclofenac, Mixtures, Pathway analysis, HepG2 cells, *Danio rerio*, Intergenerational bioassay

RESUMO

As substâncias nocivas têm graves repercussões para a vida selvagem e para a saúde humana, não apenas devido à poluição incidental, mas também à exposição crónica a misturas de poluentes. À gama de poluentes tradicionais, como os hidrocarbonetos aromáticos, acrescentamos continuamente novos produtos, como os fármacos, que são reclassificados como "emergentes". Tendo o diclofenac (DFC), um dos anti-inflamatórios não esteroides (AINEs) mais tóxicos para a vida selvagem, e o PAH cancerígeno benzo[*a*]pireno (B[*a*]P) como substâncias modelo, revelamos que as misturas binárias causam efeitos de interação *in vivo* e *in vitro*, mesmo em concentrações realisticamente baixas. Comparando ambos, o DFC causou alta mortalidade embrionária no peixe-zebra e lesões morfológicas mais agudas e o B[*a*]P foi mais citotóxico para as células do hepatoma humano HepG2, no entanto todos estes efeitos pareceram diminuir ou retardar na co-exposição. A genotoxicidade foi inferior à aditiva, *in vivo* e *in vitro*, indicando antagonismo em exposições curtas. A bioinformática e o RNAseq geraram cerca de 300 genes diferencialmente expressos apenas em embriões de peixe-zebra co-expostos e indicaram que as vias relacionadas ao controle do ciclo celular podem parcialmente explicar o antagonismo. As descobertas indicam efeitos crónicos graves, mesmo quando as respostas toxicopatológicas e relacionadas com a genotoxicidade parecem ser reduzidas pela co-exposição, o que foi confirmado pela transferência de efeitos das gerações parentais (expostas aos poluentes durante o desenvolvimento embrionário) para os seus descendentes, embora as exposições individuais continuem a ter implicações mais elevadas do que as misturas. A complexidade geral dos efeitos e mecanismos dependeu da dose e da duração da exposição. Em conjunto, os aspetos mecanicistas e a toxicopatologia nas misturas indicam um risco significativo de doenças crónicas ao longo do ciclo de vida dos organismos. Os ensaios *in vitro*, por sua vez, foram fundamentais para testar múltiplas misturas binárias e permitiram refinar a pesquisa em direção a potenciais resultados adversos e vias moleculares, o que hoje é reconhecido como fundamental para quantificar o risco em cenários realistas e associar a saúde ambiental e a exposição ocupacional humana.

Palavras chave: Benzo[*a*]pireno, Diclofenac, Misturas, Análise de metabolismo, Células HepG2, *Danio rerio*, Bioensaio intergeracional

CONTENTS

1 INTRODUCTION 1

1.1 Environmental Pollution 3

1.2 Implications of pollution to humans and wildlife 8

1.3 The new days of toxicologic evaluation: the “mixtures world” 10

1.4 Challenges and perspectives of “omics” approaches directed to toxicant mixtures 14

1.4.1 Transcriptomics 15

1.4.2 Genomics and Epigenomics 18

1.4.3 Proteomics 20

1.4.4 Metabolomics and Lipidomics 21

1.4.5 Multi-omics 23

2 OBJECTIVES AND WORKFLOW 25

3 ANTAGONISTIC EFFECTS OF A COX 1/2 INHIBITOR DRUG IN HUMAN HEPG2 CELLS EXPOSED TO AN ENVIRONMENTAL CARCINOGEN 27

3.1 Abstract 29

3.2 Introduction 29

3.3 Methods 31

3.3.1 Chemicals and cell culture 31

3.3.2 Cell viability assay 31

3.3.3 Comet assay 32

3.3.4 MN flow cytometric assay 32

3.3.5 Reactive oxygen species assay 33

3.3.6 Statistical analysis 33
3.4 Results 34
3.4.1 Binary mixtures of B[*a*]P and DFC cause antagonistic effects on cytotoxicity 34
3.4.2 Dose-dependent antagonism on genotoxicity 36
3.4.3 Additive effects on ROS induction 38
3.5 Discussion 40
3.6 Conclusions 42
4 TECHNICAL UPDATES TO THE COMET ASSAY *IN VIVO* FOR ASSESSING DNA DAMAGE IN ZEBRAFISH EMBRYOS FROM FRESH AND FROZEN CELL SUSPENSIONS 45
4.1 Abstract 47
4.2 Introduction 47
4.3 Methods 48
4.3.1 Zebrafish embryos 48
4.3.2 Cell harvesting 49
4.3.3 Comet assay 49
4.3.4 Statistical analysis 51
4.4 Results and Discussion 51
4.5 Conclusions 56
5 A MECHANISTIC STUDY ON THE INTERACTION EFFECTS BETWEEN LEGACY AND POLLUTANTS OF EMERGING CONCERN: A CASE STUDY WITH B[*A*]P AND DICLOFENAC 57
5.1 Abstract 59
5.2 Introduction 59
5.3 Methods 61
5.3.1 Chemicals 61
5.3.2 Test organisms 61
5.3.3 Acute toxicity 62
5.3.4 Histopathology 63
5.3.5 Genotoxicity assessment 63
5.3.6 Statistics 64

5.3.7 RNA-Seq 64
5.3.8 Validation of RNA-Seq data 65
5.4 Results 66
5.4.1 Acute toxicity and genotoxicity of DFC, B[*a*]P and their mixtures 66
5.4.2 Inferring toxicological mode-of-action of DFC and B[*a*]P mixtures from gene expression profiles 70
5.5 Discussion 75
5.6 Conclusions 78
6 THE INTERACTION EFFECTS TOXICANTS AND EMERGING POLLUTANTS IN *DANIO RERIO*: A GENERATIONAL CHRONIC ASSAY 81
6.1 Abstract 83
6.2 Introduction 83
6.3 Methods 85
6.3.1 Chemicals and test animals 85
6.3.2 Experimental design 85
6.3.3 Histopathology 87
6.3.4 Immunohistochemistry 87
6.3.5 Statistics 88
6.4 Results 88
6.4.1 Parental generation zebrafish: Juveniles 88
6.4.2 Parental generation zebrafish: Adults 93
6.4.3 Reproductive performance of the parental generation and the consequences for first filial generation embryos 98
6.5 Discussion 101
6.6 Conclusions 104
7 CONCLUDING REMARKS 105
A APPENDIX TO CHAPTER 5 139
B APPENDIX TO CHAPTER 6 163

LIST OF FIGURES

Figure 1.1. Levels of legacy and emerging model toxicants in environment. 7

Figure 1.2. A representation of the One Health concept. 8

Figure 1.3. The gene expression path from DNA sequence (upstream) to functional enzymes, yielding concomitant changes to metabolism (downstream). 14

Figure 1.4. Simplified flowchart linking the environmental exposome with the employment of "omics" methods to address the mode-of-action of toxicants and toxicants mixtures. 15

Figure 1.5. Simplified diagram of the RNA-Seq workflow. 17

Figure 2.1. Project workflow illustrating the autonomous tasks and their interlinks. 26

Figure 3.1. Assessment of cellular viability at 48 h by Alamar Blue test. 35

Figure 3.2. Toxicant interaction analyses of HepG2 viability exposed to DFC, B[*a*]P and their mixtures. 36

Figure 3.3. Assessment of DNA strand breaks (% DNA tail) by Comet assay at 6, 24 and 48 h. 37

Figure 3.4. Micronuclei induction assessment by flow cytometry. 38

Figure 3.5. Assessment of intracellular Reactive Oxygen Species (ROS) measured using the DCFH-DA assay. 39

Figure 4.1. Representative nucleoids of Comet classes based on % DNA in Tail in zebrafish embryos, obtained using software CometScore 1.6. 52

Figure 4.2. Results from scoring metrics obtained from whole zebrafish embryo cells, fresh or frozen at -80ºC for 1 or 2 weeks, the latter in either for PBS or PBS complemented with 10% m/v DMSO (PBS+DMSO). 54

Figure 5.1. Examples of histopathologic alterations in zebrafish embryos (96 hpf). 67

Figure 5.2. Principal component analysis (PCA) plots highlighting the relationships between mortality and pathological alterations (toxicopathological or developmental) rates in zebrafish embryos exposed to B[*a*]P, DFC or their mixtures. 69

Figure 5.3. Damage to DNA strand (measured through the Comet assay) in zebrafish embryos exposed to B[*a*]P, DFC or their mixture. 70

Figure 5.4. Transcriptomics (RNA-Seq) analyses in zebrafish embryos exposed to B[*a*]P, DFC or their mixture. 71

Figure 5.5. Gene ontology/ Gene enrichment analysis. 74

Figure 5.6 Protein-protein interaction network retrieved using STRING from whole-transcriptomes of zebrafish embryos exposed to mixture of B[*a]*P and DFC. 75

Figure 6.1 - Experimental design. 86

Figure 6.2 – Histopathological alterations in F0 juvenile zebrafish exposed to DFC, B[*a*]P and their mixtures during embryonic development. 89

Figure 6.3 – Immunostaining of PCNA in intestinal epithelia of F0 juvenile zebrafish. 91

Figure 6.4 – Immunostaining of PCNA in the kidney of F0 juvenile zebrafish. 92

Figure 6.5 – Histopathological alterations in adult F0 zebrafish that were exposed to DFC, B[*a*]P and corresponding mixtures during embryonic development. 94

Figure 6.6 – Histopathological alterations in kidneys of F0 adult zebrafish exposed to DFC, B[*a*]P and corresponding mixtures during embryonic development. 95

Figure 6.7 – Immunostaining of PCNA in intestinal epithelia of adult F0 zebrafish. 96

Figure 6.8 – Immunostaining of PCNA in kidney of adult F0 zebrafish. 97

Figure 6.9 – Histopathological alterations in the gonads of F0 zebrafish exposed during embryonic stage to DFC and B[*a*]P, isolated and combined, after the couples are used in crosses to obtain the F1 embryos. 99

Figure 6.10 – Heatmap and hierarchical clustering of experimental conditions and endpoints determined in zebrafish exposed to DFC, B[*a*]P and their combination during embryonic development. 100

Figure A3.1. Mortality global model statistical analysis (model validation). 159

Figure A3.2. Development and pathological alterations global model statistical analysis (model validation). 160

Figure B1.1. PCNA expression individual channels and RGB composite in intestine epithelium and kidney of F0 juvenile zebrafish (30 dpf). 165

Figure B1.2. PCNA expression individual channels and RGB composite in intestine epithelium and kidney of F0 adult zebrafish (90 dpf). 166

LIST OF TABLES

Table 4.1. Summary of the Comet Assay Protocol Proposed for DNA Strand Breakage Analysis in Whole-Body Zebrafish Embryos 51

Table 5.1. Zebrafish primer design for RT-PCR. 66

Table 5.2. Generalised linear model (GLM) for mortality. 68

Table 5.3. Generalised linear model (GLM) for pathological alterations. 68

Table 5.4. KEGG pathways associated to total genes from B[*a*]P and DFC treatments and mixture of both contaminants. 73

Table 6.1 - Anti-PCNA antibody signal and histopathological traits in target organs relatively to controls. The table summarises the results from juvenile F0 zebrafish exposed to DFC and B[*a*]P, isolated and combined, during the embryonic development. 93

Table 6.2 - Anti-PCNA antibody signal and histopathological traits in target organs relatively to controls. The table summarises the results from adult F0 zebrafish exposed to DFC and B[*a*]P, isolated and combined, during embryonic development. 97

Table A1.1. Summary of experimental conditions for the acute bioassays with zebrafish embryos with single of combined toxicants. 141

Table A3.1. RNAseq top 5 genes overexpressed and underexpressed in zebrafish embryos exposed to B[*a*]P (0.4 µM), DFC (2.5 µM) and corresponding mixture. 161

ABBREVIATIONS

AChE	Acetylcholine esterase
Ahr	Aryl hydrocarbon receptor
AKRs	Aldo-keto reductases
AOPs	Adverse Outcome Pathways
B[*a*]P	Benzo[*a*]pyrene
COX	Cyclooxygenases
CYP	Cytochrome P450
DAPI	4',6-Diamidino-2-Phenylindole, Dihydrochloride
DCFH-DA	Dichloro-fluorescein diacetate
DDA	Data-dependent acquisition
DEGs	Differentially expressed genes
DFC	Diclofenac
DIA	Data-independent acquisition
DMSO	Dimethyl sulfoxide
DNA	Deoxyribonucleic acid
EC	European Commission
EDA	Effects-Directed Analysis
EDCs	Endocrine-disrupting chemicals
EEA	European Environment Agency
EPA	Environmental Protection Agency
ERA	Environmental Risk Assessment

ESQ	Environmental Quality Standards
EU	European Union
GSH	Glutathione
GWAS	Genome-wide association studies
H&E	Harris' Hematoxylin and Eosin Y stain
HepG2	Human hepatocellular carcinoma cell line
HILIC	Hydrophilic Interaction Chromatography
HMPA	High melting point agarose
IARC	International Agency for Research on Cancer
IC_{50}	Half-maximal inhibitory concentrations
iTRAQ	Termed Isobaric Tag for Relative and Absolute Quantitation
KEGG	Kyoto Encyclopedia of Genes and Genomes
LMPA	Low melting point agarose
MALTI-ToF-MS	Matrix-Assisted Laser Time-of-Flight MS
MEM	Minimum Essential Medium
MN	Micronucleus
MOA	Mode-of-action
MS	Mass spectrometry
NGS	Next-generation sequencing
NMR	Nuclear magnetic resonance
NOAEL	Observed adverse effect level
NOEC	Observed effect concentration
NSAIDs	Non-steroidal anti-inflammatory drugs
nUPLC-nESI-TOFMS	Nanoflow ultra-Perfomance Liquid Chromatography-nanoelectrospray ionization-Time-of-Flight Mass Spectrometry
OCPs	Organochlorine pesticides
PAHs	Polycyclic aromatic compounds
PAS&H	Periodic acid-Schiff's and Harris' Hematoxylin stain
PBS	Phosphate-buffered saline

PCBs	Polychlorinated biphenyls
PCNA	Protein proliferating cell nuclear antigen
PG	Prostaglandin
PPCs	Pharmaceuticals and personal care products
qRT-PCR	Quantitative reverse-transcription PCR
QSAR	Quantitative Structure-Activity Relationship
REEs	Rare earth elements
RNA	Ribonucleic acid
RNAseq	Ribonucleic acid sequencing
ROS	Reactive oxygen species
SDGs	Sustainable Development Goals
SNPs	Single-nucleotide polymorphisms
SQGs	Sediment Quality Guidelines
SRM	Selected Reaction Monitoring
SSH	Suppression subtractive hybridization
SWATH	Sequential Window Acquisition of all Theoretical fragment-ion spectra
UGTs	UDP-glucuronosyltransferases
UN	United Nations Organization
UNIDO	United Nations Industrial Development Organization
WFD	Water Framework Directive
WGBS	Whole-Genome Bisulfite Sequencing
WHO	World Health Organisation

1

INTRODUCTION

The present section was partially adapted from the follow article produced and published during this thesis:

Martins, C., Dreij, K. & Costa, P. M. (2019). The state-of-the art of environmental toxicogenomics: Challenges and perspectives of “omics” approaches directed to toxicant mixtures. International Journal of Environmental Research and Public Health, 16(23), 1–16. https://doi.org/10.3390/ijerph16234718

1.1 Environmental Pollution

Throughout the centuries, the human society has relied on knowledge and industriousness for its expansion, but the Industrial Revolution would be responsible for the fastest and most abrupt changes in civilisation, albeit arguably with a high price for the environment and the health of human populations. Despite the developments in environmental policy of the last decades and the growing awareness of society towards pollution and other drivers of global change, every day large amounts of urban (including pharmaceutical), industrial, plus veterinarian and agricultural contaminants are released to the environment. Soils, air and water are the first recipients of these contaminants, but due to many different factors such as rain or wind, these compounds meet their ultimate fate in rivers, lakes, groundwater and ultimately the ocean, creating complex patterns of toxicants. Contamination, of the environment i.e., the levels of a substance over the baseline threshold, can become pollution when the levels of contamination are sufficiently elevated to cause adverse biologic effects to communities (see Chapman, 2007 for disambiguation of terms). Modern risk assessment strategies rely on understanding the unpredictable "frontier" where contamination becomes pollution, which implies investigating the underlying mechanisms of toxicity and their downstream implications for the health and survival of living systems.

In the 1960s and 1970s the term "pollution", mostly coupled to the three main types of pollution (air, water, and soil), began to be seriously discussed not only by researchers but also by the general public and lawmaker. At that time Russell (1974) compiled the definition that is still considered quite valid today: "*Pollution is best considered an activity of man, which directly or indirectly results in the addition to water, air or soil, of matter or energy which has a deleterious effect on living organisms or structures it is desirable to preserve, or which reduces the quality of water, air or soil for any subsequent use*". Nowadays, the term "pollution" is also used associated to natural sources as volcanic eruptions or windblown dust, thus not being exclusively associated to anthropogenic activities. Even though exposure to pollutants had been a concern at least since the days of Paracelsus, two centuries before the Industrial Revolution, the 1960s and 1970s witnessed the birth of environmental activism. During these early years of rising concern about anthropogenic pollution, the scientific community sought to alert not only governments, urging to impose rules to industry and agriculture, but also attract the attention of the general public. The environmental science book "Silent Spring" by Rachel Carson, a marine biologist, published in 1962, which focused on the indiscriminate use of pesticides and their persistence in ecosystems may be considered one of the pillars of ecotoxicology. In fact, it generated a cascade of events than eventually led to a ban on DDT (1972) for agricultural uses and with the reformulation of U.S. pesticide policy.

Global interventions were organized and new environment agencies and polices have been created since the 1960s, with the major objective of reversing, mitigating or remediating anthropogenic pollution. In 1970, the United States Environmental Protection Agency (EPA) was created with the

mission to protect humans and ecosystems from adverse anthropogenic alterations to the environment, including pollution. Indeed, the Priority Pollutant List developed by the EPA in 1977 was one of the most important endeavours of the Agency's early years. In its turn, the European Union (EU), virtually from its start (then called EEC), also revealed concerns about pollution and a substantial effort was issued to design guidelines for environment conservation, which effectively started in the 1970s with the first Programme of Action of the European Communities on the Environment (Boehmer-Christiansen, 1995). However, the European Environment Agency (EEA), the twin environmental agency of the U.S. EPA, would only be officially established in 1990.

Since the late 1980s until now, several important guidelines and directives meant to safeguard environmental quality were published by the European Commission (EC). We may highlight, for instance, the Drinking Water Directive (Directive 98/83/EC), created to promote the quality of water intended for human consumption. Followed by Water Framework Directive (WFD) and the Environmental Quality Standards Directive (ESQ) (Directives 2000/60/EC and 2008/105/EC, respectively), both recently amended by the Directive 2013/39/EU on "*priority substances in the field of water policy*". In turn, the consolidated Ambient Air Quality Directive (Directive 2004/107/EC), aims at setting the safety thresholds for several harmful airborne substances, including polycyclic aromatic compounds (PAHs). The Sewage Sludge Directive (86/278/EEC) and the EU Regulation 2019/1009; that regulates EU agriculture fertiliser products should also be highlighted. The recent environmental policy in Europe culminates with the "European Green Deal" with three main goals: i) setting the EU as the first climate-neutral area by 2050; ii) curtailing at least 55 % of net greenhouse gas emissions by 2030, compared to 1990 levels, and iii) plant 3 billion additional trees by 2030 (Fetting, 2020). It should be noted that, firstly, these examples are a small part of the bulk of the environmental legislation in the EU, which also includes norms for controlling radioactive and noise pollution. Secondly, the Directives are not restricted to specific habitats but the European environment as a whole. Finally, legislation ultimately intends to preserve human and wildlife health for a sustainable society that ensured the needs of future generations.

On a global scale, the United Nations Organization (UN), launched in 2016 its ambitious "2030 Agenda for Sustainable Development" whose main objective is "*end poverty and set the world on a path of peace, prosperity and opportunity for all on a healthy planet*" (United Nations, 2020). The Agenda describes seventeen Sustainable Development Goals (SDGs) that should be met to in both developed and developing countries. Between SDGs can be highlighted the goals 3 (*Good Health and Well-being*) and 6 (*Clean Water and Sanitation*) which promote human and wildlife health allied to reduction of environmental pollution, plus goals 14 (*Life Below Water*) and 15 (*Life On Land*) in conservation of ecosystems and natural resources. Regarding the objectives of these four goals, it should be noticed that disparities on environmental legislation between developed and developing countries is leaving developing countries more susceptible to increased effects of pollution, in large part due the fast increase of highly populated urban areas and rapid reduced-cost industrialization, all of which without proper sanitary norms (Rehman et al., 2015; Selwe et al., 2022). The UN reported that in 2017, 4.2

billion of people still lack safely managed sanitation. Developed countries benefit of having the capability to build more efficient and sustainable wastewater and sanitation systems, for instance, just as well as profiting from the relocation of highly polluting industries to developing countries (Muhammad et al., 2022).

Nowadays, a global effort, where the EU has a high and active participation, is in motion to decrease the levels of pollution "on source" and to seek the remediation of highly contaminated sites. Aquatic environments, especially freshwater and brackish, deserve particularly attention, since these tend, by far, to be the most impact by industrialisation, intensive agriculture and urbanism. The EEA report of 2018 for European waters (EEA, 2018) mentioned that 46 % of surface waters failed to achieve good chemical status (as defined by the EQS Directive for priority substances). This may, in most part, result from diffuse sources pollution, spanning from agriculture to atmospheric deposition; and point sources mainly pertain to urban and industrial waste and wastewater treatment (EEA, 2019). Nevertheless, the Report of Air quality in Europe 2022 (EEA, 2022) disclosed a continuous decline, between 2005 and 2019, in emissions of almost all air pollutants considered priority in the EU (e.g., B[a]P -18 %; SO_2 -76 %; PM_{10} -27 % and $PM_{2.5}$ -29 %), which can contribute to the pollution decrease in aquatic environments. Independently of the source, it is clear that pollution is rarely caused by a single major toxicant. In most cases, the environment is impacted by complex patterns of chemicals from various natural and anthropogenic sources, chemical contamination that are nowadays categorised as legacy ('traditional') and emerging ('novel') pollutants.

Legacy pollutants with urban, agricultural or industrial sources (or even naturally, due to geological events) were introduced in environment over decades or even centuries until the present day. We may highlight chemicals resulting from combustion and fossil fuels such as PAHs, organochlorine pesticides (OCPs) from agriculture activities, which were introduced about a century ago, the wide-purpose (from insulators to lubricants) polychlorinated biphenyls (PCBs) and, of course, metals. These contaminants share their persistency as well as their toxicity to humans and wildlife. At the time when the levels of legacy pollutants in the environment first rose to alarming levels, there was little knowledge of effective causality, mechanism and long-term effects of exposure eventually leading to chronic disease such as cancer. Even nowadays, despite, the growing pool of knowledge on legacy pollutants, the policies mentioned above, as well as the resultant improvement of wastewater treatment systems and air particle filtering, the levels of legacy pollutants like carcinogenic PAHs in the environment remain worryingly high and often rising (Dat & Chang, 2017). Among these, benzo[*a*]pyrene (B[*a*]P) became the first of such compounds to be identified (Kennaway, 1924) and a model toxicant. It is chiefly originated by incomplete combustion of petrogenic and biomass fuels of domestic and industrial use, cigarette smoke and industrial waste. This five-ring PAH (CAS: 50-32-8) is since 1973 considered by the International Agency for Research on Cancer (IARC) as holding carcinogenic risk to humans and with sufficient evidence to be carcinogenic to other animals (Boström et al., 2002; IARC, 1983). As representative of carcinogenic PAHs, B[*a*]P is on the initial EPA Priority Pollutant List, since 1977. Additionally, in European Union its EQS for surface waters was established

at 0.05 µg/L (Directive 2008/105/EC), which was lowered in subsequent revisions (Directive 2013/39/EU) to 1.70E-04 µg/L. Indeed, the levels of this carcinogen and similar carcinogens in the environment exceed EU and World Health Organisation (WHO) guidelines in many regions worldwide. In Europe for instance, the 2022 Air quality report (EEA, 2022) described B[*a*]P concentrations exceeding the EU target value (1 ng/m³) and the WHO guidelines (0.12 ng/m³). This situation trends to occur especially in eastern Europe countries, where environmental awareness is a comparatively recent phenomenon (Figure 1.1A). It must be noted that the genotoxic and mutagenic proprieties this particular PAH are largely associated to the formation of DNA adducts, mainly through binding the highly reactive B[*a*]P diol epoxides to guanine, after bioactivation by CYP1A1 and CYP1B1 during phase I of detoxification (Moorthy et al., 2015; Shimada & Fujii-Kuriyama, 2004). Nowadays, there is awareness that the binding site of metabolites, forming bulky adducts that are not easily removed to DNA repair enzymes, thus increasing the odds of faulty repair and fixation of mutations, is not random. Instead, the metabolites appear to bear high affinity to certain regions of proto-oncogenes (such as *ras* family) and in the p53 tumour suppressor gene, promoting or inhibiting their expression respectively, therefore favouring cell proliferation with prejudice of DNA checkpoints, therefore increasing the chances of neoplasia (Denissenko et al., 1996; Ross & Nesnow, 1999; Shimada, 2006). To all these alterations is added increased production of oxidative radicals during phase I and subsequent release of pro-inflammatory cytokines, which also enhances cell and proliferation (Nebert et al., 2000).

In turn, emerging pollutants (also termed chemicals of emerging concern), comprise mostly novel engineered chemicals or compounds derived from the advancing human society whose presence in the environment poses a significant threat. The class includes a wide range of substances, from pharmaceuticals and personal care products (PPCs) to endocrine-disrupting chemicals (EDCs) such as natural and synthetic hormones, plus flame retardants and some rare earth elements (REEs) used in new technologies (Arman et al., 2021; Itoh et al., 2021). As previous, the potential adverse impacts caused by these chemicals were not immediately foreseen and recent studies were responsible for raising the awareness of the European and other international environmental agencies to control and regulate their use and establish threshold levels to mitigate risk. Depending on substance, the sources of emerging pollutants can be as varied (or even similar) to those of legacy toxicants, however, their inefficient removal by wastewater treatment plants has been established as a major pollution factor, particularly for pharmaceuticals, PCPs and EDCs (Arman et al., 2021; Verlicchi et al., 2012). Not surprisingly, among these, non-steroidal anti-inflammatory drugs (NSAIDs) raise particularly concerns due to their widespread (and growing) use and their known chronic effects at low concentrations that, in aquatic invertebrates, for instance, may not be sufficient to trigger acute toxicity (Parolini, 2020). For these reasons, these pharmaceutical and veterinarian drugs are in the list of substances of concern detected in surface, drinking and groundwaters in all the five UN regional groups, which spans through six continents (aus der Beek et al., 2016; Parolini, 2020). Diclofenac (DFC), in particular, rose to become a model NSAID because it is widely used in human and non-human animal medicine, with the highest

concentrations being recorded in surface waters of Europe, Latin America (Brazil), Africa and Asia (Pakistan) (Figure 1.1B).

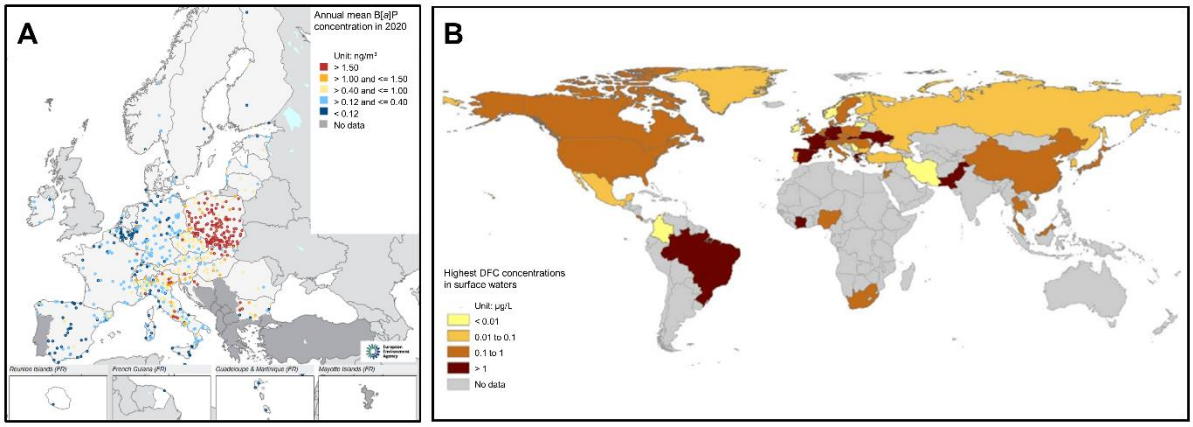

Figure 1.1. Levels of legacy and emerging model toxicants in environment. **A)** Atmospheric B[*a*]P concentrations in Europe. Image retrieved from the Air quality in Europe 2022 report (EEA). **B)** Maximum DFC concentrations reported in surface waters per country, in the early 2010s. Image from aus der Beek et al. (2016)

Many studies indicate that DFC is one of the most toxic NSAIDs for wildlife (see the reviews by Lonappan et al., 2016; Parolini, 2020). A paradigmatic base is the situation of vulture populations in India and Pakistan, which faced a near-extinction situation following renal failure caused by feeding on the carcasses of farm animals treated with DFC (Oaks et al., 2004). The alert so far issued by the scientific community led policy makers in Europe to include DFC in the water EQS list under Directive 2013/39/EU (0.1 µg/L) and in 2015 it was integrated on the1st Watch List for substances in surface waters (Commission Implementing Decision (EU) 2015/495), urging for continuous monitoring (at least) until 2018. The toxicity of DFC results mostly from the reactive metabolites 4'-hydroxydiclofenac and 5'-hydroxydiclofenac produced by cytochrome P450 (mainly CYP2C9 and CYP3A4) during phase I (Boelsterli, 2003; Leemann et al., 1993). Additionally, Boelsterli (2003) indicated a certain level of hepatotoxicity of the reactive DFC acyl glucuronide resulted from UDP-glucuronosyltransferases (UGTs) metabolization during phase II but there is still no clear and unambiguous evidence if this is true. High doses or prolongated exposure to DFC can cause hepatotoxicity due to excessive oxidative stress or even gastrointestinal and acute myocardial disorders (A. Inoue et al., 2004; K. Inoue et al., 2020). Additionally, DFC as other NSAIDs, at high doses, can negatively affect leukocyte migration to affected tissue, thus limiting the production of pro-inflammatory cytokines needed to promote acute inflammation, which may even affect tissue recovery (Paskauskas et al., 2011). This aspects relates directly with the mode-of-action of the drug, as it inhibits cyclooxygenase family members COX-1 and COX-2, which promotes the disruption of arachidonic acid cascade and prostaglandin (PG), mainly PGE_2 (Gan, 2010). An interesting fact mentioned by some authors is the possible anti-cancer properties associated to DFC because of its anti-inflammatory activity, which includes its interference with angiogenesis and general cytokine signalling (Arisan et al., 2018; Duval et al., 2019; J. Kaur & Sanyal, 2011).

Altogether, it is clear that the current relevance of both legacy and emerging pollutants is beyond dispute, which implies cautions when mixtures are not only possible but highly likely in many regions of the world, Europe included. Furthermore, as the mechanisms of toxicity between toxicants may overlap, e.g., during biotransformation, generation of oxidative radicals and cell cycle control, for instance (as between B[*a*]P and DFC), we may expect hindrances in determining risk as predicting outcomes in humans and wildlife. Similarly, we may challenge single-substance environmental standards and their real efficacy for risk assessment. The present study thus derives from the hypothesis that understanding the effects and mechanisms from exposure to mixed toxicants is vital, especially in a time where chronic disease and ageing are acknowledged to be linked to occupational exposure and lifestyle in humans which calls also for assessing toxicity not only for representative toxicants but also under realistic concentrations for both environmental and human health.

1.2 Implications of pollution to humans and wildlife

Anthropogenic pollution is unquestionably one of the factors that contribute the most to unbalance the equilibrium between ecosystems and the human society that arguably depends on it. Nowadays, the growing Humanity's awareness for the need to safeguard environmental status as a means to uphold our own quality of life and achieve sustainable societies. For such reason, in the last fifteen years the One Health concept (Figure 1.2) supported by the WHO has been introduced to explore the interconnection between society and environment through multisectoral and transdisciplinary policies (Adisasmito et al., 2022; Destoumieux-Garzón et al., 2018). The One Health concept is defined as a "*collaborative effort of multiple disciplines-working locally, nationally, and globally – to attain optimal health for people, animals and our environment*" (One Health Initiative Task Force, 2008).

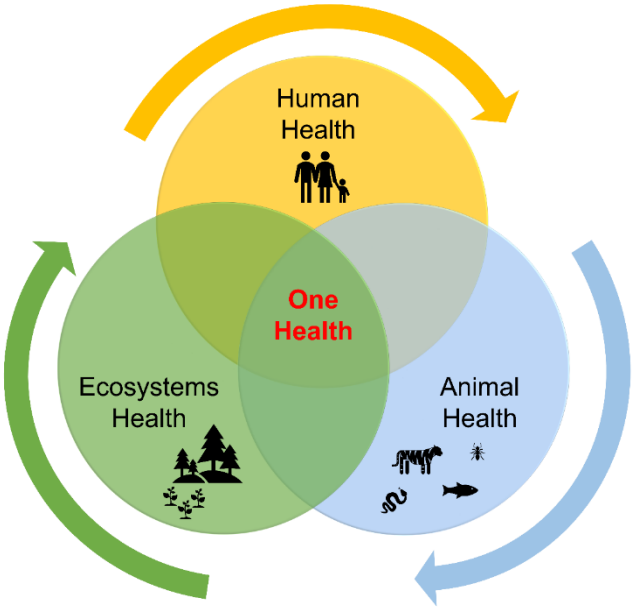

Figure 1.2. A representation of the One Health concept. Adapted from Adisasmito et al. (2022).

The good state of ecosystems health is the base of survival and progression for wildlife and humans. Globally, national and transnational programs for the identification, remediation and eventual restoration of affected ecosystems. For instance, an international collaboration between EC, the not-for-profit organization Pure Earth and the United Nations Industrial Development Organization (UNIDO) created the Toxic Sites Identification Program for assisting the association between local communities, mainly in low- and middle-income countries, and governments to identify and solve problems caused by pollution (EU/UNIDO, 2019). In the EU, the last European Commission's Joint Research Centre report, published in 2014, identified around 127,000 contaminated sites in Europe of which about 45 % (58,000) have been remediated (Liedekerke et al., 2014). Also in Europe, a successful ecosystem restoration example was the Emscher Industrial Park in Ruhr region of Germany, a massive industrial area with mining operations and steel plants that ceased activities in 1983 after about 200 years of production, leaving behind a large legacy of highly contaminated areas. These impacted grounds and water bodies were restored and now form an area occupied by sustainable communities where biodiversity has, inclusively, significantly recovered. Also, in Portugal a pilot project successfully remediated the acidified soils largely impacted with several metals in Lousal pyrite mines in operation for 88 years. Nowadays host a historical and geological interpretation centre with a regenerating endemic flora.

Animals including humans are invariably subjected to deleterious health effects of environmental contamination either by ingestion or occupational exposure, which may lead to morbidity, chronic illness and even death. For instance, Fuller et al. (2022) in their review mentioned a substantial increase of human fatalities due to pollution on a global scale over the past 20 years, with special incidence in low- and middle-income countries. In fact, WHO already reported that, by 2012, environmental hazards were responsible for 23 % of deaths worldwide and for 22 % of the global burden of disease (Prüss-Üstün et al., 2016). With this respect, EDCs and chemical carcinogens can be highlighted amongst pollutants due to their severe and often irreversible effects as in wildlife or in humans. In fact, EDCs alone can alter the balance between birth ratios of male and females, impar fertility or modify sexual behaviour of animals, from fishes and amphibians to reptiles and mammal, humans included (e.g., Bernanke & Köhler, 2009; Gonçalves et al., 2014; Gonsioroski et al., 2020; Kloas et al., 2009). Environmental carcinogens, in turn, can pose a wide and not yet fully disclosed span of effects from reproduction and development impairment to hindered immunity, neoplasia and other chronic diseases, in both humans and wildlife.

Carcinogenic chemicals form a critical group of environmental contaminants that bear the aggravating risk factor of preferentially displaying chronic effects. The IARC World Cancer Report of 2020 reported that polluted air containing known human carcinogens is the most important environmental factor for the risk of cancer, being invariably linked to water and food contamination as well, mainly affecting high-risk populations near industrial sites (Wild et al., 2020). Report from IARC (2020) also, pointed cancer as the main cause of premature death (ages 30 – 69 years) in around 70 % of the 183 studied countries, with higher incidence in developed countries. Carcinogenic contaminants comprise several categories of chemicals, including legacy and emerging pollutants. The well-known

PAHs (WHO, 2021) were identified as carcinogens the 1920s, although two centuries before the physician Percivall Pott had already linked soot (known to contain PSHs) to testicular squamous cell carcinoma in chimney sweepers. These compounds are causative agents of chronic disease even at low doses exposures, whereas acute symptoms such as inflammation or skin irritation often precede severe effects that may culminate in fatal cancer (see review of Kim et al., 2013). Among these, B[*a*]P is the most study PAH and curiously the only one included Group 1, "carcinogenic to humans", by IARC, in large part due to difficulties in determining the aetiology of such a complex systemic disease and the fact that only recently has toxicological mechanisms been considered pivotal in establishing causation (see the review by Vitorino & Costa, 2023). Still within the carcinogenic legacy pollutants group we may refer metals as cadmium, which was included in Group 1 by IARC in 1993is due the elevate risk for lung cancer (Hartwig, 2013; IARC, 1993). We may add well-known carcinogens such as asbestos (a fibrous form of silicate mineral widely used in construction), which has been linked to pulmonary carcinoma (Vorwald & Karr, 1938) and the metalloid arsenic, largely associated to skin cancer (Hughes, 2002). Between the carcinogenic emerging pollutants, we may underline, for instance, synthetic oestrogen used in menopausal hormone therapy that has been associated to the increase of breast cancer risk (Kohn et al., 2019). Additionally, the "safe" glyphosate, globally used as herbicide, has recently been reclassified by IARC as "probably carcinogenic to humans" due its genotoxicity and the possible ability to increase the risk of non-Hodgkin lymphoma in humans (IARC, 2017). Altogether, these emerging compounds show that carcinogenic chemicals are not restrained to legacy pollutants.

1.3 The new days of toxicologic evaluation: the "mixtures world"

Expecting that humans and wildlife are exposed to single toxicants or classes of toxicants is unrealistic. As the basic principle upon which Paracelsus set the foundations for modern toxicology, "*it is only the dose which makes a thing a poison*", we must be aware that every biological system is constantly exposed to a multitude of potential hazards whose hazards can differ of the sum of its parts. In brief, in mixtures, the concept of additivity is the straight sum of single effects of contaminants. In turn, additivity sets the baseline of effects for non-additivity namely antagonism and synergism. In case of antagonism the mixture effects are less than the sum of the individual effects. Conversely, in synergism, the mixture effects are larger or even distinct than the sum of the individual effects (Hernández et al., 2017). Besides very exceptional cases in which pollution (i.e., contamination rising to the point of causing deleterious effects) is caused by a single substance, establishing causal relationships between hazardous substances and deleterious effects to life is one of the toxicologist's major challenges. Among the few cases, we count the Minamata disease from incident with methylmercury (Harada, 1995), and the known associations between occupational exposure to asbestos and human cancer, first disclosed by Doll (1955). The most realistic situation in mixture assays is certainly the harvest of contaminated samples from water, air or sediment, known as "environmental" mixtures, to be used in exposure (e.g.,

Dreij et al., 2017). However, the mixtures defined in laboratory permits a higher control in number and dose of contaminants, which is advantage to more easily allow the specialists trace the line between mechanisms and effects from specific compounds interaction. Altogether, it is clear that if establishing causality for single substances is already a challenging enterprise, then more so is addressing exposure to two or more. In its turn, dealing with multiple or even countless substances that form part of an organism's exposome throughout its entire lifespan can seem dystopic. Nonetheless, exposure to mixtures whose toxicants are not entirely (or at all) known a priori is the realistic scenario for occupational toxicologists and environmental toxicologists or ecotoxicologists. Developing strategies for the evaluation of risk and safety strategies for chemical mixtures has long been deemed a priority, with many specialised workgroups already being constituted.

In result of the increased awareness for the problem of toxicant mixtures, a sizable number of new analytical approaches have been released in the past decades, with emphasis on statistical procedures, computational tools and bioassays with *in vitro* and *in vivo* models. The reader may refer, for instance, to the works by Allan et al.(2012) or Perkins et al. (2017); as well as to the recent review by Kar and Leszczynski (2019) on computational approaches to determine the toxicity of mixtures. These range from the traditional Quantitative Structure-Activity Relationship (QSAR) models to machine learning. However, these approaches are designed to address known mixtures of toxicants and not the undefinable mixture that characterises the exposome, human or otherwise. There are, nonetheless, invaluable cases that determined the toxicity thresholds of specific toxicants of classes of toxicants within complex environmental matrices and mixtures of chemicals. It is the case of the Sediment Quality Guidelines (SQGs) derived by Macdonald et al. (1996) for major toxicant in marine coastal sediments such as metals, pesticides and PAHs, which resulted from empirical models based on vast amounts of chemical and biological data. In essence, these methods were developed to identify toxicological thresholds and not mechanism.

In vitro assays have many logistical, ethical and procedural advantages in comparation with *in vivo* assays. In particularly, assays in cells involving mixtures of toxicants can accommodate more combinations and concentrations of tested chemicals, with much more reduced inter-replicate variability. An important advantage of cell-based assays is the variety of cell lines (normal or cancer) available in the market that can be chosen in function of the study objective. For example, the relative ability to metabolise toxicants, while providing some measure of risk to human health, despite obvious differences between *in vivo* and *in vitro*. In studies involving drug-induced hepatoxicity and xenobiotic metabolization, hepatocyte-derived human cell lines, normal or cancer, are largely used, such as the primary hepatocytes and liver carcinoma (HepG2) cell lines, respectively. Primary hepatocytes may be considered preferential because they have the potential to mimic at some extent the normal hepatic milieu, however, they are not as easily cultured. In turn, HepG2 immortalized cell line with adherent properties, originally derived from the liver of a 15-year-old caucasian male who had a well-differentiated hepatocellular carcinoma. This cell line is commonly used in replacement of primary hepatocytes due to the fact that it is easy to maintain in the laboratory, bearing high proliferation rates without being

tumorigenic (unable to form a solid tumour). Additionally, HepG2 cells have a stable phenotype that does not depend on donor characteristics and are capable of maintaining their levels of metabolism following propagation, contrary to primary hepatocytes after some passages (Wilkening et al., 2003). Despite being hepatoma-derived, HepG2 cells keep all major functions of human hepatocytes, including CYP-based bioactivation of toxicants, even though the expression of drug-metabolizing enzymes is generally lower than primary hepatic cells. In last year's was set a new line, the HepaRG, that is considered an alternative for primary human hepatocytes. While HepaRG, as a human normal cell line, could be considered a better *in vitro* liver model for realistic interpretation of results, extensive toxicological research with HepG2 has been proven a more promising *in vitro* hepatic model for predictive toxicogenomic studies in the area of chemical carcinogenesis, in good part due to its neoplastic nature and robustness (Jennen et al., 2010). In any case, human cell-based systems are valued models to increase relevance for human health in hazard and risk assessment of environmental contamination.

In vivo assays are still the logical approach for assessing both essential toxicological descriptors/thresholds) and mechanistic process. There are, however, constraints at ethical, economic and logistical plus economical levels. Still, small aquatic vertebrate animals, can be a "3R"-compliant alternative, being easy to breed and maintain in a laboratory and normally have a large number of descendants. The principle of the "3Rs" (Replacement, Reduction and Refinement) was proposed by Directive 2010/63/EU for the protection of animals used for scientific purposes, with the replacement and reduction of the use of animals in procedures and the refinement of animal care during assays. Among the "3R"-compliant aquatic vertebrate animals, we may primarily highlight laboratory strains of the zebrafish (*Danio rerio*), a growing biomedical model. This species has been used as models for disease and toxicity testing since the 1990s and in, mane instance, they replace murine models efficiently (Ablain & Zon, 2013; Modarresi Chahardehi et al., 2020). The zebrafish is easy to maintain in laboratory, their small size demands low space for growth and adults can reproduce weekly with high production of gametes. The logistics for toxicologic assays is also easier in comparison with mice since is possible have more replicates in less space (embryo assays are even performed on Petri dishes). The zebrafish is a genetically tractable organism, amenable to genetic manipulation, and its genome shows an important degree of similarity to the human genome, with around 70 % of its genes to have a human orthologue, which is pivotal when the study aims at establishing a bridge towards human health (Howe et al., 2013). Other relevant features are the first maturation age, usually around 2- or 4-months (Lawrence et al., 2012) and the short embryonic phase.

The majority of approaches to study mixtures, using both *in vitro* and *in vivo* assay models, aim at predicting at what dose they cause damage and not how. This means that Effects-Directed Analysis (EDA) may overlook unknown consequences of exposure, e.g., because they require time to develop (like neoplasms and chronic disease) or because these effects are subtle and not targeted by paradigmatic biomarkers. Nonetheless, EDA and mode-of-action (MOA) are not (and must not be) self-exclusive. The importance of understanding the toxicological MOA underlying exposure to mixtures of

chemicals is a paramount component of risk assessment strategies even for regulatory purposes (see for instance Franzellitti et al., 2013; Kienzler et al., 2016). In the first place, toxicodynamics, which aims at disclosing the interaction between chemicals and living systems is positioned at the basis of biomarker discovery (or pattern of biomarkers), which requires solid mechanistic knowledge to ascertain biological plausibility and specificity. Toxicokinetics, aims at the rate of uptake, distribution, metabolization and elimination of noxious chemicals which unquestionably depends on toxicological mechanism as well. Altogether, both subdisciplines are regarded as integrated elements of the toxic response, which means that knowledge on both is required to determine exposure and predict the probability of harm, i.e., risk. Molecular toxicologists aim thus at fine-tuning their research onto the subcellular targets plus the effects and responses triggered by exposure to toxicant mixtures at the level of genes and proteins, which forms the core of the approach commonly termed toxicogenomics (see, e.g., Chen et al., 2012 and the classic work by Schmidt, 2002).

Recent advances in molecular "omics" tools and the computational tools for the analyses of massive amounts of resulting data expanded toxicogenomics from the study of the expression of a few genes of interest toward the quantification of changes in whole-genomes, transcriptomes, proteomes and metabolomes (Figure 1.3). Naturally, "omics" and the bioinformatics required to analyse such large datasets became a key component of Systems Toxicology, a derivative of Systems Biology perspective that ultimately aims at building truly quantitative and predictive models from the integration of biological data at various levels of organisation: from molecule to environment (Hood et al., 2004). Under the Systems Toxicology paradigm, toxicogenomics aims at deriving toxicological mechanism and disclosing Adverse Outcome Pathways (AOPs), which are defined as direct associations between specific molecular networks and deleterious effects to biological systems that can be used as predictors of adversity and, therefore, have relevance for risk assessment. By other words, AOPs offer a mechanism-based perspective on the classical concept of "biomarker". Interestingly, the term AOP was first introduced by ecotoxicologists, who quickly adopted "omics" up to the point of becoming pioneers amongst toxicologists, in large part due to the success of these methods on organisms with low or incipient genomic annotation (Ankley et al., 2010). Besides ecotoxicology, the concepts underlying Systems Toxicology and "omics" methods are being applied to nearly every subdomain of toxicology to address isolated or combined toxicants, from nanotoxicology to emerging fields such as evolutionary toxicology, the latter of which aims at studying intergenerational exposure to environmental toxicants (see or instance Costa & Fadeel, 2016; Oziolor et al., 2017). Even though the relevance of "omics" for studying the toxicology of mixtures has been pointed out years back (Altenburger et al., 2012) now is the time to review the subject in face of novel technical achievements, with emphasis on multi-omics approaches, bioinformatics tools, plus their failures and successes in the collusion between traditional and emerging toxicants. Additionally, the AOP framework also permits increasing the relevance of environmental toxicology though human health by exploring the mechanistics of effects in *in vitro*, in silico or *in vivo* models of biomedical relevance (e.g., Clippinger et al., 2018).

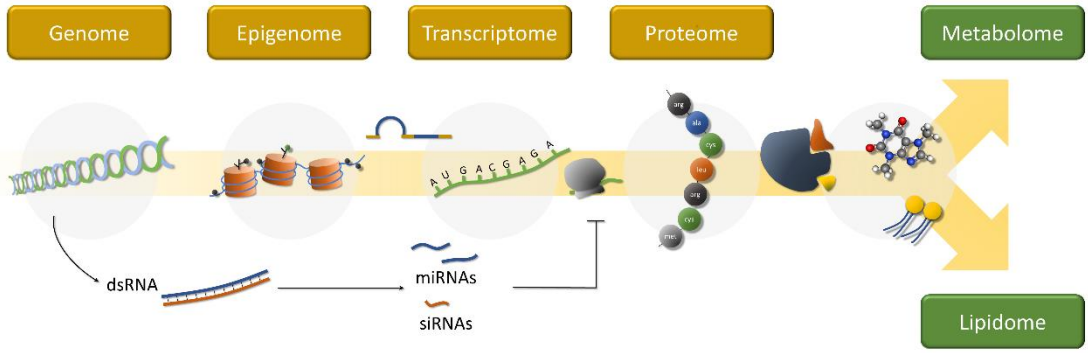

Figure 1.3. The gene expression path from DNA sequence (upstream) to functional enzymes, yielding concomitant changes to metabolism (downstream). The toxicogenomics approach can focus on any or multiple levels of the molecular cascade than can be impacted by toxicological challenge, either as response to chemical insult or as effect. These levels are, nonetheless, two-way interlinked: enzymes are involved every step, from epigenomic modifications and the regulation of transcription and mRNA maturation, for instance. Changes to the proteome will thus affect upstream effects. Bioreactive metabolites can, in their turn, interfere with protein structure and function, as well as with chromatin.

1.4 Challenges and perspectives of "omics" approaches directed to toxicant mixtures

The term "omics" is an informal neologism that applies to various methods designed at the detection, characterisation and quantification of large batches of biomolecules in single runs. The essential methods vary according to target, like, for instance, mass spectrometry (MS) for proteins, microarrays and next-generation sequencing (NGS) for mRNAs and gDNAs or nuclear magnetic resonance (NMR) for metabolites. The last decade witnessed a tremendous surge in new or improved "omics" methods and the bioinformatics tools required to analyse the massive outputs, whether these refer to sequences, counts or other forms of quantitative data, and the technical advances appear at an astonishing rate, allowing increased output, sensitiveness and accuracy and low sample input. Nonetheless, validation of findings with single-endpoint methods such as qRT-PCR of a few genes or Western Blot for representative proteins is nowadays considered good practice when handling "omics". The reader is then alerted to the need to elect the most adequate quality assessment strategy from current guidelines and available literature.

As an illustrative example, in a few years proteomics shifted from one- or two-dimensional gel fractionation procedures coupled to MS-MS detectors for data-dependent acquisition (DDA) to gel independent, highly sensitive data-independent acquisition (DIA) through shotgun methods; Selected Reaction Monitoring (SRM), or Sequential Window Acquisition of all Theoretical fragment-ion spectra (SWATH)-MS that can quantify thousands of peptides in highly complex samples (e.g. Simbürger et al., 2016; Vidova & Spacil, 2017). Similarly, epigenetics expanded from the analysis DNA methylation using, .e.g., gene arrays (which are not considered "omics", though) to methods, like Whole-Genome Bisulfite

Sequencing (WGBS), which, coupled with NGS, can screen whole-genomes for the reversible epigenetic alterations that modulate expression such as methylation and histone modifications (Kernaleguen et al., 2018). Toxicologists swiftly adopted these methods and indisputably contributed to their development as the advantages of detecting and quantifying large sets of molecules in single reads from individual samples. This tremendous asset now allows, instead of surveying single or few endpoints that may or not produce clear results, to explore gene and protein sets, for instance, and draw molecular pathways and gene expression signatures resulting from exposure. If properly phenotypic anchoring is provided (e.g. toxicopathology) and toxicodynamics are addressed (as toxicant burdens plus dose- and time-responsiveness), then a link between pathway and effect is established, then determining AOPs for mixtures (Figure 1.4).

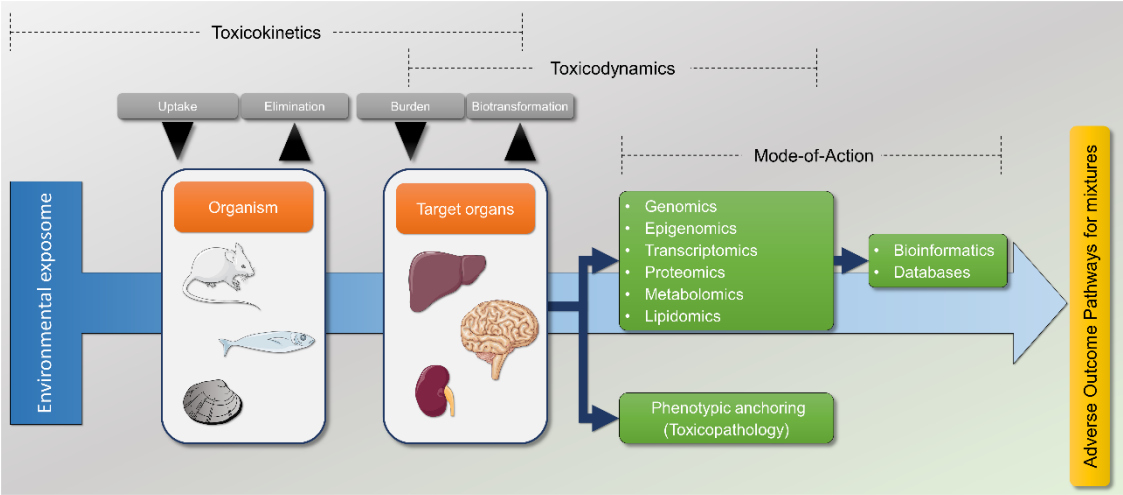

Figure 1.4. Simplified flowchart linking the environmental exposome with the employment of "omics" methods to address the mode-of-action of toxicants and toxicants mixtures. Mechanism is one of the fundamental steps of the process of disclosing specific adverse outcome pathways which, in turn, are paramount to develop quantitative and predictive models for Environmental Risk Assessment (ERA).

"Omics" approaches are, nonetheless, challenging in terms of computation and interpretation, technically demanding and highly expensive, which poses serious constraints to experimental design, number of samples and multi-omics approaches. Therefore, this project focused only on transcriptomics techniques. To understand the relevance of transcriptomics in the disclosure of toxicological mechanisms and AOPs, we must first briefly compare the main "omics" approaches and their aims. As the technicalities of each "omics" is worthy of a textbook on its own, they will only be briefly explored here.

1.4.1 Transcriptomics

Transcriptomics addresses global changes to gene expression by targeting mRNAs. Transcriptomics, together with proteomics, is likely one of the most widely employed "omics" by toxicologists. Comparatively to traditional qRT-PCR, transcriptomics methods can target thousands of

single mRNAs in a single run, which may render analyses highly cost-effective. The most common methods are microarrays and a form of RNA-directed NGS commonly termed RNA-Seq (Figure 1.5). It is now clear that the latter, which does not rely on cDNA templates (therefore less dependent of genomic annotation), is effectively able to analyse whole-transcriptomes, generating data on more differentially expressed genes (DEGs), albeit being more challenging to analyse and interpret (refer to Rao et al., 2019 for a comparison between methods in a toxicological study with the rat model). Commercial or customised gene arrays for qRT-PCR and suppression subtractive hybridization (SSH), are methods that gained some notoriety within other branches of life science. The first is strictly target-directed but SSH is designed to isolate mRNAs that are presenting in significantly differing number of copies between a control and a treatment, which are then amplified by qRT-PCR and identified by sequencing. As they quantify a reduced number of transcripts (up to a few hundreds) they are a sort of "semi-omics" that is useful and accurate, but not particularly cost-effective. Still, as an example, Evrard et al. (2010) used SSHs to study alteration to the transcriptome in the livers of European flounder (*Platichthys flesus*) exposed to mixed herbicides.

Microarrays remain popular in many fields of research, toxicology included, in part due to relatively reduced costs. However, this method requires high genomic annotation because the fundamental principal is to attach known cDNAs to a chip, to which complementary mRNAs will hybridise. Not surprisingly, commercial chips are available for humans, murine, zebrafish, rainbow trout and other standard models. The applications of the method are wide, from single-particle type nanotoxicology to studies involving combined pesticides and PAHs in fish feed, and complex mixtures mimicking crude oil spills, diesel exhausts, on a various range of model organisms (from rats to mussels) using commercial or customised oligonucleotide chips, just to sample a few (e.g. Costa et al., 2018; Jensen et al., 2016; Søfteland et al., 2014; Tilton et al., 2015). The list of cases is likely too long to be comprehensively presented here but the most important lesson learned is the success of microarrays in complex studies, providing paramount information for risk assessment from toxicological mechanism where traditional limited-endpoint studies fail (see Jensen et al., 2016, and references therein). Most importantly, the use of microarrays led toxicologists to use special bioinformatics tools to investigate mechanism, such as gene ontology and gene enrichment-based pathway and network analyses, effectively disclosing or at least contributing to disclose true AOPs for intricate toxicant mixtures. With this respect, we can highlight the works by Zare et al. (2018) with the freshwater fish *Pimephales promelas* (the fathead minnow) exposed to mixed EDCs. This was preceded by Lichtensteiger et al. (2015), with Wistar rats exposed to complex mixtures of EDCs. In this case, the authors specifically targeted the brain and used an Affymetrix chip designed for rat brain. Another interesting case study is that of Martínez-Pacheco et al. (2014), who exposed a normal mouse fibroblast cell line to mixed metals (Cd, Pb) and As and combined microarray analyses with the expression of miRNAs (determined using a commercial qRT-PCR array). Using, Ingenuity Pathway Analysis (IPA) software suite (www.qiagenbioinformatics.com/products/ingenuity-pathway-analysis), the authors revealed a combination of pathways linked to cell death, inflammation and others. Similarly, Curtis et al. (2017),

used microarray data from the head kidney of rainbow trout (*Oncorhynchus mykiss*) exposed to complex mixtures of PAHs to analyse susceptibility for infection with the pathogenic bacterium Aeromonas salmonicida. These authors retrieved canonical biological pathways from gene enrichment tools (Huang et al., 2009a) using a free (unlike IPA) online software suite called DAVID (Huang et al., 2009b), disclosing de-activation of immune- and infection-related pathways.

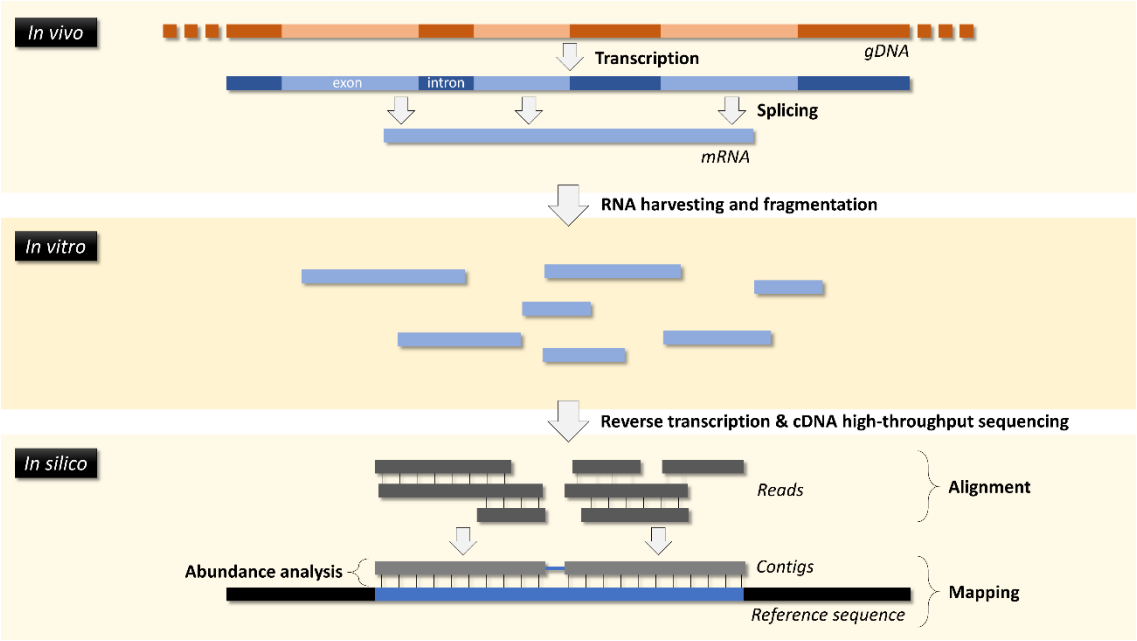

Figure 1.5. Simplified diagram of the RNA-Seq workflow. The method implies harvesting total RNAs from a biological sample, which is then fragmented, reverse-transcribed to double-stranded cDNA. The cDNA fragments are then sequenced, producing short reads, which are aligned to produce contigs to be mapped against a reference sequence (such as a known transcriptome). The abundance ("counts") of reads or aligned contigs permits estimating relative expression between experimental conditions.

The employment of RNA-Seq by environmental toxicologists and ecotoxicologists may be, comparatively to microarrays, in its infancy, but it is already showing its potential for investigating the mechanisms of disease, such as cancer (e.g., Q. Chen et al., 2022; Lao et al., 2023; White, 2016). As it produces far more data than microarrays and is less reliant on annotation, this method can generate even larger data sets from which more a more comprehensive list of pathways can be produced. Nonetheless, these same advantages make RNA-Seq data more cumbersome to analyse and interpret. Fortunately, there is a huge effort to adapt statistical procedures to RNA-Seq data, like those available for the open-source software suite R (Ihaka & Gentleman, 1996), which now accommodates several packages, such as edgeR (McCarthy et al., 2012), especially conceived for NGS data, as it does for microarrays.

Perhaps not surprisingly, RNA-Seq rapidly gained momentum within ecotoxicologists. A recent example comes from the work by Yadetie et al. (2018), who employed the method in precision-cut liver slices of the Atlantic cod (*Gadus morhua*) exposed to isolated and binary mixture of the carcinogenic

PAH benzo[*a*]pyrene (B[*a*]P) and 17α-ethynylestradiol (EE2), revealing putative pathways in which vitellogenin production and the aryl hydrocarbon receptor (Ahr) pathways overlap. These authors also used R for data processing and essential statistics, plus gene enrichment and pathway analysis through DAVID and also the STRING and STICH databases and online tools for surveying gene and protein networks (Szklarczyk et al., 2015, 2016). In another example with emerging pollutants, H. Chen et al. (2019) surveyed signalling pathways related to reproduction in female zebrafish recurring exposed to mixed phthalate plasticizers. The authors contrasted DEGs against the canonical pathways in the Kyoto Encyclopedia of Genes and Genomes (KEGG). This is a database allocates biological pathway data for a large number of species, the zebrafish included due to its acknowledged and expanding value as model organism (Kanehisa et al., 2014). Furthermore, physiological condition indices and toxicological traits (e.g. number of viable oocytes) provided important phenotypical anchoring in this same work. To these examples we may add the *in vitro* study with primary human hepatocytes exposed to insecticides and insect repellents by Mitchell et al. (2016), more directed to human risk and therefore better lodged within the domain of environmental toxicology and ecotoxicology, as the previous. These examples illustrate the diversity of research on toxicant mixtures in which RNA-Seq-based transcriptomics has been proving its worth, likely to expand in the near future.

1.4.2 Genomics and Epigenomics

The genome sets the essential layout for all living organism, which means that minute changes may have a deep impact at all levels of biological organisation, from cell to population. Moreover, genotoxicity and mutagenesis have a very significant link with tumorigenesis (see Basu, 2018 for a recent review). Nonetheless, whole-genome analysis in toxicology is still lagging despite the extraordinary advances in sequencing methods, bioinformatics and machine learning. The high costs of analysis are just a part of the problem. Indeed, reduced or absent genomic annotation of unconventional model organisms and wildlife (unlike murines, zebrafish and humans) is a serious constraint to ecotoxicologists. Interesting prospects arise from state-of-the-art approaches such as genome-wide association studies (GWAS), which mostly focus on single-nucleotide polymorphisms (SNPs) to detect variants across the genomes of different individuals from the same species or strain. The findings are then matched against phenotypical pathological traits, from resistance to drugs and toxicants to cancer and other diseases (e.g. Giacomini et al., 2017). The approach requires, however, access to batches of sequenced genomes and, so far, has been mostly employed in human toxicity and pharmacology of single substances, with the outcomes being made publicly available in repositories such as the GWAS Catalogue (https://www.ebi.ac.uk/gwas/).

Whereas genotoxicologists were more initially focused on quantifying the amount of DNA damage resulting from exposure to chemicals with direct or indirect genotoxic properties (e.g. adducts and those resulting from hindered repair), there is growing interest in the analysis of polymorphisms either as a consequence of fixed mutations or as indicators of susceptibility to environmental stressors. Despite early promises, either perspective is lagging within toxicology, of mixtures or otherwise. The

latter perspective has been proposed for linking human health and environmental stressors, chemicals included, just after the first human full-genome sequencing (Olden & Guthrie, 2001). This strategy assisted, for instance, the discovery of genes that confer resistance in mice to tetrachlorodibenzodioxin (TCDD), a potent mutagen that is an Ahr agonist and therefore able to induce CYP1A expression (Prokopec et al., 2019). The analysis of polymorphisms resulting from exposure to toxicants is acknowledged to be particularly challenging due to limitations in the detection of the low levels of somatic mutations, even by current NGS methods (Maslov et al., 2015) and blocking of polymerases due to DNA lesions. Still, recent advances in NGS sensitivity, error handling and bioinformatics are beginning to produce interesting results, even if not yet linked to the problem of mixed toxicants. Indeed, technical advances and special adaptations of NGS are being developed for the detection of rare mutations and low amounts of DNA damage caused by various agents, chemical included, including Damage-seq, a sequencing method that immunoprecipitates damaged sites, or Endo-Seq, which circumvents polymerase blocking by forcing strand-breakage at damaged locations (see the recent reviews by Du et al., 2017; Sloan et al., 2018). Additionally, a recent work (Wamucho et al., 2019) identified significantly increased incidence of SNPs in the nematode model (*Caenorhabditis elegans*) exposed to Ag nanoparticles in a multigenerational study. Matsumura et al. (2018), developed a whole-genome mutation detection procedure in bacteria (*Salmonella typhimurium* strain TA100) as a test to detect the signatures of mutagens, deploying model DNA alkylating agents, namely ethylnitrosourea, methylnitrosourea and ethyl methansulphonate (EMS). These authors disclosed that the assay is able to detect alkylating signatures similar to those registered in human cancer. These findings showed the growing potential of genomic approaches in toxicology, albeit still at their début, in correlation to the advances that are introduced in sequencing technology and computational tools.

Assisted by NGS methods, pyrosequencing (a sequencing method based on the luciferase system during synthesis) and PCR quantification, epigenomics aims at detecting and quantifying epigenetic modifications to the whole genome and identify specific modifications to genes that may compromise their expression. These modifications play a massive role in transcription control by modulating the accessibility to DNA-binding enzymes, which means that epigenetic mechanisms can literally turn on or off certain genes. This must not be confused with simply measuring the total levels of DNA methylation. Although of importance (for instance Duca et al., 2018, for an example on toxicant mixtures, PAHs, in the case, on DNA and RNA total methylation in rats), this strategy does not allow inferring on which genes have their expression inhibited or favoured, with consequences for downstream pathways. Methylation of DNA and post-translation histone modifications (forming the “histone code”) are arguably the best-known epigenetic phenomena and are regulated by a battery of enzymes whose function can be modified or compromised by toxicant action (see Marczylo et al., 2016, for a review).

Epigenomics has already been applied to the study of toxicant mixtures, in complex matrices inclusively. As example, Ding et al. (2016) discovered differential levels of global DNA methylation between lungs and blood cells in rats exposed in situ to traffic-polluted air for up to seven days. In another example, Desaulniers et al. (2009), analysed DNA methylation in the livers of pregnant rats

exposed to isolated and mixtures of organochlorine pesticides, methylmercury (meHg) and PCBs, disclosing reduced global genome methylation in the liver, consistent with reduced expression of a methyltransferase. Even though these works have not addressed upstream effects, they illustrate the significance of exploring changes with potentially high impact on gene expression and its regulation. Specifically, they show that epigenetic processes are significantly modulated by exposure to complex mixtures.

1.4.3 Proteomics

Proteomics is essentially the study of the proteome, i.e., the set of proteins and peptides that account for structure and metabolic signalling, transport and defence processes in living systems, not excluding cell division and death, differentiation and biomolecule digestion and recycling, for instance. The proteome is essentially the final product of gene expression and, albeit subject to significant interference on all steps that link genes and functional proteins, it can provide a more factual overview of the true metabolic condition of cells and tissues. For disambiguation, the term secretomics applies to a part of proteomics that focuses on secreted proteins. In toxicological studies, proteomics is used to determine how the proteome is modulated by chemical challenge. Proteomics is likely the longest standing “omics” within toxicology and the advances in bioinformatics MS methods that allow higher and more accurate throughput plus peptide quantification, will rightfully guarantee its sustenance in the future. Comparatively to transcriptomics, though, the number of target hits is, traditionally, reduced, which makes it somewhat less cost-effective. In spite of these constraints, the positioning of the proteome downstream in the gene expression cascade and higher independence from genomic annotation comparative to microarrays, renders proteomics an omics of choice in Systems Toxicology (see the review by Titz et al., 2014).

Proteomics has long been widely employed in environmental toxicology and ecotoxicology, of mixtures inclusively. Among the many examples, there are works dealing with unconventional organisms (such as clams and flatfishes) and pollutant complex matrices such as natural estuarine sediments (e.g. Costa et al., 2012; Romero-Ruiz et al., 2006). These works are essentially focused on biomonitoring and environmental risk assessment (ERA) strategies. In many cases, proteomics is often coupled with more traditional biomarker approaches. Proteomics has, nonetheless, been successfully applied in more mechanistic studies of mixtures, binary or more complex, in many cases in ecologically relevant organisms. It is the example of work with a flatfish (*Solea senegalensis*) exposed to Cd and B[*a*]P, during which the mechanisms of tissue damage and clearance were investigated by proteomics and phenotypic anchoring with multiple toxicopathological traits, histopathology included (Costa et al., 2010). In a similar context but deploying the mussel *Mytilus galloprovincialis* as model in a work more oriented towards biomarker-search, Maria et al. (2013) surveyed changes caused by Cu and B[*a*]P. Interestingly, among other discoveries, the authors revealed chitin synthase to be de-regulated by mixture and individual toxicants. In fact, in either case, as mandated by good practices in toxic mixture assessment, the bioassays (laboratorial) included co-exposure and isolated substance treatments. Still,

these short-term studies deployed relatively high concentrations of the toxicants to force a noticeable response, which contrasts with the ecological relevance of the two works mentioned in the first place. Demonstrating the importance of modern bioinformatics and available databases in studies involving proteomics, Galland et al. (2015) used STRING to demonstrate differential regulation of networks involved in multiple functions, from oxidative stress and metabolite conjugation via glutathione (GSH) recycling to betaine demethylation, in European flounder (*P. flesus*) laboratorially-exposed via feed to mixtures of PAHs and PCBs.

Proteomics has also been applied in studies more focused on potential human health effects. It is the case of Hooven and Baird (2008) who exposed MCF-7 cells (human breast cancer) to coal tar and diesel exhaust extracts, as well as to a few individual PAHs. Whereas common mechanisms were found, the authors also concluded that each individual PAH elicits its own pattern of proteome responses. Altogether, these findings sustain caution when establishing causality from exposure to intricate mixtures of pollutants due to potential synergistic effects, i.e., unattainable to individual compounds alone. The zebrafish model, which already joined the ranks of relevant biomedical surrogate models, provides further illustrative examples. Yin et al. (2014) exposed wildtype (AB strain) zebrafish (30-90 days post-fertilization juveniles) to mixtures of diketone antibiotics. The authors combined 2DE with Matrix-Assisted Laser Time-of-Flight MS (MALTI-ToF-MS), validated by qRT-PCR, with toxicopathology to demonstrate the relationship between trace concentrations of the antibiotics with cardiac loss-of-function and damaged structure, providing then paramount toxicopathological validation of their findings.

1.4.4 Metabolomics and Lipidomics

Comparatively to other “omics” metabolomics and lipidomics are less commonly employed by toxicologists. In a way, both the metabolome and the lipidome can be considered downstream elements of the toxicological mechanisms impacting “omes”, hence being co-joined in a single section. The rising number of works dealing with these “omics” show, nonetheless that technical improvements made in the last few years, including pathway-driven bioinformatics and expanding curated databases for small biomolecules, are steadily convincing toxicologists of to their purpose and value.

Metabolomics is the “omics” that embraces identification and quantification of metabolites. The term is often used interchangeably with metabonomics, but the current consensus seems to ascribe metabolomics to the study of endogenous metabolome whereas metabonomics refers to understanding how the metabolome is modulated by external or internal factors, microbiome included (see for instance Robertson, 2005). For simplification purposes, we will restrain to the most common term, metabolomics. The work horses of metabolomics are MS and NMR. In mixture toxicology, most studies are based on NMR data, with aquatic animals being the most common biological models which once again attests how ecotoxicologists are pioneering the use of “omics” in studies whose complexity is augmented by the need to analyse organisms whose physiology is as uncanny and unknown as their genomes. Jordan et al. (2012), for instance, used NMR-based metabolomics to investigate the effects of mixtures of EDCs

(bisphenol-A, di-(2-ethylhexyl)-phthalate and nonylphenol, all of which are acknowledged emerging pollutants of concern) in the liver and gonads of male goldfish, *Carassius auratus*, exposed via water for 10 days to ecologically-relevant concentrations of the toxicants (within the ng/L range). The authors retrieved almost fifty individual metabolites from each organ, matched to KEGG identities and used the IPA suite to disclose a series of modulated intracellular signalling in a synergistic form. Other examples, such as that with the mussel *Perna viridis* exposed to Cd and Cu (H. Wu & Wang, 2010) and with Limnodynastes peronii tadpoles exposed to mixed pharmaceuticals (Melvin et al., 2017) show the diversity of applications of NMR-based toxicometabolomics. In its turn, GC-MS metabolomics was used by Xu et al. (2017) to identify oxidative damage and disrupted of energy metabolism in the liver of rats exposed to the insecticide chlorpyrifos and Cd. Other techniques include nanoflow ultra-Perfomance Liquid Chromatography-nanoelectrospray ionization-Time-of-Flight Mass Spectrometry (nUPLC-nESI-TOFMS), used by David et al. (2017) to analyse metabolites in the blood plasma of roach (*Rutilus rutilus*) exposed to wastewater treatment plant effluents contaminated by pharmaceuticals and their metabolites. Also, Tufi et al. (2016) used Hydrophilic Interaction Chromatography (HILIC) coupled with ToF-MS to detect and quantify metabolites in the central nervous system of the freshwater snail *Limnaea stagnalis* exposed to agricultural surface water extracts containing mixed pesticides and other common pollutants. Spectra were then contrasted against a metabolite database and a large assay of standards for identification. The same authors complemented the MOA approach with endpoints commonly used for EDA such as acetylcholine esterase (AChE) activity and thorough the identification of target chemicals in extracts.

Lipidomics is a relatively recent subdiscipline that is gaining momentum in high-profile biomedical research, particularly due to the link between metabolic dysfunction and fatty diseases (Chiappini et al., 2017), many of which, like hepatic steatosis and phospholipidosis, are well-acquainted to toxico-histopathologists and cytopathologists. Lipidomics, which is nowadays mostly based on MS and special fractioning for hydrophobic compounds, has yet to conquer its own territory within environmental toxicology and ecotoxicology, related to toxicant mixtures in particular. For these reasons, we are compelled to introduce this important emerging “omics”. An interesting example derives from the application of multiple “omics” to address the problems of mixtures, an issue will be addressed in a section of its own. Phillips et al. (2017) studied the toxicity of the main components of electronic cigarettes, as a mixture that among other substances contains nicotine and glycerol, on Sprague-Dawley rats exposed via inhalation and applied transcriptomics, proteomics and a simplified form of lipidomics to detect and quantify the major classes of lipids in blood serum and lung. The authors showed reduced effects resulting from the aerosol exposure, albeit changes at molecular and metabolic levels in rats (liver inclusively). Despite the relatively low throughput from the lipidomics analyses, the work, which combines histopathological analyses and other common endpoints in toxicology, is an interesting example of the Systems Toxicology flowchart.

1.4.5 Multi-omics

Multi-omics (or poly-omics, as often referred to) can circumvent gaps in toxicological mechanism. Toxicologists must keep in mind that noxious substances can interact differently, yet simultaneously, with different molecular target. As example, they can modify the active centre of enzymes involved in pathways as distinct as DNA methylation, repair and transcription; protein folding; lipid peroxidation, etc. These effects and responses, regardless if they are direct or indirect can potentially affect all downstream cell functions, which renders multi-omics an extraordinary tool to disclose a toxicant's MOA (see for instance Borgert, 2007). It is thus reasonable to assume that, when looking for mechanisms in the dark meanders of supra-additive and synergistic consequences of exposure to complex combinations of toxicants, employing methods that can screen various levels is molecular organisation is a major asset. The advantages are, however, just as broad as the challenges they pose in terms of cost, experimental and sampling design, interpretation and computation. Having noted this, it is clear that multi-omics is far from routine in environmental toxicology and ecotoxicology of mixtures but the withstanding examples shed light on paths to be trod.

As before, important lessons can be learned from ecotoxicologists. For instance, Song et al. (2016, 2017) revealed alterations to the proteome, based on a gel-independent methodology termed Isobaric Tag for Relative and Absolute Quantitation (iTRAQ) and the metabolome (though NMR) of gills and digestive glands of green-lipped mussel following combined exposure to an organochlorine pesticide and a PAH, hitherto revealing changes at multiple levels: from basal oxidative stress response to cell death and even reproduction. Williams et al. (2014) combined microarrays and NMR-based metabolomics to address the effects and responses of exposure to contaminated marine sediments (by recreating a mesocosms in the lab) in European Flounder. The authors combined these analyses with environmental chemistry and traditional biomarkers (such as the Comet assay), in an attempt to concatenate mechanism with toxicodynamics and, at least in part, toxicokynetics. This same work, which is yet another good example of the application of the systems Toxicology workflow, tracked immune response and apoptosis pathways to be modulated by exposure when genes related to traditional biomarkers failed to respond. Even though much has to be done with respect to the disclosure for specific AOPs for this mixture and its application in predictive toxicology, this work shows that risk assessment of complex mixtures, especially in an environmentally-relevant scenario, cannot rely on traditional target-oriented effects.

2

OBJECTIVES AND WORKFLOW

Ultimately, the present thesis is a contribution to understand the effects and mechanisms underlying exposure to mixtures of environmental toxicants, ultimately as a means to better evaluate hazards and risks for the aquatic milieu and, most importantly, the health of human population that depend upon it. It is hypothesised that the toxicological mechanisms underneath exposure to carcinogenic PAHs and pharmaceutical drugs, namely NSAIDs can overlap via phase I biotransformation, hypothetically leading to an interaction at levels of inflammation regulation plus cell cycle control and cell proliferation. As such, we elected as model toxicants the ubiquitous aquatic toxicants NSAID diclofenac (DFC) as representative of emerging pollutant and the carcinogenic PAH and legacy toxicant benzo[*a*]pyrene (B[*a*]P).

The zebrafish (*Danio rerio*) and the human hepatoma HepG2 cell line were selected as *in vivo* and *in vitro* biological models, respectively, both with proven value in environmental toxicology. In particular, the value of laboratorial strains of the zebrafish in research on mutagenesis and neoplasia must be highlighted, rendering it an important model for both environmental and biomedical sciences, which is co-adjuvated by the growing level of genomic resources for the organism. The design of the current workplan is settled upon three important but often disregarded premises: i) the need to safeguard environmental relevance, ii) to contrast *in vivo* and *in vitro* approaches, since it has been pointed out that the discrepancies between the two strategies may be compromising risk assessment for emerging pollutants, and iii) integrating mechanism of toxicity and effects can provide a more robust measure of risk, especially in cases where realistic concentrations of individual toxicants should indicate low or null risk.

Specifically, the project aimed at:

1. Understand the effects and risk of mixtures of environmental toxicants, taking DFC and the B[*a*]P as model substances, using the zebrafish and HepG2 cell line as models.
2. Evaluate the effects of the interaction between the two toxicants on the mechanisms associated to the pathways linking genotoxicity, cell cycle regulation and immunity.

3. Infer on the potential of *in vitro* testing as a consistent and realistic procedure to expeditiously perform toxicity evaluation tests for mixtures.

To address these main goals, the project was designed as a set of interlinked but autonomous tasks, as illustrated in Figure 2.1. These include bio and cytoassays and a battery of acknowledged methods for toxicity assessment combined with RNA-Seq based transcriptomics and bioinformatics to address toxicological mechanism and unravel adverse outcome pathways for toxicants and their mixtures.

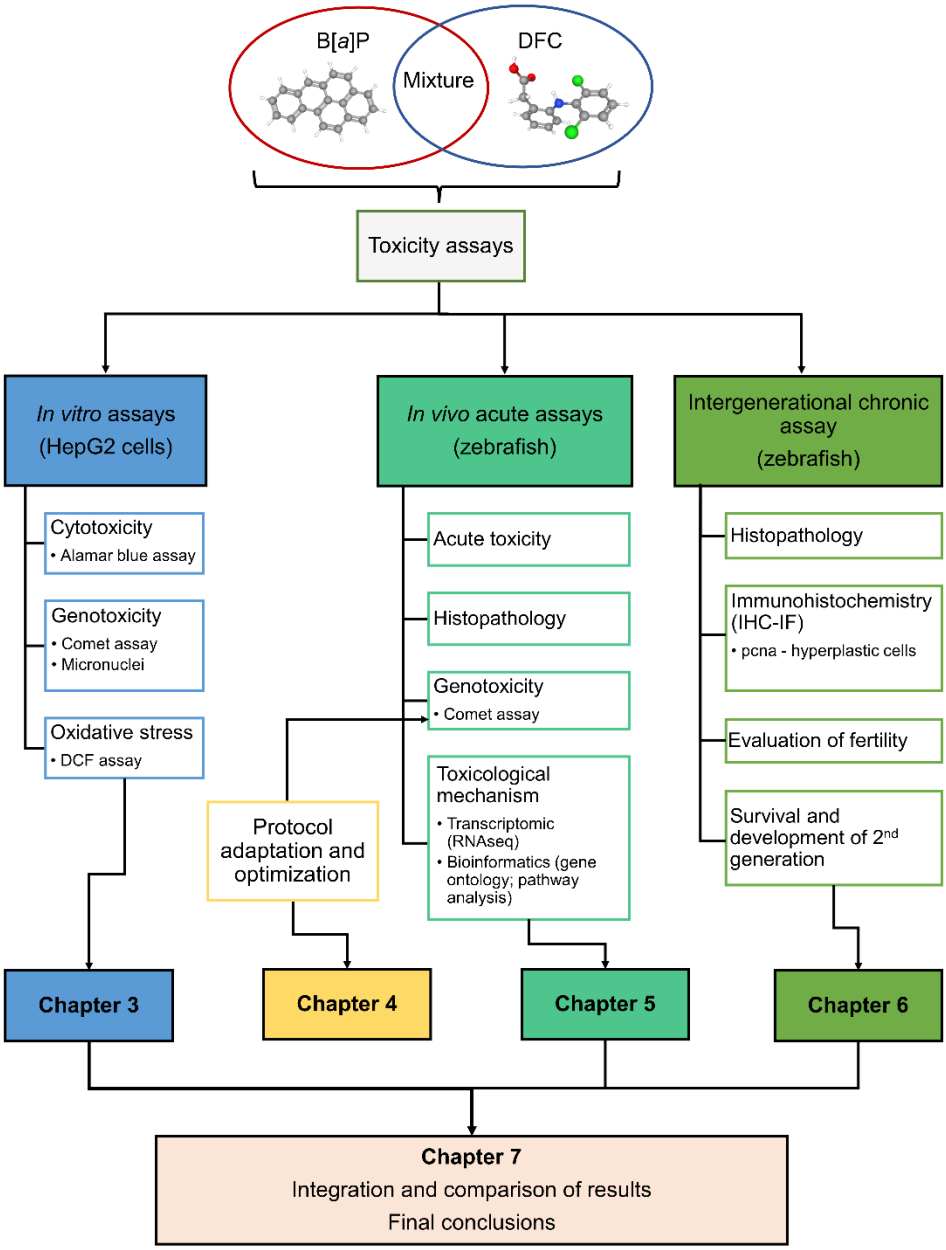

Figure 2.1. Project workflow illustrating the autonomous tasks and their interlinks.

3

ANTAGONISTIC EFFECTS OF A COX 1/2 INHIBITOR DRUG IN HUMAN HEPG2 CELLS EXPOSED TO AN ENVIRONMENTAL CARCINOGEN

3.1 Abstract

Understanding interactions between legacy and emerging pollutants has important implications for risk assessment, especially when involving mutagens and carcinogens whose critical effects are chronic and therefore difficult to predict. The current work aimed to investigate potential interactions between the carcinogenic polycyclic aromatic hydrocarbon (PAH) benzo[*a*]pyrene (B[*a*]P) and diclofenac (DFC), an anti-inflammatory COX1/2 inhibitor and one of the most widespread non-steroidal anti-inflammatory drugs (NSAIDs). Exposure to binary mixtures of these pollutants resulted in substantially reduced cytotoxicity to human hepatoma cells (HepG2) compared to the effects of single-chemical exposure. Significant antagonistic effects were found following exposure to high concentrations of B[*a*]P in combination with DFC at IC50 and 1/5 IC50. Despite observing a similar dose-dependent antagonism for induction of DNA strand breaks by the mixtures, the impact on intracellular reactive oxygen species contrasted by displaying additive effects. In addition, the frequency of micronuclei (MN) yielded a significant increase in cells exposed to mixed pollutants, but still less than the sum of individual effects, suggesting some level of antagonism. Antagonistic effects between B[*a*]P and DFC from genotoxicity and cytotoxicity assessments, but not oxidative stress, indicate a significant degree of reciprocal interference in xenobiotic CYP metabolization and mode-of-action. Overall, the findings further support the increasing concern that co-exposure to environmental toxicants and their non-additive interactions can be a confounding factor that should not be neglected in environmental and human health risk assessment.

3.2 Introduction

The advancing human society is releasing increasing amounts and diversity of domestic, urban, industrial, and agricultural toxicants to the environment, with serious implications for both wildlife and human health (Bernanke & Köhler, 2009; Pereira et al., 2015). As a result, the environment is contaminated by increasingly complex mixtures of legacy and emerging pollutants. It is critical to address effects of mixtures as a means to establish more realistic monitoring policies and guidelines for risk assessment toward environmental and human health (Beronius et al., 2020; Martin et al., 2021; Silins & Högberg, 2011). The hazard and risk assessment of mixtures is based upon the concepts of additivity and interaction in accordance with the individual chemicals' mode of action (Cassee et al., 1998). Interaction effects can be categorized as antagonistic or synergistic, depending on their relationship with the summative effects of the individual contaminants (Hernández et al., 2017). In both cases they can produce unexpected outcomes and pose a serious confounding factor in pharmacological, environmental, and occupational toxicology. Most notably, interaction effects constitute a further challenge since they depend not only on the compounds' mode-of-actions but also on the number of contaminants in the mixture, the concentration range of each chemical and their ratios (Altenburger et al., 2012; Ferreira et al., 2008; Nys et al., 2015).

The problem of toxicant interactions was further exacerbated by the end of 20th century, when it became clear that the exponential use of pharmaceutical drugs created another generation of pollutants to be added to the range of substances of emerging concern (Escher et al., 2011; Ternes, 1998). These emerging pollutants (and their derivatives) have turned into very significant pollutants of surface waters in both developed and developing countries, either due to inefficient or absence of wastewater treatment and proper environmental guidelines (Rehman et al., 2015; Selwe et al., 2022; Verlicchi et al., 2012). Legacy pollutants have been and are still a serious global health hazard, and while emissions of for example carcinogenic PAHs are decreasing in some parts of the world, they do not in others and cause high incidences of both acute and chronic health effects (WHO, 2021). The interaction between emerging and legacy pollutants is not only a realistic issue but also a serious challenge for environmental health risk assessment. For instance, recent studies suggest distinct health effects from exposure to mixtures of legacy and emerging poly/perfluoroalkyl substances (Luo et al., 2022; Roth et al., 2021). This issue is especially relevant since pharmaceuticals such as non-steroidal anti-inflammatory drugs (NSAIDs) that inhibit cyclooxygenases (COX) and legacy pollutants can affect the same pathophysiological pathways, such as those related to inflammation and cancer. Indeed, it is suspected that cancer induced by environmental factors, especially chemicals, represent the vast majority of the cases (see for instance the reviews Lewandowska et al., 2019; Wogan et al., 2004).

The human PAH carcinogen benzo[*a*]pyrene (B[*a*]P) is a well-established model compound for legacy pollutants. The main emission sources for PAHs are wide, from incomplete combustion of petrogenic and biomass fuels to cigarette smoke and industrial waste (Boström et al., 2002). B[*a*]P is genotoxic and mutagenic, forming bulky DNA adducts after bioactivation by CYP1A1 and 1B1 into highly reactive B[*a*]P diol epoxides (Shimada & Fujii-Kuriyama, 2004). These adducts can hinder DNA replication and transcription; however, their removal can be cumbersome and result in DNA double strand breaks (DSBs) and subsequent formation of micronucleus (MN) (Harding et al., 2017; Shah et al., 2016). Most importantly, these lesions are known to cause so-called “hotspot” mutations in *ras* family oncogenes (activating transcription) and p53 tumour suppressor gene (inhibiting function), which promotes cell proliferation and inhibition of apoptosis, both of which are hallmarks of neoplasia (Denissenko et al., 1996; Ross & Nesnow, 1999). Also, the increased secretion of pro-inflammatory cytokines induced by oxidative stress resulting from B[*a*]P bioactivation may further promote cell proliferation which is a strong indicator of its potency as a complete carcinogen (Nebert et al., 2000; Shimada, 2006).

In turn, diclofenac (DFC) is a drug widely used in humans and livestock, generally considered safe albeit considered one of the most toxic NSAIDs to some domestic animals and wildlife (Oaks et al., 2004). DFC exerts is pharmacological activity by inhibiting COX-1 and COX-2, i.e., prostaglandin synthases (Gan, 2010). Metabolization by cytochrome P450 (mainly CYP2C9 and CYP3A4) during phase I and by UDP-glucuronosyltransferases (UGTs) during phase II (see for instance the review Boelsterli, 2003) produces some metabolites that are associated with hepatotoxicity and hypersensitivity (K. Inoue et al., 2020). These effects are mainly associated with the induction of intracellular reactive

oxygen species (ROS), which can influence mitochondrial integrity allied with suppression of autophagy (Jung et al., 2020) and induction of intrinsic apoptosis through caspases 9 and 3 (A. Inoue et al., 2004). In contrast to B[*a*]P, DFC has not been found to have genotoxic and carcinogenic potential *in vivo* or *in vitro* (Hartmann et al., 2021). In fact, as noted for other NSAIDs, it is suggested that DFC can hold some anti-cancer properties by inhibiting angiogenesis and cytokine signalling (Arisan et al., 2018; Duval et al., 2019; J. Kaur & Sanyal, 2011).

B[*a*]P and DFC are often found at hazardous concentrations in the environment. In the EU, their concentrations in surface waters have been found to exceed the European Environmental Quality Standards, although with a decreasing trend for surface waters (Johnson et al., 2013; Škrbić et al., 2018; Toušová et al., 2019; Vystavna et al., 2018). This makes them relevant model toxicants to study possible mixture interactions between legacy and emerging pollutants, which is the main goal of the present work with emphasis on potential effects to humans and implications for risk assessment strategies. To accomplish this, we exposed the hepatoma derived HepG2 cell line to single compounds and binary mixtures of B[*a*]P and DFC. HepG2 cells were chosen as *in vitro* model due to their high metabolic capacity (Knasmüller et al., 1998). Considering the genotoxic properties of B[*a*]P, the scope of the current work centred on endpoints related to cytotoxicity, oxidative stress, and DNA damage.

3.3 Methods

3.3.1 Chemicals and cell culture

Benzo[*a*]pyrene (B[*a*]P) (CAS 50-32-8, > 95 %) was purchased from TCI EUROPE (Zwijndrecht, Belgium) and sodium diclofenac (DFC) (CAS 15307-79-6, 98 %) from Acros organics (Geel, Belgium). Stock solutions of B[*a*]P and DFC were prepared in dimethyl sulfoxide (DMSO, 99 %) from Sigma Aldrich (St. Louis, MO). The human hepatocellular carcinoma HepG2 cell line was acquired from the American Type Culture Collection (Rockville, MD). Cells were cultured in Corning® T-75 flasks with 10 mL of Minimum Essential Medium (MEM) supplemented with penicillin-streptomycin (100 IU/mL penicillin and 100 µg/mL streptomycin), 10 % v/v foetal bovine serum, sodium pyruvate (1 mM) and non-essential amino acid solution (0.1 mM), all purchased from Gibco by Life Technologies (Stockholm, Sweden). Cells were kept in an incubator, with humified atmosphere at 5 % CO_2 and 37 °C to maintain the proper cell growth during culture and assays.

3.3.2 Cell viability assay

The impact of B[*a*]P and DFC on cell viability, individually and as mixtures, was determined using Alamar Blue (Invitrogen, Carlsbad, CA) after 48 h of exposure (Rampersad, 2012). Cells were seeded (1.5E4 cells/mL) in 96-well plates that included wells with the vehicle control (0.1 % v/v DMSO) and medium-only to subtract background fluorescence. After 24 h incubation, cells were exposed to individual compounds (final volume of 200 µL per well). B[*a*]P concentration ranged from 3.2E-3 to

10 µM, and DFC from 3.2E-3 to 1000 µM. These assays were used to determine B[*a*]P and DFC half-maximal inhibitory concentrations (IC_{50}). Subsequently, cells were exposed to IC_{50} and 1/5 IC_{50} concentrations of either compound mixed with the full range of concentrations of the other. After exposure, 20 µL of Alamar Blue was added to each well and the cells incubated for further 2 h. Fluorescence intensity (excitation 540 nm, emission 590 nm) was recorded using a microplate reader (Infinite F 200 PRO, fitted with the software: Magellan 7.2, all from Tecan, Austria). Every exposure was performed in triplicate technical replicates per plate, with four independent experimental replicates (*n* = 4).

3.3.3 Comet assay

The alkaline Comet assay was performed in mini-gel version as described (di Bucchianico et al., 2017). Cells were seeded in 24-well plates (6.0E4 cells/mL) and incubated for 24 h. Cells were then exposed to: i) 1/5 IC_{50} B[*a*]P (0.39 µM) and 1/5 IC_{50} DFC (58 µM) and their respective mixture (Mixture 1); ii) 1/2 IC_{50} B[*a*]P (1 µM) and 1/2 IC_{50} DFC (150 µM) and their mixture (Mixture 3) plus a mixture containing 1 µM B[*a*]P + 58 µM DFC (Mixture 2). All plates included vehicle control (0.1 % v/v DMSO), negative control (cells in medium only) and positive control (cells exposed to 25 µM hydrogen peroxide for 5 min, on ice). After 6, 24 and 48 h of exposure, the medium was aspirated and cells washed twice with warm phosphate-buffered saline (PBS). Cells were then trypsinized and centrifuged, after which the supernatant was discarded, and the pellet resuspended in PBS and placed on ice. Cells were embedded in 0.75 % m/v type VII, low gelling temperature agarose (Sigma-Aldrich A-4018) and placed on a microscopy slide previously coated with 0.3 % agarose (two mini-gels per slide). Two technical replicates were made by treatment, with three independent experimental replicates (n = 3). After solidification on ice, slides were placed in cold lysis buffer (pH 10, 1 % Triton X-100, 2.5 M NaCl, 10 mM Tris, 0.1 M EDTA) for 60 min, followed by 40 min in cold alkaline buffer (pH 13, 0.3 M NaOH, 1 mM EDTA), both in the dark. Electrophoresis was run at 1.15 V/cm (29 V) in the same alkaline buffer during 30 min, in cold and dark conditions. Slides were then neutralized in 0.4 M Tris pH 7.8 (5 min + 5 min) and washed twice for 5 min in dH2O. Slides were allowed to dry in the dark and then fixed for 5 min in methanol for archiving. Slides were stained for 15 min in cold SYBR green (Life Technologies) diluted in TAE (tris-acetate-EDTA) buffer (1:10000). One-hundred nucleoids per experimental replica were scored under a DMLB model epifluorescence microscope (Leica Microsystems, Wetzlar, Germany) using the Comet assay IV software (Perspective Instruments, Suffolk, UK).

3.3.4 MN flow cytometric assay

The induction of micronucleus (MN) was evaluated by flow cytometry in cells exposed to 1/2 IC_{50} concentrations of individual B[*a*]P (1 µM) and DFC (150 µM) and their respective mixture, in three independent experiments (*n* = 3). The *In Vitro* Microflow Kit (Litron Laboratories, Rochester, NY) was employed following manufacturer's instructions and previous adaptations (le Bihanic et al., 2016; McCarrick et al., 2019). In brief, cells were seeded in 96-well plate (2.5E4 cells/mL), incubated for 24 h

and exposed to the three treatments plus the vehicle control (0.1 % v/v DMSO), a negative (cells in medium only) and positive control (etoposide, 0.2 µg/mL). After 72 h of exposure, medium was aspirated, and cells were incubated with ethidium monoazide (EMA) on ice for 30 min under cold white light to allow stain photoactivation. Subsequently, cells were lysed and stained with SYTOX® Green nucleic acid stain for 1.5 h in the dark at 37 °C. Samples were analysed using a Accuri C6 flow cytometer (BD Bioscience, Franklin Lakes, NJ) with flow set to 30 µL/min, run limit to 175 µL and 10000 gated nuclei events per sample. Each well was manually resuspended before acquisition to avoid sedimentation.

3.3.5 Reactive oxygen species assay

The quantification of intracellular reactive oxygen species (ROS) was performed using the dichloro-fluorescein diacetate (DCFH-DA) assay (Wang & Joseph, 1999). In brief, cells were seeded in black 96-well plates with clear bottom (Corning Incorporated, NY), at 2.5E5 cells/mL. After 24 h incubation, cells were subject to the same experimental design as described for the Comet assay, including a positive control (1 mM Tert-Butyl hydroperoxide, Sigma-Aldrich, St. Louis, MO). The exposure times ranged between 3 and 12 h. Medium was aspirated after each treatment and cells washed with Hank's Balanced Salt Solution (HBSS) from Gibco Life Tech (Carlsbad, CA), at 37 ºC. Subsequently, cells were incubated with 5 µM DCFH-DA (45 min, at 37 ºC and 5 % CO_2, in the dark). Cells were then washed with warm HBSS, and fluorescence (excitation 485 nm, emission 530 nm) was recorded immediately. Three independent assays were performed (n = 3), each with three technical replicates.

3.3.6 Statistical analysis

The IC_{50} was estimated by log(inhibitor) vs. normalized response function using the GraphPad Prism 9 statistical software (GraphPad Inc., San Diego, CA). The same software was used for statistical analysis of MN data by one-way ANOVA followed by Dunnett's multiple comparison test. All other analyses were computed using R (Ihaka & Gentleman, 1996). After invalidation of normality and homogeneity of variances, determined by Shapiro-Wilk's and Levene's tests, respectively, Kruskal-Wallis ANOVA-by-Ranks H followed by Dunn's test was used for multiple comparisons. The significance level α was set at 0.05 for all analyses and the results are expressed as means ± standard error of mean (SEM). For detecting synergistic or antagonistic mixture interactions the Biochemically Intuitive Generalized Loewe Model (BIGL) package (van der Borght et al., 2017) was used followed by meanR/maxR statistical tests, which allow for identification of statistically significant combined effects and their deviation from the null model (additivity). This strategy was applied to data from cytotoxicity, Comet, and ROS assays.

3.4 Results

3.4.1 Binary mixtures of B[*a*]P and DFC cause antagonistic effects on cytotoxicity

The IC_{50} for B[*a*]P in cells was found to be almost 150-fold lower than for DFC, i.e. 1.95 µM and 290 µM, respectively (Figures 3.1A-B). In fact, only concentrations higher than 500 µM DFC caused significant decrease in cell viability, whereas this threshold for B[*a*]P was 1 µM. Notably, the effects were lower than expected when cells were exposed to binary mixtures (Figure 3.1C-F). Co-exposing cells to increasing concentrations of B[*a*]P with a set concentration of DCF at either IC_{50} or 1/5 IC_{50} resulted in apparent IC_{50} for B[*a*]P at 15 and 14 µM, respectively (Figure 3.1C-D), approximately 7-fold lower than what was found for exposure to B[*a*]P alone. Similarly, the cytotoxicity of the mixture was about 3- and 2-fold lower in cells exposed to increasing concentrations of DCF and B[a]P at IC_{50} and 1/5 IC_{50}, respectively, compared to DCF alone (Figures 3.1E-F).

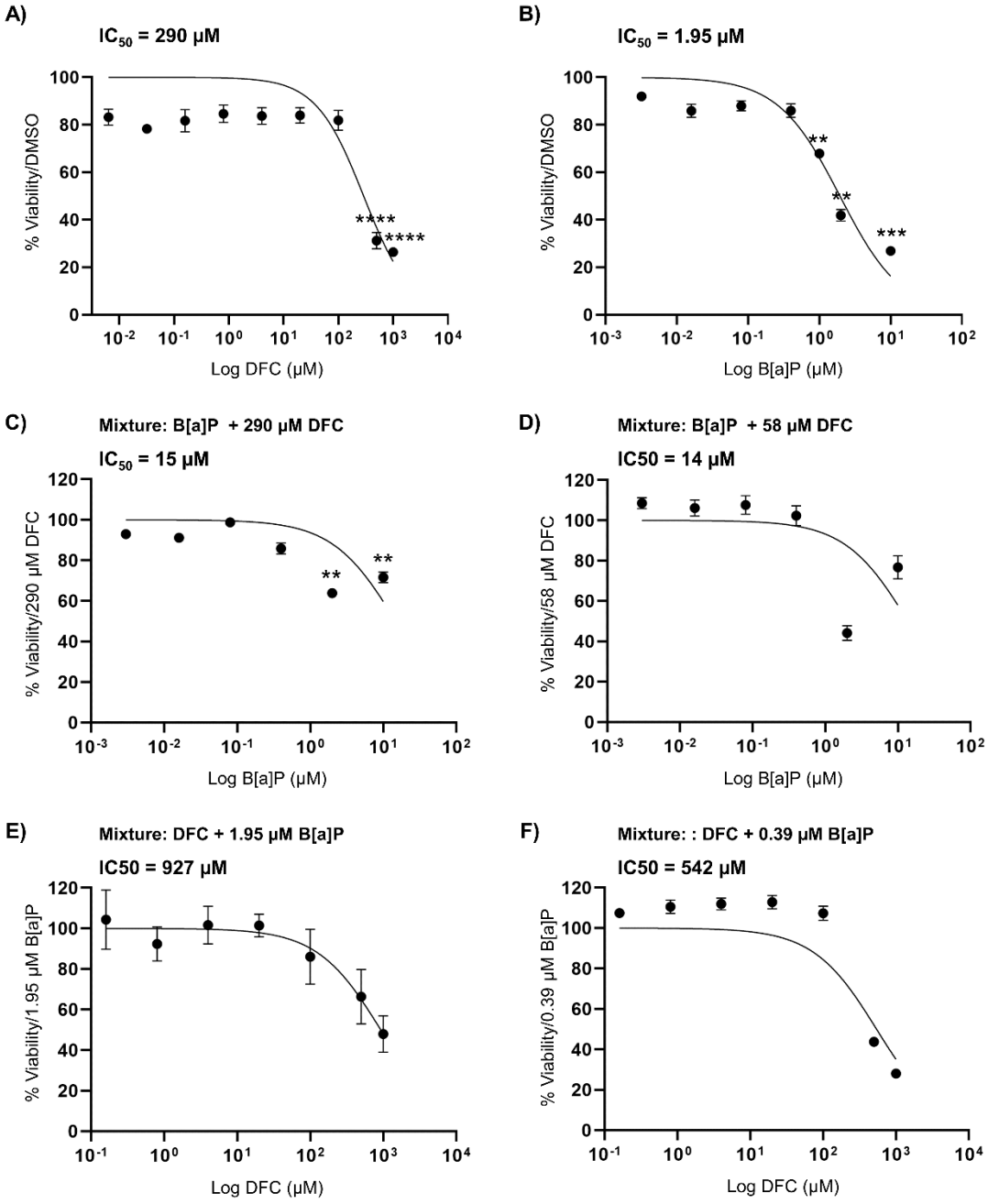

Figure 3.1. Assessment of cellular viability at 48 h by Alamar Blue test. HepG2 cells were exposed to several single concentrations of diclofenac (DFC) **(A)**, benzo[*a*]pyrene (B[*a*]P) **(B)** and binary mixtures **(C - F)**. Data shows mean ± SEM, n = 4, * $p < 0.05$, ** $p < 0.01$, ***$p < 0.001$, **** $p < 0.0001$ as compared with control through Dunn's test.

Accordingly, toxicant interaction analyses using BIGL confirmed the antagonistic effects on cytotoxicity (Figure 3.2). Antagonism was most obvious in cells exposed to binary mixtures consisting of 10 µM B[*a*]P and IC_{50} or 1/5 IC_{50} of DFC (BIGL, $p < 0.05$). In contrast, a synergistic effect was observed for the combination of the higher DFC concentration (1000 µM) and B[*a*]P IC_{50} (BIGL, $p = 0.02$).

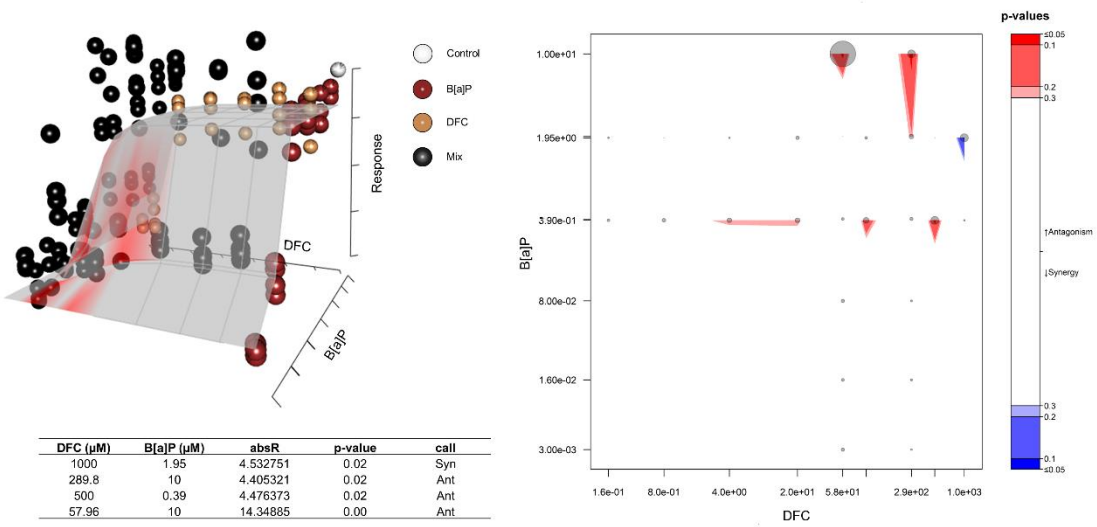

DFC (µM)	B[a]P (µM)	absR	p-value	call
1000	1.95	4.532751	0.02	Syn
289.8	10	4.405321	0.02	Ant
500	0.39	4.476373	0.02	Ant
57.96	10	14.34885	0.00	Ant

Figure 3.2. Toxicant interaction analyses of HepG2 viability exposed to DFC, B[*a*]P and their mixtures. The colours in both graphs indicate synergy and antagonism by blue and red, respectively. Generalized Loewe model followed by meanR/maxR statistic (effects are considered significant if $p < 0.05$).

3.4.2 Dose-dependent antagonism on genotoxicity

The induction of DNA strand breaks in cells exposed to low doses of B[*a*]P and DFC was only significant compared to control (Dunn's test, $p < 0.05$) in response to the mixture (Mixture 1: 0.39 µM B[*a*]P + 58 µM DFC) following 24 h of exposure (Figure 3.3A). As expected, induction of DNA strand breaks were altogether stronger following exposure to higher doses of either toxicant and their mixture (1 µM B[*a*]P and 150 µM DFC), albeit more obvious at shorter time points (Dunn's test, $p < 0.05$, Figure 3.3B). Mixture interaction analyses indicated antagonistic effects on the induction of DNA strand breaks for all exposure times (Figure 3.3C). However, only Mixture 2 (1 µM B[*a*]P + 58 µM DFC) at 24 h displayed significant antagonistic effects on levels of DNA strand breaks (BIGL, $p = 0.04$).

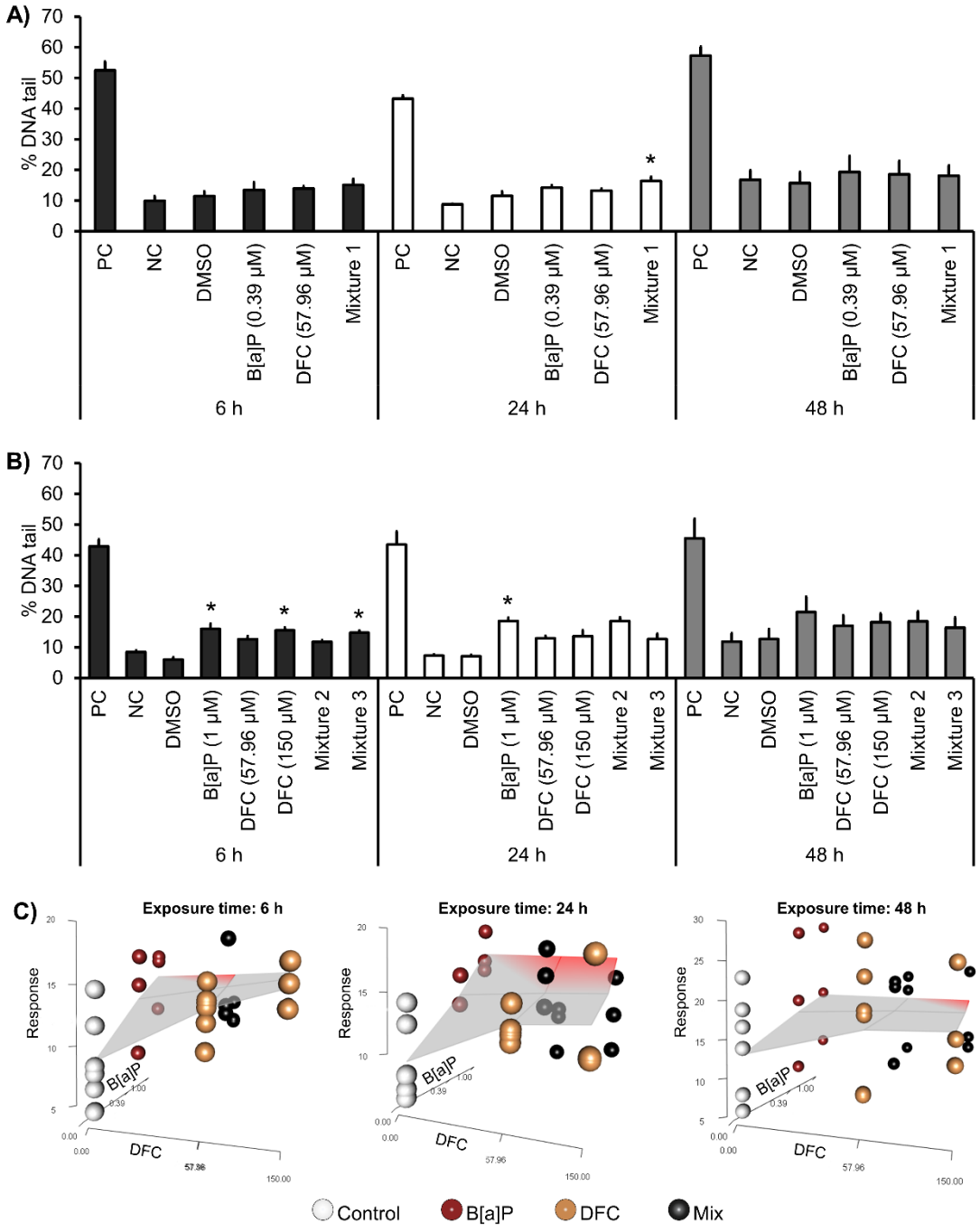

Figure 3.3. Assessment of DNA strand breaks (% DNA tail) by Comet assay at 6, 24 and 48 h. **A)** HepG2 cells were exposed to low concentrations (1/5 IC50) of individual contaminants and Mixture 1 (0.39 µM B[*a*]P + 57.96 µM DFC). **B)** Exposure to high concentrations (≈1/2 IC50) of individual contaminants, Mixture 2 (1 µM B[*a*]P + 57.96 µM DFC) and Mixture 3 (1 µM B[*a*]P + 150 µM DFC). Data in A and B shows mean ± SEM, n = 3, * $p < 0.05$ as compared with DMSO-control through Dunn's test. **C)** Mixture interaction analyses of HepG2 genotoxicity exposed

to DFC, B[a]P and their mixtures. Red surfaces indicate antagonism (Generalized Loewe model followed by meanR/maxR statistic, effect considered significant if $p < 0.05$).

Induction of MN (Figure 3.4A-B) was assessed in response to high concentrations and the results displayed similar results as the Comet assay with B[*a*]P (1 µM) and the mixture significantly inducing MN compared to control (Dunn's test, $p < 0.01$). Although only one mixture was tested, the observed effects were less than the sum of individual effects, which suggests some level of antagonism.

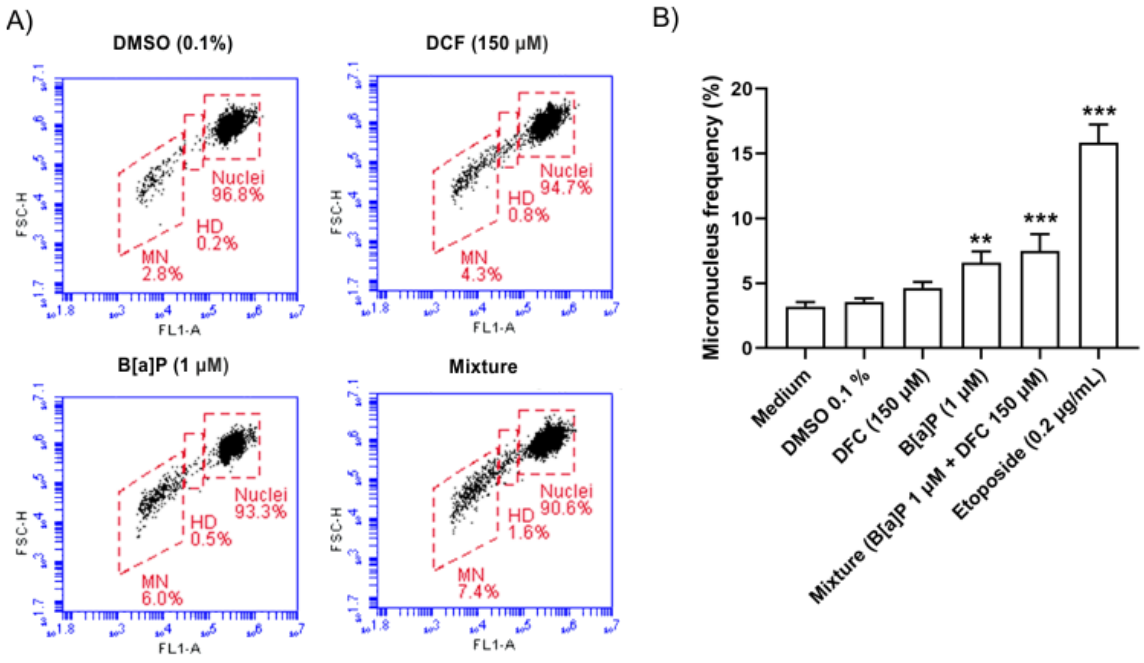

Figure 3.4. Micronuclei induction assessment by flow cytometry. **A)** Representative flow cytometry plots including populations of nuclei, hypodiploid nuclei (HD) and micronuclei (MN) in control (DMSO-only) cells, DFC, B[*a*]P and mixture. **B)** Micronuclei frequency in HepG2 cells exposed to 1/2 IC50 of individual contaminant concentrations and the respective mixture. Data is presented as mean ± SEM (n = 8 - 17). ** $p < 0.01$, ***$p < 0.001$ indicate significant differences to control (Dunnett's test).

3.4.3 Additive effects on ROS induction

ROS quantification followed the same setting as used in genotoxic analyses, with exposures to single and binary mixtures with low (0.39 µM B[*a*]P and 58 µM DFC) and high (1 µM B[*a*]P and 150 µM DFC) concentrations of B[*a*]P and DFC. Intracellular ROS was moderately increased in cells exposed to both low and high concentrations of B[*a*]P, individually and in mixture (Figure 3.5A-B). At low concentrations, the levels of ROS were significantly increased at 6 h for B[*a*]P and Mixture 1 (0.39 µM B[*a*]P + 58 µM DFC), up to 1.5-fold comparative to the control (Dunn's test, $p < 0.05$, Figure 3.5A). In addition, Mixture 1 induced a 1.3-fold increase in ROS after 12 h exposure (Dunn's test, $p < 0.05$). At high concentrations, significant levels were only found at 12 h and for individual B[*a*]P (1 µM) and Mixture 2 (1 µM B[*a*]P + 58 µM DFC) (Dunn's test, $p < 0.05$, Figure 3.5B). In contrast to the other

endpoints, no antagonistic effects were found on intracellular ROS generation, but rather additive effects by the mixtures (BIGL, $p < 0.05$, Figure 3.5C).

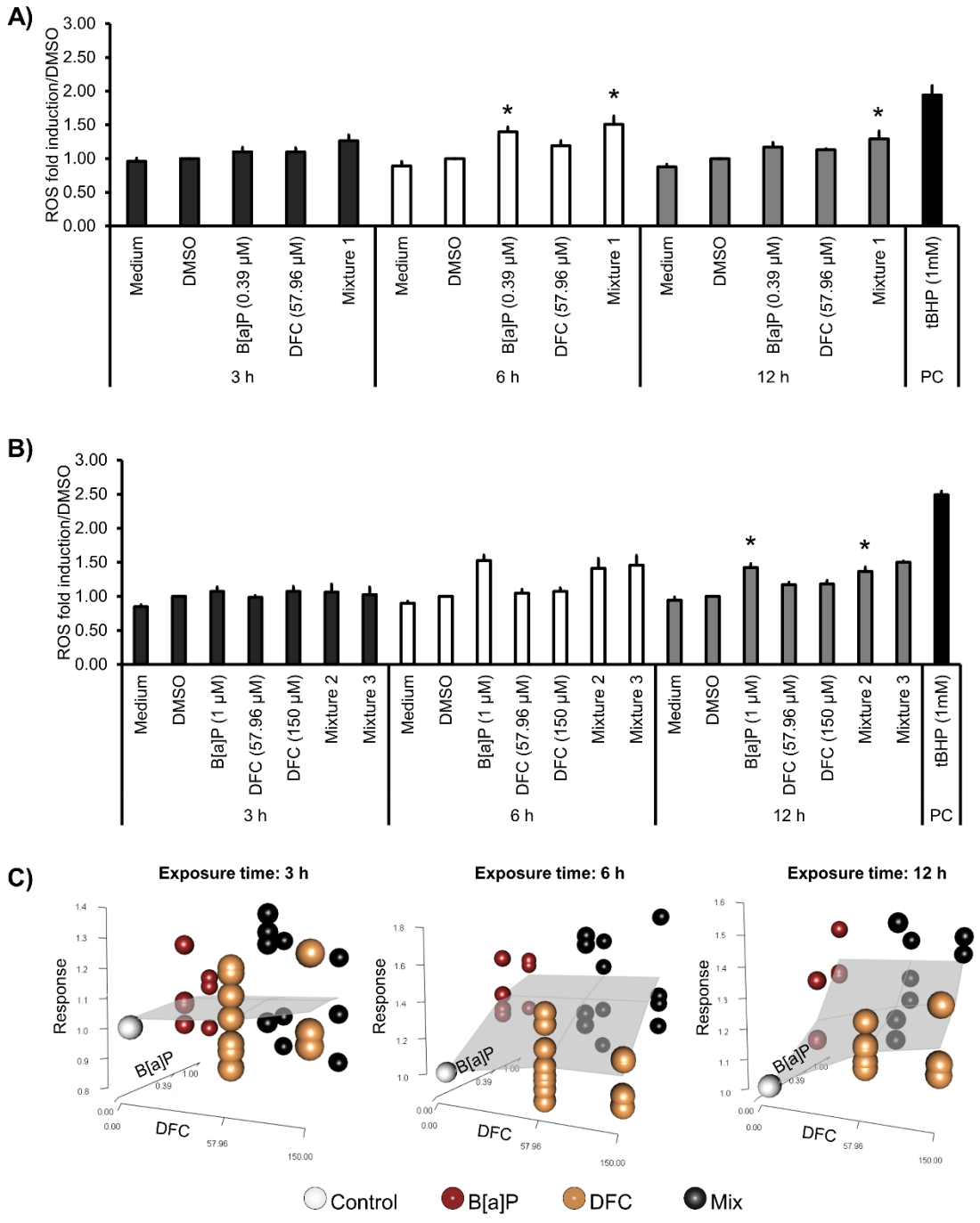

Figure 3.5. Assessment of intracellular Reactive Oxygen Species (ROS) measured using the DCFH-DA assay. **A)** HepG2 cells exposed to low concentrations (1/5 IC50) of individual contaminants and Mixture 1 (0.39 µM B[*a*]P + 57.96 µM DFC). **B)** Exposure to high concentrations (≈1/2 IC50) of individual contaminants, Mixture 2 (1 µM B[*a*]P + 57.96 µM DFC) and Mixture 3 (1 µM B[*a*]P + 150 µM DFC). Data in A and B shows mean ± SEM, n = 4, * p <

0.05, ** p < 0.01, ***p < 0.001 as compared with control (DMSO-only) through Dunn's test. **C)** Additive ROS effects in HepG2 exposed to DFC and B[*a*]P mixtures, demonstrated by the absence of blue or red surfaces in graphs (Generalized Loewe model followed by meanR/maxR statistic, effect considered significant if p < 0.05).

3.5 Discussion

Even though B[*a*]P, a well-known carcinogenic model PAH, and the NSAID diclofenac are expected to have different modes-of-action, the underlying metabolic networks may sufficiently overlap to trigger unforeseen interaction effects. Our findings revealed that HepG2 cells respond unpredictably when exposed to binary mixtures of B[*a*]P and DFC compared to exposure to the individual compounds, showing antagonistic effects on induction of cytotoxicity and genotoxicity and additivity for the induction of intracellular ROS. Although antagonistic effects were predominant in this study, the observed non-additive effects on the time and dose response for several biomarkers can be a significant confounding factor in mixtures evaluation. These results further corroborate the long-foreseen problem of contaminant mixtures in surface waters of industrialised regions compromising risk assessment for humans and wildlife (Cassee et al., 1998).

Our results showed that B[*a*]P was more than 100-fold more cytotoxic than DCF (IC_{50} of 1.95 µM vs. 290 µM). This agrees with previous studies performed in hepatocytes: Lim et al. (2015) and Ünlü Endirlik et al. (2023) reported an IC_{50} for B[*a*]P (48 h) of 1.5-2.0 µM in HepG2 cells and Ellepola et al. (2022) reported an IC_{50} for DCF in HepG2 cells (48 h) at > 250 µM. Relatively high IC_{50} for DCF (> 700 µM) were also observed in HepG2 cells at 24 h (Bort et al., 1999; Granitzny et al., 2017; Y. Wu et al., 2016). Notably, the cytotoxicity of combined exposure to B[*a*]P and DFC diverged from simple additive effects and yielded a significant reduction of cytotoxic effects compared to the exposure to individual compounds. Both compounds are metabolized into reactive metabolites by CYPs, and addition of specific CYP inhibitors can block the cytotoxic effects of B[*a*]P and DCF *in vitro*. Inhibition of CYP1A1 significantly reduces both cytotoxicity and genotoxicity of B[*a*]P in mammalian cells (Babich et al., 1988; Shimada & Guengerich, 2006). Similarly, co-exposure with an inhibitor against CYP2C significantly increased the viability of primary rat hepatocytes and immortalized human HC-04 hepatocytes exposed to DFC. Moreover, the decreased cell viability by DFC were associated with induction of oxidative stress responsive genes in these two models, of which the latter was significantly reduced by addition of CYP2C inhibitor (Lauer et al., 2009; M. S. Lim et al., 2006). In all, this highlights the importance of metabolism and induction of ROS in the cytotoxicity of these chemicals. The possible mechanisms for interactions between B[*a*]P and DCF resulting in antagonism of cytotoxicity is discussed below.

As expected, B[*a*]P was a more potent genotoxicant than DCF. Our findings are accordant with previous works reporting induction of DNA strand breaks in HepG2 cells exposed to B[*a*]P from 0.1 µM to 1 µM (Genies et al., 2013; H. Lim et al., 2015; Park et al., 2006; Stepnik et al., 2015). Our results were similarly in agreement for the induction of MN (Shah et al., 2016), which is an important biomarker

for chromosomal instability linked to genomic mutation and tumour development (Fenech et al., 2020; Terradas et al., 2010).The potency of B[*a*]P as genotoxicant and mutagen results mainly from the formation of reactive metabolites by CYPs and aldo-keto reductases (AKRs) resulting in B[*a*]P diol epoxides and quinones, respectively (Penning, 2014; Shimada & Fujii-Kuriyama, 2004). While the diol epoxides are responsible for forming bulky DNA adducts, the quinones can redox cycle resulting in ROS formation and oxidative DNA damage. Both routes of metabolism can cause DNA strand breaks that may persist and lead to formation of MN, either as result of replication stress due to replicative blockage by the bulky adduct, or due to extensive oxidative DNA damage due to ROS (Fischer et al., 2018; Penning, 2014). In contrast to B[*a*]P, DFC only induced significant genotoxicity in cells exposed to the highest dose (150 µM) and the shorter time of exposure (6 h). In accordance, several *in vivo* and *in vitro* studies on DFC genotoxicity report the absence of genotoxic effects, as summarized by Hartmann et al. (2021). The low level of genotoxicity may be linked to the suggested mechanism of carboxylic acid drugs like DFC involving the formation of reactive but short-lived acyl glucuronides during phase II metabolism that can damage DNA via glycation or glycoxidation resulting in DNA strand breaks (Grillo et al., 2003; Sallustio et al., 2006). It is not impossible that the induced genotoxicity of DFC observed at high concentrations could be linked to the formation of these metabolites at early stages of exposure. Similar to the effects on cytotoxicity, we observed significant antagonistic mixture effects on the induction of DNA strand breaks, and an indication for antagonism also for MN formation. For all endpoints, this was most clearly observed at higher concentrations and in contrast to the more commonly observed synergistic effects on viability and genotoxicity due to secondary toxicity mechanisms activated at elevated concentrations (Boobis et al., 2011). The reason for these antagonistic effects is unclear but most likely related to their metabolism, induction of oxidative stress, and pro-inflammatory signalling.

The two chemicals are preferentially metabolized by different CYPs. B[*a*]P is mainly metabolized into reactive metabolites by CYP1A1 or 1B1 (Shimada & Fujii-Kuriyama, 2004) whereas the most reactive DFC metabolites are produced by CYP2C9 and CYP3A4 (Bort et al., 1999; Leemann et al., 1993; Shen et al., 1999). However, interactions may occur either due to substrate overlap, enzyme inhibitions or induction of CYP gene expression. Indeed, even though DFC metabolization by CYP1 is not reported, B[*a*]P can be metabolized into 3-hydroxyl B[*a*]P by CYP2C and CYP3A families (Bauer et al., 1995; Yun et al., 1992). The few available data on CYP1A inhibition by DFC is contradicting with negative results in Rainbow trout liver microsomes but positive results in primary Rainbow trout hepatocytes (Burkina et al., 2018; Laville et al., 2004). However, DFC has been shown to moderately induce CYP1A gene expression in Japanese medaka, Rainbow trout and human hepatocytes (Hong et al., 2007; Lauer et al., 2009; Mehinto et al., 2010), potentially leading to increased bioactivation of B[*a*]P. In all, and even though these studies imply caution when associating mixture effects on metabolism to the observed antagonistic effects between B[*a*]P and DFC, this indicates that metabolic pathways for these compounds may superimpose, potentially leading to competition for active sites and or hindering/enhancing bioactivation/deactivation. However, the observed additive effects on ROS induction diverge from this model, possibly due the fact that both contaminants can contribute to the

induction of ROS. In fact, DFC hepatotoxicity is associated with induction of ROS during bioactivation leading to compromised mitochondrial integrity and induction of apoptosis (A. Inoue et al., 2004; K. Inoue et al., 2020). These issue need, nonetheless, further enhancement.

Antagonistic affects resulting from co-exposure to B[*a*]P and DCF may, in fact, be predominantly linked with the role of both contaminants in the inflammatory cascade and regulation of the NF-kβ pathway. The formation of genotoxic B[*a*]P metabolites either through CYP1 (B[*a*]P diol-epoxides) or through dihydrodiol dehydrogenase (B[*a*]P-quinones) increase intracellular ROS, therefore influencing the cell redox signalling chain (Cavalieri & Rogan, 1992; Penning et al., 1999). The formation of oxidative radicals (and indirectly even DNA damage) triggers the prostaglandin E2 (PGE2) – prostaglandin E receptor subtype 2 (EP2) signalling, which directly activates the NF-kβ pathway leading to increased secretion of pro-inflammatory cytokines (Aoki et al., 2017; Conner & Grisham, 1996; Liu et al., 2017; Ranjit et al., 2018). In the present study, increased genotoxicity and ROS in HepG2 cells exposed to B[*a*]P accords with a pro-inflammatory scenario, whereas DFC yielded limited effects. Indeed, DFC, a COX-inhibitor NSAID (see Schwartz et al., 2008), disrupts the prostaglandin chain by hindering the production of PGE2, therefore inhibiting the NF-kβ pathway and the downstream progression of the inflammatory cascade (Aoki et al., 2017; Fredriksson et al., 2011; Liu et al., 2017). It should be noted that the NF-kβ pathway is active in HepG2 cells and is sensitive to pro- and anti-inflammatory chemicals (Alnahdi et al., 2019; Heo et al., 2019).

It was not surprising that co-exposure increased genotoxicity in HepG2 cells, however the combined effect was smaller than the expected sum of individual effects, indicating a clear measure of antagonism between the two xenobiotics that was not extended to intracellular ROS induction, which yielded additive effects. Antagonistic affects can thus result from the inhibition of the NF-kβ pathway by DFC, therefore promoting pro-apoptotic and anti-proliferative effects (see review by Liu et al., 2017), leading to reduced survival of cells with high levels of B[a]P-induced DNA damage. Additionally, NF-kβ inhibition by DFC should also lower DNA repair (S. Kaur et al., 2013; Volcic et al., 2012), which may not only explain some modest genotoxicity in cells exposed to DFC but also prevent highly damaged cells exposed to mixture to recover and invest in survival. It must be emphasised that the Comet and MN assays determine DNA damage in individual living cells, thus it is most likely that the pro-apoptotic effect of DFC in mixtures contributed to eliminate cells with higher levels of DNA damage, hence the overall reduction in expected genotoxicity that, nonetheless, may not be indicative of fixed mutations.

3.6 Conclusions

The antagonistic effects of co-exposure to B[*a*]P and DFC in HepG2 cells tend to be consistent, regardless of individual dose. Indeed, dose-responsiveness, seems to be a significant factor for the induction of DNA damage and ROS, which reveals a more hindrance of molecular processes related to signalling and cell survival in co-exposure scenarios than could be anticipated. Mutually, DFC and B[*a*]P can be responsible for antagonist responses, even though molecular competition for cytochrome P450

can be involved, the most important factor may be the interference in ROS-mediated inflammatory process and subsequent unbalancing of cell survival and proliferation, contributing to eliminate the most damaged cells and favouring the survival of the most viable. Our findings demonstrate that exposure to mixed toxicants whose MOA and detoxification pathways may partly overlap can produce unexpected outcomes hindering risk assessment. This issue is of particular importance when dealing with ubiquitous carcinogens and the rising problem of long, occupational, exposure to pharmaceutical drugs and their metabolites.

4

TECHNICAL UPDATES TO THE COMET ASSAY *IN VIVO* FOR ASSESSING DNA DAMAGE IN ZEBRAFISH EMBRYOS FROM FRESH AND FROZEN CELL SUSPENSIONS

This chapter has been published in the following paper:

Martins, C. & Costa, P. M. (2020). Technical Updates to the Comet Assay *In Vivo* for Assessing DNA Damage in Zebrafish Embryos from Fresh and Frozen Cell Suspensions. Zebrafish, 00(00), 1–9. https://doi.org/10.1089/zeb.2020.1857

4.1 Abstract

The Single-Cell Gel Electrophoresis, simply known as the Comet assay, is a sensitive and quick technique used to quantitate DNA damage, widely used to assess the effects of genotoxicants and mutagens in animal cells. Still, performing the assay on peripheral or cultured cells is far more expeditious and cost effective than solid tissue, especially from small biological model like the zebrafish embryo. The current work describes and validates a highly cost-effective protocol of the updated Comet assay designed for zebrafish embryos. Compared with the few previous applications of the Comet assay on this biological model, the present method successfully simplifies the process of cell harvesting and resuspending, producing a much higher yield of viable nucleoids with reduced basal DNA damage, even from a small number of embryos, and compatible with scoring with safe fluorescent dyes. Additionally, the protocol can be just as easily performed on freshly harvested cells of cells frozen in dimethyl sulfoxide (DMSO)-containing physiological buffer, without a significant increase of DNA damage, which is another highly relevant update, especially for researchers handling high numbers of samples.

4.2 Introduction

The single-Cell Gel Electrophoresis “Comet” assay has been widely used for the evaluation of DNA strand breakage, for being a practical and sensitive technique, with proven value in diagnostics in several areas of research, with emphasis on genotoxicology. The Comet assay can be done under either neutral or alkaline conditions, the former evidencing double- and single-strand breaks, whereas the latter converts breaks and alkali-labile sites to single-strand due to the more complete denaturation of DNA, therefore increasing sensitivity (Collins et al., 2008). The protocol for the alkaline Comet assay was first developed by (Singh et al., 1988) for individual mammal lymphocytes and is, by far, the most widespread method. The versatility of the method protocol has persistently been leading to several successful modifications aiming at different kinds of biological material, from whole blood of marine fish (Costa et al., 2008) to solid tissue of various less conventional model organisms for genotoxicologists, such as bivalves or even plants (Costa, Milhinhos, et al., 2012; Jackson et al., 2013; Lee et al., 2000; Sasaki et al., 1997; Wilson et al., 1998).

The application of the Comet assay in cultured and peripheral cells have been much preferred, much owing to convenience, to solid tissue. Indeed, the latter commonly involve laborious and far less cost-effective protocols, with emphasis on the process of harvesting cells or nude nuclei. For such reasons, even the application of the Comet assay in such important toxicological models such as the zebrafish embryo (McGrath & Li, 2008; Scholz et al., 2008) has been stalling. In fact, even though protocols for the alkaline Comet assay in zebrafish embryos have been proposed in the past (Kosmehl et al., 2006; Ku-Centurión et al., 2016; Sun et al., 2004), systematic applications are essentially missing from literature, in large part owing to difficulties in harvesting sufficient viable cells from such small

organisms, reducing accessory DNA damage and handling potentially large batches of samples and experimental replicates.

Even though the many adaptations of alkaline Comet assay protocol include the same invariable steps, namely, agarose embedding, lysis, DNA unwinding, electrophoresis, and scoring, there have been many variations to adapt the method for a multiplicity of biological media, with focus on cell harvesting, lysis, and even scoring. The latter aspect, in particular, follows the attempt to ditch the use of Ethidium bromide due to its mutagenicity. Whereas some of the modifications are as simple as adding an extra layer of low melting point agarose (LMPA) to the Comet slides (Kosmehl et al., 2006; Sasaki et al., 1997), in most cases these changes imply extended preparation times and expenditures.

The preparation of cell suspensions from solid tissue, in particular, has been given particular attention, receiving additional steps such as the digestion of the extracellular matrix using collagenase and filtration of cell suspensions (Belpaeme et al., 1998; Wilson et al., 1998) such as in previous attempts to apply the Comet assay to zebrafish embryos (Kosmehl et al., 2006, 2008), resulting in lagging and laborious procedures that may compromise workflow and cell viability. It must at this stage be stressed that the Comet assay requires live cells, as cell death greatly increases DNA fragmentation, for example, caused by internucleosomal cleavage during apoptosis. Notwithstanding, faster protocols tend to increase the viability of cells. On the other hand, as these modifications greatly increase the expenditures of the method, especially in toxicological assays, which tend to consider a large number of samples, cryopreservation of cell suspensions and tissue with adequate freezing buffers has already been proposed as a convenient alternative (Al-Salmani et al., 2011; Belpaeme et al., 1998; Hu et al., 2002; Jackson et al., 2013), although in need of conditions possibly not accessible for all laboratories.

In accord with all the points stressed above, the present work aimed at developing and testing a modified, simple and quick Comet assay protocol, from cell harvesting to slide dying, adapted to whole-body zebrafish embryos especially, but not exclusively, directed to toxicologists and genotoxicologists.

4.3 Methods

4.3.1 Zebrafish embryos

Danio rerio eggs were collected from several adult couples (AB incross) at early morning hours. The adults were maintained in a six-rack recirculating system from Tecniplast supplied by a reverse osmosis unit under controlled conditions: conductivity of 800 lS, pH 7.0, at 28ºC on a 14-h light/10-h dark cycle and fed daily with ZEBRAFEED and Artemia (ZM Systems). Viable eggs were dechorionated mechanically using tweezers (Henn & Braunbeck, 2011), after 2 h post-fertilization (hpf). The dechorionated eggs, with 4 hpf, were randomly divided by glass Petri dishes (two sets of animals with four replicas each). In each dish were placed twenty embryos and 15 mL of embryo medium (distilled water supplemented with NaCl, KCl, CaCl22H2O, and MgSO47H2O). The embryos were conditioned

in an incubator at 28ºC during 48 h. Two-day-old (48 h) embryos were elected to ascertain the employment of still small-sized individuals without the needed of large pools of animals. It represents an intermediate term between fertilization and the standard 96-h embryos used for acute testing. The medium was changed after 24 h (90 %) to minimize medium stagnation and oxygen depletion.

4.3.2 Cell harvesting

The alkaline Comet assay protocol was modified from the procedures previously set for solid molluscan tissue (M. Martins et al., 2013; Raimundo et al., 2010). At the end of the 48 h, the 20 zebrafish embryos of each replica were placed in 1.5-mL tubes with 2 different buffers (1 individual per 10 µL of buffer): the first animal set of 4 replicas (n = 4) was placed in 200 µL of cold (4ºC) Dulbecco's phosphate-buffered saline (PBS); and the second set (n = 4) in 200 µL of 10 % v/v dimethyl sulfoxide (DMSO) in PBS, pH 7.4. Embryos were gently minced with a scissor followed by soft pipetting.

The process was followed by a low-power centrifugation at 250 g, at 4ºC, for 2 min, to promote deposition of tissue and cellular debris. The supernatant was collected to new tubes to prevent the damage to live cells by nucleases and other enzymes in the pellet. At this point, the total volume of the supernatant was divided into three ≈ 60–80 µL aliquots: (1) fresh sample; (2) sample to be stored at -80ºC for 1 week, and (3) sample to be stored at -80ºC for 2 weeks. Cellular viability was assessed with the Trypan Blue exclusion method. Both fresh and frozen samples from the two animal sets, suspended in PBS and PBS+DMSO, were processed under the same conditions and in accordance with the Comet assay protocol detailed below.

4.3.3 Comet assay

The first step was the embedding of 20 µL of the supernatant in 180 µL of molten (37ºC - 40ºC) 1 % m/v LMPA prepared in PBS. Two 80-µL drops of LMPA with the incorporated samples were placed in slides precoated with 1.2 % m/v high melting point agarose (HMPA) prepared in TAE buffer. The precoated slides were allowed to dry for at least 48 h. The slide was immediately covered with a coverslip to permit even spread of molten agarose. No additional layer of LMPA was added, resulting in a faster and equally effective protocol. Two slides were prepared per sample.

After solidification for 15 min at 4ºC, the coverslips were gently removed, and the slides placed in cold lysis buffer (2.64 % m/v NaCl, 3.72 % m/v EDTA, and 5 mM Tris, pH 10), supplemented with 10 % v/v DMSO and 1 % v/v Triton X-100 just before use. Lysis was done during 1 h at 4ºC, in the dark. Following, slides were transferred to cold electrophoresis buffer (1 mM EDTA and 300 mM NaOH, pH 13) during 40 min to allow unwinding of DNA and enhance the expression of alkali-labile sites. Electrophoresis was run for 30 min at 25 V, in cold (4ºC) and dark conditions, using a CSLCOM20 Comet Assay Tank (Cleaver Scientific). Dark and cold (4ºC) were enforced to prevent accessory DNA degradation and gel detachment. Finally, slides were neutralized in cold 0.1 M Tris-HCL buffer (pH 7.5)

lasting 15 min and dehydrated in cold methanol for 15 min for archiving, if not stained and analysed immediately.

After neutralization, or rehydration of archived slides in cold ultrapure water (30 min), the preparations were stained with GreenSafe Premium (Nzytech), diluted to 1:500 in ultrapure water, to our knowledge the first application of this safe DNA fluorophore in the Comet protocol. Each slide received two 40 µL drops of the diluted dye and were mounted with a coverslip. The dye was allowed to bind to DNA for 10 min in the dark, at room temperature, before visualization of nucleoids in a DM 2500 LED model microscope equipped with an EL6000 model ultraviolet source and a MC 190 HD camera (all from Leica Microsystems). Micrographs of Comet fields were obtained in 8-bit grayscale mode at 400 × magnification, to increase sensitivity.

Scoring of micrographs was done using the software CometScore 1.6 (TriTek). Between 50 and 150 nucleoids per treatment, replicates were measured in accordance with three main metrics: % DNA in Tail; Tail Moment, and Olive Moment (Azqueta & Collins, 2013; Collins, 2004; Kumaravel et al., 2009; Olive & Banáth, 2006). Results are expressed as mean scores among replicates ± standard deviation (n = 4). Additionally, the nucleoids were also distributed in five classes of % DNA in Tail, based on data retrieved from software, for statistical analyses, and quality assessment, since the unimodal distribution of DNA damage is indicative of negligible interference of cell death. The detailed protocol is summarized in Table 4.1.

Table 4.1. Summary of the Comet Assay Protocol Proposed for DNA Strand Breakage Analysis in Whole-Body Zebrafish Embryos

Step	Buffer / Procedure	Duration
Cells suspension	Prepare with Dulbecco's PBS and 10% of DMSO in Dulbecco's PBS, pH 7.4, 4˚C	
Separation of cells	Centrifuge at 250 × g, 4˚C	2 min
Sample incorporation	20-µL supernatant + 180-µL LMPA (37-40˚C)	
Lamina preparation	Two 80-µL drops of incorporated sample in each slide pre-covered with dried HMPA. Cover quickly with coverslip	
Agarose solidification	Reserve slides in the dark at 4˚C	15 min
Cell lysis	Supplemented lysis buffer, pH 10, 4˚C, dark	1 h
Incubation	Electrophoresis solution, pH 13, 4˚C, dark	40 min
Electrophoresis	Electrophoresis solution, pH 13, 25V, 4˚C, dark	30 min
Neutralization	Neutralization buffer, pH 7.5, 4˚C, dark	15 min
Dehydration (optional)	Methanol, 4˚C	15 min
Re-hydration (optional)	Ultrapure water, 4˚C	30 min
Staining	Two 40-µL drops of GreenSafe Premium (Nzytech, Portugal), or similar safe intercalating agent, dark	10 min
Strand-breakage analysis	Employment of relative metrics	

DMSO, dimethyl sulfoxide; HMPA, high melting point agarose; LMPA, low melting point agarose; PBS, phosphate-buffered saline.

4.3.4 Statistical analysis

Statistical analysis was computed with the software R The data for % DNA in Tail complied with the three assumptions to parametric test (independency, normality of the data, and homogeneity of variances), the latter of which being checked by Shapiro–Wilk's and Levene's tests, respectively. Taking storage condition as independent variable, % DNA in Tail data were then analyzed by F test-based analysis of variance (ANOVA) followed by Tukey's Honest Significant Difference Test for post hoc comparisons. On the other hand, Tail Moment, Olive Moment, and frequency of cells per % DNA in Tail class failed to meet the assumptions for parametric tests and were analyzed by the nonparametric Kruskal–Wallis ANOVA-by-Ranks H, followed by Dunn's test for multiple comparisons. The significance level a was set at 0.05 for all analyses.

4.4 Results and Discussion

The methods yielded good-quality nucleoids, regardless of experimental condition (Figure 4.1), with 90.8 % – 4.20 % and 92.2 % – 0.68 % of cell viability in fresh samples for suspension in PBS+DMSO and PBS, respectively. Nucleoids revealed uniform distribution on the slides in all of the

six experimental conditions (see Figure 4.2A for further details). Freshly collected cell suspensions yielded % DNA in Tail <30 % (Figure 4.2B), which is accordant with previous applications on solid tissue (M. Martins et al., 2013). These samples showed a high percentage of cells in the first class of % DNA in Tail (0 % – 20 %), with only <2 % of cells pertaining to the class of highest DNA damage (80 % – 100 % DNA in tail), as shown in Figure 4.2C. In general, the distribution of nucleoids per class was clearly unimodal, which indicates reduced interference from apoptotic or necrotic cells. Altogether, the findings from these fresh samples reflect what is expected from normal cells and are indicative of successful adaptation and functionality of the comet assay protocol in zebrafish embryos.

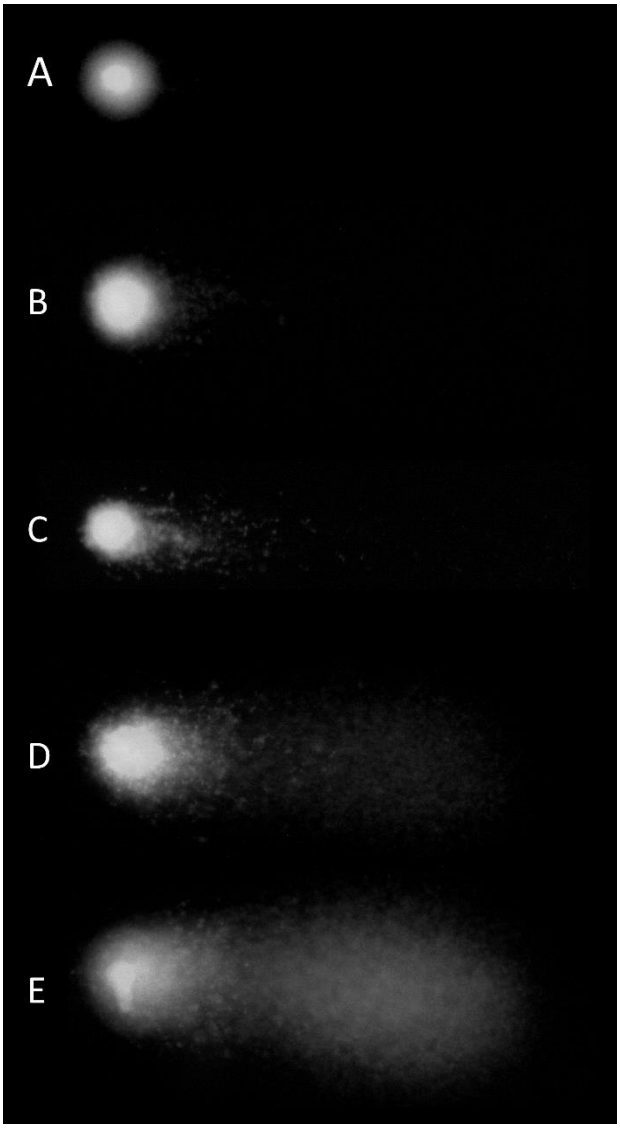

Figure 4.1. Representative nucleoids of Comet classes based on % DNA in Tail in zebrafish embryos, obtained using software CometScore 1.6. **A)** 0% – 20% where the DNA strand breakage is most reduced. **B)** 20% – 40%.

C) 40% – 60%. **D)** 60% – 80%. **E)** 80% – 100%, where massive DNA strand breakage is evident (“hedgehog” comet).

Contrary to many previous studies that applied the Comet assay on solid tissue (Belpaeme et al., 1998; Kosmehl et al., 2006; Sun et al., 2004; Wilson et al., 1998), the current protocol did not apply or seemingly require additional digestion steps for the removal of the extracellular matrix for cell harvesting, as well as filtration of cell suspensions, since the proportion of viable cells was sufficient to obtain sound outcomes. This allied to the importance of obtaining a unimodal distribution of nucleoids per % DNA in Tail class, as recorded for every experimental condition (Figure 4.2C).

In similarity to recent works with other biological models for which extraction of peripheral cells is complicated, such as bivalve molluscs (M. Martins et al., 2013), it has been demonstrated that gentle mincing with pliers followed by gentle pipetting is sufficient to extract sufficient cells from zebrafish embryos. Comparatively, the most recent attempt to apply the Comet assay in zebrafish embryos relied only on soft pipetting for cell harvesting, producing a much more reduced number of nucleoids and required pooling the various experimental replicates per treatment, plus the removal of higher tail intensity nucleoids from analysis to avoid skewing toward hedgehog comets (Ku-Centurión et al., 2016). On the contrary, the present work yielded hundreds of analysis-ready nucleoids per slide, from both fresh DMSO-frozen cell suspensions, enabling true biological replication from a small number of embryos. In addition, filtration can be replaced by low-power centrifugation to provide a clean cell suspension (supernatant), which greatly simplifies the process and permits, comparatively, reduced accessory DNA damage.

The % DNA in Tail metric, although suggested by some authors (Kumaravel & Jha, 2006) as a good measure of DNA damage, is less used than other metrics, as Tail Moment or Olive Moment, in Comet assay protocols involving solid tissue. Similar results were obtained with the moment metrics (Figure 4.2D, E), which shows intercompatibility of these acknowledged measurements.

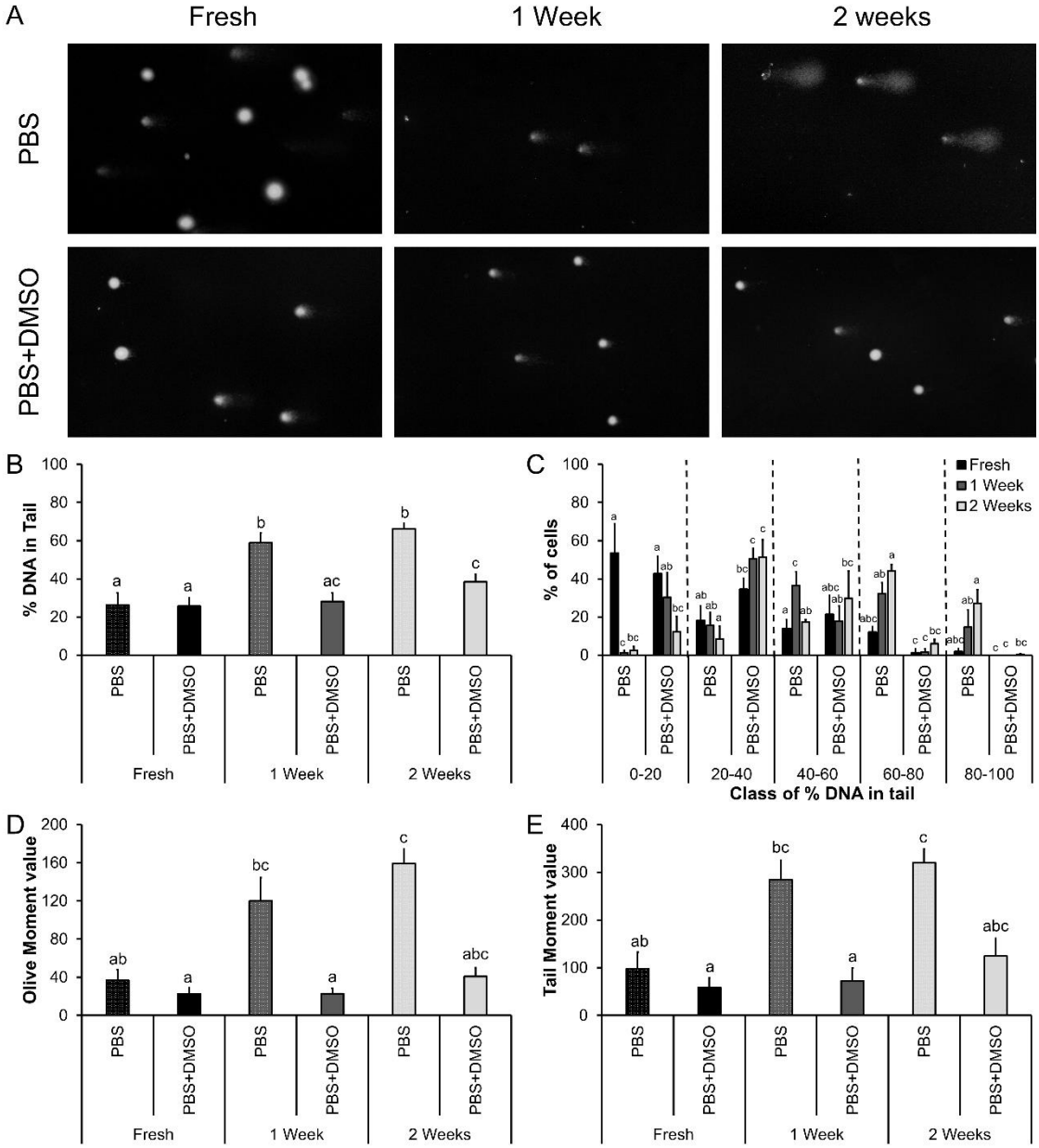

Figure 4.2. Results from scoring metrics obtained from whole zebrafish embryo cells, fresh or frozen at -80ºC for 1 or 2 weeks, the latter in either for PBS or PBS complemented with 10% m/v DMSO (PBS+DMSO). **A)** Representative Comet fields from each tested condition, 200 × magnification. **B)** % DNA in Tail. The letters indicate significant differences ($p < 0.05$, ANOVA + Tukey's HSD) between cells resuspended in PBS or PBS+DMSO fresh or frozen for 1 and 2 weeks. **C)** Relative frequency of nucleoids per % DNA in Tail class (given in percentage of cells per class), comparing buffers and storage (fresh vs. frozen) conditions. Letters indicate the significant differences ($p < 0.05$, Kruskal–Wallis ANOVA-by-Ranks H + Dunn's test) within the same % DNA in Tail class. **D)** Olive Moment metric scores. **E)** Tail Moment scoring. Different letters are indicative of significant differences ($p < 0.05$, Kruskal–Wallis ANOVA-by-Ranks H + Dunn's test) between samples preserved in PBS or PBS+DMSO, fresh and frozen for 1 and 2 weeks. All the results are expressed as mean (n = 4), with error bars representing the SD.

ANOVA, analysis of variance; DMSO, dimethyl sulfoxide; HSD, honest significant difference; PBS, phosphate buffered saline; SD, standard deviation.

Performing the Comet assay on frozen cells, immediately after thawing is essential for genotoxicity assessment, as it allows assessing DNA status upon harvesting, rather than allowing the cells to recover or cell death to occur. Indeed, DNA repair in eukaryotes is very efficient and can be very fast (Boiteux & Jinks-Robertson, 2013), which would then render unreliable the Comet assay if cells are not analysed immediately. However, the samples frozen in simple PBS (i.e., without DMSO) increased significantly to 33 % DNA in Tail and 40 % after 1 and 2 weeks of storage at -80ºC, respectively, when compared with fresh samples (Figure 4.2B). Caution is thus required when performing the Comet assay with whole-embryo cells harvested in uncomplemented PBS. In its turn, the sample storage at -80ºC in PBS containing 10 % DMSO only increased to 2 % DNA in Tail and 13 % after 1 and 2 weeks, respectively, which was not a statistically significant difference to fresh samples (Figure 4.2B). It is thus inferable that DMSO helped improve cell stabilization and provided protection against DNA strand breakage during the freezing, in accordance with previous works (Hu et al., 2002).

Most importantly, only minute and not significant differences in DNA damage were recorded between samples frozen for 1 and 2 weeks, regardless of buffer. In fact, the % DNA in Tail from the first to the second week of storage, was overall translated into mere mean increases of 7 % and 10 % in samples stored in PBS and PBS + DMSO, respectively. It must be noted, though, that samples frozen in uncomplemented PBS, particularly after 2 weeks, showed a high percentage of cells in the two last classes (60 % – 80 % and 80 % – 100 %) revealing a clear interference of freezing in cell stability and the increase of basal DNA damage, yielding reduced sensitivity of the assay or compromising its soundness altogether. Complementarily, the total yield of nucleoids per Comet field was hitherto reduced up to 20 %. However, in samples archived in PBS + DMSO, the number of nucleoids was not only seemingly unchanged as the frequency of nucleoids pertaining to the highest % DNA in Tail classes was not significant (Figure 4.2C).

The same trend was observed regarding Olive and Tail Moment metrics (Figure 4.2D, E). It must be noticed, however, that moment metrics tend to be more conservative than the % DNA in Tail (Costa, Milhinhos, et al., 2012). As an example, PBS-treated cells yielded a significant increase of moment metrics only after 2 weeks of freezing relatively to freshly harvested cells. In any case, all metrics yielded the same pattern of responses and are likely interchangeable. It must also be noted that the Comet assay is, by essence, comparative and highly reliant on the constancy of protocol conditions among samples. It is thus likely that moderate increases in basal DNA damage do not compromise the assessment, as seen in the present work and in previous studies (Belpaeme et al., 1998; Hu et al., 2002; Jackson et al., 2013; Riesco et al., 2012). It must be emphasized, nonetheless, that the method analysis DNA damage in cells from all organs of the embryo, which likely have differential abilities to respond to genotoxic challenge, from bioactivation of xenobiotics to DNA repair. As such, the application of the Comet assay in zebrafish embryos must be interpreted as a whole-individual measure of DNA

lesions in which highly sensitive cells are diluted with those less prone to suffer from genotoxic challenge.

Finally, it must also be noted that the GreenSafe Premium dye used in this study (in a dilution of 1:500), a first-time application in the Comet assay protocol, produced excellent results, yielding high sensitivity to small DNA fragments (single-stranded, inclusively, as they occur in alkali media) and a good signal-to-noise ratio. Being described as innocuous, this dye can be an effective substitute of Ethidium Bromide in the staining of Comets nucleoids. We also noted that the green fluorescence kept the intensity during the potentially long process of collecting micrographs for scoring under the microscope, given that the dye is allowed to intercalate for 10 min at room temperature, in the dark.

4.5 Conclusions

Besides the acknowledged sensitivity to alkali-expressed DNA lesions, one of the major advantages of the Comet assay is its expediency. In this study, it has been shown that the key to improve the Comet assay with respect to cell yield and integrity is simplification. Although the protocol introduced in this study one of the most important biological models, the zebrafish embryo, although mostly neglected by toxicologists outside the scope of acute toxicity testing, has better grounds to prove its value for genotoxicologists. The modifications resulted in a simple and effective Comet assay, with emphasis on cell harvesting and retrieval of viable cells. Deep-freezing cells in DMSO-containing physiological buffer for posterior analyses is possible, considering the minor increase of the basal level of DNA damage, with reduced differences between 1 and 2 weeks of storage. This finding shows that freezing can assist the hefty logistics of the Comet assay protocol, which otherwise requires immediate processing of cells.

5

A Mechanistic Study on the Interaction Effects Between Legacy and Pollutants of Emerging Concern: A Case Study with B[*a*]P and Diclofenac

5.1 Abstract

Exposure to mixtures of environmental toxicants can have serious and unforeseen acute or chronic consequences to humans and wildlife due to intricate toxicodynamics and molecular mechanisms of interaction. We explored possible interaction mechanisms and downstream effects between legacy and emerging pollutants through binary mixtures of benzo[*a*]pyrene (B[*a*]P) and the non-steroid inflammatory drug diclofenac (DFC) in them zebrafish embryo model. The results disclosed higher mortality of DFC, albeit a potential antagonistic interaction with B[*a*]P. Antagonism was also noticed on genotoxicity plus some molecular pathways that upon co-exposure ceased to be affected, namely those associated to RNA degradation, cell proliferation, apoptosis and cell-cycle control. Most importantly, the combination of next-generation transcriptomics and toxicopathology suggested two potential molecular mode-of-action linked to adverse outcome (AOs) from DFC and B[*a*]P co-exposure. The formation of pericardial cavity and yolk sac oedemas in embryos can be an AO resulting from exposure to DFC isolated or combined. This AO follows key events (KE) involving cell cycle arrest and apoptosis via p53 and MAPK pathways. In this case, the molecular initiating event (MIE) is not genotoxicity but rather inflammation triggered by oxidative stress. Another AO is impaired ocular function by action of DFC and B[*a*]P combined. This AO is caused by ocular degeneration as KE, caused by the underexpression of critical genes such as prph2b and pdca, whose mutations are known to cause blindness in humans. As an AO, blindness was also caused by exposure to DFC, but no prospective molecular pathway could hitherto be found. To summarise, the results from toxicologic and genotoxic biomarkers indicated a predominance of antagonistic effects in mixtures, but the integration of mechanism with toxicopathology suggested interactions between DFC and B[*a*]P when the toxicants are present in environmentally-relevant concentrations that may lead to chronic impacts on the control of key aspects such as inflammation and cell cycle control.

5.2 Introduction

The growing human society allied to new-technology development has been releasing large amounts of diverse urban, industrial and agricultural toxicants to the environment with critical repercussions for wildlife and human health. Consequently, contamination of the environment is seldom attributed to single substances but rather by a complex mixture of legacy and emerging toxicants whose combined effects are not immediately predictable even if each substance is present in relatively low concentrations. This means that legacy (‘traditional’) contaminants like carcinogenic polycyclic aromatic compounds (PAHs) , which are some of the most ubiquitous pollutants worldwide (Dat and Chang, 2017), can co-occur with pollutants of emerging concern like pharmaceuticals and derivatives, whose concentrations in surface waters are increasing in large part due to inefficient removal by wastewater treatment plants, the growing diversity and use of medical and veterinarian drugs and also the growing human population, either in industrialised or developing regions (Arman et al., 2021; Verlicchi et al.,

2012; Zhou et al., 2019). Despite the paramount effort to produce regulatory guidelines and safety levels of individual contaminants such as the EU Environmental Quality Standards (EQSs), it remains challenging to derive risk for complex mixtures, as pollutants invariably occur, especially in cases of prolonged occupational exposure to low levels of individual compounds. Understanding the toxicological mechanism underlying the 'cocktail effect' of pollutant mixtures can thus be pivotal to understand hazard and risk. Indeed, understanding the toxicological mode-of-action is increasingly acknowledged as key to predict adverse effects and established effective measure to safeguard humans and environmental health (e.g., Cassee et al., 1998; Silins and Högberg, 2011; Vitorino and Costa, 2022).

Toxicant interaction effects can be complex and categorized as additive, antagonistic or synergistic, depending on their relationship with the mode-of-action of individual chemicals (Hernández et al., 2017). New omics approaches, which can deliver multiple endpoints in single runs, if anchored by toxicopathological traits, can be used to associate adverse outcomes (AOs) with key events (KEs) and upstream molecular initiating evens (MIEs) triggered by exposure to mixtures of pollutants, i.e., the risk factor (Madeira & Costa, 2021; C. Martins et al., 2019). Consequently, AOPs can be derived even in cases where reduced levels of individual toxicants would render difficult to establish causal networks between toxicants and effects, with emphasis on chronic disease such as cancer (e.g., Hayes et al., 2019; Vitorino and costa, 2023).

The toxicant interaction addressed in this work combined the PAH benzo[*a*]pyrene (B[*a*]P), a well-known model carcinogen, as representative of legacy toxicants and the pharmaceutical drug diclofenac (DFC), one of the most widely used non-steroid anti-inflammatory drugs (NSAIDs) worldwide. Zebrafish (*Danio rerio*) was the selected biological model given its versatility as a vertebrate model in aquatic systems and due the genetic similarity to humans offers toxicological answers in biomedical field, stablishing the bridge between contamination and consequences in human health and wildlife (Ablain & Zon, 2013; Howe et al., 2013; Modarresi Chahardehi et al., 2020). Both contaminants had the concern of EU, with DFC listed as a 'pollutant of emerging concern' and B[*a*]P included on the European list of priority pollutants (Directive 2008/105/EC) where its EQS was established at 0.05 µg/L. This value was reviewed to low values in Directive 2013/39/EU (1.70E-04 µg/L). Like most PAHs, its main sources are the combustion of fossil fuels, biomass, cigarette smoke or industrial waste (Boström et al., 2002). This compound is described as genotoxic and mutagenic largely associated to the formation of bulky DNA adducts (mainly though binding of diol-epoxide metabolite to guanine, which are difficult to remove by DNA repair mechanisms and therefore increase the odds of fixation of mutations (Costa, 2022). The toxicant can promote proliferation of neoplastic cells via mutation in protooncogenes like *ras* and inactivate tumour suppressors genes such as p53, to which is added the activation of pro-inflammatory cytokines following bioactivation by cytochrome P4501A/B during phase I (Denissenko et al., 1996; Moorthy et al., 2015; Nebert et al., 2000; Ross & Nesnow, 1999; Shimada, 2006). In turn, DFC, which is broadly used in human and livestock, is listed on water EQS list under Directive 2013/39/EU (0.1µg/L) and in 2015 was integrated on the 1st Watch List for substances in surface waters by Commission Implementing Decision (EU) 2015/495 for a continuous monitoring. The important decision of monitoring

the levels of DFC in surface waters was mainly due its risk to wildlife (Oaks et al., 2004). For instance, the study of Diniz et al. (2015) reports significant increase of oxidative stress in *D. rerio* exposed to DFC and its by-products comparatively to other two NSAIDs. Additionally, a review of Parolini (2020) identified DFC as one of the most toxic NSAIDs to freshwater invertebrates, as *Daphnia magna*, in acute and chronic exposure. This drug, which controls inflammation by inhibiting cyclooxygenase family members COX-1 and COX-2 disrupting the prostaglandin pathway (Gan 2010), is chiefly biotransformed via glucuronidation, nonetheless, it can also be metabolized by cytochrome P450 members (CYP), especially CYP2C and CYP3A, the latter of which is responsible for generating the most reactive metabolites (Leemann et al., 1993). Indeed, several DFC derivatives were linked to mechanisms of hepatotoxicity associated to oxidative stress and mitochondrial dysfunction (Inoue et al. 2004). Interesting, the influence of DFC in inflammation process may be linked to anti-cancer proprieties by interfering with angiogenesis and cytokine signalling, although the full pathway has not yet been described (Arisan et al., 2018; Duval et al., 2019; J. Kaur & Sanyal, 2011).

Besides the environmental relevance of B[*a*]P and DFC, they may share metabolization via CYPs and can hypothetically interact through pathways related to inflammation and cell proliferation neoplasia processes. However, interaction mechanisms and downstream effects remain, at the current stage, conjectural. The present work aimed primarily at investigating a possible mechanistic network for the interaction between these two model toxicants in vertebrates, at environmentally-relevant concentrations, that can be used to derive an AOP apt for risk assessment strategies.

5.3 Methods

5.3.1 Chemicals

Benzo[*a*]pyrene (CAS: 50-32-8) was acquired from TCI EUROPE (Zwijndrecht, Belgium) and diclofenac sodium (CAS: 15307-79-6) from Acros organics (Geel, Belgium). Stock solutions of B[*a*]P (0.4 and 4 mM) and DFC (3.1 and 31.4 mM) were prepared in dimethyl sulfoxide (DMSO) and sterilised ultrapure water, respectively.

5.3.2 Test organisms

Zebrafish embryos were obtained from wildtype *Danio rerio* (AB incross). Adults were maintained in a six-rack recirculating system (Tecniplast, Buguggiate, Italy) equipped with a reverse osmosis unit, under controlled conditions, namely conductivity set at 800 µS, pH 7.0, at 28 °C on a 14 h light/10 h dark cycle. Animals were fed daily with ZEBRAFEED and *Artemia* (ZM Systems, Winchester, UK). Eggs were collected from multiple couples at early morning hours. After 2 h post-fertilisation (hpf), viable eggs were dechorionated mechanically using tweezers as in Henn and Braunbeck (2011). Before exposure, dechorionated eggs (4 hpf), were randomly divided by glass Petri dishes with embryo medium (distilled water supplemented with NaCl, KCl, $CaCl_2$ and $MgSO_4$). During all assays, embryos were

placed in an incubator at 28˚C and the medium was changed with fresh spiked (contaminated), control (vehicles only) or blank (medium only) every 24 h (90%) to minimise stagnation and oxygen depletion.

5.3.3 Acute toxicity

Acute toxicity bioassays were conducted to assess mortality plus developmental and toxicopathological alterations in zebrafish exposed to toxicants and their combination between sphere stage (4 hpf) to early larva (96 hpf). The experiments followed standard guidelines for zebrafish embryo toxicity tests (OECD, 2013), with some adaptations. In brief, the assays were performed with dechorionated eggs that were placed in glass Petri dishes with 10 mL of total volume (medium + vehicle + drug) for 96 h. Each experimental condition held ten embryos (n = 10) and was performed in duplicate. The entire experimental set-up was replicated four times. Spiking guaranteed < 0.1% of DMSO, as recommended by Maes et al. (2012). Individual toxicant concentrations and corresponding binary mixtures were tested, plus control (i.e., spiking with DMSO + H_2O) and blank (see Table A1.1 in Appendix to Chapter 5).

The selection of test concentrations was based on realistic thresholds reported in available literature (Table S1). The two lowest B[*a*]P and DFC concentrations were defined in accordance with the EU EQSs (Directive 2008/105/EC and Directive 2013/39/EU) and highest concentrations recorded in the environment in EU surface water (Gonzalez-Rey & Bebianno, 2014; Heberer, 2002; Manoli & Samara, 1999). High concentrations of B[*a*]P tested in acute assays, were primarily based on the 8.9 µg/L (4.00E-2 µM) threshold indicated as able to disturb the development the central nervous system in the zebrafish, with consequent neurodegenerative syndromes in adults (Gao et al., 2017). The highest concentration of B[*a*]P was set at 89 µg/L (0.4 µM), corresponding to 1/10 no observed adverse effect level (NOAEL), as defined by (Knecht et al., (2017), which falls within the range of maximum concentration of total PAHs (0.0598 µg/L - 127.7 µg/L) measured in highly impacted rivers (X. Wu et al., 2021). In turn, the highest concentrations of DFC were set using as reference the no observed effect concentration (NOEC) for zebrafish embryos (Ferrari et al., 2003), more specifically 1/5 NOEC 800 µg/L (2.5 µM), 1/10 NOEC 400 µg/L (1.3 µM) and 1/50 NOEC 80 µg/L (0.3 µM). The highest DFC concentration (800 µg/L) follows the highest recorded level of DFC (836 µg/L) found in riverine waters immediately adjacent to a wastewater effluent inlet (Ashfaq et al., (2017).

Mortality, developmental malformations (lack of somite formation, lack of detachment of the tail-bud from the yolk sac, lack of heartbeat and abnormal pigmentation) and toxicopathological traits (e.g., spinal deformations, oedemas and small eye/blindness) , were scored in embryos at 24 h, 48 h, 72 h and 96 h of exposure. The scores of developmental malformations and toxicopathological traits were combined into the single variable “pathological alterations”, for statistical purposes and in the presentation of results. Micrographs of surviving embryos after 96 h of exposure were obtained using a DM 2500 LED model microscope equipped with a MC 190 HD camera (Leica Microsystems, Wetzlar, Germany).

5.3.4 Histopathology

After 96 h of exposure, surviving embryos were fixed in 2.5% v/v glutaraldehyde in 0.1 M Sorensen's phosphate-buffered saline (PBS) pH 7.4, for c.a. 2 h. Samples were then washed in PBS (3 × 10 min) and post–fixed in 1% m/v osmium tetroxide in PBS, in the dark, o/n (all at room temperature). After washing in ultrapure water (3 × 10 min), samples were dehydrated in a progressive series of acetone (30-100%) and embedded in Epon resin (Sigma-Aldrich, St. Louis, MO, USA), following Luft's mixture (Sigma-Aldrich, St. Louis, MO, USA). Intermediate infiltration was done with Epon : Polypropylene oxide (2:1), followed by Epon : Polypropylene oxide (1:1) and Epon : Polypropylene oxide (2:1), 30 min each. Sections (2 µm) were produced using a RM 2125 RTS rotary microtome (Leica Biosystems) equipped with a tungsten carbide blade and stained with Toluidine Blue. Histopathological analyses were made using the microscope referenced above.

5.3.5 Genotoxicity assessment

Genotoxicity (DNA strand damage) was determined using the alkaline Comet assay (Singh et al., 1988) from a series of 48-h bioassays conducted with non-lethal concentrations, i.e., B[*a*]P 0.4 µM (89 µg/L) and DFC 2.5 µM (800 µg/L), under the same conditions described above. The Comet assay in whole-embryos was performed as described by Martins and Costa (2020). At the end of the 48 h, ten embryos from each of the three replicates were placed in 100 µL cold (4˚C) Dulbecco's PBS, pH 7.4 (one embryo per 10 µL). Embryos were then gently minced with scissor and soft-pipetting to resuspend cells. The process was followed by low-speed centrifuging at 250 × g at 4˚C (2 min) to remove cellular debris. The fresh supernatant was promptly collected to new tubes to prevent the damage to live cells by nucleases and other enzymes in the pellet. Following, 20 µL of the supernatant was embedded in 180 µL of molten (37 – 40ºC) 1% m/v low melting point agarose (LMPA) prepared in PBS. Two 80-µL drops were placed on dried slides pre-coated with 1.2% m/v high melting point agarose (HMPA) prepared in TAE buffer. The slide was immediately covered with a coverslip to permit even spread of molten agarose. Two slides were prepared per sample. After solidification for 15 min at 4˚C, the coverslips were gently removed and the slides immersed for 1 h in cold lysis buffer (2.64% m/v NaCl, 3.72% m/v EDTA and 5 mM Tris, pH 10), supplemented with 10% v/v DMSO and 1% v/v Triton-X100, in the dark. Slides were afterwards transferred to cold electrophoresis buffer (1 mM EDTA and 300 mM NaOH, pH 13) during 40 min to allow unwinding of DNA and enhance the expression of alkali-labile sites. Electrophoresis was run for 30 min at 25 V, in cold (4˚C) and dark conditions, using a CSL-COM20 Comet Assay Tank (Cleaver Scientific), followed by neutralization in cold 0.1 M Tris-HCL buffer (pH 7.5), during 15 min. Slides were then dehydrated in cold methanol for 15 min for archiving. Archived slides were hydrated in cold ultrapure water (30 min) and stained with GreenSafe Premium (Nzytech, Lisbon, Portugal) during 10 min in the dark, at room temperature. Nucleoid observation and microphotography (8-bit greyscale mode at 400 × magnification) were done in the microscope referenced above using an EL6000 UV source (also from Leica Microsystems). Scoring was done using

CometScore™ 1.6 (TriTek Corp, Sumerduck, VA, USA). The mean % DNA in tail (from ≈100 nucleoids per slide) was employed as metric.

5.3.6 Statistics

Statistical analyses were computed in R (Ihaka and Gentleman, 1996). The significance level α was set at 0.05 for all analyses. Data were checked for normality and homogeneity of variances using Shapiro-Wilk's and Levene's Tests, respectively. Parametric data were as analysed using *F* test-based ANOVA followed by Tukey's Honest Significant Difference (HSD) test for post-hoc comparisons. Following invalidation of at least one assumption, non-parametric statistics were employed, namely the Kruskal-Wallis ANOVA-by-Ranks H, followed by Dunn's test for multiple comparations. The non-parametric Mann-Whitney U-test for between-sample pair comparisons and Spearman's correlation R statistics were also employed.

Analysis of variance (ANOVA) of discrete (count) data (mortality and alteration scores) was done using generalised linear models (GLM) through a Poisson regression with a log link taking B[*a*]P and DFC concentrations plus exposure time as categorial predictors (Faraway, 2010; McCullagh & Nelder, 1989). Statistical inference on explanatory variables was achieved though deviance analysis by sequential variable addition and χ^2 tests. The model was validated by randomness and normality of standardised Pearson residuals plus Cook's *h* statistic for biasing. Principal component analysis (PCA) based on Pearson's *r* was employed as reduction statistics to ascertain the interlink over time between drug concentrations, mortality and alterations data.

5.3.7 RNA-Seq

Total RNA was extracted from embryos subjected to a third series of bioassays performed under the same conditions and chemical concentrations (B[*a*]P 0.4 µM, DFC 2.5 µM and mixture) as those for genotoxicity assessment. After the 48-h exposure, the embryos were collected, pooled per experimental replicate, infiltrated with RNA Later (Qiagen, Hilden, Germany) and stored at -80˚C until further processing. Extraction was done using the RNeasy Protect Mini Kit (Qiagen, Hilden, Germany) following manufacturer instructions. Contaminant DNA was digested in-column with DNase I (RNase-free DNase set from Qiagen) during 15 min at room temperature. Elution was done in 25 µL RNase-free water. Quality and concentration were first analysed using a Nanodrop 1000 spectrophotometer (Thermo Fisher Scientific, Wilmington, DE, USA). Samples were stored at -80 °C until further analyses. The RNA integrity number (RIN) for each sample was determined in an Agilent 2100 Bioanalyzer (Agilent Technologies, Santa Clara, CA, USA), with all samples being found within suitable parameters, i.e., intact or partially degraded samples with RIN ≥ 7, input of ≥ 1 µg total RNA, free of contaminating DNA (Schroeder et al., 2006). Library preparation was done using Kapa Stranded mRNA Library Preparation Kit and the generated RNA fragments were sequenced in an Illumina HiSeq 4000 platform, using 150bp paired-end sequencing reads at the scale of 40-80 M reads.

Transcriptomes were mapped against the reference transcriptome of *D. rerio* (Ensembl v99, GRCz11) using Kallisto (Bray et al., 2016), followed by gene expression analyses in R. Expression analyses was conducted using packages edgeR (McCarthy et al., 2012; Robinson et al., 2009) and limma (Ritchie et al., 2015). Gene ontology (GO) and gene enrichment (GE) analyses through GO term and KEGG (Kyoto Encyclopaedia of Genes and Genomes) were also performed with R, using packages Biomart (Durinck et al., 2009), org.Dr.eg.db (Carlson, 2019) and multiGSEA (Canzler & Hackermüller, 2020). Pathway analysis was performed through the FGSEA (fast gene set enrichment analysis) test applied to all genes whereas GO statistics were based on the Fisher test on DEGs in each treatment. In GO/GE analysis functional enrichments with an adjusted p-value (FDR) < 0.05 were considered significant. Additionally, STRING 11.0 (Szklarczyk et al., 2019) provided a simulation of protein-protein interaction networks (medium confidence was set at 0.4). Command line and R transcript for the code of all transcriptomic analyses can be found in A2 Appendix to Chapter 5.

5.3.8 Validation of RNA-Seq data

Experimental validation was achieved by quantitative reverse-transcription PCR (qRT-PCR). The cDNAs were produced from total RNA using the NZY First-Strand cDNA Synthesis Kit (NZYTech) as per manufacturer instructions. Specific primers for *cyp1a1*, *pou3f1*, *hsp70l* and the housekeeping genes *EF1a* and *18S* were designed with MEGA-X software (Kumar et al., 2018) and Primer-BLAST tool (see Table 5.1). After resolving PCR products by gel electrophoresis following amplification using a Thermocycler Biometra 96 apparatus (Analytik Jena, Jena, Germany) and confirmation by Sanger sequencing, expression was quantified using a Corbett Rotor-Gene 6000 thermal cycler (Qiagen, Hilden, Germany) with the NZY qPCR Green Master Mix (NZYTech). The qPCR programme (50 cycles) was set as: denaturation (94 ºC, 45s), annealing (52 ºC, 35s) and extension (72 ºC, 30s). Primer melting analysis was also conducted to verify specificity of hybridisation. Expression was quantified by the $\Delta\Delta$Ct method (Livak & Schmittgen, 2001). The results were statistically validated by applying the *F* test-based ANOVA followed by Tukey's Honest Significant Difference (HSD) test for post-hoc comparisons between control and treatments gene expression, for *cyp1a* and *hsp70l* genes.

Table 5.1. Zebrafish primer design for RT-PCR.

Gene ID	Accession	Primer	Primer sequence (5'–3')	Amplicon size (bp)	Tm (ºC)
cyp1a1	NM_131879	Forward	CCTGGGCGGTTGTCTATCTA	184	63.65
		Reverse	TGAGGAATGGTGAAGGGAAG		62.23
pou3f1	NM_131161.1	Forward	ATCCAACCATGGAGGACGTT	195	64.46
		Reverse	TGTCAGCGAACTCTTCCCAA		64.29
hsp70l	NM_001113589.1	Forward	GACCTCTTCAGGGGAACACTA	168	63.76
		Reverse	AATGCTCTTGTTCAGTTCTCTG		61.41
EF1a (housekeeping)	L23807.1	Forward	TTTGCTGTGCGTGACATGAG	151	64.00
		Reverse	CAACCTTTGGAACGGTGTGA		63.91
18S (housekeeping)	KY486501.1	Forward	GTAGTTGGATCTCGGGAGTG	200	62.39
		Reverse	CCATTATTCCTAGCTGCGGTA		61.95

5.4 Results

5.4.1 Acute toxicity and genotoxicity of DFC, B[*a*]P and their mixtures

Embryos exposed to the highest DFC concentration (2.5 µM), isolated or combined, registered the highest mortality rate with an increase of 4-fold between 48 h and 96 h of exposure. Also, the number of embryos with pathological alterations, *in vivo*, triple after 48h of exposure to these treatments. Histopathological alterations at 96 hpf were mostly found in zebrafish embryos exposed to the highest DFC concentrations, both individually (1.3 µM and 2.5 µM) and combined with B[*a*]P, with the embryos having a normal development in the remaining treatments (Figure 5.1A). Between histopathological alterations were observed an evident formation of massive oedemas (Figure 5.1B) in the pericardial cavity and yolk-sac. The heart, well visible in the pericardial cavity, was found to have a normal anatomy (Figure 5.1B - *Inset*), despite decreased heartbeat and blood circulation noted *in vivo* during the acute assay. In addition, whereas control embryos presented normal tails and all the properly-formed thirty somite pairs along of the notochord (Figure 5.1C), embryos exposed to treatments where the highest DFC concentrations (1.3 µM and 2.5 µM) were involved showed a complete absence of somite formation and muscle degeneration (Figure 5.1D) accompanied by severe spinal curvature (scoliosis). The same affected embryos also notice, ocular degeneration or developmental delay (compare Figures 5.1E, F). In general, embryo eyes presented normal development at 24 h regardless of experimental conditions, which should indicate that most ocular alterations may be toxicopathological rather that developmental. Loss of retinal melanin pigmentation was noticeable 48 h onwards. At 96 h the retina and lens exhibited severe degeneration (Figure 5.1F).

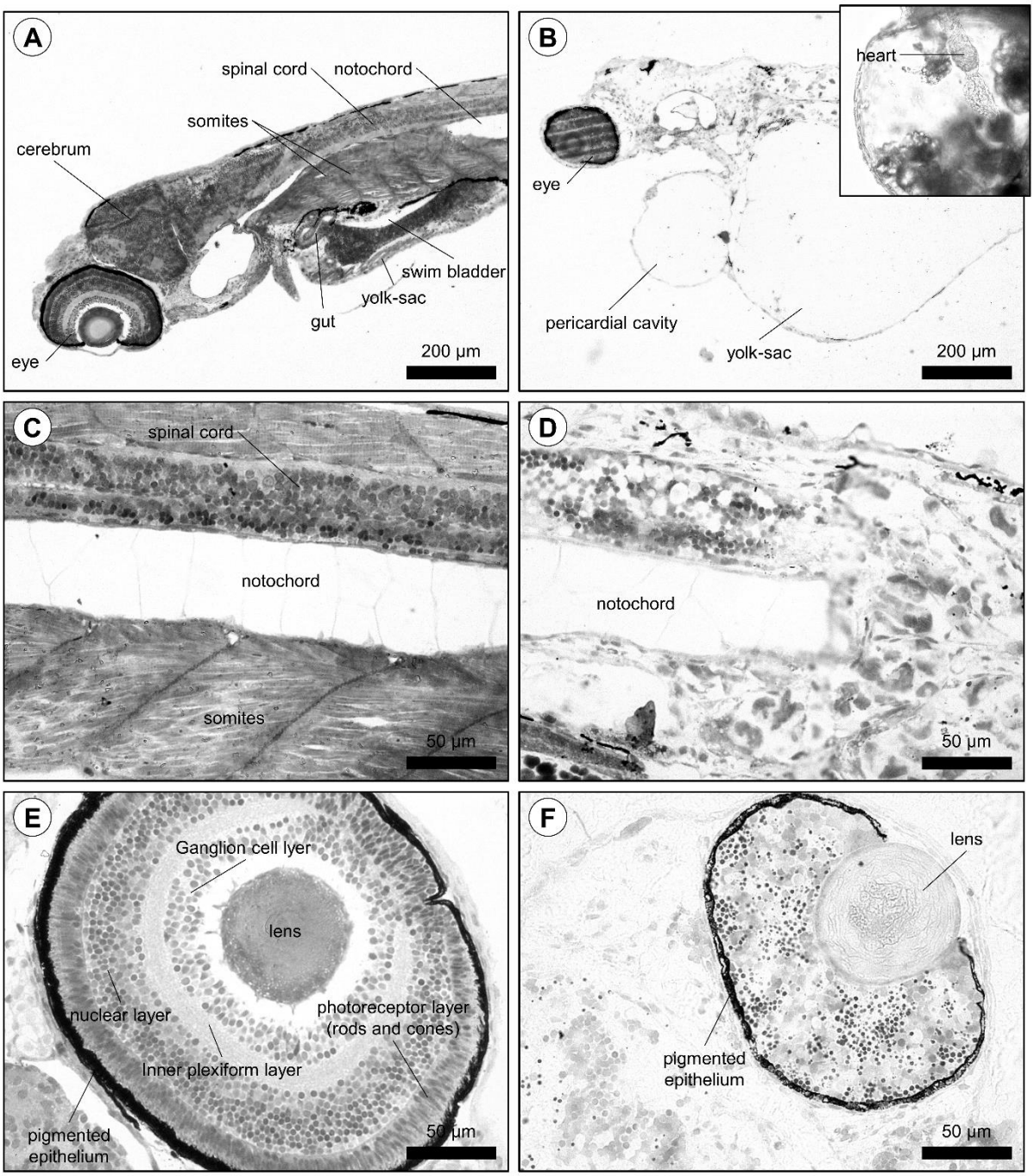

Figure 5.1. Examples of histopathologic alterations in zebrafish embryos (96 hpf). **A)** Normal microanatomy observed in a control embryo. **B)** Embryo subjected to the mixture of highest concentrations of B[*a*]P and DFC (0.4 µM B[*a*]P + 2.5 µM DFC), showing pericardial cavity and yolk-sac oedemas. *Inset*: Detail heart amidst an oedema (embryo exposed to highest concentration of DFC (2.5 µM). **C)** Detail of the normal somites and notochord from a control embryo. **D)** Absence of somite formation in embryos exposed to mixture (0.4 µM B[*a*]P + 2.5 µM DFC) E) Normal eye in a control embryo. **F)** Eye of an embryo exposed to 2.5 µM DFC presenting serious malformations. Staining: Toluidine blue (epoxy resin sections).

Mortality (Table 5.2) and pathological alterations (Table 5.3) GLM analyses (see Figures A3.1 and A3.2 in Appendix to Chapter 5, for validation details) revealed that DFC concentration and exposure

time were comparatively, the variables with highest influence in both endpoints. These facts are confirmed by DFC concentration positive link with mortality and alterations rates after 48h (PCA - Figure 5.2A,B). The global correlation (conjoining all treatments and exposure times) between mortality and alteration rates was weak (Spearman's R = 0.243, p = 1.1E-15), which is further highlighted by PCA analyses (Figure 5.2C, D).

Table 5.2. Generalised linear model (GLM) for mortality. The significance of each predictor (explanatory variable) was assessed by deviance analysis and ANOVA chi-square test.

Coefficients	Deviance	Resid. Df	Resid. Dev	Pr(>Chi)	
Exposure time (h)	14.86	1182	2341.3	0.0001161	***
[B[a]P]	15.37	1181	2325.9	8.83E-05	***
[DFC]	389.39	1180	1936.5	< 2.20E-16	***
Exposure time (h) : [B[a]P]	0.2	1179	1936.3	0.6559287	
Exposure time (h) : [DFC]	550.9	1178	1385.5	< 2.20E-16	***
[B[a]P] : [DFC]	0.71	1177	1384.8	0.4006577	
Exposure time (h) : [B[a]P] : [DFC]	2.49	1176	1382.3	0.1149048	

Signif. codes: (***) 0.001; (**) 0.01; (*) 0.05; (.) 0.1

Table 5.3. Generalised linear model (GLM) for pathological alterations. The significance of each predictor (explanatory variable) was assessed by deviance analysis and ANOVA chi-square test.

Coefficients	Deviance	Resid. Df	Resid. Dev	Pr(>Chi)	
Exposure time (h)	16.50	1182	2137.9	4.86E-05	***
[B[a]P]	3.44	1181	2134.4	0.0637507	.
[DFC]	1063.30	1180	1071.2	< 2.20E-16	***
Exposure time (h) : [B[a]P]	0.09	1179	1071.1	0.7634414	
Exposure time (h) : [DFC]	11.63	1178	1059.4	0.0006496	***
[B[a]P] : [DFC]	0.61	1177	1058.8	0.4334506	
Exposure time (h) : [B[a]P] : [DFC]	0.45	1176	1058.4	0.5006677	

Significance levels: (***) < 0.001; (**) < 0.01; (*) < 0.05; (.) < 0.1

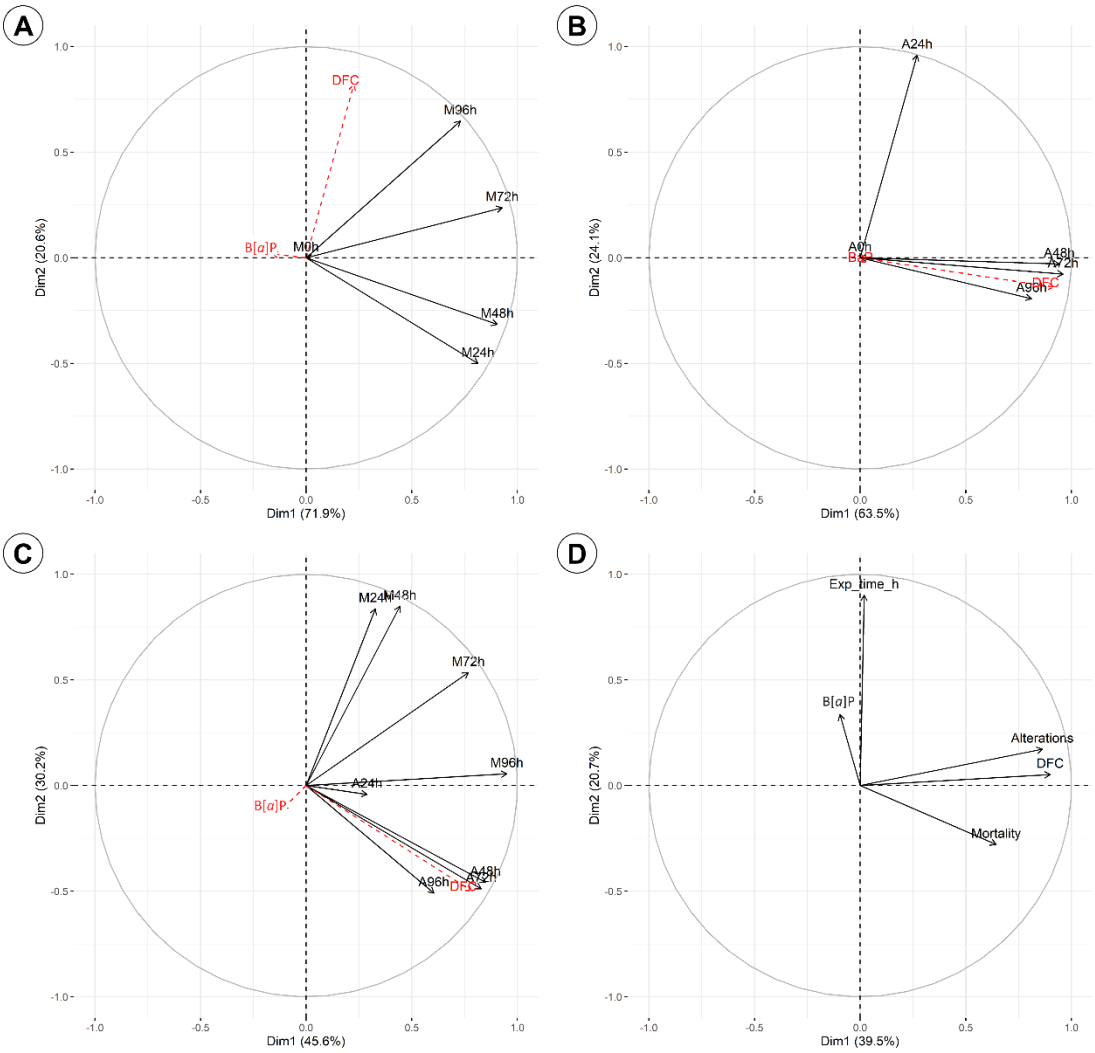

Figure 5.2. Principal component analysis (PCA) plots highlighting the relationships between mortality and pathological alterations (toxicopathological or developmental) rates in zebrafish embryos exposed to B[*a*]P, DFC or their mixtures. **A)** Mortality at different time points (M24h to M96h) contrasted against B[*a*]P and DFC concentrations as supplementary variables. **B)** Same as previous panel for combined embryo pathological alterations at the different time points (A24h to A96h). **C)** PCA combining mortality and pathological alterations. **D)** Analysis combining all variables (mortality and pathological alteration rates; B[*a*]P and DFC concentrations and exposure time).

Genotoxicity was found to be significantly influenced by B[*a*]P concentration, in contrast to the acute toxicity endpoints (mortality and pathological alteration rates), which were mostly influenced by DFC concentration. The induction of DNA damage was highest (Tukey's HSD test, $p < 0.05$) in zebrafish embryos subjected to mixture (DFC 2.5 µM + B[*a*]P 0.4 µM) and B[*a*]P-only (0.4 µM) treatments when compared to control (Figure 5.3A). Altogether, B[*a*]P-only treatment yielded the highest average frequency (Dunn's test, $p < 0.05$) of nucleoids in classes 3 (40-60%) and 4 (60-80%) of % DNA in tail comparatively to control (Figure 5.3B).

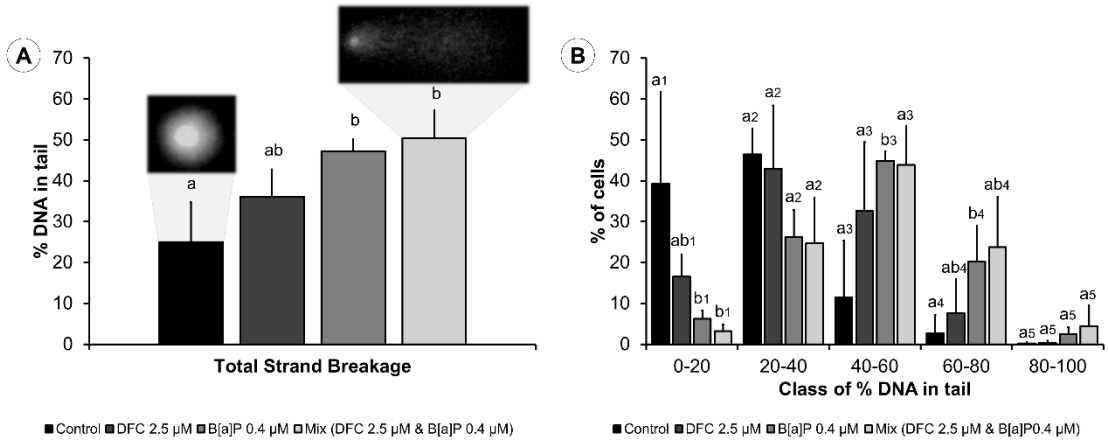

Figure 5.3. Damage to DNA strand (measured through the Comet assay) in zebrafish embryos exposed to B[*a*]P, DFC or their mixture. **A)** Percentage of DNA in Tail. The letters indicate significant differences between treatments (Tukey's HSD test, $p < 0.05$). **B)** Relative frequency of nucleoids per % DNA in Tail class (given in percentage of cells per class). Letters indicate significant differences within the same % DNA in Tail class (Dunn's test, $p < 0.05$).

5.4.2 Inferring toxicological mode-of-action of DFC and B[*a*]P mixtures from gene expression profiles

Transcriptomic analysis by RNA-Seq unveiled differences between global gene expression profiles in embryos exposed to either chemical or their combination. The raw data can be found at Gene Expression Omnibus (GEO) under the accession number GSE232729. Validation of RNA-Seq results was provided by qPCR analyses of *cyp1a* (Figure 5.4A) and *hsp70l* genes (Figure 5.4B). In total, exposure to DFC (2.5 µM), B[*a*]P (0.4 µM) plus their mixture (B[*a*]P 0.4 µM + DFC 2.5 µM), yielded about 1,300 differentially-expressed genes (DEGs), relatively to control. Around 300 genes were differentially expressed in the mixture treatment only (Figure 5.4C). Individual B[*a*]P (0.4 µM) treatment unveil the lowest number of DEGs (30 genes), relatively to control, which only 9 genes were exclusive of this treatment.

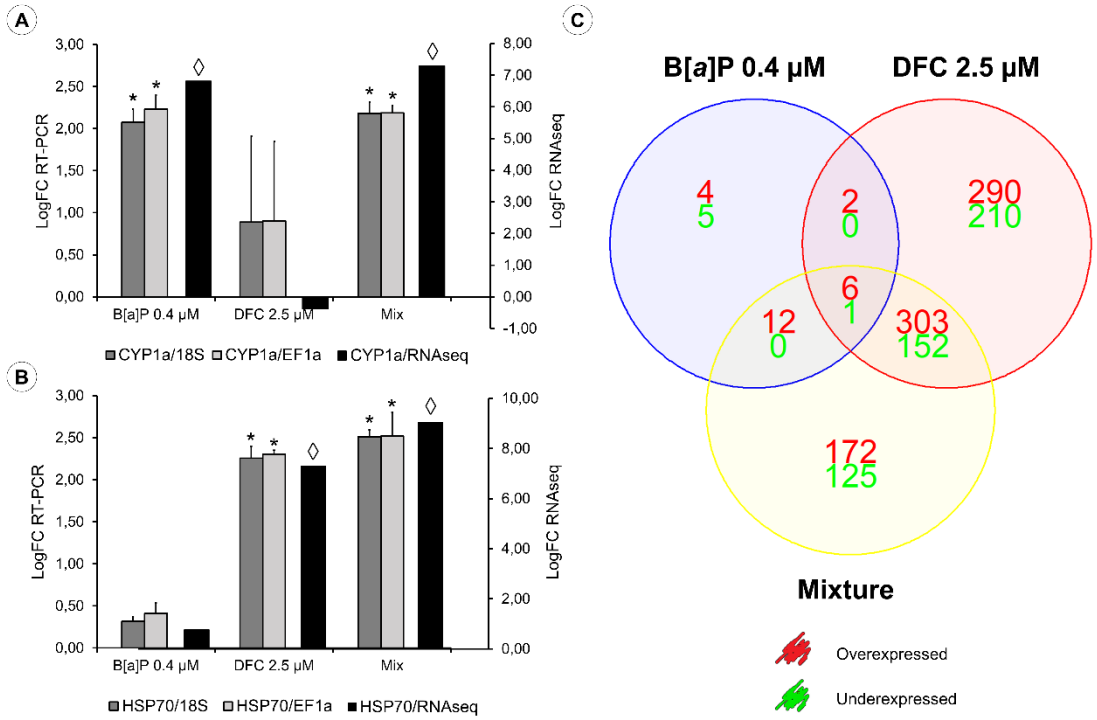

Figure 5.4. Transcriptomics (RNA-Seq) analyses in zebrafish embryos exposed to B[*a*]P, DFC or their mixture. Validation of data was provided by comparing CYP1a **(A)** and HSP70 **(B)** gene expression between treatments by qPCR and RNA-Seq counts. The symbols indicate significant differences between treatments (Tukey's HSD test, $p < 0.05$). **C)** Venn diagram illustrating the distribution of overexpressed and underexpressed genes relative to control (RNA-Seq).

The top five over- or underexpressed genes were generally distinct between treatments (Table A3.1 in Appendix to Chapter 5), with few exceptions, such as the as *pou3f1* gene (involved in brain development and embryonic morphogenesis), which was found to be overexpressed in all three treatments. Mixture and DFC-only treatments also share two underexpressed genes, *cuedc1a* and *ddb2*, linked to DNA repair and protein ubiquitination. Embryos exposure to the mixture also revealed top overexpressed genes connected to stress response (*hsp70* and *hsp70l*) and RNA binding (*rpl21*) plus underexpressed genes associated to transcription (*znf143b*), translation (*eif2b2*) and glutathione metabolism (*gstr*). In turn, the top five overexpressed genes in DFC treatment were connected to immune and heat shock responses (*ier5* and *ptmaa*), transcription and translation initiation (*btf3* and *rpl32*). The remaining DFC top five underexpressed genes, not shared with mixture treatment, were involved in neuronal development (*mbpa*) and lipid metabolism (*apoa4b.2*). On the other hand, embryos exposed to B[*a*]P showed a more exclusive top five genes, where the overexpressed genes were related to regulation of RNA polymerase II (*med6*), DNA damage response (*ints7*), muscle differentiation (*myog*) and xenobiotic metabolization evidencing the cytochrome P450 1A (*cyp1a*). To these are added underexpressed genes involved in heme biosynthesis (*alad*), glycogen metabolism regulation (*ppp1r3ca*), cellular response against oxidative stress (*rpe*) plus cell proliferation (*CU207215.1*, activator of AKT family member).

Pathway analyses based on GO terms and GE through the KEGG database of zebrafish embryos yielded more significant number of significantly altered canonical pathways and GO terms in embryos exposed to the mixture (B[*a*]P 0.4 µM + DFC 2.5 µM), and DFC-only (2.5 µM), comparatively with control. Nonetheless, three significant enriched KEGG pathways (FDR-adjusted $p < 0.05$) were noticed in embryos subjected to the B[*a*]P (0.4 µM) treatment (Table 5.4), although without any significant GO term associated (Figure 5.5A). These pathways were mainly connected with xenobiotic biotransformation, including metabolization by CYPs (Figure 5.5A). Contrarily embryos exposed to DFC yielded thirteen significantly-enriched KEGG pathways (FDR-adjusted $p < 0.05$). These were mostly related to RNA degradation, apoptosis, cell proliferation and cell cycle regulation, of which we highlight the MAPK, p53, VEGF and FoxO signalling pathways (Table 5.4). The GO/GE analysis indicated that overexpressed DEGs promote significant Biological Processes linked to immune response, DNA replication and transcription (orange bars in Figure 5.5B). In turn, the underexpressed DEGs indicated suppression of ion transport and the 'chemical synaptic transmission' (blue bars in Figure 5.5B).

The mixture treatment revealed alterations in nine significantly-enriched KEGG pathways that essentially amalgamate the pathways indicated above concerning B[*a*]P- and DFC-only treatments. However, several molecular pathways linked to RNA degradation, cell proliferation, apoptosis and cell-cycle control lost their relative enrichment significance when compared to single-exposure treatments (Table 5.4). In general, most GO terms retrieved from the mixture treatment were common to the DFC-only experiment and essentially associated to regulation of transcription by RNA polymerase II and ion transport (Figure 5.5C). Interestingly, 'lens development in camera-type eye' and 'visual perception' were GO terms within Biological Processes exclusively affected by exposure to the mixture treatment. In addition, under Molecular Function, 'protein heterodimerization activity' potentiation and suppression of 'structural constituent of eye lens' were also exclusive to the mixture treatment (see Figure 5.5D for further details).

From overexpressed (Figure 5.6A) and underexpressed (Figure 5.6B) DEGs exclusive to the mixture treatment, two sets of networks based on protein-protein interactions were provided by STRING. Several processes can be hypothetically potentiated (Figure 5.6A, left) such as xenobiotic response with Cyp26a1 being representative of phase I of biotransformation and Ugt1a1 involved in glucuronidation of phase II. The Cyp26a1 protein is also linked with cholesterol metabolism along with Sqlea and Ch25h. Likewise, Cyp26a1, partakes in the set of proteins connected to embryonic development together with Cdx4, Cad, Sst2, Atoh1a, Wnt11. Cellular antioxidant defence, DNA repair and ubiquitination were processes that can be potentiated by exposure to the mixed toxicants according to predicted protein-protein interactions. The mitogen-activated protein kinase (MAPK) pathway (Figure 5.6A, right) was seemingly upheld by co-exposure. Here we highlight a subdivision in two groups, the first associated to apoptosis and the second to cell proliferation, with Mapk12b protein activating the Sgk2b kinase and the heat shock protein Hsp90aa1.2. The up-regulation of Jun (protein coding gene of Jun proto-oncogene) and Mapk12b (enable MAP kinase activity), can be associated to the regulation of apoptosis and cell proliferation. There is a probable duality in regulation of apoptosis and cell proliferation

associated to Jun and Mapk12b protein interaction, which works both ways and can be related with the metabolic stimulus at a given time. In turn, underexpressed DEGs (Figure 5.6B) suggest potential down-regulation of proteins and subsequent hindering or suppression of eye development (Hsf4, Lgsn) and phototransduction (Pdca, Prph2b), nervous system development and function regulation, cell survival and proliferation (KCNAB3, Ntrk2a, Fgf6b), plus transmembrane transport (Rhbg, Slc22a7b, C6, Gc). It is noteworthy that C6 and Gc genes can also be linked to immune response.

Table 5.4. KEGG pathways associated to total genes from B[*a*]P and DFC treatments and mixture of both contaminants.

	KEGG Pathway	**Padj (FDR)**	**NES**	**Size**
Total B[*a*]P	Tryptophan metabolism	4.56E-03	2.323818	52
	Steroid hormone biosynthesis	5.26E-03	2.372632	69
	Metabolism of xenobiotics by cytochrome P450	2.59E-02	2.513161	61
Total DFC	MAPK signalling pathway	3.39E-05	1.927695	397
	Cytokine-cytokine receptor interaction	9.59E-03	1.808769	184
	Apoptosis	1.16E-02	1.90573	172
	Herpes simplex virus 1 infection	1.16E-02	1.776337	165
	NOD-like receptor signalling pathway	1.75E-02	1.859701	134
	Adipocytokine signalling pathway	1.86E-02	1.909814	82
	RNA degradation	2.93E-02	1.769055	16
	Toll-like receptor signalling pathway	2.93E-02	1.770994	99
	p53 signalling pathway	2.93E-02	1.946374	85
	VEGF signalling pathway	3.05E-02	1.816578	79
	FoxO signalling pathway	3.78E-02	1.63135	166
	Caffeine metabolism	3.83E-02	-1.56162	4
	Steroid biosynthesis	4.46E-02	1.710755	22
Total Mix	MAPK signalling pathway	2.27E-04	1.895394	397
	Apoptosis	2.35E-03	2.031882	172
	Metabolism of xenobiotics by cytochrome P450	3.96E-03	2.065028	61
	Toll-like receptor signalling pathway	1.73E-02	1.833873	99
	NOD-like receptor signalling pathway	1.73E-02	1.861289	134
	Herpes simplex virus 1 infection	1.73E-02	1.77273	165
	p53 signalling pathway	1.73E-02	2.009452	85
	Steroid hormone biosynthesis	1.73E-02	1.989381	69
	Adipocytokine signalling pathway	3.37E-02	1.909841	82

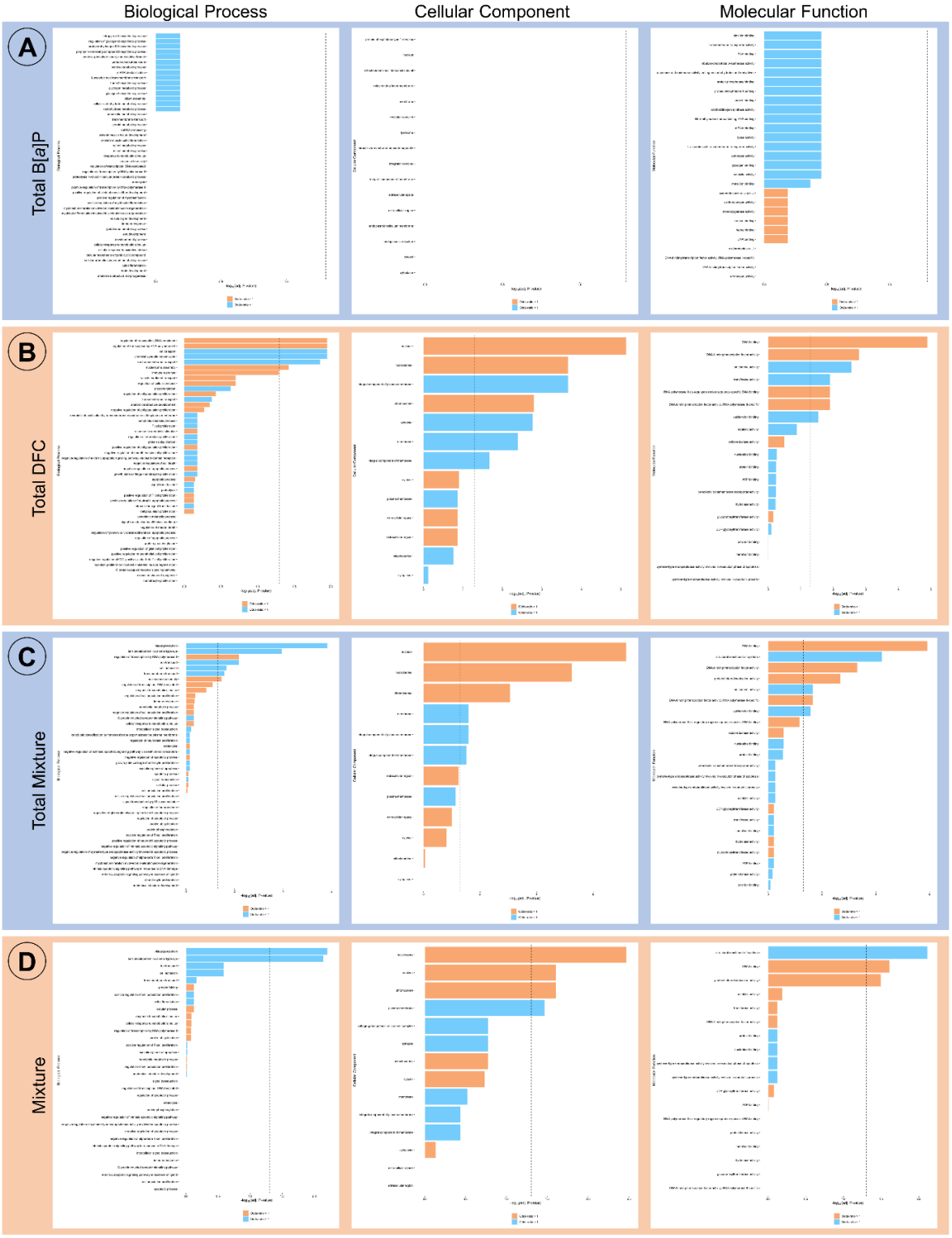

Figure 5.5. Gene ontology/ Gene enrichment analysis (Fisher test, FDR<0.05) using the top10 GO-terms plus GO-terms of interest from DEGs in treatments. **A)** Analysis of total DEGs in B[*a*]P-only treatment. **B)** Analysis of total DEGs in DFC-only treatment. **C)** Analysis of total DEGs in mixture treatment. **D)** Analysis of DEGs exclusive to mixture treatment.

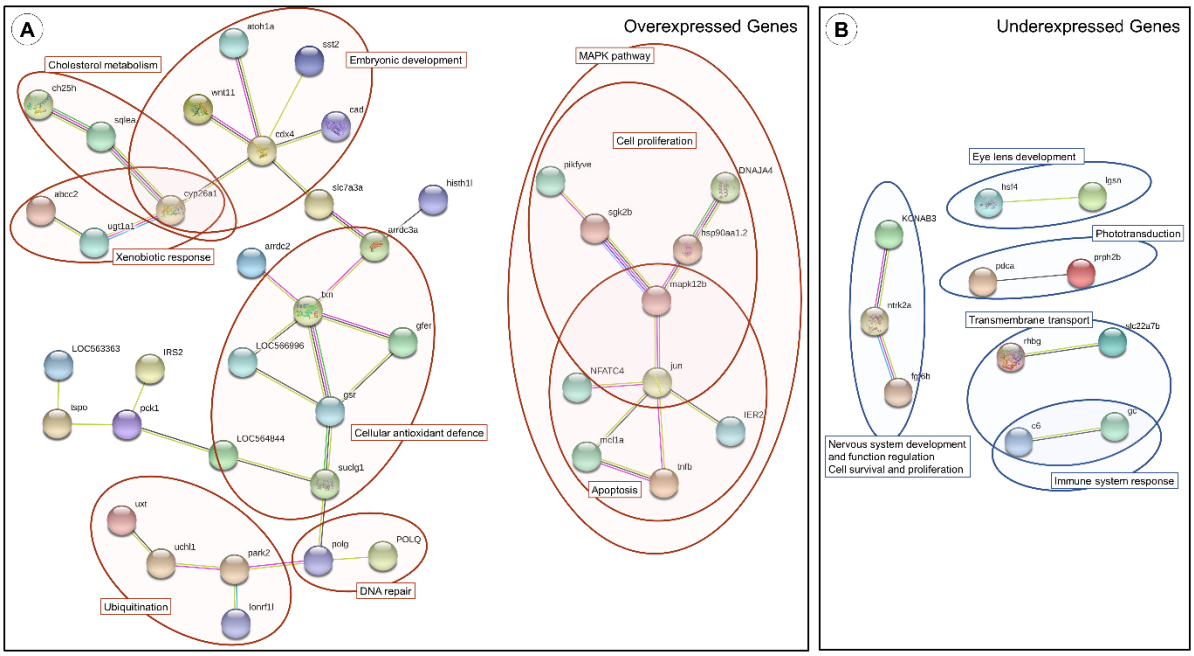

Figure 5.6 Protein-protein interaction network retrieved using STRING from whole-transcriptomes of zebrafish embryos exposed to mixture of B[*a*]P and DFC. The networks were reconstructed from overexpressed **(A)** and underexpressed **(B)** DEGs exclusive to mixture treatment.

5.5 Discussion

Addressing toxicant mixtures arguably partakes in the next level of toxicological risk assessment for humans (occupational exposure) and wildlife. In this work, we explored potential interaction effects between realistic mixtures of B[*a*]P and DFC, which are representative models of legacy and emerging contaminants, respectively, taking the *in vivo* zebrafish embryo as biological model. It must be noted that addressing the toxicity of mixtures is long acknowledged to be a challenge with evidence for unexpected diverging effects as these can be co-dependent of individual chemical dose and the single mode of action, for instance, as reviewed already by Bopp et al. (2019). Novel molecular and computational tools based on 'omics' methods anchored with toxicopathological endpoints can arguably provide better insights on mechanism and therefore biological plausibility, which is one of the pillars to establish causality (see Hayes et al., 2019; Martins et al., 2019; Vitorino and costa, 2023). In addition, understanding mechanism can also lead to retrieving adverse outcome pathways (AOPs) linking exposure to specific deleterious effects even in cases of exposure to complex mixtures (see Ankley et al., 2010).

Transcriptomic analysis revealed around 300 DEGs that are exclusive to the mixture treatment, complemented by gene ontology results displaying a deactivation of biological processes and molecular functions linked to eye development and activation of molecular heterodimerization activity in embryos co-exposed to B[*a*]P and DFC, which overall suggested a synergistic interaction. However, when gene expression is translated to molecular networks the loss of relative enrichment significance of pathways

in mixture treatment that were seemingly relevant in embryos exposed to single toxicants, namely those associated to RNA degradation, cell proliferation, apoptosis and cell-cycle control may suggest antagonistic interaction. These findings imply a cautionary tale when suggesting that some specific toxicopathic outcomes result from synergism or antagonism since further analysis should be necessary to determine the implications of these changes in zebrafish growth, health and reproduction. Altogether, this means that interactions effects must be analysed and interpreted by integrating molecular mechanism with toxicopathic effects. Degradation of RNA, for instance, is a key and complex pathway in cells. Its deregulation can lead to the accumulation of defective RNAs or intermediates, with severe consequences for the regulation of gene expression (Houseley and Tollervey, 2009). We may hypothesize the reduced significance of this pathway in zebrafish embryos subjected to the mixture treatment can be linked to reduced expression in some of the top five genes involved in transcription and translation, such as *znf143b* and *eif2b2*, respectively.

One of the most significant crosslinks between toxicopathic effects and molecular mechanism concerns the formation of pericardial cavity and yolk sac oedemas in embryos from exposure to DFC isolated or combined. This adverse outcome (AO) follows key events (KE) associated with the regulation of ribosomal proteins with P53 function, thus leading to a hindrance of cell cycle arrest and apoptosis. More than 50 % of total DEGs retrieved from the mixture treatment were in common with those isolated from the DFC-only exposure (recall Venn diagram in Figure 5.4C), which uncovered the high influence of DFC exposure in mixture. Among the most overexpressed genes from this subset we found *rpl32* (exposure to DFC) and *rpl21* (mixture treatment). These genes encode for ribosomal proteins and are both involved in translation; however, the resulting proteins have both been linked to cancer progression and metastasis development via degradation of P53 and activation of the FAK/paxillin/ERK signalling pathway (Xie et al., 2020; Zhu et al., 2023). Moreover, DFC and mixture treatments shared the underexpressed genes *cuedc1a* and *ddb2*, both linked to DNA repair and protein ubiquitination, that may also have implications for the p53-related apoptosis pathways, as seen from GE analysis. It should be noted that DNA damage was significantly increased in embryos exposed to B[*a*]P and mixture treatments but not in DFC, which suggests that alterations to P53 regulation may not be related with molecular initiating event (MIE) as DNA damage caused by exposure to the NSAID. In fact, DFC was considered not genotoxic either *in vivo* or *in vitro* assays by Hartmann et al. (2021) although Gómez-Oliván et al. (2014) registered significant DNA damage in *Daphnia magna* after 48-h exposure to 9.7 mg/L of DCF, but this is more than ten times higher than the DFC concentration used in this study. Additionally, in animals exposed to DFC and mixtures, we found the activation of biological process “DNA replication” and molecular function “DNA binding”, which added to the alterations mentioned suggest an investment in cellular proliferation that may be connected to the impairment of cell cycle arresting and onset of apoptosis that may not necessarily be linked to genotoxicity.

According to Brown and Benchimol (2006), the p53-related apoptotic cascade and cell cycle arrest can be activated or deactivated depending on the progression of mitogen-activated protein kinase (MAPK) pathway. Indeed, we must recall that the GE results from DFC and mixture-exposed embryos

indicated significant alterations in MAPK pathway. In turn, protein-protein interaction networks associated to overexpressed genes in embryos subjected to the mixture treatment (see Figure 5.6) also suggest activation of the MAPK pathway. It must also be noted that despite the reduced genotoxicity by DFC, this compound can induce intracellular reactive oxygen species (ROS) and subsequent mitochondrial dysfunction, which, in turn, can also induce further ROS (Jung et al., 2020; Thai et al., 2023). This causes inflammation, with secretion of pro-inflammatory cytokines and growth factors that can stimulate the MAPK/ERK/Raf pathway (Manzoor & Koh, 2012; Mittal et al., 2014). This pathway leads to further inflammation, cell growth, cell proliferation and apoptosis. It should be noted that the ERK pathway was significantly altered in DFC and mixture treatments and that there are indications of activation of inflammatory and oxidative stress response in embryos subjected to mixed toxicants, as revealed, again, by protein-protein interaction networks. Finally, to a potential adverse outcome pathway (AOP) can be derived by linking inflammatory cascade to the AO as formation of oedemas and increased mortality in embryos exposed to DFC 2.5 µM isolated or combined with B[*a*]P. In fact, oedemas are an accumulation of liquid in tissue after pro-inflammatory molecules overpromote vascular permeability (Teixeira & Faria, 2021).

Embryos from co-exposure to DFC and B[*a*]P revealed another AO linked to the impaired ocular function, which combined with molecular alterations indicating the mode-of-action of these toxicant interaction. Gene ontology revealed that mixture-exclusive DEGs were found to be connected to the suppression of biologic processes and molecular functions involved in eye development and its functionalities. The potential consequences of eye-related processes suppression can be reflected in histology with 96 hpf embryos exhibited eye degeneration (recall Figure 5.1F). After comparation with other studies (Dahm et al., 2007; Schmitt & Dowling, 1994) the scenario of development delay was discarded since in the affected eyes remain a small pigment layer of pigment and an individualized lens protruding from the optic cup that in normal development are both only visible after 84 hpf. The blindness hypothesis of these affected embryos subjected caused by ocular degeneration as KE could be related with protein-protein interaction networks (recall Figure 5.6B) associated to underexpressed genes in mixture treatment. For instance, *prph2b* (peripherin 2, also known as retinal degeneration slow, RDS) and *pdca* (phosducin a) connected to formation of rod and cone photoreceptor outer segments and phototransduction progression, respectively (Herrmann et al., 2010; Stuck et al., 2016; Tebbe et al., 2020). Inclusive an alteration of expression or even mutation in *prph2b* gene was widely related to eye degenerative diseases as retinitis pigmentosa, an incurable blindness, or cone-rod dystrophy (Gill et al., 2019; Kajiwara et al., 1991; Wells et al., 1993). Nonetheless, the eye degeneration was also seen in DFC-only treatments even the gene *prph2b* not be included in the DGEs list of this treatment, which reflects once again the complexity of molecular mechanisms where alterations in the expression of distinct genes can ultimately trigger an identical AO.

The molecular mechanisms behind the acute effects are not always possible to trace considering these complexity, therefore, some pathological alterations (recall Figure 1) have only been associated to the concentrations of each substance. For example, in embryos where DFC highest

concentrations (1.3 and 2.5 µM) were used, as in individual or mixture exposure, were registered the highest development alterations rates. Severe alterations as shorter body length, smaller eye, muscle degeneration, pericardial and body oedema, and abnormal pigmentation, similar to those detected in this study at high DFC concentrations, were observed by Chen et al. (2014), however only at concentrations above 3.38 µM. Also, the same study reported only about 26.7% of embryo lethality at DFC 3.38 µM despite we registered, for the same time of exposure, above 70% mortality for low DFC concentrations (2.5 µM). The use of dechorionated eggs in our assays can be the reason for the discrepancy among effects in each range of DFC concentrations, since the chorion acts as a chemical protection barrier (Henn & Braunbeck, 2011). At this point the qualitative evaluation of pathological alterations and even mortality seems do not tend to present differences for the effects registered in high DFC-only treatments and the mixtures where these concentrations are involved, however, statistical results are evidenced a trend to antagonism in mixtures, with the loss of DFC influence in both mortality and alterations when in mixture.

The lack of acute effects in B[*a*]P treatments and the apparent low influence in mixtures can be explained by the known capacities of B[*a*]P in induce predominantly chronic or long-term adverse effect, i.e., the dysfunctions from B[*a*]P exposure only have visible repercussions after some time. Lin et al. (2020) observed neurotoxic effects, with alterations in nervous system development in zebrafish embryos exposed to B[*a*]P concentrations (10 and 20 µM) even higher than those used in this study, without any apparent morphological alteration. Despite this, embryos exposed to B[*a*]P (0.4 µM) highest concentration and mixture revealed more DNA damage than DFC treatment, what contradict the lack of influence of B[*a*]P and enhance its long-term adverse effect capacity. An antagonistic trend was also present in genotoxic evaluation where although DNA damage was higher in embryos exposed to mixture this damage is less than the sum of the individual genotoxic levels of DFC and B[*a*]P treatments. Effectively, B[*a*]P is a known genotoxic component at relatively low concentrations, such as in *Danio rerio* embryos exposed to B[*a*]P for 6 days revealing significant DNA damage at concentrations of 0.001 µM and 0.01 µM (Šrut et al., 2015) or a significant DNA damage in *Oryzias latipes* embryos after 48 h exposure to 20 µg/L (Dasgupta et al., 2014), about one-third of the B[*a*]P concentration used in our study (89 µg/L). Genotoxicity of B[*a*]P derive from DNA adducts formed after B[*a*]P bioactivation by CYP450 during phase I leading to the formation of reactive B[*a*]P diol-epoxides (Tarantini et al., 2009), and the metabolism of xenobiotics by CYP450 emerges as one of the pathways significantly affected in both B[*a*]P-only and mixture treatments, which reveal other point of influence of this compound in mixture.

5.6 Conclusions

Novel molecular and computational tools based on ‘omics’ methods enabled a better understanding on how toxicopathological effects and molecular mechanisms are linked upon exposure to toxicant mixtures. This association pointed toward potential AOPs in zebrafish embryos. The AOs

reported in animals exposed to combined DFC and B[*a*]P can follow two relevant AOPs, one linked to eye development and another to inflammation, cell cycle arrest and apoptosis via p53 and MAPK pathways. This last AOP permitted tracing the molecular line to verified downstream toxicopathological effects such as DNA damage and the forming of oedemas. In either case we detected high influence of DFC in toxicopathic effects but low interaction between DFC and B[*a*]P when the toxicants are present in environmentally-relevant concentrations. However, we found an antagonistic interaction onto genotoxicity and some molecular pathways that upon co-exposure ceased to be affected, namely associated to RNA degradation, cell proliferation, apoptosis and cell-cycle control. We must highlight that B[*a*]P tends to cause serious chronic effects, regardless of interaction effects, which means that the full span of consequences can only be understood after analysing the whole zebrafish life cycle. Altogether, it is clear interaction between toxicants can hinder risk assessment of toxicants in mixtures. Nonetheless, the discovery of potentially mixture-specific AOPs can indicate biological plausibility and therefore assist establishing causation.

6

THE INTERACTION EFFECTS TOXICANTS AND EMERGING POLLUTANTS IN *DANIO RERIO*: A GENERATIONAL CHRONIC ASSAY

6.1 Abstract

Society has grown and developed over the centuries and with it also the legacy and emerging pollutants released into the environment at levels that can be harmful to wildlife and human health. The unpredictability of the consequences rises when we looked to the environmental pollution as a complex junction of unexpected effects from toxicants mixtures at several doses and ratios. However, is critical draw a realistic scenario considering the risks of exposure throughout the organisms' life cycle or intergenerational effects. Therefore, the main aim of this study was assessing the chronic effects in juveniles and adults associated with co-exposure during their embryonic development stage to legacy benzo[*a*]pyrene (B[*a*]P) and emerging diclofenac (DFC) toxicants and determining the costs for reproductive performance and the intergenerational carry-over effects to first filial generation embryos. The intergenerational assay was initiated with the F0 embryo exposure followed by growth and reproduction in clean environment and finalised with development evaluation of F1 embryos. Despite the short-term exposure during embryonic stage, exposure to B[*a*]P and DFC, was responsible for toxicopathological traits in F0 juveniles and adults, namely cellular/nuclear pleomorphisms and hyperaemia in livers, renal hydropic degeneration, and a few cases of apoptotic hepatocytes and haemorrhage in kidney. Additionally, kidney and the intestinal epithelium revealed the most notorious increase in PCNA regulation in F0 juvenile but after reach adulthood the alterations in PCNA signal were reduced when compared with control. The gonads from F0 reproductive adults showed reduced effects however B[*a*]P had high interference in reproductive success but not when combined with DFC. The F1 embryos showed developmental malformations mostly in isolated DFC and B[*a*]P treatments, with mixtures revealing antagonistic effects. Overall, we can concluded that realistic exposure to mixtures can be heavily affected by life stage, with exposure during developmental phases bearing serious consequences not only for the entire life cycle of the individual but also for the offspring generation.

6.2 Introduction

Environmental contamination by mixed toxicants is arguably the rule and not the exception in impacted areas, affecting both humans and wildlife. Co-exposure to what often constitutes an intricate matrix of toxicants renders environmental risk assessment challenging, especially when guidelines and safety thresholds are directed toward individual compounds. In additions, little information is available concerning risks of exposure throughout the organisms' life cycle or generational effects. Considering the chronic nature of diseases that may be chemically-induced, such as neoplasms, these gaps are a serious handicap for both environmental protection and human occupational health. It must be noticed that the joint effects of mixed toxicants in an organism can expand beyond additivity into the domain of synergy, leading into consequences unattainable by individual compounds, or even antagonistic (see Hernández et al., 2017 for concept clarification), which can be hypothesise to depend not only on the components of the mixture but also factors raging from age and duration of exposure to target organism

and co-morbidities. In any case, nowadays, predicting risk in realistic scenarios, which arguably includes mixtures of chemicals, is a priority for occupational toxicologists and environmental toxicologists or ecotoxicologists, as it can lead to the development of more effective guidelines for environmental monitoring; development of strategies for the evaluation of risk and outlining safety plus remediation strategies. Nonetheless addressing the toxicology of mixtures is a challenge due to multiple aspects expanding beyond intricate pharmacokinetics, beginning with the mode-of-action of each chemical and how it is modulated by variables like number, concentration and even the proportion of contaminants in the mixture (Bopp et al., 2019). In addition, we must bear in mind that searching for realistic scenarios implies also considering evaluating long-term effects either ensuing chronic exposure of persistent effects after acute exposure, which, in any case can have a profound and often unpredictable impact on health.

The evaluation of potential intergenerational effects following parental exposure to complex toxicant matrices are seldom the first approach in building realistic chronic scenarios, even though there is evidence for such occurrences through laboratory bioassays with model organisms. We may refer, for instance, to the recent work of Philibert et al. (2023) who described intergenerational endocrine-disrupting effects in mice parentally exposed to (realistically low) levels of combined non-steroid anti-inflammatory drugs (NSAIDs) and ethinylestradiol (EE2). Also, Swank et al. (2021) described altered behaviour in both larvae and adults of the freshwater fish *Pimephales promelas* after exposure to environmentally relevant concentrations of chemicals of emerging concern (CECs) that includes compounds as pharmaceutics, cosmetics or hormones. In fact, these authors even mention a magnification of effects in F1 and F2 generations. In this study, the combination of zebrafish as toxicologic model with a choice of relevant representatives of legacy and emerging pollutants should enable a more realistic assessment of the chronic toxicity of this mixture in an intergenerational context.

The carcinogenic PAH benzo[*a*]pyrene (B[*a*]P) and diclofenac (DFC), a non-steroid anti-inflammatory drug (NSAID) were the legacy and emerging pollutants, respectively, chosen due its relevant interaction in zebrafish embryos after acute exposure described in Chapter 5. For instance, an antagonistic interaction was observed in genotoxic effects and some molecular pathways that upon co-exposure ceased to be affected, namely associated to RNA degradation, cell proliferation, apoptosis and cell-cycle control (see Chapter 5 for more information). The acute exposure study was thus the basis for develop a strategi in order to understand the full extent of consequences for whole zebrafish life cycle and their offspring after a short co-exposure to B[*a*]P and DFC. Regarding the selected pollutants, B[*a*]P is mostly from the incomplete combustion of petrogenic and biomass fuels, cigarette smoke and industrial waste and since 1973 it is considered chemical with carcinogenic risk to humans (Boström et al., 2002; IARC, 1983). Additionally, B[*a*]P is also recognized by its genotoxic and mutagenic proprieties, particularly those associated to the formation of diolepoxides-DNA adducts after bioactivation by CYP1A1 and 1B1 (see for instance Moorthy et al., 2015; Shimada & Fujii-Kuriyama, 2004). B[*a*]P can promote proliferation of neoplastic cells via mutation in *ras* family oncogenes with activation of transcription and in p53 tumour suppressor gene, inhibiting this main function or via

activation of pro-inflammatory cytokines (Denissenko et al., 1996; Nebert et al., 2000; Ross & Nesnow, 1999; Shimada, 2006). In turn, DFC is widely used in human and farm animal medicine, albeit being regarded as one of the most toxic NSAIDs for wildlife (Lonappan et al., 2016; Parolini, 2020). The toxicity of DFC seemingly results mostly from the production of reactive metabolites cytochrome P450 (albeit mainly by CYP2C9 and CYP3A4) during phase I and by UDP-glucuronosyltransferases (UGTs) during phase II (Boelsterli, 2003; Leemann et al., 1993). DFC can also limit the production of pro-inflammatory cytokines essential to acute inflammation progression linked to its inhibitor action over the cyclooxygenase family members, COX-1 and COX-2 (Gan, 2010; Paskauskas et al., 2011). In fact, the inflammation process seems to be a point of interaction between B[*a*]P and DFC combining the individual mode-of-action described to these two pollutants with the alterations in pathways (p53 and MAPK) linked to inflammation found in zebrafish embryos by transcriptomic analyses (see Chapter 5).

In the aftermath of our preceding work, we aimed primarily as investigating the consequences the combined toxicants in adult organisms following exposure during early life stages. As such, the main objectives of this study were assessing the chronic effects in juvenile and adult zebrafish associated with exposure during their embryonic development stage to mixed legacy and emerging toxicants (DFC and B[*a*]P) and determining the costs for reproductive performance and the intergenerational carry-over effects to first filial generation embryos.

6.3 Methods

6.3.1 Chemicals and test animals

Benzo[*a*]pyrene (B[*a*]P) (CAS: 50-32-8) was acquired from TCI EUROPE (Zwijndrecht, Belgium) and diclofenac (DFC) Sodium salt (CAS: 15307-79-6) from Acros organics (Geel, Belgium). Stock solutions of B[*a*]P and DFC were prepared in dimethyl sulfoxide (DMSO) and sterilised ultrapure water, respectively. Adult wildtype *Danio rerio* (AB incross) were maintained in a six-rack recirculating system (Tecniplast, Buguggiate, Italy) equipped with a reverse osmosis unit, under controlled conditions, namely conductivity set at 800 µS, pH 7.0, at 28 °C on a 14 h light/10 h dark cycle. Zebrafish were fed daily with ZEBRAFEED and Artemia (ZM Systems, Winchester, UK). The exposure assay was performed with viable dechorionated eggs (Henn & Braunbeck, 2011), between 2 and 4 h post-fertilisation (hpf) and collected from multiple couples.

6.3.2 Experimental design

The intergenerational chronic assay was performed in four serial steps: (I) exposure of parental generation zebrafish (F0) during embryonic development from 4 to 96 hpf; (II) F0 growth in clean environment; (III) F0 reproduction and assessment of fertility performance; and (IV) development of first filial generation zebrafish (F1) embryos until their larval stage, i.e., from 0 to 96 hpf (see experimental design in Figure 6.1). Exposure (Step I) was conducted according to our previously developed

experimental design (Chapter 5). In brief, F0 dechorionated eggs (4 hpf), were randomly divided by glass Petri dishes with embryo medium (distilled water supplemented with NaCl, KCl, $CaCl_2$ and $MgSO_4$), for which each experimental condition had two replicates and each one held forty embryos (*n* = 40). During the 96 h of assay, embryos were placed in an incubator at 28 ˚C and the medium was changed with fresh spiked (contaminated), control (DMSO + H2O) or blank (medium) every 24 h (90%) to minimise stagnation and oxygen depletion. Embryos were monitored at 24, 48 and 72 hpf of exposure in a stereo microscope in order to remove any dead embryo. Chemical concentrations used in individual and binary mixtures exposure were chosen considering the mortality and pathological effects from the acute assays. Thus, for lowest concentrations were selected the EU Environmental Quality Standards (EQS), B[*a*]P 1.98E-4 µM (0.05 µg/L) and DFC 3.14E-4 µM (0.1 µg/L). The highest concentrations of B[*a*]P 0.4 µM (89 µg/L) and DFC 0.3 µM (80 µg/L), corresponding to 1/10 and no observed adverse effect level (NOAEL) and to 1/50 no observed effect concentration (NOEC), respectively (Ferrari et al., 2003; Knecht et al., 2017).

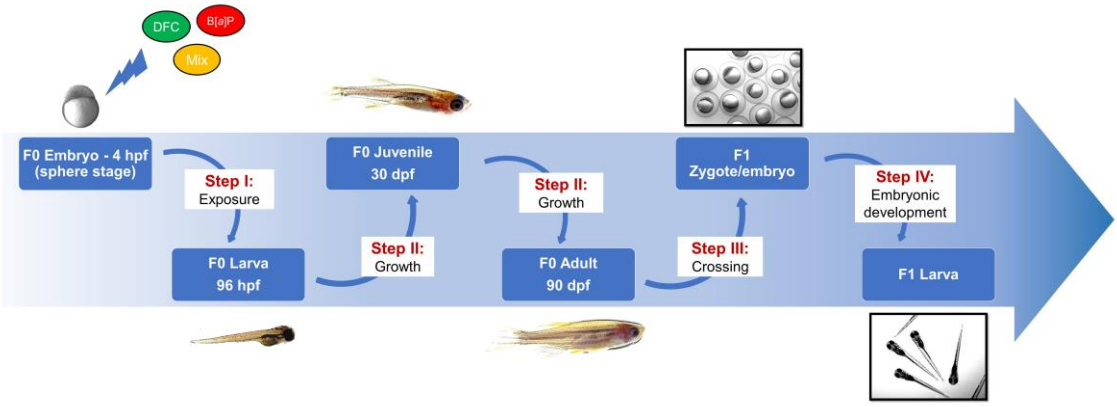

Figure 6.1 - Experimental design. The intergenerational bioassay was divided in four steps: (I) exposure of parental generation zebrafish (F0) during embryonic development from 4 to 96 hpf; (II) F0 growth in clean environment; (III) F0 reproduction and assessment of fertility performance; and (IV) development of first filial generation zebrafish (F1) embryos until their larval stage, i.e., from 0 to 96 hpf.

After 96 h of exposure live F0 zebrafish larvae were collected and transferred to Petri dishes with fresh uncontaminated medium, divided in according to replicates and experimental conditions. At 6 days post-fertilization (dpf), larvae were transferred to tanks with a recirculating system of clean freshwater, onsetting step II. Here, fish were allowed to reach adulthood under the same conditions mentioned in subsection 6.2.1. Samples for histopathological and immunohistochemical analyses were collected at 30 dpf (F0 juveniles) and 90 dpf (F0 adults). At both sampling times, two animals by replicate, independently of sex, were sampled and fixed in Davidson fixative for 30 h. Weight and length were registered to all sampled animals. The remain adult's F0 zebrafish were left to growing in clean environment until they reached maturity.

In step III, four F0 zebrafish couples by replicate were selected for weekly crosses, during six weeks (between 110 and 160 dpf old), in single-pair breeding. The reproductive fitness of couples F0 was verified by calculating the Spawning rate (number of successful crosses / total number of crosses) and Fertilization rate (total of fertilized eggs / total of eggs). Finally in step IV, all eggs after the first hour's check were left to develop in clean medium until the end of their embryonic phase (96 hpf). Embryos, now termed F1 for disambiguation, were monitored at 24 and 96 hpf for evaluation of Survival 96 hpf rate (total of live embryos at 96hpf / total of fertilized eggs), Normal embryos 24 hpf rate (normal embryos 24 hpf / total of live embryos at 24 hpf) and Normal embryos 96 hpf rate (normal embryos 96 hpf / total of live embryos at 96 hpf). Zebrafish (F0) couples used in crosses were ultimately sampled and fixed in Bouin's fixative for 48 h for histopathological assessment. Weight and length were registered for all animals.

6.3.3 Histopathology

The preparation of samples for histopathological analyses was similar for all sampling times (i.e., 30 dpf, 90 dpf and F0 adults after crossing). Briefly, after fixation samples were washed three times in ultrapure water before being subjected to a dehydration in a progressive gradient of ethanol (70%, 96% and 100%), an intermediate infiltration step using xylenes and finally allowed to infiltrate in molten paraffin (Paraplast) o/n at 60ºC. Paraffin–embedded samples were sectioned (5 µm thickness) with a Jung RM2035 model rotary microtome (Leica Microsystems, Wetzlar, Germany). Zebrafish whole body sections were stained with Harris' Hematoxylin (differentiated with tap water) and counterstained with alcoholic Eosin Y (H&E). Periodic acid-Schiff's contrasted with Harris' Hematoxylin (PAS&H) for polysaccharides with free hydroxyl groups was also performed on some slides. After staining, sections were dehydrated using a crescent gradient of ethanol, cleared in xylol, and mounted with DPX mounting agent (Sigma-Aldrich, Portugal). Histological analyses were made using a DM2500 LED model microscope equipped with a MC 190 HD camera (Leica Microsystems).

6.3.4 Immunohistochemistry

The regulation of proliferating cell nuclear antigen (PCNA) was localised using Immunohistochemistry for fluorescence microscopy (IHC-IF) to detected potential hyperplastic foci in 30 and 90 dpf zebrafish (i.e., juveniles and adults, respectively). The anti-PCNA Polyclonal Rabbit IgG Antibody (PA5-27214) primary antibody was diluted to a 1:1100 (100 µg/L) working solution, while the secondary fluorochrome-labelled antibody was a Goat anti-Rabbit IgG (H+L) Cross-Adsorbed Secondary Antibody, Alexa Fluor™ 568 (A-11011) diluted to 1:20000 (100 µg/L). both antibodies were purchased from Invitrogen/Thermo Fisher Scientific, Massachusetts, EUA). All dilutions were prepared in PBS containing 2% BSA and 0.1% Triton X-100.

Two histological slides per replicate were analysed, corresponding to negative control (incubated with the secondary antibody only) and assay (incubated with both primary and secondary antibodies). In brief, samples were deparaffinated and rehydrated in a regressive series of ethanol down

to phosphate-buffered saline (PBS), pH 7.4. Afterwards, sections were treated with 0.1% Triton X-100 in PBS for antigen retrieval. Slides were then transferred to a humidified chamber and incubated during 30 min with the blocking solution (2% BSA in PBS with 0.1% Triton X-100). Posteriorly slides were washed in PBS and the primary antibody was applied for o/n incubation 4ºC under a coverslip. Slides were washed again before the 2-h incubation with the secondary antibody and mounted with an aqueous DAPI-containing mounting agent (Sigma-Aldrich, Portugal). This dye is a nuclear-contrasting agent that stains the adenine-thymine (AT) rich regions of double-strand DNA (dsDNA) with fluorescent blue under UV light. Analysis was performed immediately using an DM2500 model LED microscope fitted with an MC190 model HD camera and a EL6000 model fluorescence light source (Leica Microsystems). Images were processed using ImageJ (Schneider et al., 2012).

6.3.5 Statistics

Statistical analysis was computed in R 4.2.1 (Ihaka and Gentleman, 1996). All data were checked for normality and homogeneity of variances using Shapiro-Wilk's and Levene's Tests, respectively. Parametric data (body length) were analysed using F test-based ANOVA followed by Tukey's Honest Significant Difference (HSD) test for post-hoc comparisons. Following invalidation of at least one assumption, the remaining data were analysed using the non-parametric Kruskal-Wallis ANOVA-by-Ranks H, followed by Dunn's test for multiple comparations. The data from parental generation zebrafish (F0) fertility performance and first filial generation zebrafish embryos (F1) development were analysed by hierarchical clustering though Ward's method employing Euclidean distances as metric and the significance level α was set at 0.05 for all analyses.

6.4 Results

6.4.1 Parental generation zebrafish: Juveniles

Parental generation (F0) juveniles exposed to toxicants, isolated and combined, during the embryonic stage revealed significant histopathological alterations mostly in livers and kidneys, even though, as general rule, these 30 dpf animals tended to show as expected full development and organ functioning, plus adult-like fins and pigmentation. In addition, zebrafish from control and B[*a*]P-only treatments were significantly larger (Standard body length ≈10 mm against ≈8 mm) than animals from other treatments (Tukey's HSD, $p < 0.05$). Compared with the control liver (Figure 6.2A), pleomorphic cells and nuclei were common especially in the two mixture treatments that combined the highest and lowest concentrations of both toxicants. Interestingly, they were also recurrent in zebrafish exposed to the lowest concentration of B[*a*]P (Figure 6.2B). The nuclear pleomorphism is a regressive alteration identified by the increase of hepatocyte nuclei size ultimately affected cell size and shape (see Figure 6.2B – *Inset*). Hyperaemia was recorded in fish exposed to mixtures where the higher B[*a*]P concentration (0.4 µM) was involved (Figure 6.2C). In most treatments (isolated toxicants and mixtures),

exposed females revealed increased prevalence of liver vacuolization not reactive to PAS, indicative lipid contain that was eventually washed in histologic procedures (Figure 6.2B, D). In turn, kidney from zebrafish treated with the lower concentration of DFC (3.14E-4 µM) exhibited cloudy swelling in renal tubules (hydropic degeneration) accompanied by glomerular degeneration (Figure 6.2F). In addition to these major alterations, a few cases of atresia (Figure 6.2D and *Inset* for further detail) and an apparent rupture of liver and ovary membranes (see Figure 6.2B) were verified in animals exposed to B[*a*]P-only treatments and co-exposure to lowest toxicant concentrations.

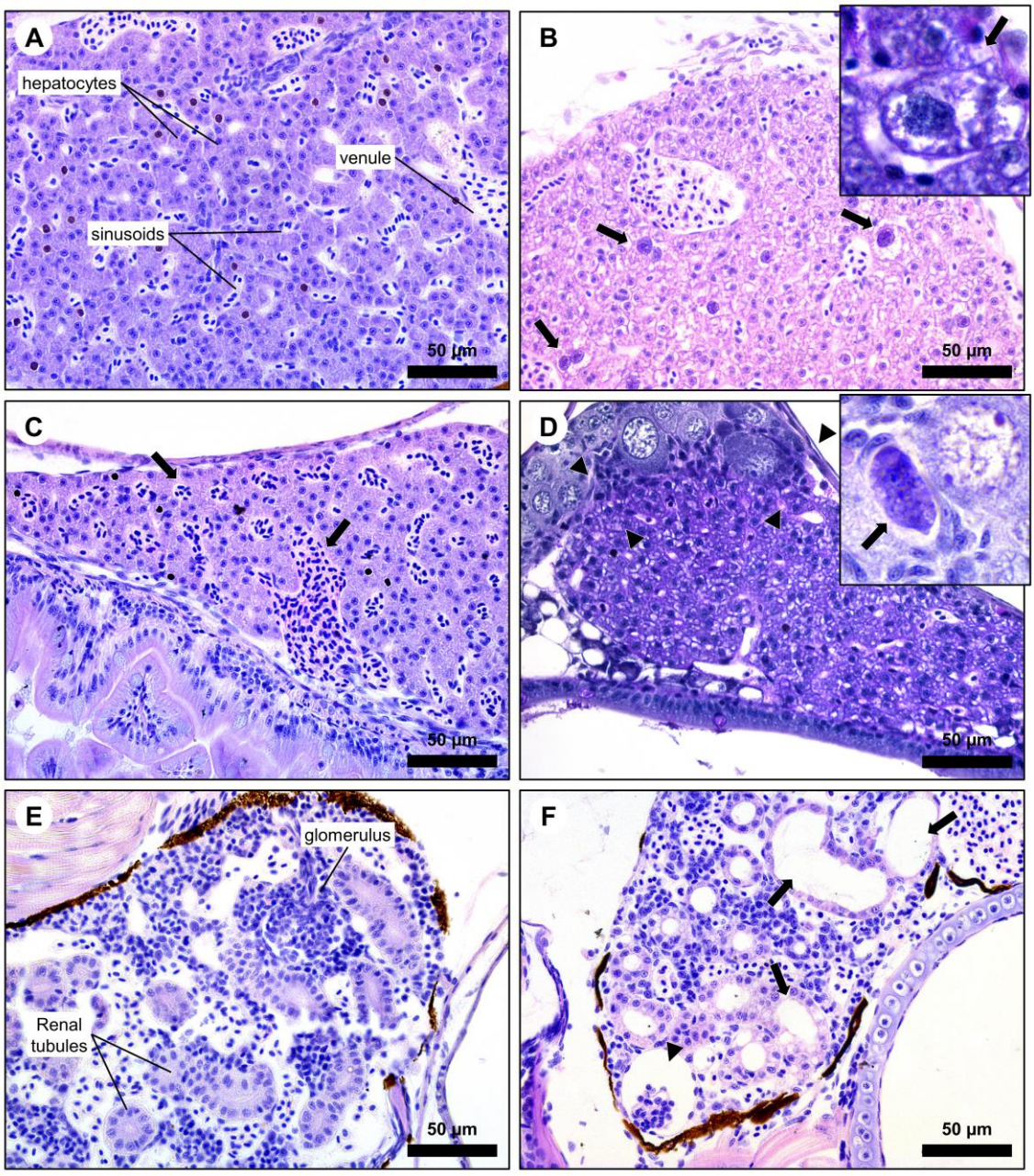

Figure 6.2 – Histopathological alterations in F0 juvenile zebrafish exposed to DFC, B[*a*]P and their mixtures during embryonic development. **A)** Liver from a control zebrafish showing the expected architecture of the organ. **B)** Liver

with numerous cellular and nuclear pleomorphisms (arrows) plus signs of vacuolization from a zebrafish exposed to mixture B[*a*]P 1.98E-4 µM + DFC 3.14E-4 µM. *Inset*: detail of a pleomorphic hepatocyte and respective nucleus. **C)** Liver from a zebrafish exposed to mixture B[*a*]P 0.4 µM + DFC 3.14E-4 µM with a comparatively high prevalence of hyperaemia (arrows). **D)** Apparent rupture of liver and ovary membranes (between arrowheads) leading to organ fusion; plus hepatocytes with increased lipid vacuolization from a female exposed to B[*a*]P 0.4 µM. *Inset:* detail of an atretic oocyte being engulfed/phagocytised by a macrophage (arrow) **E)** Kidney from a normal control zebrafish. **F)** Cloudy swelling of renal tubules (arrows) and glomerular degeneration (arrowheads) in the kidney of a zebrafish exposed to from DFC 3.14E-4 µM. All sections were stained with H&E, except **D**, stained with PAS&H.

The intestine (Figure 6.3) and kidney (Figure 6.4) were the organs that revealed obvious alterations in PCNA expression comparatively to control (Figures 6.3A and 6.4A, respectively). Immunohistochemistry revealed the presence of the red-labelled PCNA antigen in the nucleus (see examples in Figure B1.1 in Appendix to Chapter 6, for original split-channel images). Highest signal of PCNA was found on intestinal epithelia of F0 juveniles exposed to the highest concentration of DFC (0.3 µM), as shown in Figure 6.3B. This was followed by the intestinal epithelia of animals exposed to mixtures involving the same concentration of DFC (Figures 6.3C,D). Additionally, zebrafish that had been exposed to the highest concentration of B[*a*]P (0.4 µM) also showed evidence for PCNA up-regulation in the intestinal epithelium, however with comparatively lower signal. Similarly, kidney sections also indicated PCNA up-regulation in zebrafish that had been exposed to DFC (0.3 µM) and their mixtures (Figure 6.4B, C, D), albeit without a clear distinction between the various conditions. The signal was mainly detected in the nephrogenic zone.

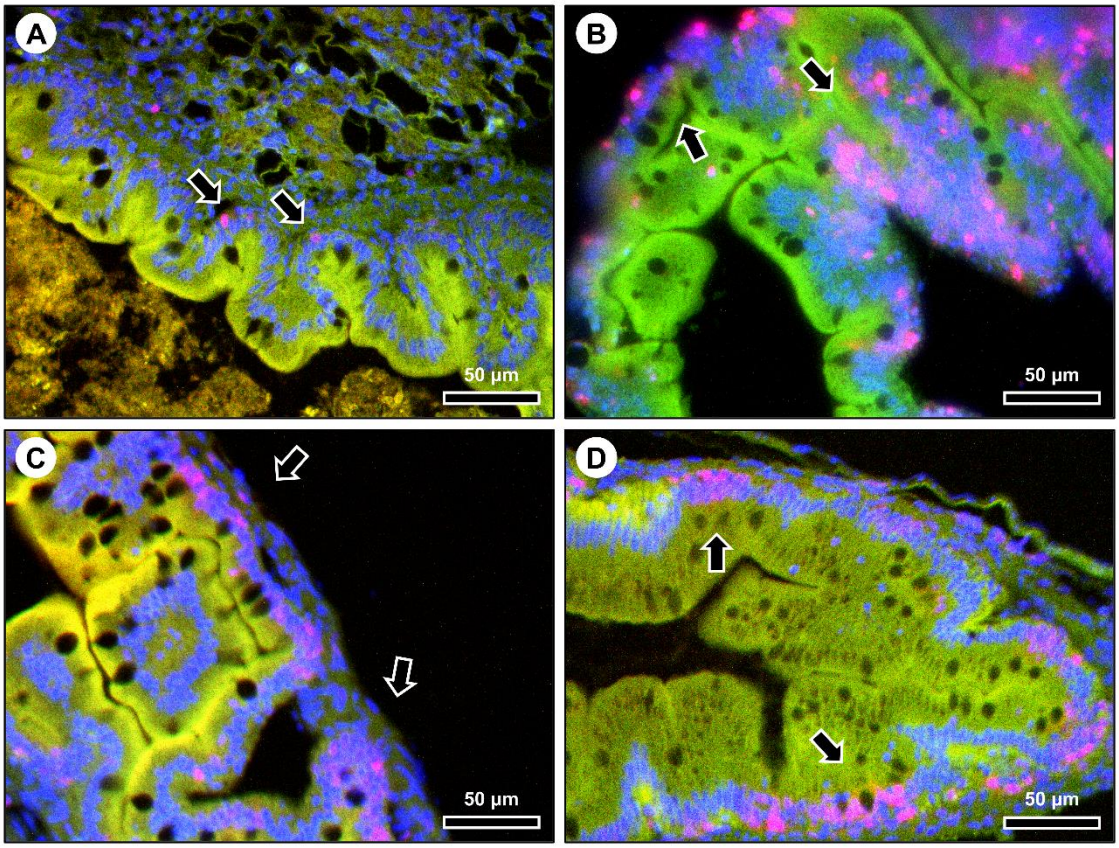

Figure 6.3 – Immunostaining of PCNA in intestinal epithelia of F0 juvenile zebrafish. Arrows indicate the localisation of the red-labelled probe in nuclei, often in conjunction with DAPI. **A)** Intestinal epithelium of a control zebrafish that yielded low signal. **B)** Intestinal epithelium of a fish exposed during embryogenesis to the highest concentration of DFC (0.3 µM) with the highest level of PCNA expression compared to control. Animals exposed to mixtures, **C)** B[*a*]P 1.98E-4 µM + DFC 0.3 µM and **D)** B[*a*]P 0.4 µM + DFC 0.3 µM, presented similar levels of PCNA regulation, albeit both elevated relatively to controls.

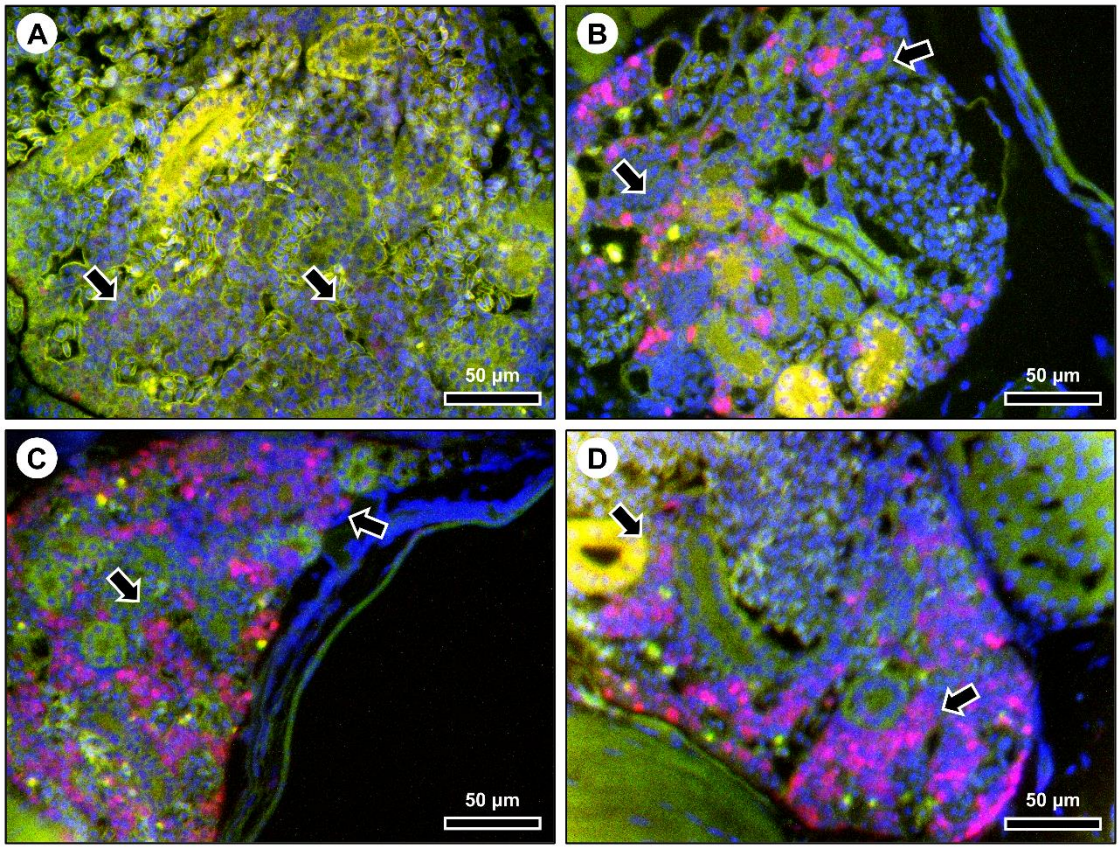

Figure 6.4 – Immunostaining of PCNA in the kidney of F0 juvenile zebrafish. Arrows indicate the localisation of the red-labelled probe in nuclei, often in conjunction with DAPI. **A)** Control zebrafish with low signal. Zebrafish exposed to **B)** DFC-only treatment (0.3 µM) plus mixtures **C)** B[*a*]P 1.98E-4 µM + DFC 0.3 µM and **D)** B[*a*]P 0.4 µM + DFC 0.3 µM, presented high levels of PCNA regulation than control, however without a clear distinction between the three conditions.

Overall, the liver, kidney and intestinal epithelia were the most affected structures in F0 juvenile zebrafish. The liver showed the most significant histopathological alterations, while the kidney and the intestinal epithelium revealed the most notorious increase in PCNA regulation. The combination of both analyses (Table 6.1) highlighted the induction of PCNA regulation and histopathological alterations like hyperaemia and nuclear pleomorphisms in animals that had been exposed to the highest concentrations of either toxicant or their mixtures.

Table 6.1 - Anti-PCNA antibody signal and histopathological traits in target organs relatively to controls. The table summarises the results from juvenile F0 zebrafish exposed to DFC and B[*a*]P, isolated and combined, during the embryonic development.

	Intestinal epithelium	**Kidney**	**Liver**
DFC 3.14E-4 µM	=	= (a)	=
B[*a*]P 1.98E-4 µM	=	=	= (a)
DFC 0.3 µM	+ + +	+ + +	=
B[*a*]P 0.4 µM	+	=	=
B[*a*]P 1.98E-4 µM + DFC 3.14E-4 µM	=	=	= (a)
B[*a*]P 1.98E-4 µM + DFC 0.3 µM	+ +	+ + +	=
B[*a*]P 0.4 µM + DFC 3.14E-4 µM	=	=	= (a)
B[*a*]P 0.4 µM + DFC 0.3 µM	+ +	+ + +	= (a)

"=" similar to controls; "+" PCNA up-regulation; "-" PCNA down-regulation; "(a)" recurrent histopathological alterations (namely cellular and nuclear pleomorphisms, hyperaemia and hydropic degeneration)

6.4.2 Parental generation zebrafish: Adults

Regardless of toxicant, adult parental generation (F0) zebrafish (90 dpf) showed a normal maturation and a mean of standard body length of 21 mm, with no significant differences between control and exposed fish (Tukey's HSD, $p < 0.05$). The F0 adults registered evident histopathological alterations relatively to controls, mainly in liver and kidney, albeit moderate alterations in the regulation of PCNA when compared to F0 juveniles. Nuclear pleomorphisms (see Figure 6.5A and corresponding *Inset* for details) continued to be noticeable in the livers of adult F0 that had been exposed to the lower B[*a*]P concentration (1.98E-4 µM) and its mixture with the lower DFC (3.14E-4 µM) concentration. Zebrafish that had been exposed to B[*a*]P 1.98E-4 µM also displayed a trend to accumulate defence cells (mostly macrophages) in the hepatic portal area (Figure 6.5B). In turn, hyperaemia (Figure 6.5C) was recorded in the livers of zebrafish previously exposed to the highest DFC (0.3 µM) concentration. Foci of cell death were uncommon (Figure 6.5D) and were typically recognised as programmed cell death due to the presence of apoptotic bodies and cells with a distinctive "blebbed" membrane, plus being accompanied by defence cells (Figure 6.5D - *Inset*). Similar to what had been observed in F0 juveniles, a few adult females also had liver vacuolization, not reactive to PAS (Figure 6.5E). In turn, kidneys from fish subjected to all drug treatments (B[*a*]P and DFC, isolated and combined) exhibited hydropic degeneration in tubule cells, also named cloudy swelling, characterized by cell engorgement due to excessive accumulation of water (Figure 6.6A and 6B). A most advanced stage of hydropic degeneration of renal tubules was observed in animals subjected to DFC-only treatments (Figure 6.6C). In addition, haemorrhage was common in the kidneys of zebrafish that had been exposed to the highest B[*a*]P concentration plus respective mixtures (Figure 6.6A).

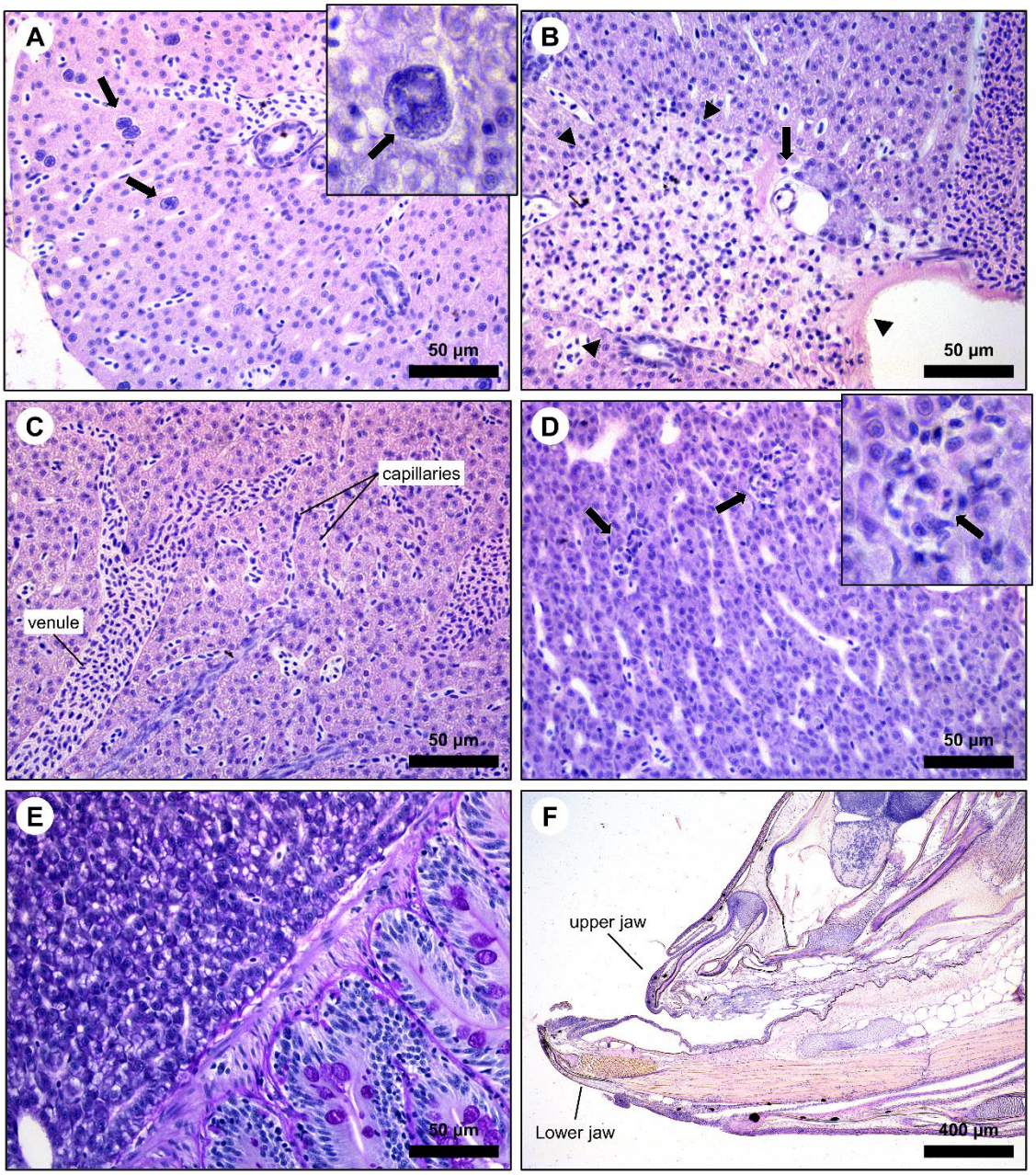

Figure 6.5 – Histopathological alterations in adult F0 zebrafish that were exposed to DFC, B[*a*]P and corresponding mixtures during embryonic development. **A)** Liver with numerous nuclear pleomorphisms (arrows) from a zebrafish exposed to B[*a*]P 1.98E-4 µM. *Inset:* detail of a hepatocyte with a nuclear pleomorphism. **B)** Zebrafish exposed to B[*a*]P 1.98E-4 µM also displayed a massive accumulation of defence cells on a liver vessel (between arrowheads) and a degenerated bile duct (arrow). **C)** Liver from a zebrafish exposed to DFC 0.3 µM with relatively high prevalence of hyperaemia (increased blood flow with respective dilation of venules and capillaries). **D)** Small foci of apoptosis (arrows) in liver from zebrafish exposed to mixture B[*a*]P 0.4 µM + DFC 0.3 µM. *Inset:* detail of apoptotic bodies (arrow) accompanied by defence cells. **E)** Increased hepatocyte vacuolization (PAS-negative vacuole contents) in the liver of a female exposed to B[*a*]P 0.4 µM. **F)** Abnormal growth of lower jaw of a zebrafish exposed to B[*a*]P (1.98E-4 µM). All sections stained with H&E except **E** (PAS&H).

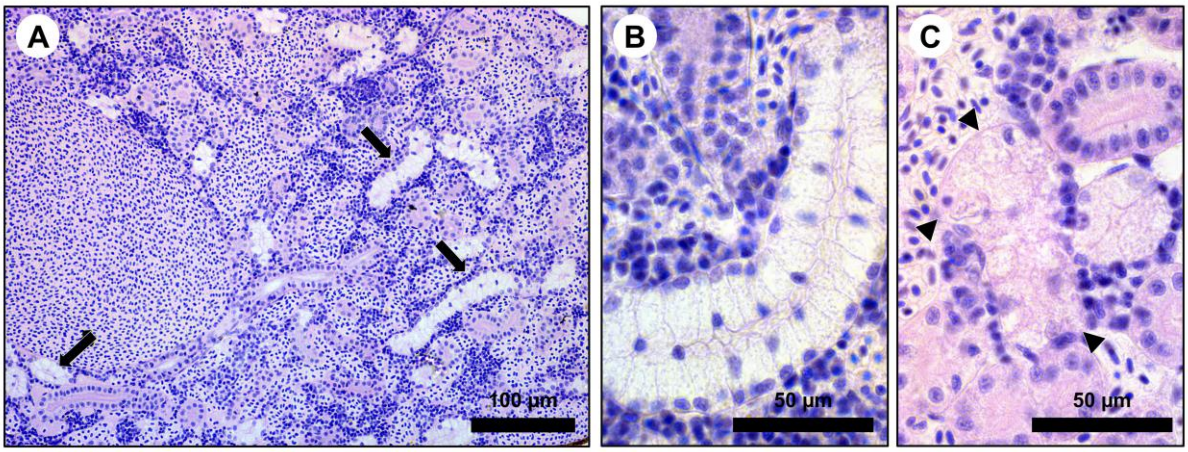

Figure 6.6 – Histopathological alterations in kidneys of F0 adult zebrafish exposed to DFC, B[*a*]P and corresponding mixtures during embryonic development. **A)** Cloudy swelling (hydropic degeneration) of the renal tubule cells (arrows) and a severe hyperaemia and haemorrhage in a zebrafish exposed to mixture B[*a*]P 0.4 µM + DFC 0.3 µM. **B)** Detail of a renal tubule with cell hydropic degeneration from a zebrafish exposed to B[*a*]P 1.98E-4 µM. **C)** Detail of renal tubule (arrowheads) in a most advanced stage of hydropic degeneration of renal tubules in animals that had been subjected to DFC-only treatments (3.14E-4 µM). All sections stained with H&E.

In F0 adults the immunohistochemical signal for PCNA was considerably fainter than in juveniles, although the organs that exhibited the most significant alterations remained the same, i.e., intestine and kidney (for original split-channel images see examples in Figure B1.2 in Appendix to Chapter 6). Contrary to juveniles, no signal was detected in the intestinal epithelium of control zebrafish (Figure 6.7A). Conversely, reduced signal was detected in adult fish previously subjected to the single-toxicant treatments, specifically, in intestinal epithelia of animals exposed to lower DFC and the highest B[*a*]P concentrations (Figure 6.7B), plus in animals exposed to several mixtures of toxicants, albeit in any case without a clear dose-response pattern. Still, fish subjected to mixtures tended to yield higher signal for PCNA (Figure 6.7C, D). In the kidneys, we noted a reduced but conspicuous signal in control zebrafish (Figure 6.8A), which curiously decreased in fish that had been subjected to B[*a*]P-only treatments (Figure 6.8B). The same mixtures identified with the highest signal in intestine, were the ones that yielded increased regulation of PCNA comparatively to control, in both nephrogenic zone and renal tubule epithelia (Figure 6.8C, D), once again without a clear dose-response pattern.

As for F0 juveniles, the liver, kidney and intestinal epithelia were the most affected tissues in adults. The juxtaposition of histopathological alterations and PCNA regulation (Table 6.2) emphasised the mixture of the lowest concentrations of either toxicant (B[*a*]P 1.98E-4 µM + DFC 3.14E-4 µM) as the treatment with responsible for the most significant alterations.

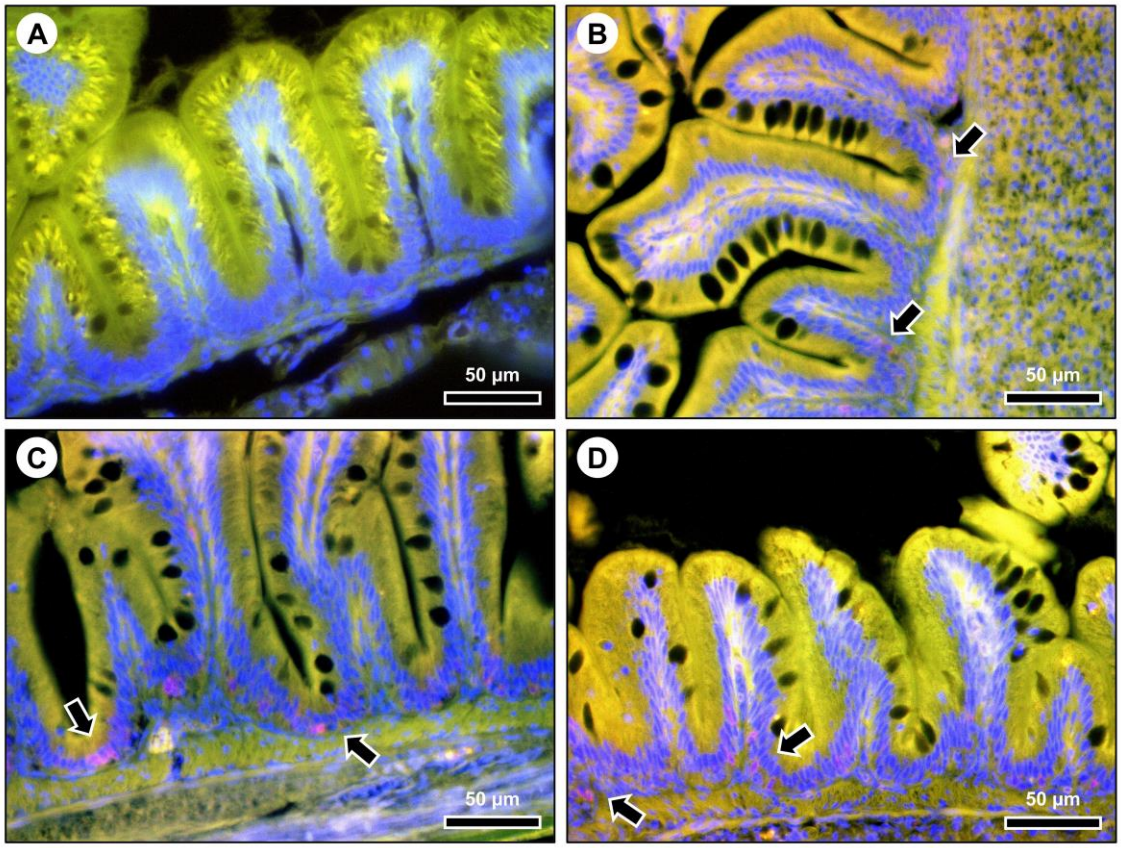

Figure 6.7 – Immunostaining of PCNA in intestinal epithelia of adult F0 zebrafish. Arrows localise of the red-labelled probe in nuclei, often in conjunction with DAPI. **A)** Control zebrafish (no signal. **B)** Intestine epithelium from a fish exposed during embryogenesis to the highest concentration of B[*a*]P (0.4 µM) with low levels of PCNA expression. Animals exposed to mixtures **C)** B[*a*]P 1.98E-4 µM + DFC 0.3 µM and **D)** B[*a*]P 0.4 µM + DFC 3.14E-4 µM presented the highest levels of PCNA regulation.

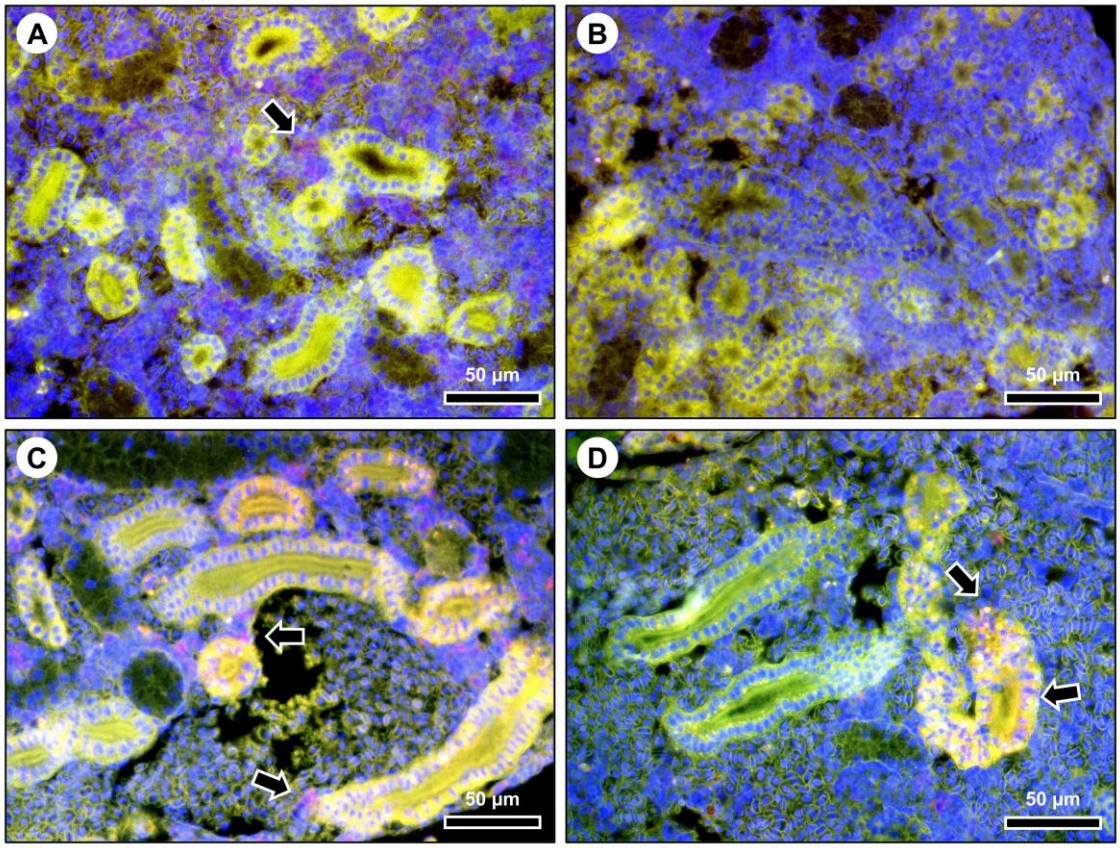

Figure 6.8 – Immunostaining of PCNA in kidney of adult F0 zebrafish. Arrows localise of the red-labelled probe in nuclei, often in conjunction with DAPI. **A)** Control zebrafish with low signal. **B)** Kidney from a zebrafish exposed to the highest concentration of B[*a*]P (0.4 µM) without PCNA signal, what means a decreasing of PCNA expression relatively to control. Animals exposed to mixtures **C)** B[*a*]P 1.98E-4 µM + DFC 0.3 µM and **D)** B[*a*]P 0.4 µM + DFC 3.14E-4 µM presented the highest levels of PCNA regulation, comparatively to control.

Table 6.2 - Anti-PCNA antibody signal and histopathological traits in target organs relatively to controls. The table summarises the results from adult F0 zebrafish exposed to DFC and B[*a*]P, isolated and combined, during embryonic development.

	Intestinal epithelium	**Kidney**	**Liver**
DFC 3.14E-4 µM	+	= (a)	=
B[*a*]P 1.98E-4 µM	=	- (a)	= (a)
DFC 0.3 µM	=	= (a)	= (a)
B[*a*]P 0.4 µM	+	- (a)	=
B[*a*]P 1.98E-4 µM + DFC 3.14E-4 µM	+	= (a)	= (a)
B[*a*]P 1.98E-4 µM + DFC 0.3 µM	+ +	+ (a)	=
B[*a*]P 0.4 µM + DFC 3.14E-4 µM	+ +	+ (a)	=
B[*a*]P 0.4 µM + DFC 0.3 µM	=	= (a)	= (a)

"=" similar to controls; "+" PCNA up-regulation; "-" PCNA down-regulation; "(a)" recurrent histopathological alterations (namely nuclear pleomorphisms, hyperaemia, apoptotic cell, haemorrhage and hydropic degeneration)

6.4.3 Reproductive performance of the parental generation and the consequences for first filial generation embryos

Zebrafish F0 breeders showed overall good reproductive performance, with the exception of animals that had been subjected to individual B[*a*]P treatments, namely the for the highest B[*a*]P concentration (0.4 µM), which simultaneously, revealed a decline of 30% in fertilization and ≈40% in spawning rates, relatively to control. Whereas male gonads did not show significant histopathological lesions (Figure 6.9A), female gonads endured scant histopathological alterations compared with control (Figure 6.9B). Alterations in female gonads were restricted to an increase in lipofuscin deposits in oogonia, occasionally associated to small inflammatory foci (Figure 6.9C), plus large encapsulated yellow-brownish agglomerates of lipofuscin (Figure 6.9D). These alterations only were found in females that had been exposed to isolated DFC and B[*a*]P treatments plus the mixture of higher concentrations (B[*a*]P 0.4 µM + DFC 0.3 µM).

In generation F1 zebrafish embryos, the most significant deformities (recorded *in vivo* at 96 hpf) were pericardial cavity and yolk-sac oedemas, typically accompanied by severe spinal curvature and curved tails. However, deformities were noted already at 24 hpf, when some embryos presented delayed development, defective somitogenesis and head malformation with absent formation of eve. At 24 hpf, the normal embryo rate was lower in embryos from parents exposed to low concentrations of isolated DFC (3.14E-4 µM) and B[*a*]P (1.98E-4 µM) however, after 96 hpf the F1 embryos exposed to DFC 0.3 µM and B[*a*]P 0.4 µM (highest individual concentrations) showed the lowest rate.

Hierarchical clustering associated treatments and endpoints two main clusters each. While mixture treatments were clustered with the control (Figure 6.10 – blue cluster); exposure to individual contaminants, regardless of concentration, were grouped together (Figure 6.10 – red cluster). The latter comprised two subclusters, where exposure to the higher B[*a*]P concentration (0.4 µM) was placed afar. The segregation of the former seemingly reflects significantly lower endpoints in most cases, from spawning and fertilization to survival at 96 hpf. Overall, the adverse effects linked to both F0 adult couples and F1 embryos were higher in animals subjected to individual DFC and B[*a*]P exposures than mixture treatments, despite the high survival rate of F1 embryos after 96 hpf (≈80%) for all treatments, including controls.

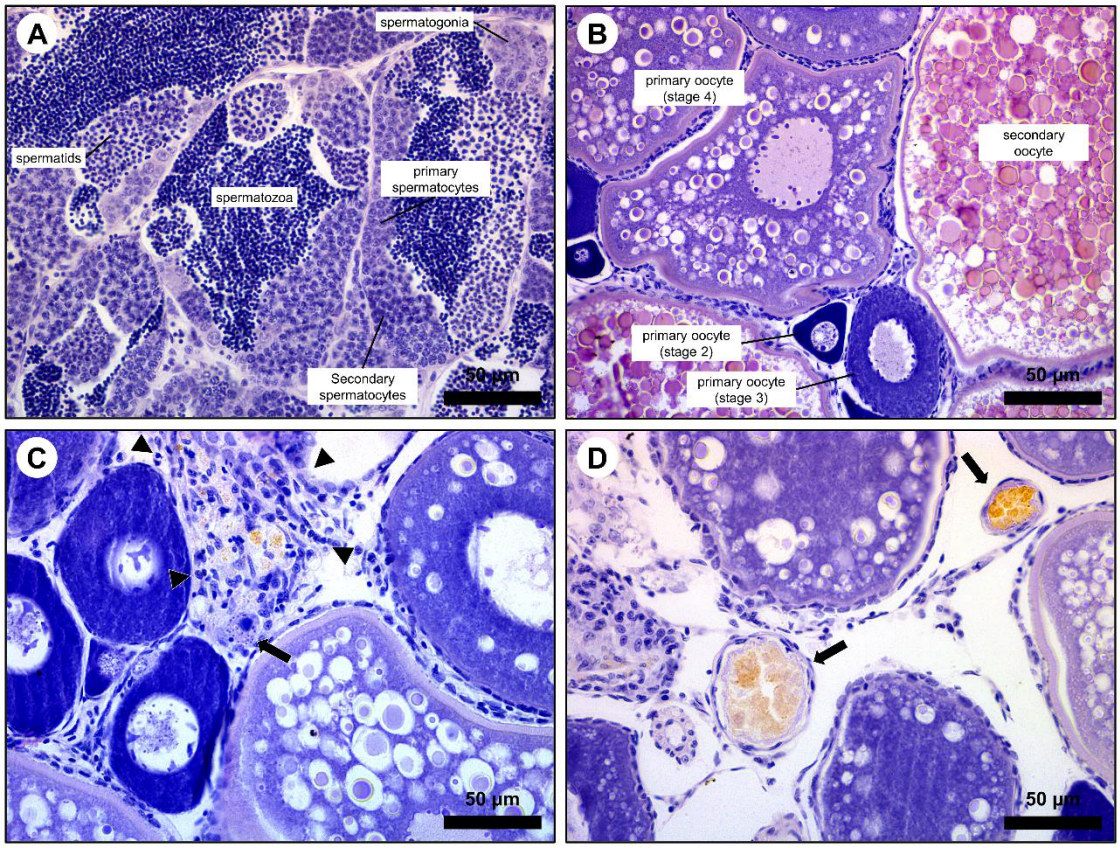

Figure 6.9 – Histopathological alterations in the gonads of F0 zebrafish exposed during embryonic stage to DFC and B[*a*]P, isolated and combined, after the couples are used in crosses to obtain the F1 embryos. Male gonads did not show any alterations relatively to controls **(A).** However, comparatively to controls **(B)**, female gonads presented significant alterations. **C)** Females exposed to individual DFC and B[*a*]P treatments plus the mixture with higher concentrations (B[*a*]P 0.4 µM + DFC 0.3 µM) presented increased lipofuscin deposits occasionally associated to small inflammatory foci (between arrowheads), with visible recruitment of macrophages (arrow). **D)** Encapsulated yellow-brownish agglomerates of lipofuscin in a female from mixture of higher concentrations (B[*a*]P 0.4 µM + DFC 0.3 µM). All sections stained with H&E.

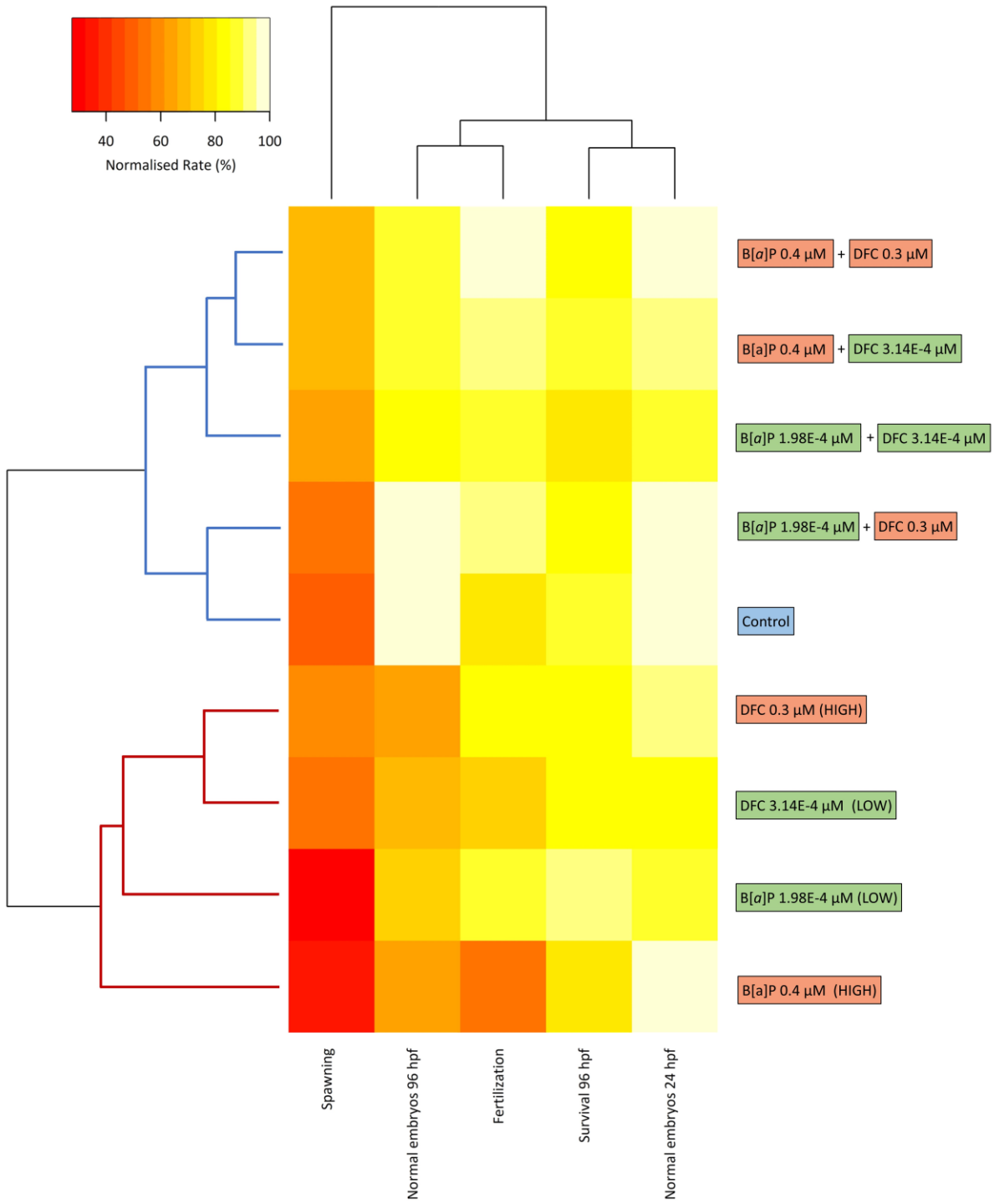

Figure 6.10 – Heatmap and hierarchical clustering of experimental conditions and endpoints determined in zebrafish exposed to DFC, B[*a*]P and their combination during embryonic development: spawning and fertilization rates of F0 breeders; plus normal embryos at 24 and 96 hpf rates, and survival rate of fertilized eggs after embryonic development associated to F1 embryos. Clustering was done through Ward's method employing Euclidean distances as metric.

6.5 Discussion

Even though environmental contamination by complex mixtures of chemicals is arguably the most realistic scenario, risk assessment approaches are most often directed to single substances. In addition, many other aspects than can potentially modulate the consequences of environmental, or occupational, exposure to pollutants besides mixtures and dose. One of such factors is the stage of the life cycle during which exposure occurs and the carryover of effects into reproductive adulthood and eventually onto offspring, which is altogether more critical when addressing the problem of mutagens, as shown by the present study. Our results showed that not only can the toxicants interact and produce unexpected outcomes, but also that there can be significant carryover of effects from parental (F0) to offspring (F1) generations, even in a case where exposure was limited to a short period of time during embryonic development of F0 zebrafish.

Zebrafish (F0) that were co-exposed to DFC and B[*a*]P during embryonic phase failed to show a clear trend for the amplification or attenuation of effects in animal development until reach adulthood when compared with individual treatments. Contrariwise, exposure to individual toxicants seems to have higher implications in reproductive performance and therefore on the success of offspring than DFC and B[*a*]P mixtures which may indicate an antagonistic effect under these circumstances of exposure. Altogether, the results indicate that the short-term embryo exposure to DFC and B[*a*]P, isolated or combined, can produce chronic affects in zebrafish affecting both F0 and F1 generations even under realistic conditions of assessment, suggesting transgenerational carryover. In fact, the F1 embryos from F0 zebrafish subjected to the lowest concentrations of individual toxicants, i.e., the EU EQS levels for surface waters, revealed critical histopathological effects after the absence of visible effects in F0 larvae acutely exposed to same concentrations (see Chapter 5).

Liver, kidney and intestine epithelia were the most affected organs in both juvenile and adults of the parental generation (F0). It must be emphasized, though, that the kidney displayed histopathological alterations, like hydropic degeneration of renal tubules and hyperaemia, while enduring PCNA up-regulation (thus suggesting cell proliferation). Hydropic degeneration, found namely in F0 adults, is caused by fluid retention in cells that, in turn, occurs due to changes in intracellular osmotic potential, e.g., due to alterations in ion transport through the plasmalemma. This can be explained by the downregulation of biological processes linked to ion transport reported in Chapter 5, in zebrafish embryos acutely exposed to DFC, isolated and combined with B[*a*]P, despite the difference in DFC concentration (eight times more in acute exposure). Interestingly, although the hydropic degeneration was most progressed in F0 adults from the DFC-only treatment (recall Figure 6C), the simultaneity of histopathological alterations and PCNA upregulation only occurs in some mixtures (involving the highest concentrations of B[*a*]P and DFC) but without signs of inflammation. Therefore, PCNA upregulation in the nephrogenic zone adjacent to renal tubules can actually be related with DNA replication and repair mechanisms instead of cell proliferation. Knowing the important role of PCNA in DNA replication and repair, as a central protein in both DNA processes (Essers et al., 2005), a higher

incidence of this biomarker can lead to tissue regeneration after damage, in this case possibly caused by both B[*a*]P and DFC exposure. Also, the direct combination of the highest concentrations (B[*a*]P 0.4 µM + DFC 0.3 µM) caused, in juveniles, a sizable increase in PCNA regulation in kidneys and intestinal epithelia. At the same time, it caused critical histopathological alterations like hepatic hyperaemia and increased frequency of nuclear pleomorphisms. This setting would indicate an amplification of effects and likely an increased response to exposure, leading to increased effort to promote cell survival and DNA repair. In fact, our previous work showed that embryos co-exposed to DFC and B[*a*]P endured up-regulation of biologic processes linked to DNA replication (see Chapter 5 for more information). This upregulation of PCNA not association to cell proliferation corroborates the hypothesis that chronic exposure can inconspicuously lead to changes potentially only detected at the genetic level. Altogether, this calls attention to a better understanding of the mechanisms behind chronic environmental/occupational exposure and its impacts in the incidence of diseases like cancer.

In both juvenile and adult zebrafish co-exposed to DFC and B[*a*]P, the findings indicate an important degree of variability that ultimately results in unclear dose-effect responsiveness. Such variation should, at least in part, be explained by intricate toxicokinetics and toxicodynamics, especially under relatively low doses and short duration of exposure. Nonetheless, there is a global tendency towards antagonism in animals exposed to mixture of lowest concentrations of both contaminants. As an illustrative example, zebrafish exposed to this mixture did not yield the severe hydropic degeneration in kidney verified in animals exposed to the low DFC concentration, suggesting an attenuation of toxicopathic effects by co-exposure with B[*a*]P. In fact, the renal toxicity of DFC is reported by several clinical human studies (see review Ungprasert et al., 2015) and animals as vultures (Oaks et al., 2004) or rats where was identified a severe degeneration kidney tubules (Aycan et al., 2018). As other COX2 inhibitor, DFC promote the reduction of renal prostaglandins that have an important role in tubular transport (G.-H. Kim, 2008). In turn, B[*a*]P can promote the transcription of COX2 and the increase of prostaglandins levels via binding of NF-kβ to DNA (Yan et al., 2000), originate a point of interaction between B[*a*]P and DFC. However, exposure to mixture of lowest concentrations and to the low isolated B[*a*]P (1.98E-4 µM) treatments share a key histopathologic alteration that is the increased frequency of pleomorphic nuclei in hepatocytes. This alteration has long been considered a hallmark of carcinogenesis, which, in this case, can be reasonably linked to the B[*a*]P ability of promoting cell proliferation and neoplasia (see for instance Denissenko et al., 1996; Nebert et al., 2000; Ross & Nesnow, 1999). It has, inclusively, been positively associated with PCNA up-regulation by Akyol et al. (1999), however in this study no PCNA upregulation was registered in livers, even in treatments where pleomorphic nuclei in hepatocytes were observed.

In adults that had been exposed to lowest individual B[*a*]P concentration, we also noted increased presence of inflammatory cells, predominantly macrophages, in the portal area. Indeed, the zebrafish liver has resident macrophages (known as Kupffer cells in mammals) that eliminate noxious compounds and pathogens while promoting the recruitment of peripheral immune cells like monocyte-derived macrophages (Shwartz et al., 2019). Liver macrophages may also contribute to limit the

progression of hepatocellular carcinoma, then shifting towards the promotion of cell proliferation (Tian et al., 2019). Another interesting occurrence was finding an adult fish that had been exposed to this low concentration of B[*a*]P (isolated) revealed a particular anomaly in the mouth, where the lower jaw protruding past the upper jaw. Keer et al. (2019) linked similar alterations with hyperthyroidism, a condition that Movahedinia et al. (2018) reported to occur in the fish *Liza abu* exposed to B[*a*]P. Rurale et al. (2022) also reported B[*a*]P affecting the thyroid function in zebrafish, however with a tendency to cause hypothyroidism. All these findings illustrate that B[*a*]P can affect multiple functions in fish and likely other vertebrates, which also helps explaining the variability of effects.

Co-exposure to DFC and B[*a*]P followed a visibly antagonistic trend in key aspects such as the reproductive performance of F0 animals or developmental effects in F1 embryos. Conversely, the reproductive performance was clearly affected by B[*a*]P-only exposure, even at lower concentrations, resulting then in affected both spawning and fertilization. Gao et al. (2018) already described a significant reduction of reproductive performance in zebrafish exposed to relatively low concentrations (0.0126–12.6 µg/L) of B[*a*]P during embryonic development, in fact close to the lowest concentration tested in the present study (0.05 µg/L). However, histopathological alterations in gonads were found by us to be limited to lipofuscin deposits in females that had been exposed to individual DFC and B[*a*]P, plus mixture of higher concentrations (B[*a*]P 0.4 µM + DFC 0.3 µM). These alterations can be linked with the final stage of atresia, which, it must be recalled, is defined as a normal process of degeneration and resorption of unviable follicles (see Miranda et al., 1999). Still, there is a variety of xenobiotics that may increase the level of follicular atresia (e.g., Vidal & Dixon, 2018), with implications to reproductive performance. Curiously, some authors reported this alteration in rats exposed to B[*a*]P to be triggered by hormonal disturbances (Jorge et al., 2021). It must at this stage be recalled that we registered cases of oocyte degeneration in juveniles previously exposed to B[*a*]P-only treatments.

Most importantly, the offspring embryos (F1) resulting from couples exposed to individual B[*a*]P revealed a high rate of deformities and other deviations to the normal embryonic development, including dorsal curvature and pericardial oedema. This is consistent with the alterations reported by Gao et al. (2018) in embryos whose parental generation had been exposed to B[*a*]P during embryonic development, which reiterates transgenerational carryover of effects. Such effects may be explained by alterations to the DNA molecule, as expected to occur following exposure to potent mutagens (and teratogens) like B[*a*]P. In our study, parental (F0) exposure to DFC also resulted in increased deformity rates in the offspring (F1), as oedemas in pericardial cavity and yolk-sac or spinal curvature, suggesting important carryover of teratogenic effects, an issue that should be further investigated in the future. Still, according to Chen et al. (2014), DFC teratogenicity to zebrafish may indeed occur, as the compound, can inhibit genes involved in development of the cardiovascular and nervous systems and cause malformations similar to the pathologic alterations seen in F1 embryos.

6.6 Conclusions

Despite the short-term exposure to the model toxicants B[*a*]P and DFC, isolated or combined, during zebrafish embryonic stages, the current study showed not only the retention of toxicopathic effects in juveniles and reproductive adults but also transgenerational carryover of effects to the offspring, translated into developmental malformations and reduced reproductive success. This occurrence can be due to changes to the DNA molecule (via mutagenesis), but this issue needs further research. Very importantly, some of the effects retained in adults can be regarded primary markers of neoplasia, in fish exposed to B[*a*]P and some mixtures. The toxicodynamics of these binary mixtures, which combined a carcinogen and an anti-inflammatory agent, therefore with potentially antagonistic effects are complex and prone to significant variability under the circumstances of exposure, which can hinder risk assessment and dilute dose- and time-responsiveness. Still, there are indications that the modulation of regulators of cell cycle like PCNA can bear an opposite trend to tissue-level lesions and alterations by action of DCF, which controls inflammation by tackling the response to oxidative radicals. Most importantly these effects are clearly delayed following exposure. Altogether we demonstrated realistic exposure to mixtures of these model and ubiquitous toxicants can be heavily affected by life stage, with exposure during developmental phases bearing serious consequences not only for the entire life cycle of the individual but also for the offspring generation, even in scenarios were biomarkers of exposure to potent carcinogens like B[*a*]P should indicate low risk for the individual.

7

CONCLUDING REMARKS

The health status of an individual results from the balance between exposure and defence against endogenous and exogenous agents, among which complex mixtures of noxious chemicals of environmental origin are included. However, the concept of exposome is not exhausted within the lifetime of an organism. Rather, there is a growing understanding that factors affecting the germline of ancestors can have a profound impact on the offspring and therefore on the fitness of entire populations. Environmental risk assessment is therefore a challenging enterprise that should be holistic whether is applies to ecosystem, human health or the rim between the two, as they are unavoidably link, as conceptualised through the “One Health” concept upheld by the World Health Organization. In addition, it must be emphasised that ecotoxicologists were major players in introducing, developing and applying modern approaches to risk assessment rooted in the Systems Biology framework, from ‘omics’ and bioinformatics to drawing adverse outcome pathways and ultimately attempting to model the outcomes of exposure to noxious chemicals under realistically challenging scenarios.

The current work focused on understanding the mechanistic of toxicant interactions by investigating the alterations triggered by co-exposure to two ubiquitous model toxicants, the non-steroidal anti-inflammatory drug (NSAID) diclofenac (DFC) and the carcinogenic PAH benzo[*a*]pyrene (B[*a*]P), representatives of emerging and legacy pollutants, respectively. Aiming at the human-environment interface, we selected biological models that are acknowledged adequate surrogates, namely the HepG2 human hepatoma cell line (the *in vitro* model) and the growing biomedical model, the zebrafish (*Danio rerio* – AB strain), especially the embryo (*in vivo* model). In addition, the deployment of these models enabled performing multiple binary mixtures that included realistic concentrations of exposure while ensuring a significant number of biological replicates. Most importantly, the high level of genomic resources for these models, with emphasis on the zebrafish, permitted exploring mechanistic toxicology using “omics” and computational biology and study effects during the life cycle.

The current work showed that the two model toxicants elicit different responses in either model and that co-exposure causes effects that can surpass additivity into the domain of antagonism. These findings have important implications for environmental risk assessment, especially under circumstances of assessment that implied realistic concentrations. Nonetheless, the findings also showed that before

dwelling into the complex mechanisms underneath exposure to mixed toxicants, we must understand the effects of each individual compounds. In the zebrafish model, the current study showed that exposure to the legacy pollutant B[*a*]P tended to cause to chronic effects that can lead to the carryover of adverse consequences to future generations via damage to the DNA molecule. However, the expanding of effects to the offspring is a novel subject that needs further research. In fact, as expected the genotoxicity of B[*a*]P was undoubtedly more relevant than the DFC both *in vitro* (HepG2 cells) and *in vivo* (zebrafish), indicated the possibility of a high degree of mutagenesis that can be linked to adverse chronic alterations. In zebrafish, this hypothesis was notoriously demonstrated not only by the severe reduction of reproductive performance of F0 generation but also by the developmental malformations in F1 embryos. It is worth highlighting that, in the generational *in vivo* assay, these effects resulted from a short period of exposure during the embryonic phase of F0 animals and even at relatively low concentrations, namely the EU EQS levels for surface waters. These important results also highlight the sensitivity of early life stages to pollutants and that even short-term exposures during early development can imply serious chronic effects to adults and even their offspring. In turn, the emerging pollutant DFC revealed acute and chronic toxicity that varies with the exposure concentration in either model, although in HepG2 cells DFC was less cytotoxic than B[*a*]P. The zebrafish embryo acute assays showed higher mortality and malformation rates caused by concentrations of DFC equivalent to highly/contaminated surface waters. At low concentrations (as the EU EQS levels for surface waters), DFC caused chronic alterations in F0 juveniles and adults and severe malformations in F1 embryos despite, unlike B[*a*]P, the absence of effects in F0 reproductive performance. These data confirm that NSAIDs are extremely toxic to aquatic organisms.

Co-exposure to B[*a*]P and DFC, as other contaminant mixtures reported in available literature, triggered a complex pattern of effects that depends on biological model, dose, exposure time and endpoint. The present work showed complex toxicodynamics and even more complex mechanistics of interaction. In general, the results from co-exposure of zebrafish (acute and generational chronic assays) and HepG2 cells to DFC and B[*a*]P consistently revealed antagonistic effects, i.e., the mixture effects were lower than the combination of the individual effects caused by exposure to DFC and B[*a*]P. In brief, the cytotoxicity was lower in HepG2 cells exposed to mixtures than to individual contaminants (Chapter 3); in zebrafish embryos, mortality and malformation rates indicated a low degree of toxicity in animals that were subjected to mixture treatments (Chapter 5). Finally, the effects in reproductive performance of F0 and the embryonic development of F1 generation were found to be less compromised in fish that had been exposed to mixtures (Chapter 6). Genotoxicity was the most obvious consequence impacted by antagonistic effects of co-exposure in both HepG2 cells and zebrafish embryos. It should be highlighted that the Comet assay is a very versatile and expeditious technique to evaluate DNA damage in models as distinct as cell cultures, tissue and even in *in vivo*, as we proved after the protocol optimization for use in zebrafish embryos (Chapter 4). Still, it should be noted that some of the adverse outcomes (AOs) leaned towards simple additivity. We may refer, for instance, to in the induction of reactive oxygen species (ROS) in HepG2 cells, independently of dose or exposure time (Chapter 3).

Simultaneously, histopathological traits in zebrafish larva (96 hpf) from acute assays were consistently similar to those observed in animals from DFC individual treatments, namely those subjected to the highest concentrations (Chapter 5).

After integrating the results from the three major toxicant interaction studies in this thesis, we can conclude that the interaction between B[*a*]P and DFC was denoted in AOs derived from *in vivo* and *in vitro* toxicity evaluation. Co-exposure in of zebrafish enabled the possibility to investigate interactions at the molecular level. Through computational tools , transcriptomics and the crosslink between molecular alterations and effects we may indicate two potential adverse outcome pathways (AOPs) in animals exposed to combined DFC and B[*a*]P. The first one is linked to needs further enhancement ocular deformation and is associated with the underexpression of important genes related with eye development and eye degeneration diseases. A second AOP permitted tracing molecular events down inflammation, linking cell cycle arrest and apoptosis via p53 and MAPK pathways, to verified downstream toxicopathological effects such as DNA damage and formation of oedemas. Additionally, we found that some molecular pathways that ceased to be affected upon co-exposure, namely some processes associated to RNA degradation, cell proliferation, apoptosis and cell-cycle control, altogether pointing once more to an antagonistic interaction between DFC and B[*a*]P that, nonetheless, need further investigation. The short-term exposure during embryonic stages, alterations to molecular pathways were sufficient to trigger traceable toxicopathological effects in F0 juveniles and adults, with repercussions for F1 embryos from the intergenerational experiment. However, the toxicodynamics and underlying mechanisms of these binary mixtures, which combined a carcinogen and an anti-inflammatory agent, therefore with potentially antagonistic effects are complex and need further enhancement and validation, as well as the projected AOPs here proposed. Exploring transcriptomics in animals subjected to further doses and their concentrations, as well as investigating changes in gene expression and their protein products along the organism's different life stages would be critical to refine and validate novel AOPs.

An important outcome of the work relates to the indication that the modulation of cell cycle regulators like PCNA can bear an opposite trend to tissue-level lesions and alterations by action of DCF, which controls inflammation by tackling the response to oxidative radicals. In turn, the induction of DNA damage and ROS in HepG2, indicated a potential interference of molecular processes related to inflammatory process and subsequent unbalancing of cell survival and proliferation in co-exposure scenarios. In fact, our findings demonstrate that exposure to mixed toxicants whose mode-of-action (MOA) and detoxification pathways may partly overlap, as DFC and B[*a*]P via cytochrome P450 (CYP) oxidases, can produce unexpected outcomes hindering risk assessment. In the future, it would be of highest interest to further infer about the potential competition for cytochrome P450 bindings sites. In addition, using transcriptomics and proteomics in HepG2 cells to reconstruct molecular pathways underlying co-exposure and compare these to the findings from the zebrafish model. This strategy would provide paramount information on the applicability of HepG2 cells for environmental risk assessment of

mixtures ultimately aiming at human occupational health. Nonetheless, the zebrafish model already provided important hints on AOPs that should be considered in other vertebrate models and humans.

In association with these final questions, it is important to mention that the global outcomes of the work permitted inferring on the potential of *in vitro* testing for toxicity testing of for mixtures. Altogether, we may reiterate that reinforce that at least hepatoma cell lines can be consistent models to obtain expeditiously a first toxicity screening of complex sets of binary mixtures or other combinations of toxicants and explore several exposure scenarios, including multiple doses. This screening can then be used as a potent tool to refine research towards mechanism and modelling of effects using *in vivo* models such as the zebrafish.

REFERENCES

Ablain, J., & Zon, L. I. (2013). Of fish and men: using zebrafish to fight human diseases. *Trends in Cell Biology*, *23*(12), 584–586. https://doi.org/10.1016/j.tcb.2013.09.009

Adisasmito, W. B., Almuhairi, S., Behravesh, C. B., Bilivogui, P., Bukachi, S. A., Casas, N., Cediel Becerra, N., Charron, D. F., Chaudhary, A., Ciacci Zanella, J. R., Cunningham, A. A., Dar, O., Debnath, N., Dungu, B., Farag, E., Gao, G. F., Hayman, D. T. S., Khaitsa, M., Koopmans, M. P. G., … Zhou, L. (2022). One Health: A new definition for a sustainable and healthy future. *PLOS Pathogens*, *18*(6), e1010537. https://doi.org/10.1371/journal.ppat.1010537

Akyol, G., Dursun, A., Poyraz, A., Uluoglu, Ö., Ataoglu, Ö., Edalý, N., & Memis, L. (1999). P53 and proliferating cell nuclear antigen (PCNA) expression in non-tumoral liver diseases. *Pathology International*, *49*(3), 214–221. https://doi.org/10.1046/j.1440-1827.1999.00849.x

Allan, S. E., Smith, B. W., Tanguay, R. L., & Anderson, K. A. (2012). Bridging environmental mixtures and toxic effects. *Environmental Toxicology and Chemistry*, *31*(12), 2877–2887. https://doi.org/10.1002/etc.2018.Bridging

Alnahdi, A., John, A., & Raza, H. (2019). Augmentation of Glucotoxicity, Oxidative Stress, Apoptosis and Mitochondrial Dysfunction in HepG2 Cells by Palmitic Acid. *Nutrients*, *11*(9), 1979. https://doi.org/10.3390/nu11091979

Al-Salmani, K., Abbas, H. H. K., Schulpen, S., Karbaschi, M., Abdalla, I., Bowman, K. J., So, K. K., Evans, M. D., Jones, G. D. D., Godschalk, R. W., & Cooke, M. S. (2011). Simplified method for the collection, storage, and comet assay analysis of DNA damage in whole blood. *Free Radical Biology and Medicine*, *51*(3), 719–725. https://doi.org/10.1016/j.freeradbiomed.2011.05.020

Altenburger, R., Scholz, S., Schmitt-Jansen, M., Busch, W., & Escher, B. I. (2012). Mixture toxicity revisited from a toxicogenomic perspective. *Environmental Science and Technology*, *46*(5), 2508–2522. https://doi.org/10.1021/es2038036

Ankley, G. T., Bennett, R. S., Erickson, R. J., Hoff, D. J., Hornung, M. W., Johnson, R. D., Mount, D. R., Nichols, J. W., Russom, C. L., Schmieder, P. K., Serrrano, J. A., Tietge, J. E., & Villeneuve, D. L. (2010). Adverse outcome pathways: A conceptual framework to support ecotoxicology

research and risk assessment. *Environmental Toxicology and Chemistry*, *29*(3), 730–741. https://doi.org/10.1002/etc.34

Aoki, T., Frosen, J., Fukuda, M., Bando, K., Shioi, G., Tsuji, K., Ollikainen, E., Nozaki, K., Laakkonen, J., & Narumiya, S. (2017). Prostaglandin E2-EP2-NF-κB signaling in macrophages as a potential therapeutic target for intracranial aneurysms. *Science Signaling*, *10*(465), 1–18. https://doi.org/10.1126/scisignal.aah6037

Arisan, E. D., Ergül, Z., Bozdağ, G., Rencüzoğulları, Ö., Çoker-Gürkan, A., Obakan-Yerlikaya, P., Coşkun, D., & Palavan-Ünsal, N. (2018). Diclofenac induced apoptosis via altering PI3K/Akt/MAPK signaling axis in HCT 116 more efficiently compared to SW480 colon cancer cells. *Molecular Biology Reports*, *45*(6), 2175–2184. https://doi.org/10.1007/s11033-018-4378-2

Arman, N. Z., Salmiati, S., Aris, A., Salim, M. R., Nazifa, T. H., Muhamad, M. S., & Marpongahtun, M. (2021). A review on emerging pollutants in the water environment: Existences, health effects and treatment processes. *Water (Switzerland)*, *13*(22), 1–31. https://doi.org/10.3390/w13223258

Ashfaq, M., Nawaz Khan, K., Saif Ur Rehman, M., Mustafa, G., Faizan Nazar, M., Sun, Q., Iqbal, J., Mulla, S. I., & Yu, C. P. (2017). Ecological risk assessment of pharmaceuticals in the receiving environment of pharmaceutical wastewater in Pakistan. *Ecotoxicology and Environmental Safety*, *136*(October 2016), 31–39. https://doi.org/10.1016/j.ecoenv.2016.10.029

aus der Beek, T., Weber, F.-A., Bergmann, A., Hickmann, S., Ebert, I., Hein, A., & Küster, A. (2016). Pharmaceuticals in the environment-Global occurrences and perspectives. *Environmental Toxicology and Chemistry*, *35*(4), 823–835. https://doi.org/10.1002/etc.3339

Aycan, İ. Ö., Elpek, Ö., Akkaya, B., Kıraç, E., Tuzcu, H., Kaya, S., Coşkunfırat, N., & Aslan, M. (2018). Diclofenac induced gastrointestinal and renal toxicity is alleviated by thymoquinone treatment. *Food and Chemical Toxicology*, *118*, 795–804. https://doi.org/10.1016/j.fct.2018.06.038

Azqueta, A., & Collins, A. R. (2013). The essential comet assay: a comprehensive guide to measuring DNA damage and repair. *Archives of Toxicology*, *87*(6), 949–968. https://doi.org/10.1007/s00204-013-1070-0

Babich, H., Sardanaand, M. K., & Borenfreund, E. (1988). Acute cytotoxicities of polynuclear aromatic hydrocarbons determined *in vitro* with the human liver tumor cell line, HepG2. *Cell Biology and Toxicology*, *4*(3), 295–309. https://doi.org/10.1007/BF00058738

Basu, A. K. (2018). DNA damage, mutagenesis and cancer. *International Journal of Molecular Sciences*, *19*(4). https://doi.org/10.3390/ijms19040970

Bauer, E., Zeldin, D., Guo, Z., Ueng, Y. F., Bell, L. C., & Guengerich, F. P. (1995). Oxidation of Benzo[a]pyrene by Recombinant Human Cytochrome P450 Enzymes. *Chemical Research in Toxicology*, *8*(1), 136–142. https://doi.org/10.1021/tx00043a018

Belpaeme, K., Cooreman, K., & Kirsch-volders, M. (1998). Development and validation of the *in vivo* alkaline comet assay for detecting genomic damage in marine flatfish. *Genetic Toxicology and Environmental Mutagenesis*, *415*(3), 167–184. https://doi.org/10.1016/S1383-5718(98)00062-X

Bernanke, J., & Köhler, H.-R. (2009). The Impact of Environmental Chemicals on Wildlife Vertebrates. In *Reviews of Environmental Contamination and Toxicology Volume 198* (Vol. 198, pp. 1–47). Springer New York. https://doi.org/10.1007/978-0-387-09647-6_1

Beronius, A., Zilliacus, J., Hanberg, A., Luijten, M., van der Voet, H., & van Klaveren, J. (2020). Methodology for health risk assessment of combined exposures to multiple chemicals. *Food and Chemical Toxicology*, *143*(July), 111520. https://doi.org/10.1016/j.fct.2020.111520

Boehmer-Christiansen, S. (1995). The Politics of the European Environment Policy. *Energy & Environment*, *6*(3), 169–195. http://www.jstor.org/stable/43734266

Boelsterli, U. A. (2003). Diclofenac-induced liver injury: A paradigm of idiosyncratic drug toxicity. *Toxicology and Applied Pharmacology*, *192*, 307–322. https://doi.org/10.1016/S0041-008X(03)00368-5

Boiteux, S., & Jinks-Robertson, S. (2013). DNA repair mechanisms and the bypass of DNA damage in Saccharomyces cerevisiae. *Genetics*, *193*(4), 1025–1064. https://doi.org/10.1534/genetics.112.145219

Boobis, A., Budinsky, R., Collie, S., Crofton, K., Embry, M., Felter, S., Hertzberg, R., Kopp, D., Mihlan, G., Mumtaz, M., Price, P., Solomon, K., Teuschler, L., Yang, R., & Zaleski, R. (2011). Critical analysis of literature on low-dose synergy for use in screening chemical mixtures for risk assessment. In *Critical Reviews in Toxicology* (Vol. 41, Issue 5, pp. 369–383). https://doi.org/10.3109/10408444.2010.543655

Bopp, S. K., Kienzler, A., Richarz, A. N., van der Linden, S. C., Paini, A., Parissis, N., & Worth, A. P. (2019). Regulatory assessment and risk management of chemical mixtures: challenges and ways forward. In *Critical Reviews in Toxicology* (Vol. 49, Issue 2, pp. 174–189). Taylor and Francis Ltd. https://doi.org/10.1080/10408444.2019.1579169

Borgert, C. J. (2007). Predicting interactions from mechanistic information: Can omic data validate theories? *Toxicology and Applied Pharmacology*, *223*(2), 114–120. https://doi.org/10.1016/j.taap.2007.01.002

Bort, R., Ponsoda, X., Jover, R., Gómez-Lechón, M. J., & Castell, J. V. (1999). Diclofenac toxicity to hepatocytes: a role for drug metabolism in cell toxicity. *The Journal of Pharmacology and Experimental Therapeutics*, *288*(1), 65–72. http://www.ncbi.nlm.nih.gov/pubmed/9862754

Boström, C. E., Gerde, P., Hanberg, A., Jernström, B., Johansson, C., Kyrklund, T., Rannug, A., Törnqvist, M., Victorin, K., & Westerholm, R. (2002). Cancer risk assessment, indicators, and

guidelines for polycyclic aromatic hydrocarbons in the ambient air. *Environmental Health Perspectives*, *110*(SUPPL. 3), 451–488. https://doi.org/10.1289/ehp.110-1241197

Bray, N. L., Pimentel, H., Melsted, P., & Pachter, L. (2016). Near-optimal probabilistic RNA-seq quantification. *Nature Biotechnology*, *34*(5), 525–527. https://doi.org/10.1038/nbt.3519

Brown, L., & Benchimol, S. (2006). The Involvement of MAPK Signaling Pathways in Determining the Cellular Response to p53 Activation. *Journal of Biological Chemistry*, *281*(7), 3832–3840. https://doi.org/10.1074/jbc.M507951200

Burkina, V., Sakalli, S., Pilipenko, N., Zlabek, V., & Zamaratskaia, G. (2018). Effect of human pharmaceuticals common to aquatic environments on hepatic CYP1A and CYP3A-like activities in rainbow trout (Oncorhynchus mykiss): An *in vitro* study. *Chemosphere*, *205*, 380–386. https://doi.org/10.1016/j.chemosphere.2018.04.080

Canzler, S., & Hackermüller, J. (2020). multiGSEA: a GSEA-based pathway enrichment analysis for multi-omics data. *BMC Bioinformatics*, *21*(1), 1–13. https://doi.org/10.1186/s12859-020-03910-x

Carlson, M. (2019). *org.Dr.eg.db: Genome wide annotation for Zebrafish. R package version 3.8.2.* https://bioconductor.org/packages/release/data/annotation/html/org.Dr.eg.db.html

Cassee, F. R., Groten, J. P., Van Bladeren, P. J., & Feron, V. J. (1998). Toxicological evaluation and risk assessment of chemical mixtures. *Critical Reviews in Toxicology*, *28*(1), 73–101. https://doi.org/10.1080/10408449891344164

Cavalieri, E. L., & Rogan, E. G. (1992). The approach to understanding aromatic hydrocarbon carcinogenesis. The central role of radical cations in metabolic activation. *Pharmacology and Therapeutics*, *55*(2), 183–199. https://doi.org/10.1016/0163-7258(92)90015-R

Chapman, P. M. (2007). Determining when contamination is pollution — Weight of evidence determinations for sediments and effluents. *Environment International*, *33*(4), 492–501. https://doi.org/10.1016/j.envint.2006.09.001

Chen, J. Bin, Gao, H. W., Zhang, Y. L., Zhang, Y., Zhou, X. F., Li, C. Q., & Gao, H. P. (2014). Developmental toxicity of diclofenac and elucidation of gene regulation in zebrafish (Danio rerio). *Scientific Reports*, *4*, 1–7. https://doi.org/10.1038/srep04841

Chen, H., Feng, W., Chen, K., Qiu, X., Xu, H., Mao, G., Zhao, T., Ding, Y., & Wu, X. (2019). Transcriptomic analysis reveals potential mechanisms of toxicity in a combined exposure to dibutyl phthalate and diisobutyl phthalate in zebrafish (Danio rerio) ovary. *Aquatic Toxicology*, *216*(May), 105290. https://doi.org/10.1016/j.aquatox.2019.105290

Chen, M., Zhang, M., Borlak, J., & Tong, W. (2012). A decade of toxicogenomic research and its contribution to toxicological science. *Toxicological Sciences*, *130*(2), 217–228. https://doi.org/10.1093/toxsci/kfs223

Chen, Q., Wang, Y., Yang, L., Sun, L., Wen, Y., Huang, Y., Gao, K., Yang, W., Bai, F., Ling, L., Zhou, Z., Zhang, X., Xiong, J., & Zhai, R. (2022). PM2.5 promotes NSCLC carcinogenesis through translationally and transcriptionally activating DLAT-mediated glycolysis reprograming. *Journal of Experimental & Clinical Cancer Research*, *41*(1), 229. https://doi.org/10.1186/s13046-022-02437-8

Chiappini, F., Coilly, A., Kadar, H., Gual, P., Tran, A., Desterke, C., Samuel, D., Duclos-Vallée, J.-C., Touboul, D., Bertrand-Michel, J., Brunelle, A., Guettier, C., & le Naour, F. (2017). Metabolism dysregulation induces a specific lipid signature of nonalcoholic steatohepatitis in patients. *Scientific Reports*, *7*(November 2016), 1–17. https://doi.org/10.1038/srep46658

Clippinger, A. J., Allen, D., Behrsing, H., BéruBé, K. A., Bolger, M. B., Casey, W., DeLorme, M., Gaça, M., Gehen, S. C., Glover, K., Hayden, P., Hinderliter, P., Hotchkiss, J. A., Iskandar, A., Keyser, B., Luettich, K., Ma-Hock, L., Maione, A. G., Makena, P., … Jarabek, A. M. (2018). Pathway-based predictive approaches for non-animal assessment of acute inhalation toxicity. *Toxicology in Vitro*, *52*, 131–145. https://doi.org/10.1016/j.tiv.2018.06.009

Collins, A. R. (2004). The Comet Assay for DNA Damage and Repair: Principles, Applications, and Limitations. *Molecular Biotechnology*, *26*(3), 249–261. https://doi.org/10.1385/MB:26:3:249

Collins, A. R., Oscoz, A. A., Brunborg, G., Gaivao, I., Giovannelli, L., Kruszewski, M., Smith, C. C., & Stetina, R. (2008). The comet assay: topical issues. *Mutagenesis*, *23*(3), 143–151. https://doi.org/10.1093/mutage/gem051

Conner, E. M., & Grisham, M. B. (1996). Inflammation, free radicals and antioxidants. In *Nutrition* (Vol. 12, Issue 4, pp. 274–277). https://doi.org/10.1016/S0899-9007(96)00000-8

Costa, P. M. (2022). Current aspects of DNA damage and repair in ecotoxicology: a mini-review. *Ecotoxicology*, *31*(1), 1–11. https://doi.org/10.1007/s10646-021-02487-2

Costa, P. M., Chicano-Gálvez, E., Caeiro, S., Lobo, J., Martins, M., Ferreira, A. M., Caetano, M., Vale, C., Alhama-Carmona, J., Lopez-Barea, J., DelValls, T. À., & Costa, M. H. (2012). Hepatic proteome changes in Solea senegalensis exposed to contaminated estuarine sediments: A laboratory and in situ survey. *Ecotoxicology*, *21*(4), 1194–1207. https://doi.org/10.1007/s10646-012-0874-7

Costa, P. M., Chicano-Gálvez, E., López Barea, J., Delvalls, T. A., & Costa, M. H. (2010). Alterations to proteome and tissue recovery responses in fish liver caused by a short-term combination treatment with cadmium and benzo[a]pyrene. *Environmental Pollution*, *158*(10), 3338–3346. https://doi.org/10.1016/j.envpol.2010.07.030

Costa, P. M., & Fadeel, B. (2016). Emerging systems biology approaches in nanotoxicology: Towards a mechanism-based understanding of nanomaterial hazard and risk. *Toxicology and Applied Pharmacology*, *299*, 101–111. https://doi.org/10.1016/j.taap.2015.12.014

Costa, P. M., Gosens, I., Williams, A., Farcal, L., Pantano, D., Brown, D. M., Stone, V., Cassee, F. R., Halappanavar, S., & Fadeel, B. (2018). Transcriptional profiling reveals gene expression changes associated with inflammation and cell proliferation following short-term inhalation exposure to copper oxide nanoparticles. *Journal of Applied Toxicology*, *38*(3), 385–397. https://doi.org/10.1002/jat.3548

Costa, P. M., Lobo, J., Caeiro, S., Martins, M., Ferreira, A. M., Caetano, M., Vale, C., DelValls, T. Á., & Costa, M. H. (2008). Genotoxic damage in Solea senegalensis exposed to sediments from the Sado Estuary (Portugal): Effects of metallic and organic contaminants. *Mutation Research - Genetic Toxicology and Environmental Mutagenesis*, *654*(1), 29–37. https://doi.org/10.1016/j.mrgentox.2008.04.007

Costa, P. M., Milhinhos, A., Simões, M., Marum, L., Oliveira, A. M., Costa, M. H., & Miguel, C. (2012). Determining DNA strand breakage from embryogenic cell cultures of a conifer species using the single-cell gel electrophoresis assay. *Tree Genetics and Genomes*, *8*(2), 425–430. https://doi.org/10.1007/s11295-011-0434-y

Curtis, L. R., Bravo, C. F., Bayne, C. J., Tilton, F., Arkoosh, M. R., Lambertini, E., Loge, F. J., Collier, T. K., Meador, J. P., & Tilton, S. C. (2017). Transcriptional changes in innate immunity genes in head kidneys from Aeromonas salmonicida-challenged rainbow trout fed a mixture of polycyclic aromatic hydrocarbons. *Ecotoxicology and Environmental Safety*, *142*(November 2016), 157–163. https://doi.org/10.1016/j.ecoenv.2017.03.044

Dahm, R., Schonthaler, H. B., Soehn, A. S., van Marle, J., & Vrensen, G. F. J. M. (2007). Development and adult morphology of the eye lens in the zebrafish. *Experimental Eye Research*, *85*(1), 74–89. https://doi.org/10.1016/j.exer.2007.02.015

Dasgupta, S., Cao, A., Mauer, B., Yan, B., Uno, S., & McElroy, A. (2014). Genotoxicity of oxy-PAHs to Japanese medaka (Oryzias latipes) embryos assessed using the comet assay. *Environmental Science and Pollution Research*, *21*(24), 13867–13876. https://doi.org/10.1007/s11356-014-2586-4

Dat, N. D., & Chang, M. B. (2017). Review on characteristics of PAHs in atmosphere, anthropogenic sources and control technologies. *Science of the Total Environment*, *609*, 682–693. https://doi.org/10.1016/j.scitotenv.2017.07.204

David, A., Lange, A., Abdul-Sada, A., Tyler, C. R., & Hill, E. M. (2017). Disruption of the Prostaglandin Metabolome and Characterization of the Pharmaceutical Exposome in Fish Exposed to Wastewater Treatment Works Effluent As Revealed by Nanoflow-Nanospray Mass Spectrometry-Based Metabolomics. *Environmental Science and Technology*, *51*(1), 616–624. https://doi.org/10.1021/acs.est.6b04365

Denissenko, M. F., Pao, A., Tang, M. S., & Pfeifer, G. P. (1996). Preferential formation of benzo[a]pyrene adducts at lung cancer mutational hotspots in P53. *Science*, *274*(5286), 430–432. https://doi.org/10.1126/science.274.5286.430

Desaulniers, D., Xiao, G. H., Lian, H., Feng, Y.-L., Zhu, J., Nakai, J., & Bowers, W. J. (2009). Effects of mixtures of polychlorinated biphenyls, methylmercury, and organochlorine pesticides on hepatic DNA methylation in prepubertal female sprague-dawley rats. *International Journal of Toxicology*, *28*(4), 294–307. https://doi.org/10.1177/1091581809337918

Destoumieux-Garzón, D., Mavingui, P., Boetsch, G., Boissier, J., Darriet, F., Duboz, P., Fritsch, C., Giraudoux, P., le Roux, F., Morand, S., Paillard, C., Pontier, D., Sueur, C., & Voituron, Y. (2018). The One Health Concept: 10 Years Old and a Long Road Ahead. *Frontiers in Veterinary Science*, *5*. https://doi.org/10.3389/fvets.2018.00014

di Bucchianico, S., Cappellini, F., le Bihanic, F., Zhang, Y., Dreij, K., & Karlsson, H. L. (2017). Genotoxicity of TiO2 nanoparticles assessed by mini-gel comet assay and micronucleus scoring with flow cytometry. *Mutagenesis*, *32*(1), 127–137. https://doi.org/10.1093/mutage/gew030

Ding, R., Jin, Y., Liu, X., Zhu, Z., Zhang, Y., Wang, T., & Xu, Y. (2016). Characteristics of DNA methylation changes induced by traffic-related air pollution. *Mutation Research - Genetic Toxicology and Environmental Mutagenesis*, *796*, 46–53. https://doi.org/10.1016/j.mrgentox.2015.12.002

Doll, R. (1955). Mortality from lung cancer in asbestos workers. *British Journal of Industrial Medicine*, *12*, 81–86. https://doi.org/10.1136/oem.12.2.81

Dreij, K., Mattsson, Å., Jarvis, I. W. H., Lim, H., Hurkmans, J., Gustafsson, J., Bergvall, C., Westerholm, R., Johansson, C., & Stenius, U. (2017). Cancer Risk Assessment of Airborne PAHs Based on *in Vitro* Mixture Potency Factors. *Environmental Science and Technology*, *51*(15), 8805–8814. https://doi.org/10.1021/acs.est.7b02963

Du, H., Pan, B., & Chen, T. (2017). Evaluation of chemical mutagenicity using next generation sequencing: A review. *Journal of Environmental Science and Health - Part C Environmental Carcinogenesis and Ecotoxicology Reviews*, *35*(3), 140–158. https://doi.org/10.1080/10590501.2017.1328831

Duca, R.-C., Grova, N., Ghosh, M., Do, J.-M., Hoet, P. H. M., Vanoirbeek, J. A. J., Appenzeller, B. M. R., & Godderis, L. (2018). Exposure to Polycyclic Aromatic Hydrocarbons Leads to Non-monotonic Modulation of DNA and RNA (hydroxy)methylation in a Rat Model. *Scientific Reports*, *8*(1), 1–9. https://doi.org/10.1038/s41598-018-28911-y

Durinck, S., Spellman, P. T., Birney, E., & Huber, W. (2009). Mapping identifiers for the integration of genomic datasets with the R/Bioconductor package biomaRt. *Nature Protocols*, *4*(8), 1184–1191. https://doi.org/10.1038/nprot.2009.97

Duval, A. P., Troquier, L., Silva, O. D. S., Demartines, N., & Dormond, O. (2019). Diclofenac potentiates sorafenib-based treatments of hepatocellular carcinoma by enhancing oxidative stress. *Cancers*, *11*(10). https://doi.org/10.3390/cancers11101453

EEA. (2018). *European waters Assessment of status and pressures 2018. Report Nº 7/2018* (Issue 7). https://doi.org/10.2800/303664

EEA. (2019). *EEA SIGNALS 2019, Land and soil in Europe*. https://doi.org/10.2800/779710

EEA. (2022). *Air quality in Europe 2022, Report Nº 05/2022*. https://doi.org/10.2800/488115

Ellepola, N., Viera, T., Patidar, P. L., & Rubasinghege, G. (2022). Fate, transformation and toxicological implications of environmental diclofenac: Role of mineralogy and solar flux. *Ecotoxicology and Environmental Safety*, *246*. https://doi.org/10.1016/j.ecoenv.2022.114138

Escher, B. I., Baumgartner, R., Koller, M., Treyer, K., Lienert, J., & McArdell, C. S. (2011). Environmental toxicology and risk assessment of pharmaceuticals from hospital wastewater. *Water Research*, *45*(1), 75–92. https://doi.org/10.1016/j.watres.2010.08.019

Essers, J., Theil, A. F., Baldeyron, C., van Cappellen, W. A., Houtsmuller, A. B., Kanaar, R., & Vermeulen, W. (2005). Nuclear Dynamics of PCNA in DNA Replication and Repair. *Molecular and Cellular Biology*, *25*(21), 9350–9359. https://doi.org/10.1128/MCB.25.21.9350-9359.2005

European Commission/UNIDO. (2019). *TOXICSITES identification programe - Initial site screening (ISS) protocol*. https://www.unido.org/sites/default/files/files/2019-10/TSIP%20Handbook%202019_0.pdf

Evrard, E., Marchand, J., Theron, M., Pichavant-Rafini, K., Durand, G., Quiniou, L., & Laroche, J. (2010). Impacts of mixtures of herbicides on molecular and physiological responses of the European flounder Platichthys flesus. *Comparative Biochemistry and Physiology - C Toxicology and Pharmacology*, *152*(3), 321–331. https://doi.org/10.1016/j.cbpc.2010.05.009

Faraway, J. J. (2010). Generalized linear models. *International Encyclopedia of Education*, 178–183. https://doi.org/10.1016/B978-0-08-044894-7.01331-2

Fenech, M., Knasmueller, S., Bolognesi, C., Holland, N., Bonassi, S., & Kirsch-Volders, M. (2020). Micronuclei as biomarkers of DNA damage, aneuploidy, inducers of chromosomal hypermutation and as sources of pro-inflammatory DNA in humans. *Mutation Research - Reviews in Mutation Research*, *786*, 108342. https://doi.org/10.1016/j.mrrev.2020.108342

Ferrari, B., Paxéus, N., Giudice, R. lo, Pollio, A., & Garric, J. (2003). Ecotoxicological impact of pharmaceuticals found in treated wastewaters: Study of carbamazepine, clofibric acid, and diclofenac. *Ecotoxicology and Environmental Safety*, *55*(3), 359–370. https://doi.org/10.1016/S0147-6513(02)00082-9

Ferreira, A. L. G., Loureiro, S., & Soares, A. M. V. M. (2008). Toxicity prediction of binary combinations of cadmium, carbendazim and low dissolved oxygen on Daphnia magna. *Aquatic Toxicology*, *89*(1), 28–39. https://doi.org/10.1016/j.aquatox.2008.05.012

Fetting, C. (2020). *"The European Green Deal", ESDN Report, December 2020 ESDN Office, Vienna*.

Fischer, J. M. F., Zubel, T., Jander, K., Fix, J., Trussina, I. R. E. A., Gebhard, D., Bergemann, J., Bürkle, A., & Mangerich, A. (2018). PARP1 protects from benzo[a]pyrene diol epoxide-induced replication stress and mutagenicity. *Archives of Toxicology*, *92*(3), 1323–1340. https://doi.org/10.1007/s00204-017-2115-6

Franzellitti, S., Buratti, S., Valbonesi, P., & Fabbri, E. (2013). The mode of action (MOA) approach reveals interactive effects of environmental pharmaceuticals on Mytilus galloprovincialis. *Aquatic Toxicology*, *140–141*, 249–256. https://doi.org/10.1016/j.aquatox.2013.06.005

Fredriksson, L., Herpers, B., Benedetti, G., Matadin, Q., Puigvert, J. C., de Bont, H., Dragovic, S., Vermeulen, N. P. E., Commandeur, J. N. M., Danen, E., de Graauw, M., & van de Water, B. (2011). Diclofenac inhibits tumor necrosis factor-α-induced nuclear factor-κB activation causing synergistic hepatocyte apoptosis. *Hepatology*, *53*(6), 2027–2041. https://doi.org/10.1002/hep.24314

Fuller, R., Landrigan, P. J., Balakrishnan, K., Bathan, G., Bose-O'Reilly, S., Brauer, M., Caravanos, J., Chiles, T., Cohen, A., Corra, L., Cropper, M., Ferraro, G., Hanna, J., Hanrahan, D., Hu, H., Hunter, D., Janata, G., Kupka, R., Lanphear, B., … Yan, C. (2022). Pollution and health: a progress update. *The Lancet Planetary Health*, *6*(6), e535–e547. https://doi.org/10.1016/S2542-5196(22)00090-0

Galland, C., Dupuy, C., Loizeau, V., Danion, M., Auffret, M., Quiniou, L., Laroche, J., & Pichereau, V. (2015). Proteomic analysis of the European flounder Platichthys flesus response to experimental PAH-PCB contamination. *Marine Pollution Bulletin*, *95*(2), 646–657. https://doi.org/10.1016/j.marpolbul.2015.04.038

Gan, T. J. (2010). Diclofenac: An update on its mechanism of action and safety profile. *Current Medical Research and Opinion*, *26*(7), 1715–1731. https://doi.org/10.1185/03007995.2010.486301

Gao, D., Lin, J., Ou, K., Chen, Y., Li, H., Dai, Q., Yu, Z., Zuo, Z., & Wang, C. (2018). Embryonic exposure to benzo(a)pyrene inhibits reproductive capability in adult female zebrafish and correlation with DNA methylation. *Environmental Pollution*, *240*, 403–411. https://doi.org/10.1016/j.envpol.2018.04.139

Gao, D., Wang, C., Xi, Z., Zhou, Y., Wang, Y., & Zuo, Z. (2017). Early-life benzo[a]pyrene exposure causes neurodegenerative syndromes in adult zebrafish (Danio rerio) and the mechanism involved. *Toxicological Sciences*, *157*(1), 74–84. https://doi.org/10.1093/toxsci/kfx028

Genies, C., Maître, A., Lefèbvre, E., Jullien, A., Chopard-Lallier, M., & Douki, T. (2013). The extreme variety of genotoxic response to benzo[a]pyrene in three different human cell lines from three different organs. *PLoS ONE*, *8*(11), 1–11. https://doi.org/10.1371/journal.pone.0078356

Giacomini, K. M., Yee, S. W., Mushiroda, T., Weinshilboum, R. M., Ratain, M. J., & Kubo3, M. (2017). Genome-wide Association Studies of Drug Response and Toxicity: An Opportunity for Genome Medicine. *Nature Reviews in Drug Discovery*, *16*(1), 1–8. https://doi.org/10.1038/nrd.2016.234

Gill, J. S., Georgiou, M., Kalitzeos, A., Moore, A. T., & Michaelides, M. (2019). Progressive cone and cone-rod dystrophies: clinical features, molecular genetics and prospects for therapy. *British Journal of Ophthalmology*, *103*(5), 711–720. https://doi.org/10.1136/bjophthalmol-2018-313278

Gómez-Oliván, L. M., Galar-Martínez, M., García-Medina, S., Valdés-Alanís, A., Islas-Flores, H., & Neri-Cruz, N. (2014). Genotoxic response and oxidative stress induced by diclofenac, ibuprofen and naproxen in *Daphnia magna*. *Drug and Chemical Toxicology*, *37*(4), 391–399. https://doi.org/10.3109/01480545.2013.870191

Gonçalves, C., Martins, M., Diniz, M. S., Costa, M. H., Caeiro, S., & Costa, P. M. (2014). May sediment contamination be xenoestrogenic to benthic fish? A case study with Solea senegalensis. *Marine Environmental Research*, *99*, 170–178. https://doi.org/10.1016/j.marenvres.2014.04.012

Gonsioroski, A., Mourikes, V. E., & Flaws, J. A. (2020). Endocrine Disruptors in Water and Their Effects on the Reproductive System. *International Journal of Molecular Sciences*, *21*(6), 1929. https://doi.org/10.3390/ijms21061929

Gonzalez-Rey, M., & Bebianno, M. J. (2014). Effects of non-steroidal anti-inflammatory drug (NSAID) diclofenac exposure in mussel Mytilus galloprovincialis. *Aquatic Toxicology*, *148*, 818–831. https://doi.org/10.1016/j.aquatox.2014.01.011

Granitzny, A., Knebel, J., Müller, M., Braun, A., Steinberg, P., Dasenbrock, C., & Hansen, T. (2017). Evaluation of a human *in vitro* hepatocyte-NPC co-culture model for the prediction of idiosyncratic drug-induced liver injury: A pilot study. *Toxicology Reports*, *4*, 89–103. https://doi.org/10.1016/j.toxrep.2017.02.001

Grillo, M. P., Knutson, C. G., Sanders, P. E., Waldon, D. J., Hua, F., & Ware, J. A. (2003). Studies on the chemical reactivity of diclofenac acyl glucuronide with glutathione: identification of diclofenac-S-acyl-glutathione in rat bile. *Drug Metabolism and Disposition*, *31*(11), 1327–1336. https://doi.org/10.1124/dmd.31.11.1327

Harada, M. (1995). Minamata disease: Methylmercury poisoning in Japan caused by environmental pollution. *Critical Reviews in Toxicology*, *25*(1), 1–24. https://doi.org/10.3109/10408449509089885

Harding, S. M., Benci, J. L., Irianto, J., Discher, D. E., Minn, A. J., & Greenberg, R. A. (2017). Mitotic progression following DNA damage enables pattern recognition within micronuclei. *Nature*, *548*(7668), 466–470. https://doi.org/10.1038/nature23470

Hartmann, A., Erkman, L., Maremanda, N., Elhajouji, A., & Martus, H. J. (2021). Comprehensive review of genotoxicity data for diclofenac. *Mutation Research - Genetic Toxicology and Environmental Mutagenesis*, *866*(February), 503347. https://doi.org/10.1016/j.mrgentox.2021.503347

Hartwig, A. (2013). Cadmium and Cancer. In *Sigel, A., Sigel, H., Sigel, R. (eds) Cadmium: From Toxicity to Essentiality. Metal Ions in Life Sciences* (Vol. 11, pp. 491–507). Springer. https://doi.org/10.1007/978-94-007-5179-8_15

Hayes, A. W., Li, R., Hoeng, J., Iskandar, A., Peistch, M. C., & Dourson, M. L. (2019). New approaches to risk assessment of chemical mixtures. *Toxicology Research and Application*, *3*, 239784731882076. https://doi.org/10.1177/2397847318820768

Heberer, T. (2002). Occurrence, fate, and removal of pharmaceutical residues in the aquatic environment: A review of recent research data. *Toxicology Letters*, *131*(1–2), 5–17. https://doi.org/10.1016/S0378-4274(02)00041-3

Henn, K., & Braunbeck, T. (2011). Dechorionation as a tool to improve the fish embryo toxicity test (FET) with the zebrafish (Danio rerio). *Comparative Biochemistry and Physiology - C Toxicology and Pharmacology*, *153*(1), 91–98. https://doi.org/10.1016/j.cbpc.2010.09.003

Heo, Y. J., Choi, S. E., Jeon, J. Y., Han, S. J., Kim, D. J., Kang, Y., Lee, K. W., & Kim, H. J. (2019). Visfatin Induces Inflammation and Insulin Resistance via the NF- κ B and STAT3 Signaling Pathways in Hepatocytes. *Journal of Diabetes Research*, *2019*. https://doi.org/10.1155/2019/4021623

Hernández, A. F., Gil, F., & Lacasaña, M. (2017). Toxicological interactions of pesticide mixtures: an update. *Archives of Toxicology*, *91*(10), 3211–3223. https://doi.org/10.1007/s00204-017-2043-5

Herrmann, R., Lobanova, E. S., Hammond, T., Kessler, C., Burns, M. E., Frishman, L. J., & Arshavsky, V. Y. (2010). Phosducin regulates transmission at the photoreceptor-to-ON-bipolar cell synapse. *Journal of Neuroscience*, *30*(9), 3239–3253. https://doi.org/10.1523/JNEUROSCI.4775-09.2010

Hong, H. N., Kim, H. N., Park, K. S., Lee, S.-K., & Gu, M. B. (2007). Analysis of the effects diclofenac has on Japanese medaka (Oryzias latipes) using real-time PCR. *Chemosphere*, *67*(11), 2115–2121. https://doi.org/10.1016/j.chemosphere.2006.12.090

Hood, L., Heath, J. R., Phelps, M. E., & Lin, B. (2004). Systems biology and new technologies enable predictive and preventative medicine. *Science*, *306*(5696), 640–643. https://doi.org/10.1126/science.1104635

Hooven, L. A., & Baird, W. M. (2008). Proteomic analysis of MCF-7 cells treated with benzo[a]pyrene, dibenzo[a,l]pyrene, coal tar extract, and diesel exhaust extract. *Toxicology*, *249*(1), 1–10. https://doi.org/10.1016/j.tox.2008.03.019

Howe, K., Clark, M. D., Torroja, C. F., Torrance, J., Berthelot, C., Muffato, M., Collins, J. E., Humphray, S., McLaren, K., Matthews, L., McLaren, S., Sealy, I., Caccamo, M., Churcher, C., Scott, C., Barrett, J. C., Koch, R., Rauch, G.-J., White, S., … Stemple, D. L. (2013). The zebrafish reference genome sequence and its relationship to the human genome. *Nature*, *496*(7446), 498–503. https://doi.org/10.1038/nature12111

Hu, M.-L., Chuang, C.-H., Sio, H.-M., & Yeh, S.-L. (2002). Simple cryoprotection and cell dissociation techniques for application of the comet assay to fresh and frozen rat tissues. *Free Radical Research*, *36*(2), 203–209. https://doi.org/10.1080/10715760290006420

Huang, D. W., Sherman, B. T., & Lempicki, R. A. (2009a). Bioinformatics enrichment tools: Paths toward the comprehensive functional analysis of large gene lists. *Nucleic Acids Research*, *37*(1), 1–13. https://doi.org/10.1093/nar/gkn923

Huang, D. W., Sherman, B. T., & Lempicki, R. A. (2009b). Systematic and integrative analysis of large gene lists using DAVID bioinformatics resources. *Nature Protocols*, *4*(1), 44–57. https://doi.org/10.1038/nprot.2008.211

Hughes, M. F. (2002). Arsenic toxicity and potential mechanisms of action. *Toxicology Letters*, *133*(1), 1–16. https://doi.org/10.1016/S0378-4274(02)00084-X

IARC. (1983). *IARC monografs on the evaluation of the carcinogenic risk of chemicals to humans*. *32*.

IARC. (1993). *Beryllium, cadmium, mercury, and exposures in the glass manufacturing industry - IARC Monographs on the Evaluation of Carcinogenic Risks to Humans* (Vol. 58).

IARC. (2017). *Some Organophosphate Insecticides and Herbicides IARC Monographs on the Evaluation of Carcinogenic Risks to Humans Volume112*. https://publications.iarc.fr/549

Ihaka, R., & Gentleman, R. (1996). R: A Language for Data Analysis and Graphics. *Journal of Computational and Graphical Statistics*, *5*(3), 299–314. https://doi.org/10.1080/10618600.1996.10474713

Inoue, A., Muranaka, S., Fujita, H., Kanno, T., Tamai, H., & Utsumi, K. (2004). Molecular mechanism of diclofenac-induced apoptosis of promyelocytic leukemia: Dependency on reactive oxygen species, Akt, Bid, cytochrome c, and caspase pathway. *Free Radical Biology and Medicine*, *37*(8), 1290–1299. https://doi.org/10.1016/j.freeradbiomed.2004.07.003

Inoue, K., Mizuo, H., Ishida, T., Komori, T., & Kusano, K. (2020). Bioactivation of diclofenac in human hepatocytes and the proposed human hepatic proteins modified by reactive metabolites. *Xenobiotica*, *50*(8), 919–928. https://doi.org/10.1080/00498254.2020.1728592

Itoh, A., Yaida, A., & Zhu, Y. (2021). Potential Anthropogenic Pollution of High-technology Metals with a Focus on Rare Earth Elements in Environmental Water. *Analytical Sciences*, *37*(1), 131–143. https://doi.org/10.2116/ANALSCI.20SAR16

Jackson, P., Pedersen, L. M., Kyjovska, Z. O., Jacobsen, N. R., Saber, A. T., Hougaard, K. S., Vogel, U., & Wallin, H. (2013). Validation of freezing tissues and cells for analysis of DNA strand break levels by comet assay. *Mutagenesis*, *28*(6), 699–707. https://doi.org/10.1093/mutage/get049

Jennen, D. G. J., Magkoufopoulou, C., Ketelslegers, H. B., van Herwijnen, M. H. M., Kleinjans, J. C. S., & van Delft, J. H. M. (2010). Comparison of HepG2 and HepaRG by Whole-Genome Gene Expression Analysis for the Purpose of Chemical Hazard Identification. *Toxicological Sciences*, *115*(1), 66–79. https://doi.org/10.1093/toxsci/kfq026

Jensen, L. K., Halvorsen, E., Song, Y., Hallanger, I. G., Hansen, E. L., Brooks, S. J., Hansen, B. H., & Tollefsen, K. E. (2016). Individual and molecular level effects of produced water contaminants on nauplii and adult females of Calanus finmarchicus. *Journal of Toxicology and Environmental Health - Part A*, *79*(13–15), 585–601. https://doi.org/10.1080/15287394.2016.1171988

Johnson, A. C., Dumont, E., Williams, R. J., Oldenkamp, R., Cisowska, I., & Sumpter, J. P. (2013). Do concentrations of ethinylestradiol, estradiol, and diclofenac in European rivers exceed proposed EU environmental quality standards? *Environmental Science and Technology*, *47*(21), 12297–12304. https://doi.org/10.1021/es4030035

Jordan, J., Zare, A., Jackson, L. J., Habibi, H. R., & Weljie, A. M. (2012). Environmental contaminant mixtures at ambient concentrations invoke a metabolic stress response in goldfish not predicted from exposure to individual compounds alone. *Journal of Proteome Research*, *11*(2), 1133–1143. https://doi.org/10.1021/pr200840b

Jorge, B. C., Reis, A. C. C., Stein, J., Balin, P. da S., Sterde, É. T., Barbosa, M. G., de Aquino, A. M., Kassuya, C. A. L., & Arena, A. C. (2021). Parental exposure to benzo(a)pyrene in the peripubertal period impacts reproductive aspects of the F1 generation in rats. *Reproductive Toxicology*, *100*, 126–136. https://doi.org/10.1016/j.reprotox.2021.01.011

Jung, S. H., Lee, W., Park, S. H., Lee, K. Y., Choi, Y. J., Choi, S., Kang, D., Kim, S., Chang, T. S., Hong, S. S., & Lee, B. H. (2020). Diclofenac impairs autophagic flux via oxidative stress and lysosomal dysfunction: Implications for hepatotoxicity. *Redox Biology*, *37*, 101751. https://doi.org/10.1016/j.redox.2020.101751

Kajiwara, K., Hahn, L. B., Mukai, S., Travis, G. H., Berson, E. L., & Dryja, T. P. (1991). Mutations in the human retinal degeneration slow gene in autosomal dominant retinitis pigmentosa. *Nature*, *354*(6353), 480–483. https://doi.org/10.1038/354480a0

Kanehisa, M., Goto, S., Sato, Y., Kawashima, M., Furumichi, M., & Tanabe, M. (2014). Data, information, knowledge and principle: Back to metabolism in KEGG. *Nucleic Acids Research*, *42*(D1), D199–D205. https://doi.org/10.1093/nar/gkt1076

Kar, S., & Leszczynski, J. (2019). Exploration of computational approaches to predict the toxicity of chemical mixtures. *Toxics*, *7*(1), 1–18. https://doi.org/10.3390/toxics7010015

Kaur, J., & Sanyal, S. N. (2011). Diclofenac, a selective COX-2 inhibitor, inhibits DMH-induced colon tumorigenesis through suppression of MCP-1, MIP-1α and VEGF. *Molecular Carcinogenesis*, *50*(9), 707–718. https://doi.org/10.1002/mc.20736

Kaur, S., Oddos, T., Tucker-Samaras, S., & D., M. (2013). Regulation of DNA Repair Process by the Pro-Inflammatory NF-κB Pathway. In *New Research Directions in DNA Repair*. InTech. https://doi.org/10.5772/54341

Keer, S., Cohen, K., May, C., Hu, Y., McMenamin, S., & Hernandez, L. P. (2019). Anatomical Assessment of the Adult Skeleton of Zebrafish Reared Under Different Thyroid Hormone Profiles. *The Anatomical Record*, *302*(10), 1754–1769. https://doi.org/10.1002/ar.24139

Kennaway, E. L. (1924). On the cancer-producing factor in tar. *British Medical Journal*, *1*(3300), 564–567. https://doi.org/10.1136/bmj.1.3300.564

Kernaleguen, M., Daviaud, C., Shen, Y., Bonnet, E., Renault, V., Deleuze, J.-F., Mauger, F., & Tost, J. (2018). Whole-Genome Bisulfite Sequencing for the Analysis of Genome-Wide DNA Methylation and Hydroxymethylation Patterns at Single-Nucleotide Resolution. In A. Jeltsch & M. G. Rots (Eds.), *Epigenome Editing: Methods and Protocols, Methods in Molecular Biology 1767* (pp. 311–350). https://doi.org/10.1007/978-1-4939-7774-1_18

Kienzler, A., Bopp, S. K., van der Linden, S., Berggren, E., & Worth, A. (2016). Regulatory assessment of chemical mixtures: Requirements, current approaches and future perspectives. *Regulatory Toxicology and Pharmacology*, *80*, 321–334. https://doi.org/10.1016/j.yrtph.2016.05.020

Kim, G.-H. (2008). Renal Effects of Prostaglandins and Cyclooxygenase-2 Inhibitors. *Electrolyte & Blood Pressure*, *6*(1), 35. https://doi.org/10.5049/EBP.2008.6.1.35

Kim, K.-H., Jahan, S. A., Kabir, E., & Brown, R. J. C. (2013). A review of airborne polycyclic aromatic hydrocarbons (PAHs) and their human health effects. *Environment International*, *60*, 71–80. https://doi.org/10.1016/j.envint.2013.07.019

Kloas, W., Urbatzka, R., Opitz, R., Würtz, S., Behrends, T., Hermelink, B., Hofmann, F., Jagnytsch, O., Kroupova, H., Lorenz, C., Neumann, N., Pietsch, C., Trubiroha, A., van Ballegooy, C.,

Wiedemann, C., & Lutz, I. (2009). Endocrine Disruption in Aquatic Vertebrates. *Annals of the New York Academy of Sciences*, *1163*(1), 187–200. https://doi.org/10.1111/j.1749-6632.2009.04453.x

Knasmüller, S., Parzefall, W., Sanyal, R., Ecker, S., Schwab, C., Uhl, M., Mersch-Sundermann, V., Williamson, G., Hietsch, G., Langer, T., Darroudi, F., & Natarajan, A. T. (1998). Use of metabolically competent human hepatoma cells for the detection of mutagens and antimutagens. *Mutation Research - Fundamental and Molecular Mechanisms of Mutagenesis*, *402*(1–2), 185–202. https://doi.org/10.1016/S0027-5107(97)00297-2

Knecht, A. L., Truong, L., Simonich, M. T., & Tanguay, R. L. (2017). Developmental benzo[a]pyrene (B[a]P) exposure impacts larval behavior and impairs adult learning in zebrafish. *Neurotoxicology and Teratology*, *59*, 27–34. https://doi.org/10.1016/j.ntt.2016.10.006

Kohn, G. E., Rodriguez, K. M., Hotaling, J., & Pastuszak, A. W. (2019). The History of Estrogen Therapy. *Sexual Medicine Reviews*, *7*(3), 416–421. https://doi.org/10.1016/j.sxmr.2019.03.006

Kosmehl, T., Hallare, A. V, Braunbeck, T., & Hollert, H. (2008). DNA damage induced by genotoxicants in zebrafish (Danio rerio) embryos after contact exposure to freeze-dried sediment and sediment extracts from Laguna Lake (The Philippines) as measured by the comet assay. *Mutation Research - Genetic Toxicology and Environmental Mutagenesis*, *650*(1), 1–14. https://doi.org/10.1016/j.mrgentox.2007.09.009

Kosmehl, T., Hallare, A. V, Reifferscheid, G., Manz, W., Braunbeck, T., & Hollert, H. (2006). A novel contact assay for testing genotoxicity of chemicals and whole sediments in zebrafish embryos. *Environmental Toxicology and Chemistry*, *25*(8), 2097–2106. https://doi.org/10.1897/05-460R.1

Ku-Centurión, M., González-Marín, B., Calderón-Ezquerro, M. C., Martínez-Valenzuela, M. C., Maldonado, E., & Calderón-Segura, M. E. (2016). DNA Damage Assessment in Zebrafish Embryos Exposed to Monceren® 250 SC Fungicide Using the Alkaline Comet Assay. *Zebrafish*, *13*(5), 442–448. https://doi.org/10.1089/zeb.2016.1265

Kumar, S., Stecher, G., Li, M., Knyaz, C., & Tamura, K. (2018). MEGA X: Molecular evolutionary genetics analysis across computing platforms. *Molecular Biology and Evolution*, *35*(6), 1547–1549. https://doi.org/10.1093/molbev/msy096

Kumaravel, T. S., & Jha, A. N. (2006). Reliable Comet assay measurements for detecting DNA damage induced by ionising radiation and chemicals. *Mutation Research - Genetic Toxicology and Environmental Mutagenesis*, *605*(1–2), 7–16. https://doi.org/10.1016/j.mrgentox.2006.03.002

Kumaravel, T. S., Vilhar, B., Faux, S. P., & Jha, A. N. (2009). Comet Assay measurements: A perspective. *Cell Biology and Toxicology*, *25*(1), 53–64. https://doi.org/10.1007/s10565-007-9043-9

Lao, Q., Zhang, Q., Qiao, Z., Li, S., Liu, L., Martin, F. L., & Pang, W. (2023). Whole transcriptome sequencing and competitive endogenous RNA regulation network construction analysis in benzo[a]pyrene-treated breast cancer cells. *Science of The Total Environment*, *861*, 160564. https://doi.org/10.1016/j.scitotenv.2022.160564

Lauer, B., Tuschl, G., Kling, M., & Mueller, S. O. (2009). Species-specific toxicity of diclofenac and troglitazone in primary human and rat hepatocytes. *Chemico-Biological Interactions*, *179*(1), 17–24. https://doi.org/10.1016/j.cbi.2008.10.031

Laville, N., Aït-Aïssa, S., Gomez, E., Casellas, C., & Porcher, J. M. (2004). Effects of human pharmaceuticals on cytotoxicity, EROD activity and ROS production in fish hepatocytes. *Toxicology*, *196*(1–2), 41–55. https://doi.org/10.1016/j.tox.2003.11.002

Lawrence, C., Adatto, I., Best, J., James, A., & Maloney, K. (2012). Generation time of zebrafish (Danio rerio) and medakas (Oryzias latipes) housed in the same aquaculture facility. *Lab Animal*, *41*(6), 158–165. https://doi.org/10.1038/laban0612-158

le Bihanic, F., di Bucchianico, S., Karlsson, H. L., & Dreij, K. (2016). *In vivo* micronucleus screening in zebrafish by flow cytometry. *Mutagenesis*, *31*(6), 643–653. https://doi.org/10.1093/mutage/gew032

Lee, R., Kim, G. B., Maruya, K. A., Steinert, S. A., & Oshima, Y. (2000). DNA strand breaks (comet assay) and embryo development effects in grass shrimp (Palaemonetes pugio) embryos after exposure to genotoxicants. *Marine Environmental Research*, *50*(1–5), 553–557. https://doi.org/10.1016/S0141-1136(00)00110-0

Leemann, T., Transon, C., & Dayer, P. (1993). Cytochrome P450TB (CYP2C): A major monooxygenase catalyzing diclofenac 4′-hydroxylation in human liver. *Life Sciences*, *52*(1), 29–34. https://doi.org/10.1016/0024-3205(93)90285-B

Lewandowska, A. M., Rudzki, M., Rudzki, S., Lewandowski, T., & Laskowska, B. (2019). Environmental risk factors for cancer - review paper. *Annals of Agricultural and Environmental Medicine*, *26*(1), 1–7. https://doi.org/10.26444/aaem/94299

Lian, L., Huang, T., Ke, X., Ling, Z., Jiang, W., Wang, Z., Song, S., Li, J., Zhao, Y., Gao, H., Tao, S., Liu, J., & Ma, J. (2022). Globalization-Driven Industry Relocation Significantly Reduces Arctic PAH Contamination. *Environmental Science and Technology*, *56*(1), 145–154. https://doi.org/10.1021/acs.est.1c05198

Lichtensteiger, W., Bassetti-Gaille, C., Faass, O., Axelstad, M., Boberg, J., Christiansen, S., Rehrauer, H., Georgijevic, J. K., Hass, U., Kortenkamp, A., & Schlumpf, M. (2015). Differential gene expression patterns in developing sexually dimorphic rat brain regions exposed to antiandrogenic, estrogenic, or complex endocrine disruptor mixtures: Glutamatergic synapses as target. *Endocrinology*, *156*(4), 1477–1493. https://doi.org/10.1210/en.2014-1504

Liedekerke, M. van, Prokop, G., Rabl-Berger, S., Kibblewhite, M., & Louwagie, G. (2014). *Progress in the management of Contaminated Sites in Europe*. https://doi.org/10.2788/4658

Lim, H., Mattsson, Å., Jarvis, I. W. H., Bergvall, C., Bottai, M., Morales, D. A., Kummrow, F., Umbuzeiro, G. A., Stenius, U., Westerholm, R., & Dreij, K. (2015). Detection of benz[j]aceanthrylene in urban air and evaluation of its genotoxic potential. *Environmental Science and Technology*, *49*(5), 3101–3109. https://doi.org/10.1021/es505458g

Lim, M. S., Lim, P. L. K., Gupta, R., & Boelsterli, U. A. (2006). Critical role of free cytosolic calcium, but not uncoupling, in mitochondrial permeability transition and cell death induced by diclofenac oxidative metabolites in immortalized human hepatocytes. *Toxicology and Applied Pharmacology*, *217*(3), 322–331. https://doi.org/10.1016/j.taap.2006.09.012

Lin, Y. C., Wu, C. Y., Hu, C. H., Pai, T. W., Chen, Y. R., & Wang, W. der. (2020). Integrated hypoxia signaling and oxidative stress in developmental neurotoxicity of benzo[a]pyrene in zebrafish embryos. *Antioxidants*, *9*(8), 1–71. https://doi.org/10.3390/antiox9080731

Liu, T., Zhang, L., Joo, D., & Sun, S.-C. (2017). NF-κB signaling in inflammation. *Signal Transduction and Targeted Therapy*, *2*(1), 17023. https://doi.org/10.1038/sigtrans.2017.23

Livak, K. J., & Schmittgen, T. D. (2001). Analysis of relative gene expression data using real-time quantitative PCR and the 2-ΔΔCT method. *Methods*, *25*(4), 402–408. https://doi.org/10.1006/meth.2001.1262

Lonappan, L., Brar, S. K., Das, R. K., Verma, M., & Surampalli, R. Y. (2016). Diclofenac and its transformation products: Environmental occurrence and toxicity - A review. *Environment International*, *96*, 127–138. https://doi.org/10.1016/j.envint.2016.09.014

Luo, K., Huang, W., Zhang, Q., Liu, X., Nian, M., Wei, M., Wang, Y., Chen, D., Chen, X., & Zhang, J. (2022). Environmental exposure to legacy poly/perfluoroalkyl substances, emerging alternatives and isomers and semen quality in men: A mixture analysis. *Science of the Total Environment*, *833*. https://doi.org/10.1016/j.scitotenv.2022.155158

Macdonald, D. D., Carr, R. S., Calder, F. D., Long, E. R., & Ingersoll, C. G. (1996). Development and evaluation of sediment quality guidelines for Florida coastal waters. *Ecotoxicology*, *5*(4), 253–278. https://doi.org/10.1007/BF00118995

Madeira, C., & Costa, P. M. (2021). *Proteomics in systems toxicology* (pp. 55–91). https://doi.org/10.1016/bs.apcsb.2021.03.001

Maes, J., Verlooy, L., Buenafe, O. E., de Witte, P. A. M., Esguerra, C. V., & Crawford, A. D. (2012). Evaluation of 14 Organic Solvents and Carriers for Screening Applications in Zebrafish Embryos and Larvae. *PLoS ONE*, *7*(10), 1–9. https://doi.org/10.1371/journal.pone.0043850

Manoli, E., & Samara, C. (1999). Polycyclic aromatic hydrocarbons in natural waters: Sources, occurrence and analysis. *TrAC - Trends in Analytical Chemistry*, *18*(6), 417–428. https://doi.org/10.1016/S0165-9936(99)00111-9

Manzoor, Z., & Koh, Y.-S. (2012). Mitogen-activated Protein Kinases in Inflammation. *Journal of Bacteriology and Virology*, *42*(3), 189. https://doi.org/10.4167/jbv.2012.42.3.189

Marczylo, E. L., Jacobs, M. N., & Gant, T. W. (2016). Environmentally induced epigenetic toxicity: potential public health concerns. *Critical Reviews in Toxicology*, *46*(8), 676–700. https://doi.org/10.1080/10408444.2016.1175417

Maria, V. L., Gomes, T., Barreira, L., & Bebianno, M. J. (2013). Impact of benzo(a)pyrene, Cu and their mixture on the proteomic response of Mytilus galloprovincialis. *Aquatic Toxicology*, *144–145*, 284–295. https://doi.org/10.1016/j.aquatox.2013.10.009

Martin, O., Scholze, M., Ermler, S., McPhie, J., Bopp, S. K., Kienzler, A., Parissis, N., & Kortenkamp, A. (2021). Ten years of research on synergisms and antagonisms in chemical mixtures: A systematic review and quantitative reappraisal of mixture studies. *Environment International*, *146*(October 2020), 106206. https://doi.org/10.1016/j.envint.2020.106206

Martínez-Pacheco, M., Hidalgo-Miranda, A., Romero-Córdoba, S., Valverde, M., & Rojas, E. (2014). MRNA and miRNA expression patterns associated to pathways linked to metal mixture health effects. *Gene*, *533*(2), 508–514. https://doi.org/10.1016/j.gene.2013.09.049

Martins, C., & Costa, P. M. (2020). Technical Updates to the Comet Assay *In Vivo* for Assessing DNA Damage in Zebrafish Embryos from Fresh and Frozen Cell Suspensions. *Zebrafish*, *00*(00), 1–9. https://doi.org/10.1089/zeb.2020.1857

Martins, C., Dreij, K., & Costa, P. M. (2019). The state-of-the art of environmental toxicogenomics: Challenges and perspectives of “omics” approaches directed to toxicant mixtures. *International Journal of Environmental Research and Public Health*, *16*(23), 1–16. https://doi.org/10.3390/ijerph16234718

Martins, M., Costa, P. M., Ferreira, A. M., & Costa, M. H. (2013). Comparative DNA damage and oxidative effects of carcinogenic and non-carcinogenic sediment-bound PAHs in the gills of a bivalve. *Aquatic Toxicology*, *142–143*, 85–95. https://doi.org/10.1016/j.aquatox.2013.07.019

Maslov, A. Y., Quispe-Tintaya, W., Gorbacheva, T., White, R. R., & Vijg, J. (2015). High-throughput sequencing in mutation detection: a new generation of genotoxicity tests? *Mutation Research - Fundamental and Molecular Mechanisms of Mutagenesis*, *776*, 136–143. https://doi.org/10.1016/j.mrfmmm.2015.03.014

Matsumura, S., Fujita, Y., Yamane, M., Morita, O., & Honda, H. (2018). A genome-wide mutation analysis method enabling high-throughput identification of chemical mutagen signatures. *Scientific Reports*, *8*(1), 1–9. https://doi.org/10.1038/s41598-018-27755-w

McCarrick, S., Cunha, V., Zapletal, O., Vondráček, J., & Dreij, K. (2019). *In vitro* and *in vivo* genotoxicity of oxygenated polycyclic aromatic hydrocarbons. *Environmental Pollution*, *246*, 678–687. https://doi.org/10.1016/j.envpol.2018.12.092

McCarthy, D. J., Chen, Y., & Smyth, G. K. (2012). Differential expression analysis of multifactor RNA-Seq experiments with respect to biological variation. *Nucleic Acids Research*, *40*(10), 4288–4297. https://doi.org/10.1093/nar/gks042

McCullagh, P., & Nelder, J. (1989). *Generalized nLinear Models Second Edition* (Second). Chapman & Hall/CRC.

McGrath, P., & Li, C. Q. (2008). Zebrafish: a predictive model for assessing drug-induced toxicity. In *Drug Discovery Today* (Vol. 13, Issues 9–10, pp. 394–401). https://doi.org/10.1016/j.drudis.2008.03.002

Mehinto, A. C., Hill, E. M., & Tyler, C. R. (2010). Uptake and Biological Effects of Environmentally Relevant Concentrations of the Nonsteroidal Anti-inflammatory Pharmaceutical Diclofenac in Rainbow Trout (Oncorhynchus mykiss). *Environmental Science & Technology*, *44*(6), 2176–2182. https://doi.org/10.1021/es903702m

Melvin, S. D., Habener, L. J., Leusch, F. D. L., & Carroll, A. R. (2017). 1H NMR-based metabolomics reveals sub-lethal toxicity of a mixture of diabetic and lipid-regulating pharmaceuticals on amphibian larvae. *Aquatic Toxicology*, *184*, 123–132. https://doi.org/10.1016/j.aquatox.2017.01.012

Miranda, A. C. L., Bazzoli, N., Rizzo, E., & Sato, Y. (1999). Ovarian follicular atresia in two teleost species: a histological and ultrastructural study. *Tissue and Cell*, *31*(5), 480–488. https://doi.org/10.1054/tice.1999.0045

Mitchell, R. D., Dhammi, A., Wallace, A., Hodgson, E., & Roe, R. M. (2016). Impact of Environmental Chemicals on the Transcriptome of Primary Human Hepatocytes: Potential for Health Effects. *J Biochem Molecular Toxicology*, *30*(8). https://doi.org/10.1002/jbt.21801

Mittal, M., Siddiqui, M. R., Tran, K., Reddy, S. P., & Malik, A. B. (2014). Reactive Oxygen Species in Inflammation and Tissue Injury. *Antioxidants & Redox Signaling*, *20*(7), 1126–1167. https://doi.org/10.1089/ars.2012.5149

Modarresi Chahardehi, A., Arsad, H., & Lim, V. (2020). Zebrafish as a Successful Animal Model for Screening Toxicity of Medicinal Plants. *Plants*, *9*(10), 1345. https://doi.org/10.3390/plants9101345

Moorthy, B., Chu, C., & Carlin, D. J. (2015). Polycyclic aromatic hydrocarbons: From metabolism to lung cancer. *Toxicological Sciences*, *145*(1), 5–15. https://doi.org/10.1093/toxsci/kfv040

Movahedinia, A., Salamat, N., & Kheradmand, P. (2018). Effects of the environmental endocrine disrupting compound benzo[a]pyrene on thyroidal status of abu mullet (Liza abu) during short-term exposure. *Toxicology Reports*, *5*, 377–382. https://doi.org/10.1016/j.toxrep.2018.02.018

Muhammad, S., Pan, Y., Agha, M. H., Umar, M., & Chen, S. (2022). Industrial structure, energy intensity and environmental efficiency across developed and developing economies: The intermediary role of primary, secondary and tertiary industry. *Energy*, *247*, 123576. https://doi.org/10.1016/j.energy.2022.123576

Nebert, D. W., Roe, A. L., Dieter, M. Z., Solis, W. A., Yang, Y., & Dalton, T. P. (2000). Role of the aromatic hydrocarbon receptor and (Ah) gene battery in the oxidative stress response, cell cycle control, and apoptosis. *Biochemical Pharmacology*, *59*(1), 65–85. https://doi.org/10.1016/S0006-2952(99)00310-X

Nys, C., Asselman, J., Hochmuth, J. D., Janssen, C. R., Blust, R., Smolders, E., & de Schamphelaere, K. A. C. (2015). Mixture toxicity of nickel and zinc to Daphnia magna is noninteractive at low effect sizes but becomes synergistic at high effect sizes. *Environmental Toxicology and Chemistry*, *34*(5), 1091–1102. https://doi.org/10.1002/etc.2902

Oaks, J. L., Gilbert, M., Virani, M. Z., Watson, R. T., Meteyer, C. U., Rideout, B. A., Shivaprasad, H. L., Ahmed, S., Chaudhry, M. J. I., Arshad, M., Mahmood, S., Ali, A., & Khan, A. A. (2004). Diclofenac residues as the cause of vulture population decline in Pakistan. *Nature*, *427*(6975), 630–633. https://doi.org/10.1038/nature02317

OECD (Organisation for Economic Co-operation and Development). (2013). *OECD Guidelines for the Testing of Chemicals*. *July*, 1–22.

Olden, K., & Guthrie, J. (2001). Genomics: Implications for toxicology. *Mutation Research - Fundamental and Molecular Mechanisms of Mutagenesis*, *473*(1), 3–10. https://doi.org/10.1016/S0027-5107(00)00161-5

Olive, P. L., & Banáth, J. P. (2006). The comet assay: A method to measure DNA damage in individual cells. *Nature Protocols*, *1*(1), 23–29. https://doi.org/10.1038/nprot.2006.5

One Health Initiative Task Force. (2008). *One Health: A New Professional Imperative.*

Oziolor, E. M., Bickham, J. W., & Matson, C. W. (2017). Evolutionary toxicology in an omics world. *Evolutionary Applications*, *10*(8), 752–761. https://doi.org/10.1111/eva.12462

Park, S. Y., Lee, S. M., Ye, S. K., Yoon, S. H., Chung, M. H., & Choi, J. (2006). Benzo[a]pyrene-induced DNA damage and p53 modulation in human hepatoma HepG2 cells for the identification of potential biomarkers for PAH monitoring and risk assessment. *Toxicology Letters*, *167*(1), 27–33. https://doi.org/10.1016/j.toxlet.2006.08.011

Parolini, M. (2020). Toxicity of the Non-Steroidal Anti-Inflammatory Drugs (NSAIDs) acetylsalicylic acid, paracetamol, diclofenac, ibuprofen and naproxen towards freshwater invertebrates: A review. *Science of The Total Environment*, *740*, 140043. https://doi.org/10.1016/j.scitotenv.2020.140043

Paskauskas, S., Parseliunas, A., Kerkadze, V., Nobiling, R., Schmidt, J., & Ryschich, E. (2011). Blockade of leukocyte haptokinesis and haptotaxis by ketoprofen, diclofenac and SC-560. *BMC Immunology*, *12*(1), 64. https://doi.org/10.1186/1471-2172-12-64

Penning, T. M. (2014). Human Aldo-Keto Reductases and the Metabolic Activation of Polycyclic Aromatic Hydrocarbons. *Chemical Research in Toxicology*, *27*(11), 1901–1917. https://doi.org/10.1021/tx500298n

Penning, T. M., Burczynski, M. E., Hung, C. F., McCoull, K. D., Palackal, N. T., & Tsuruda, L. S. (1999). Dihydrodiol dehydrogenases and polycyclic aromatic hydrocarbon activation: Generation of reactive and redox active o-quinones. *Chemical Research in Toxicology*, *12*(1), 1–18. https://doi.org/10.1021/tx980143n

Pereira, L. C., de Souza, A. O., Bernardes, M. F. F., Pazin, M., Tasso, M. J., Pereira, P. H., & Dorta, D. J. (2015). A perspective on the potential risks of emerging contaminants to human and environmental health. *Environmental Science and Pollution Research*, *22*(18), 13800–13823. https://doi.org/10.1007/s11356-015-4896-6

Perkins, J. T., Petriello, M. C., Xu, L., Stromberg, A., & Hennig, B. (2017). An open-sourced statistical application for identifying complex toxicological interactions of environmental pollutants. *Reviews on Environmental Health*, *32*(1–2), 23–26. https://doi.org/10.1515/reveh-2016-0044

Philibert, P., Déjardin, S., Girard, M., Durix, Q., Gonzalez, A.-A., Mialhe, X., Tardat, M., Poulat, F., & Boizet-Bonhoure, B. (2023). Cocktails of NSAIDs and 17α Ethinylestradiol at Environmentally Relevant Doses in Drinking Water Alter Puberty Onset in Mice Intergenerationally. *International Journal of Molecular Sciences*, *24*(6), 5890. https://doi.org/10.3390/ijms24065890

Phillips, B., Titz, B., Kogel, U., Sharma, D., Leroy, P., Xiang, Y., Vuillaume, G., Lebrun, S., Sciuscio, D., Ho, J., Nury, C., Guedj, E., Elamin, A., Esposito, M., Krishnan, S., Schlage, W. K., Veljkovic, E., Ivanov, N. v., Martin, F., … Vanscheeuwijck, P. (2017). Toxicity of the main electronic cigarette components, propylene glycol, glycerin, and nicotine, in Sprague-Dawley rats in a 90-day OECD inhalation study complemented by molecular endpoints. *Food and Chemical Toxicology*, *109*, 315–332. https://doi.org/10.1016/j.fct.2017.09.001

Prokopec, S. D., Lu, A., Lee, S. C.-E. S., Yao, C. Q., Sun, R. X., Watson, J. D., Soliymani, R., de Borja, R., Wong, A., Sam, M., Zuzarte, P., McPherson, J. D., Okey, A. B., Pohjanvirta, R., & Boutros, P. C. (2019). Comparative toxicoproteogenomics of mouse and rat liver identifies TCDD-resistance genes. *Archives of Toxicology*, *93*(10), 2961–2978. https://doi.org/10.1007/s00204-019-02560-0

Prüss-Üstün, A., Wolf, J., Corvalán, C. F., Bos, R., & Neira, M. P. (2016). Preventing disease through healthy environments: a global assessment of the burden of disease from environmental risks. In *World Health Organization*. https://www.who.int/publications/i/item/9789241565196

Raimundo, J., Costa, P. M., Vale, C., Costa, M. H., & Moura, I. (2010). DNA damage and metal accumulation in four tissues of feral Octopus vulgaris from two coastal areas in Portugal. *Ecotoxicology and Environmental Safety*, *73*(7), 1543–1547. https://doi.org/10.1016/j.ecoenv.2010.07.034

Rampersad, S. N. (2012). Multiple applications of alamar blue as an indicator of metabolic function and cellular health in cell viability bioassays. *Sensors (Switzerland)*, *12*(9), 12347–12360. https://doi.org/10.3390/s120912347

Ranjit, S., Sinha, N., Kodidela, S., & Kumar, S. (2018). Benzo(a)pyrene in Cigarette Smoke Enhances HIV-1 Replication through NF-κB Activation via CYP-Mediated Oxidative Stress Pathway. *Scientific Reports*, *8*(1), 1–13. https://doi.org/10.1038/s41598-018-28500-z

Rao, M. S., van Vleet, T. R., Ciurlionis, R., Buck, W. R., Mittelstadt, S. W., Blomme, E. A. G., & Liguori, M. J. (2019). Comparison of RNA-Seq and microarray gene expression platforms for the toxicogenomic evaluation of liver from short-term rat toxicity studies. *Frontiers in Genetics*, *10*(JAN), 1–16. https://doi.org/10.3389/fgene.2018.00636

Rehman, M. S. U., Rashid, N., Ashfaq, M., Saif, A., Ahmad, N., & Han, J. I. (2015). Global risk of pharmaceutical contamination from highly populated developing countries. *Chemosphere*, *138*, 1045–1055. https://doi.org/10.1016/j.chemosphere.2013.02.036

Riesco, M. F., Martínez-Pastor, F., Chereguini, O., & Robles, V. (2012). Evaluation of zebrafish (Danio rerio) PGCs viability and DNA damage using different cryopreservation protocols. *Theriogenology*, *77*(1), 122–130. https://doi.org/10.1016/j.theriogenology.2011.07.024

Ritchie, M. E., Phipson, B., Wu, D., Hu, Y., Law, C. W., Shi, W., & Smyth, G. K. (2015). Limma powers differential expression analyses for RNA-sequencing and microarray studies. *Nucleic Acids Research*, *43*(7), e47. https://doi.org/10.1093/nar/gkv007

Robertson, D. G. (2005). Metabonomics in toxicology: A review. *Toxicological Sciences*, *85*(2), 809–822. https://doi.org/10.1093/toxsci/kfi102

Robinson, M. D., McCarthy, D. J., & Smyth, G. K. (2009). edgeR: A Bioconductor package for differential expression analysis of digital gene expression data. *Bioinformatics*, *26*(1), 139–140. https://doi.org/10.1093/bioinformatics/btp616

Romero-Ruiz, A., Carrascal, M., Alhama, J., Gómez-Ariza, J. L., Abian, J., & López-Barea, J. (2006). Utility of proteomics to assess pollutant response of clams from the Doñana bank of Guadalquivir Estuary (SW Spain). *Proteomics*, *6*, S245–S255. https://doi.org/10.1002/pmic.200500444

Ross, J. A., & Nesnow, S. (1999). Polycyclic aromatic hydrocarbons: Correlations between DNA adducts and ras oncogene mutations. *Mutation Research - Fundamental and Molecular Mechanisms of Mutagenesis*, *424*(1–2), 155–166. https://doi.org/10.1016/S0027-5107(99)00016-0

Roth, K., Yang, Z., Agarwal, M., Liu, W., Peng, Z., Long, Z., Birbeck, J., Westrick, J., Liu, W., & Petriello, M. C. (2021). Exposure to a mixture of legacy, alternative, and replacement per- and polyfluoroalkyl substances (PFAS) results in sex-dependent modulation of cholesterol metabolism and liver injury. *Environment International*, *157*. https://doi.org/10.1016/j.envint.2021.106843

Rurale, G., Gentile, I., Carbonero, C., Persani, L., & Marelli, F. (2022). Short-Term Exposure Effects of the Environmental Endocrine Disruptor Benzo(a)Pyrene on Thyroid Axis Function in Zebrafish. *International Journal of Molecular Sciences*, *23*(10), 5833. https://doi.org/10.3390/ijms23105833

Russell, V. S. (1974). Pollution: Concept and definition. *Biological Conservation*, *6*(3), 157–161. https://doi.org/10.1016/0006-3207(74)90060-3

Sallustio, B. C., DeGraaf, Y. C., Weekley, J. S., & Burcham, P. C. (2006). Bioactivation of carboxylic acid compounds by UDP-glucuronosyltransferases to DNA-damaging intermediates: Role of glycoxidation and oxidative stress in genotoxicity. *Chemical Research in Toxicology*, *19*(5), 683–691. https://doi.org/10.1021/tx060022k

Sasaki, Y. F., Izumiyama, F., Nishidate, E., Ishibashi, S., Tsuda, S., Asano, N., Saotome, K., Sofuni, T., & Hayashi, M. (1997). Detection of genotoxicity of polluted sea water using shellfish and the alkaline single-cell gel electrophoresis (SCE) assay: a preliminary study. *Genetic Toxicology and Environmental Mutagenesis*, *393*(1–2), 133–139. https://doi.org/10.1016/S1383-5718(97)00098-3

Schmidt, C. W. (2002). Toxicogenomics: An emerging discipline. *Environmental Health Perspectives*, *110*(12), A750–A755. https://doi.org/10.1289/ehp.110-a750

Schmitt, E. A., & Dowling, J. E. (1994). Early-eye morphogenesis in the zebrafish, Brachydanio rerio. *Journal of Comparative Neurology*, *344*(4), 532–542. https://doi.org/10.1002/cne.903440404

Schneider, C. A., Rasband, W. S., & Eliceiri, K. W. (2012). NIH Image to ImageJ: 25 years of image analysis. *Nature Methods*, *9*(7), 671–675. https://doi.org/10.1038/nmeth.2089

Scholz, S., Fischer, S., Gündel, U., Küster, E., Luckenbach, T., & Voelker, D. (2008). The zebrafish embryo model in environmental risk assessment - Applications beyond acute toxicity testing. *Environmental Science and Pollution Research*, *15*(5), 394–404. https://doi.org/10.1007/s11356-008-0018-z

Schroeder, A., Mueller, O., Stocker, S., Salowsky, R., Leiber, M., Gassmann, M., Lightfoot, S., Menzel, W., Granzow, M., & Ragg, T. (2006). The RIN: An RNA integrity number for assigning

integrity values to RNA measurements. *BMC Molecular Biology*, *7*, 1–14. https://doi.org/10.1186/1471-2199-7-3

Schwartz, J. I., Dallob, A. L., Larson, P. J., Laterza, O. F., Miller, J., Royalty, J., Snyder, K. M., Chappell, D. L., Hilliard, D. A., Flynn, M. E., Cavanaugh, P. F., & Wagner, J. A. (2008). Comparative inhibitory activity of etoricoxib, celecoxib, and diclofenac on COX-2 versus COX-1 in healthy subjects. *Journal of Clinical Pharmacology*, *48*(6), 745–754. https://doi.org/10.1177/0091270008317590

Selwe, K. P., Thorn, J. P. R., Desrousseaux, A. O. S., Dessent, C. E. H., & Sallach, J. B. (2022). Emerging contaminant exposure to aquatic systems in the Southern African Development Community. *Environmental Toxicology and Chemistry*, *41*(2), 382–395. https://doi.org/10.1002/etc.5284

Shah, U. K., Seager, A. L., Fowler, P., Doak, S. H., Johnson, G. E., Scott, S. J., Scott, A. D., & Jenkins, G. J. S. (2016). A comparison of the genotoxicity of benzo[a]pyrene in four cell lines with differing metabolic capacity. *Mutation Research - Genetic Toxicology and Environmental Mutagenesis*, *808*, 8–19. https://doi.org/10.1016/j.mrgentox.2016.06.009

Shen, S., Marchick, M. R., Davis, M. R., Doss, G. A., & Pohl, L. R. (1999). Metabolic activation of diclofenac by human cytochrome P450 3A4: Role of 5-hydroxydiclofenac. *Chemical Research in Toxicology*, *12*(2), 214–222. https://doi.org/10.1021/tx9802365

Shimada, T. (2006). Xenobiotic-Metabolizing Enzymes Involved in Activation and Detoxification of Carcinogenic Polycyclic Aromatic Hydrocarbons. *Drug Metabolism and Pharmacokinetics*, *21*(4), 257–276. https://doi.org/10.2133/dmpk.21.257

Shimada, T., & Fujii-Kuriyama, Y. (2004). Metabolic activation of polycyclic aromatic hydrocarbons to carcinogens by cytochromes P450 1A1 and 1B1. In *Cancer Science* (Vol. 95, Issue 1, pp. 1–6). https://doi.org/10.1111/j.1349-7006.2004.tb03162.x

Shimada, T., & Guengerich, F. P. (2006). Inhibition of Human Cytochrome P450 1A1-, 1A2-, and 1B1-Mediated Activation of Procarcinogens to Genotoxic Metabolites by Polycyclic Aromatic Hydrocarbons. *Chemical Research in Toxicology*, *19*(2), 288–294. https://doi.org/10.1021/tx050291v

Shwartz, A., Goessling, W., & Yin, C. (2019). Macrophages in Zebrafish Models of Liver Diseases. *Frontiers in Immunology*, *10*. https://doi.org/10.3389/fimmu.2019.02840

Silins, I., & Högberg, J. (2011). Combined toxic exposures and human health: Biomarkers of exposure and effect. *International Journal of Environmental Research and Public Health*, *8*(3), 629–647. https://doi.org/10.3390/ijerph8030629

Simbürger, J. M. B., Dettmer, K., Oefner, P. J., & Reinders, J. (2016). Optimizing the SWATH-MS-workflow for label-free proteomics. *Journal of Proteomics*, *145*, 137–140. https://doi.org/10.1016/j.jprot.2016.04.021

Singh, N. P., Mccoy, M. T., Tice, R. R., & Scineider, E. L. (1988). A simple technique for quantification of low levels of DNA in individual cells. *Experimental Cell Research*, *175*(1), 184–191. https://doi.org/10.1016/0014-4827(88)90265-0

Škrbić, B. D., Kadokami, K., & Antić, I. (2018). Survey on the micro-pollutants presence in surface water system of northern Serbia and environmental and health risk assessment. *Environmental Research*, *166*(January), 130–140. https://doi.org/10.1016/j.envres.2018.05.034

Sloan, D. B., Broz, A. K., Sharbrough, J., & Wu, Z. (2018). Detecting rare mutations and DNA damage with sequencing- based methods. *Trends in Biotechnology*, *36*(7), 729–740. https://doi.org/10.1016/j.tibtech.2018.02.009.

Søfteland, L., Kirwan, J. A., Hori, T. S. F., Størseth, T. R., Sommer, U., Berntssen, M. H. G., Viant, M. R., Rise, M. L., Waagbø, R., Torstensen, B. E., Booman, M., & Olsvik, P. A. (2014). Toxicological effect of single contaminants and contaminant mixtures associated with plant ingredients in novel salmon feeds. *Food and Chemical Toxicology*, *73*, 157–174. https://doi.org/10.1016/j.fct.2014.08.008

Song, Q., Chen, H., Li, Y., Zhou, H., Han, Q., & Diao, X. (2016). Toxicological effects of benzo(a)pyrene, DDT and their mixture on the green mussel Perna viridis revealed by proteomic and metabolomic approaches. *Chemosphere*, *144*, 214–224. https://doi.org/10.1016/j.chemosphere.2015.08.029

Song, Q., Zhou, H., Han, Q., & Diao, X. (2017). Toxic responses of Perna viridis hepatopancreas exposed to DDT, benzo(a)pyrene and their mixture uncovered by iTRAQ-based proteomics and NMR-based metabolomics. *Aquatic Toxicology*, *192*(April), 48–57. https://doi.org/10.1016/j.aquatox.2017.09.010

Šrut, M., Štambuk, A., Bourdineaud, J.-P., & Klobučar, G. I. V. (2015). Zebrafish genome instability after exposure to model genotoxicants. *Ecotoxicology*, *24*(4), 887–902. https://doi.org/10.1007/s10646-015-1432-x

Stepnik, M., Spryszyńska, S., Smok-Pieniazek, A., Ferlińska, M., Roszak, J., & Nocuń, M. (2015). The modulating effect of ATM, ATR, DNA-PK inhibitors on the cytotoxicity and genotoxicity of benzo[a]pyrene in human hepatocellular cancer cell line HepG2. *Environmental Toxicology and Pharmacology*, *40*(3), 988–996. https://doi.org/10.1016/j.etap.2015.10.010

Stuck, M. W., Conley, S. M., & Naash, M. I. (2016). PRPH2/RDS and ROM-1: Historical context, current views and future considerations. In *Progress in Retinal and Eye Research* (Vol. 52, pp. 47–63). Elsevier Ltd. https://doi.org/10.1016/j.preteyeres.2015.12.002

Sun, L. W., Qu, M. M., Li, Y. Q., Wu, Y. L., Chen, Y. G., Kong, Z. M., & Liu, Z. T. (2004). Toxic Effects of Aminophenols on Aquatic Life Using the Zebrafish Embryo Test and the Comet Assay. *Bulletin of Environmental Contamination and Toxicology*, *73*(4), 628–634. https://doi.org/10.1007/s00128-004-0474-1

Swank, A., Wang, L., Ward, J., & Schoenfuss, H. (2021). Multigenerational effects of a complex urban contaminant mixture on the behavior of larval and adult fish in multiple fitness contexts. *Science of The Total Environment*, *791*, 148095. https://doi.org/10.1016/j.scitotenv.2021.148095

Szklarczyk, D., Franceschini, A., Wyder, S., Forslund, K., Heller, D., Huerta-Cepas, J., Simonovic, M., Roth, A., Santos, A., Tsafou, K. P., Kuhn, M., Bork, P., Jensen, L. J., & von Mering, C. (2015). STRING v10: Protein-protein interaction networks, integrated over the tree of life. *Nucleic Acids Research*, *43*(D1), D447–D452. https://doi.org/10.1093/nar/gku1003

Szklarczyk, D., Gable, A. L., Lyon, D., Junge, A., Wyder, S., Huerta-Cepas, J., Simonovic, M., Doncheva, N. T., Morris, J. H., Bork, P., Jensen, L. J., & Von Mering, C. (2019). STRING v11: Protein-protein association networks with increased coverage, supporting functional discovery in genome-wide experimental datasets. *Nucleic Acids Research*, *47*(D1), D607–D613. https://doi.org/10.1093/nar/gky1131

Szklarczyk, D., Santos, A., von Mering, C., Jensen, L. J., Bork, P., & Kuhn, M. (2016). STITCH 5: Augmenting protein-chemical interaction networks with tissue and affinity data. *Nucleic Acids Research*, *44*(D1), D380–D384. https://doi.org/10.1093/nar/gkv1277

Tarantini, A., Maitre, A., Lefebvre, E., Marques, M., Marie, C., Ravanat, J. L., & Douki, T. (2009). Relative contribution of DNA strand breaks and DNA adducts to the genotoxicity of benzo[a]pyrene as a pure compound and in complex mixtures. *Mutation Research - Fundamental and Molecular Mechanisms of Mutagenesis*, *671*(1–2), 67–75. https://doi.org/10.1016/j.mrfmmm.2009.08.014

Tebbe, L., Kakakhel, M., Makia, M. S., Al-Ubaidi, M. R., & Naash, M. I. (2020). The interplay between peripherin 2 complex formation and degenerative retinal diseases. In *Cells* (Vol. 9, Issue 3). MDPI. https://doi.org/10.3390/cells9030784

Teixeira, G., & Faria, R. (2021). Inflammatory Mediators Leading to Edema Formation through Plasma Membrane Receptors. In *Infections and Sepsis Development*. IntechOpen. https://doi.org/10.5772/intechopen.99230

Ternes, T. A. (1998). Occurrence of drugs in German sewage treatment plants and rivers. *Water Research*, *32*(11), 3245–3260. https://doi.org/10.1016/S0043-1354(98)00099-2

Terradas, M., Martín, M., Tusell, L., & Genescà, A. (2010). Genetic activities in micronuclei: Is the DNA entrapped in micronuclei lost for the cell? *Mutation Research - Reviews in Mutation Research*, *705*(1), 60–67. https://doi.org/10.1016/j.mrrev.2010.03.004

Thai, P. N., Ren, L., Xu, W., Overton, J., Timofeyev, V., Nader, C. E., Haddad, M., Yang, J., Gomes, A. V, Hammock, B. D., Chiamvimonvat, N., & Sirish, P. (2023). Chronic Diclofenac Exposure Increases Mitochondrial Oxidative Stress, Inflammatory Mediators, and Cardiac Dysfunction. *Cardiovascular Drugs and Therapy*, *37*(1), 25–37. https://doi.org/10.1007/s10557-021-07253-4

Tian, Z., Hou, X., Liu, W., Han, Z., & Wei, L. (2019). Macrophages and hepatocellular carcinoma. *Cell & Bioscience*, *9*(1), 79. https://doi.org/10.1186/s13578-019-0342-7

Tilton, S. C., Siddens, L. K., Krueger, S. K., Larkin, A. J., Löhr, C. v., Williams, D. E., Baird, W. M., & Waters, K. M. (2015). Mechanism-based classification of PAH mixtures to predict carcinogenic potential. *Toxicological Sciences*, *146*(1), 135–145. https://doi.org/10.1093/toxsci/kfv080

Titz, B., Elamin, A., Martin, F., Schneider, T., Dijon, S., Ivanov, N. v., Hoeng, J., & Peitsch, M. C. (2014). Proteomics for systems toxicology. *Computational and Structural Biotechnology Journal*, *11*(18), 73–90. https://doi.org/10.1016/j.csbj.2014.08.004

Toušová, Z., Vrana, B., Smutná, M., Novák, J., Klučárová, V., Grabic, R., Slobodník, J., Giesy, J. P., & Hilscherová, K. (2019). Analytical and bioanalytical assessments of organic micropollutants in the Bosna River using a combination of passive sampling, bioassays and multi-residue analysis. *Science of the Total Environment*, *650*, 1599–1612. https://doi.org/10.1016/j.scitotenv.2018.08.336

Tufi, S., Wassenaar, P. N. H., Osorio, V., de Boer, J., Leonards, P. E. G., & Lamoree, M. H. (2016). Pesticide Mixture Toxicity in Surface Water Extracts in Snails (Lymnaea stagnalis) by an *in Vitro* Acetylcholinesterase Inhibition Assay and Metabolomics. *Environmental Science and Technology*, *50*(7), 3937–3944. https://doi.org/10.1021/acs.est.5b04577

Ungprasert, P., Cheungpasitporn, W., Crowson, C. S., & Matteson, E. L. (2015). Individual non-steroidal anti-inflammatory drugs and risk of acute kidney injury: A systematic review and meta-analysis of observational studies. *European Journal of Internal Medicine*, *26*(4), 285–291. https://doi.org/10.1016/j.ejim.2015.03.008

United Nations. (2020). *Sustainable Development Goals*. https://unstats.un.org/sdgs/report/2020/#sdg-goals

Ünlü Endirlik, B., Wincent, E., & Dreij, K. (2023). Non-additive mixture effects of benzo[a]pyrene and pesticides *in vitro* and *in vivo*: Role of AhR signaling. *Environmental Pollution*, *316*. https://doi.org/10.1016/j.envpol.2022.120510

van der Borght, K., Tourny, A., Bagdziunas, R., Thas, O., Nazarov, M., Turner, H., Verbist, B., & Ceulemans, H. (2017). BIGL: Biochemically Intuitive Generalized Loewe null model for prediction of the expected combined effect compatible with partial agonism and antagonism. *Scientific Reports*, *7*(1), 1–9. https://doi.org/10.1038/s41598-017-18068-5

Verlicchi, P., al Aukidy, M., & Zambello, E. (2012). Occurrence of pharmaceutical compounds in urban wastewater: Removal, mass load and environmental risk after a secondary treatment-A review. *Science of the Total Environment*, *429*, 123–155. https://doi.org/10.1016/j.scitotenv.2012.04.028

Vidal, J. D., & Dixon, D. (2018). Ovary. In *Boorman's Pathology of the Rat* (pp. 523–536). Elsevier. https://doi.org/10.1016/B978-0-12-391448-4.00026-5

Vidova, V., & Spacil, Z. (2017). A review on mass spectrometry-based quantitative proteomics: Targeted and data independent acquisition. *Analytica Chimica Acta*, *964*, 7–23. https://doi.org/10.1016/j.aca.2017.01.059

Vitorino, J. D., & Costa, P. M. (2023). After a Century of Research into Environmental Mutagens and Carcinogens, Where Do We Stand? *International Journal of Environmental Research and Public Health*, *20*(2), 1040. https://doi.org/10.3390/ijerph20021040

Volcic, M., Karl, S., Baumann, B., Salles, D., Daniel, P., Fulda, S., & Wiesmüller, L. (2012). NF-κB regulates DNA double-strand break repair in conjunction with BRCA1-CtIP complexes. *Nucleic Acids Research*, *40*(1), 181–195. https://doi.org/10.1093/nar/gkr687

Vorwald, A. J., & Karr, J. W. (1938). Pneumoconiosis and pulmonary carcinoma. *The American Journal of Pathology*, *14*(1), 49-58.1. http://www.ncbi.nlm.nih.gov/pubmed/19970376

Vystavna, Y., Frkova, Z., Celle-Jeanton, H., Diadin, D., Huneau, F., Steinmann, M., Crini, N., & Loup, C. (2018). Priority substances and emerging pollutants in urban rivers in Ukraine: Occurrence, fluxes and loading to transboundary European Union watersheds. *Science of the Total Environment*, *637–638*, 1358–1362. https://doi.org/10.1016/j.scitotenv.2018.05.095

Wamucho, A., Unrine, J. M., Kieran, T. J., Glenn, T. C., Schultz, C. L., Farman, M., Svendsen, C., Spurgeon, D. J., & Tsyusko, O. v. (2019). Genomic mutations after multigenerational exposure of Caenorhabditis elegans to pristine and sulfidized silver nanoparticles. *Environmental Pollution*, *254*, 113078. https://doi.org/10.1016/j.envpol.2019.113078

Wang, H., & Joseph, J. A. (1999). Quantifying Cellular Oxidative Stress By. *Free Radical Biology & Medicine*, *27*(99), 612–616.

Wells, J., Wroblewski, J., Keen, J., Inglehearn, C., Jubb, C., Eckstein, A., Jay, M., Arden, G., Bhattacharya, S., Fitzke, F., & Bird, A. (1993). Mutations in the human retinal degeneration slow (RDS) gene can cause either retinitis pigmentosa or macular dystrophy. *Nature Genetics*, *3*(3), 213–218. https://doi.org/10.1038/ng0393-213

White, R. M. (2016). Genomic Approaches to Zebrafish Cancer. In *Advances in experimental medicine and biology* (Vol. 916, pp. 125–145). https://doi.org/10.1007/978-3-319-30654-4_6

WHO. (2021). *Human health effects of polycyclic aromatic hydrocarbons as ambient air pollutants Report of the Working Group on Polycyclic Aromatic Hydrocarbons of the Joint Task Force on the Health Aspects of Air Pollution*. https://www.who.int/europe/publications/i/item/9789289056533

Wild, C. P., Weiderpass, E., & Stewart, B. W. (2020). World Cancer report - Cancer research for cancer prevention. In *International Agency for Research on Cancer*.

Wilkening, S., Stahl, F., & Bader, A. (2003). Comparison of primary human hepatocytes and hepatoma cell line Hepg2 with regard to their biotransformation properties. *Drug Metabolism and Disposition*, *31*(8), 1035–1042. https://doi.org/10.1124/dmd.31.8.1035

Williams, T. D., Davies, I. M., Wu, H., Diab, A. M., Webster, L., Viant, M. R., Chipman, J. K., Leaver, M. J., George, S. G., Moffat, C. F., & Robinson, C. D. (2014). Molecular responses of European flounder (Platichthys flesus) chronically exposed to contaminated estuarine sediments. *Chemosphere*, *108*, 152–158. https://doi.org/10.1016/j.chemosphere.2014.01.028

Wilson, J. T., Pascoe, P. L., Parry, J. M., & Dixon, D. R. (1998). Evaluation of the comet assay as a method for the detection of DNA damage in the cells of a marine invertebrate, Mytilus edulis L. (Mollusca: Pelecypoda). *Mutation Research - Fundamental and Molecular Mechanisms of Mutagenesis*, *399*(1), 87–95. https://doi.org/10.1016/S0027-5107(97)00268-6

Wogan, G. N., Hecht, S. S., Felton, J. S., Conney, A. H., & Loeb, L. A. (2004). Environmental and chemical carcinogenesis. *Seminars in Cancer Biology*, *14*(6), 473–486. https://doi.org/10.1016/j.semcancer.2004.06.010

Wu, H., & Wang, W. X. (2010). NMR-based metabolomic studies on the toxicological effects of cadmium and copper on green mussels Perna viridis. *Aquatic Toxicology*, *100*(4), 339–345. https://doi.org/10.1016/j.aquatox.2010.08.005

Wu, X., Gao, X., Tan, T., Li, C., Yan, R., Chi, Z., Feng, Y., Gong, P., Fang, J., Zhang, X., Aihemaiti, K., & Xu, D. (2021). Sources and pollution path identification of PAHs in karst aquifers: an example from Liulin karst water system, northern China. *Journal of Contaminant Hydrology*, *241*(388), 103810. https://doi.org/10.1016/j.jconhyd.2021.103810

Wu, Y., Geng, X. chao, Wang, J. feng, Miao, Y. fa, Lu, Y. li, & Li, B. (2016). The HepaRG cell line, a superior *in vitro* model to L-02, HepG2 and hiHeps cell lines for assessing drug-induced liver injury. *Cell Biology and Toxicology*, *32*(1), 37–59. https://doi.org/10.1007/s10565-016-9316-2

Xie, J., Zhang, W., Liang, X., Shuai, C., Zhou, Y., Pan, H., Yang, Y., & Han, W. (2020). RPL32 Promotes Lung Cancer Progression by Facilitating p53 Degradation. *Molecular Therapy - Nucleic Acids*, *21*, 75–85. https://doi.org/10.1016/j.omtn.2020.05.019

Xu, M. Y., Wang, P., Sun, Y. J., & Wu, Y. J. (2017). Metabolomic analysis for combined hepatotoxicity of chlorpyrifos and cadmium in rats. *Toxicology*, *384*(April), 50–58. https://doi.org/10.1016/j.tox.2017.04.008

Yadetie, F., Zhang, X., Hanna, E. M., Aranguren-Abadía, L., Eide, M., Blaser, N., Brun, M., Jonassen, I., Goksøyr, A., & Karlsen, O. A. (2018). RNA-Seq analysis of transcriptome responses in Atlantic cod (Gadus morhua) precision-cut liver slices exposed to benzo[a]pyrene and 17A-ethynylestradiol. *Aquatic Toxicology*, *201*, 174–186. https://doi.org/10.1016/j.aquatox.2018.06.003

Yan, Z., Subbaramaiah, K., Camilli, T., Zhang, F., Tanabe, T., McCaffrey, T. A., Dannenberg, A. J., & Weksler, B. B. (2000). Benzo[a]pyrene Induces the Transcription of Cyclooxygenase-2 in Vascular Smooth Muscle Cells. *Journal of Biological Chemistry*, *275*(7), 4949–4955. https://doi.org/10.1074/jbc.275.7.4949

Yin, X., Wang, H., Zhang, Y., Dahlgren, R. A., Zhang, H., Shi, M., Gao, M., & Wang, X. (2014). Toxicological assessment of trace β-diketone antibiotic mixtures on zebrafish (Danio rerio) by proteomic analysis. *PLoS ONE*, *9*(7), 1–12. https://doi.org/10.1371/journal.pone.0102731

Yun, C.-H., Shimada, T., & Guengerich, F. P. (1992). Roles of Human Liver Cytochrome P4502C and 3A Enzymes in the 3-Hydroxylation of Benzo(a)pyrene. *Cancer Research*, *52*(7), 1868–1874.

Zare, A., Henry, D., Chua, G., Gordon, P., & Habibi, H. R. (2018). Differential Hepatic Gene Expression Profile of Male Fathead Minnows Exposed to Daily Varying Dose of Environmental Contaminants Individually and in Mixture. *Frontiers in Endocrinology*, *9*(December), 749. https://doi.org/10.3389/fendo.2018.00749

Zhou, Y., Meng, J., Zhang, M., Chen, S., He, B., Zhao, H., Li, Q., Zhang, S., & Wang, T. (2019). Which type of pollutants need to be controlled with priority in wastewater treatment plants: Traditional or emerging pollutants? *Environment International*, *131*(June). https://doi.org/10.1016/j.envint.2019.104982

Zhu, J., Long, T., Gao, L., Zhong, Y., Wang, P., Wang, X., Li, Z., & Hu, Z. (2023). RPL21 interacts with LAMP3 to promote colorectal cancer invasion and metastasis by regulating focal adhesion formation. *Cellular & Molecular Biology Letters*, *28*(1), 31. https://doi.org/10.1186/s11658-023-00443-y

A

Appendix to Chapter 5

A.1 Experimental design

Table A1.1. Summary of experimental conditions for the acute bioassays with zebrafish embryos with single of combined toxicants.

Treatments	Benzo[*a*]pyrene µg/L (µM)	Diclofenac µg/L (µM)
Blank (medium)	0 (0)	0 (0)
Control (DMSO + H_2O)	0 (0)	0 (0)
B1[1]	0.05 (1.98E-4)	0 (0)
B2[2]	0.5 (1.98E-3)	0 (0)
B4[3]	8.9 (4.00E-2)	0 (0)
B5[4]	89 (0.4)	0 (0)
D1[1]	0 (0)	0.1 (3.14E-4)
D2[2]	0 (0)	1.00 (3.14E-3)
D3[5]	0 (0)	400 (1.3)
D4[6]	0 (0)	80 (0.3)
D5[7]	0 (0)	800 (2.5)
M1 (B1+D1)	0.05 (1.98E-4)	0.1 (3.14E-4)
M2 (B1+D2)	0.05 (1.98E-4)	1.00 (3.14E-3)
M3 (B2+D1)	0.5 (1.98E-3)	0.1 (3.14E-4)
M4 (B2+D2)	0.5 (1.98E-3)	1.00 (3.14E-3)
M5 (B4+D4)	8.9 (4.00E-2)	80 (0.3)
M6 (B4+D5)	8.9 (4.00E-2)	800 (2.5)
M7 (B5+D4)	89 (0.4)	80 (0.3)
M8 (B5+D5)	89 (0.4)	800 (2.5)
M9 (B1+D4)	0.05 (1.98E-4)	80 (0.3)
M10 (B1+D5)	0.05 (1.98E-4)	800 (2.5)
M11 (B2+D4)	0.5 (1.98E-3)	80 (0.3)
M12 (B2+D5)	0.5 (1.98E-3)	800 (2.5)
M13 (B4+D1)	8.9 (4.00E-2)	0.1 (3.14E-4)
M14 (B4+D2)	8.9 (4.00E-2)	1.00 (3.14E-3)
M15 (B5+D1)	89 (0.4)	0.1 (3.14E-4)
M16 (B5+D2)	89 (0.4)	1.00 (3.14E-3)

[1] media-EQS Inland surface waters (B[*a*]P - Directive 2008/105/EC)
[2] higher concentrations in EU surface waters
[3] concentrations above that can disturber the central nervous system development of zebrafish embryos
[4] 1/10 of NOAEL (No Observed Adverse Effect Level) for zebrafish embryos
[5] 1/10 of NOEC (No Observed Effect Concentration) for zebrafish embryos
[6] 1/50 of NOEC for zebrafish embryos
[7] 1/5 of NOEC for zebrafish embryos

A.2 Computation scripts

Transcriptome mapping (Command lines for Linux):

```
## file opening line
#!/bin/bash

## import definitions
#$-V
#$-q hpc

module load kallisto-0.43.0

##1. B5R1-N039
mkdir /data/seatox/Output/B5R1-N039
kallisto quant -i /data/seatox/ZF2019/ZF.index -o /data/seatox/Output/B5R1-N039
/data/seatox/ZF2019/B5R1-N039/B5R1-N039_S4_L005_R1_001.fastq.gz /data/seatox/ZF2019/B5R1-
N039/B5R1-N039_S4_L005_R2_001.fastq.gz
##2.B5R2-N040
mkdir /data/seatox/Output/B5R2-N040
kallisto quant -i /data/seatox/ZF2019/ZF.index -o /data/seatox/Output/B5R2-N040
/data/seatox/ZF2019/B5R2-N040/B5R2-N040_S5_L005_R1_001.fastq.gz /data/seatox/ZF2019/B5R2-
N040/B5R2-N040_S5_L005_R2_001.fastq.gz
##3. B5R3-N041
mkdir /data/seatox/Output/B5R3-N041
kallisto quant -i /data/seatox/ZF2019/ZF.index -o /data/seatox/Output/B5R3-N041
/data/seatox/ZF2019/B5R3-N041/B5R3-N041_S6_L005_R1_001.fastq.gz /data/seatox/ZF2019/B5R3-
N041/B5R3-N041_S6_L005_R2_001.fastq.gz
##4. D5R1-N042
mkdir /data/seatox/Output/D5R1-N042
kallisto quant -i /data/seatox/ZF2019/ZF.index -o /data/seatox/Output/D5R1-N042
/data/seatox/ZF2019/D5R1-N042/D5R1-N0042_S224_L004_R1_001.fastq.gz /data/seatox/ZF2019/D5R1-
N042/D5R1-N0042_S224_L004_R2_001.fastq.gz
##5. D5R2-N043
mkdir /data/seatox/Output/D5R2-N043
kallisto quant -i /data/seatox/ZF2019/ZF.index -o /data/seatox/Output/D5R2-N043
/data/seatox/ZF2019/D5R2-N043/D5R2-N0043_S225_L004_R1_001.fastq.gz /data/seatox/ZF2019/D5R2-
N043/D5R2-N0043_S225_L004_R2_001.fastq.gz
##6. D5R3-N044
mkdir /data/seatox/Output/D5R3-N044
kallisto quant -i /data/seatox/ZF2019/ZF.index -o /data/seatox/Output/D5R3-N044
/data/seatox/ZF2019/D5R3-N044/D5R3-N044_S9_L005_R1_001.fastq.gz /data/seatox/ZF2019/D5R3-
N044/D5R3-N044_S9_L005_R2_001.fastq.gz
##7. M8R1-N045
mkdir /data/seatox/Output/M8R1-N045
kallisto quant -i /data/seatox/ZF2019/ZF.index -o /data/seatox/Output/M8R1-N045
/data/seatox/ZF2019/M8R1-N045/M8R1-N0045_S227_L004_R1_001.fastq.gz /data/seatox/ZF2019/M8R1-
N045/M8R1-N0045_S227_L004_R2_001.fastq.gz
##8. M8R2-N046
```

```
mkdir /data/seatox/Output/M8R2-N046
kallisto quant -i /data/seatox/ZF2019/ZF.index -o /data/seatox/Output/M8R2-N046
/data/seatox/ZF2019/M8R2-N046/M8R2-N046_S11_L005_R1_001.fastq.gz /data/seatox/ZF2019/M8R2-
N046/M8R2-N046_S11_L005_R2_001.fastq.gz
##9. M8R3-N047
mkdir /data/seatox/Output/M8R3-N047
kallisto quant -i /data/seatox/ZF2019/ZF.index -o /data/seatox/Output/M8R3-N047
/data/seatox/ZF2019/M8R3-N047/M8R3-N0047_S229_L004_R1_001.fastq.gz /data/seatox/ZF2019/M8R3-
N047/M8R3-N0047_S229_L004_R2_001.fastq.gz
##10. SCR1-N036
mkdir /data/seatox/Output/SCR1-N036
kallisto quant -i /data/seatox/ZF2019/ZF.index -o /data/seatox/Output/SCR1-N036
/data/seatox/ZF2019/SCR1-N036/SCR1-N036_S1_L005_R1_001.fastq.gz /data/seatox/ZF2019/SCR1-
N036/SCR1-N036_S1_L005_R2_001.fastq.gz
##11. SCR2-N037
mkdir /data/seatox/Output/SCR2-N037
kallisto quant -i /data/seatox/ZF2019/ZF.index -o /data/seatox/Output/SCR2-N037
/data/seatox/ZF2019/SCR2-N037/SCR2-N037_S2_L005_R1_001.fastq.gz /data/seatox/ZF2019/SCR2-
N037/SCR2-N037_S2_L005_R2_001.fastq.gz
##12. SCR3-N038
mkdir /data/seatox/Output/SCR3-N038
kallisto quant -i /data/seatox/ZF2019/ZF.index -o /data/seatox/Output/SCR3-N038
/data/seatox/ZF2019/SCR3-N038/SCR3-N038_S3_L005_R1_001.fastq.gz /data/seatox/ZF2019/SCR3-
N038/SCR3-N038_S3_L005_R2_001.fastq.gz
```

Gene expression analysis (R script):

```
##Loading necessary R packages
library(tximport)
library(edgeR)
library(seqinr)

##Data folders
folder<-"C:\\Read data\\"
samples<-dir(folder)
file<-c(paste(sep="",folder,samples,"/","abundance.tsv"))
names(file)=samples
names(file)

##Import data
ZFtsv <- tximport(file, type = "kallisto", txOut = TRUE,countsFromAbundance =
"lengthScaledTPM")
head(ZFtsv$counts)

##View in table format
View(ZFtsv$counts)
dim(ZFtsv$counts)
colnames(ZFtsv$counts)
```

```
##Create table
dir<-"C:\\Users\\Carla Martins\\Documents\\PhD\\PhD_Data\\Ensaios zebrafish\\Data_embryos\\Experiment 2_ RNAextraction\\Code_Carla\\Final_Code_results\\"
file<-"Danio_rerio.GRCz11.cdna.all.fa.gz"
ZFfa<-read.fasta(paste(sep="",dir,file),as.string = TRUE)
head(ZFfa)

ZFtxID<-getName(ZFfa)
ZFtxAnnotation<-as.character(getAnnot(ZFfa))
ZFtxAnnotation<-sapply(strsplit(ZFtxAnnotation, split="gene:", fixed=TRUE), function(x) (x[2]))
ZFtxAnnotation<-sapply(strsplit(ZFtxAnnotation, split="[Source", fixed=TRUE), function(x) (x[1]))
ZFtx2gene<-as.data.frame(cbind(ZFtxID,ZFtxAnnotation))
write.table(ZFtx2gene,paste(sep="","ZFtx2gene.csv"),sep=";",col.names=NA)

##summarize the transcripts
ZFtsv_Gene <- summarizeToGene(ZFtsv, ZFtx2gene,ignoreTxVersion = F,countsFromAbundance = "lengthScaledTPM")
head(ZFtsv_Gene$counts)
write.table(ZFtsv_Gene,paste(sep="","ZFcounts.csv"),sep=";",col.names=NA)

fullData<-read.table(paste(sep="","ZFcounts.csv"),sep=";",header=TRUE)
head(fullData)

ID<-as.data.frame(sapply(strsplit(as.character(fullData[,1]), split=" gene_biotype:protein_coding transcript_biotype:", fixed=TRUE), function(x) (x[1])))
gene<-as.data.frame(sapply(strsplit(as.character(fullData[,1]), split=" gene_biotype:protein_coding transcript_biotype:", fixed=TRUE), function(x) (x[2])))

ZFCounts<-cbind(ID,gene,
fullData$counts.B5R1.N039,
fullData$counts.B5R2.N040,
fullData$counts.B5R3.N041,
fullData$counts.D5R1.N042,
fullData$counts.D5R2.N043,
fullData$counts.D5R3.N044,
fullData$counts.M8R1.N045,
fullData$counts.M8R2.N046,
fullData$counts.M8R3.N047,
fullData$counts.SCR1.N036,
fullData$counts.SCR2.N037,
fullData$counts.SCR3.N038)

colnames(ZFCounts)<-
c("ID","Gene","B5R1","B5R2","B5R3","D5R1","D5R2","D5R3","M8R1","M8R2","M8R3","SCR1","SCR2","SCR3")
ZFGroups<- c("B5","B5","B5","D5","D5","D5","M8","M8","M8","SC","SC","SC")
```

```
ZFData<-DGEList(counts=ZFCounts[,3:14], group=ZFGroups,genes=ZFCounts[,1:2])

##Data normalization
ZFData1<-calcNormFactors(ZFData)

##Model application
ZFDesign<-model.matrix(~0+ZFGroups,data=ZFData1$samples)
colnames(ZFDesign) <- levels(ZFData1$samples$group)
ZFData2<-estimateDisp(ZFData1,ZFDesign)
ZFfit <- glmFit(ZFData2,ZFDesign)

B5vSC <- makeContrasts(B5-SC, levels=ZFDesign)
D5vSC <- makeContrasts(D5-SC, levels=ZFDesign)
M8vSC <- makeContrasts(M8-SC, levels=ZFDesign)

ZFlrtB5 <- glmLRT(ZFfit,contrast=B5vSC)
 topTags(ZFlrtB5)
write.table( topTags(ZFlrtB5),paste(sep="","top_ZFlrtB5.csv"),sep=";",col.names=NA)

ZFlrtD5 <- glmLRT(ZFfit,contrast=D5vSC)
 topTags(ZFlrtD5)
write.table( topTags(ZFlrtD5),paste(sep="","top_ZFlrtD5.csv"),sep=";",col.names=NA)

ZFlrtM8 <- glmLRT(ZFfit,contrast=M8vSC)
 topTags(ZFlrtM8)
write.table( topTags(ZFlrtM8),paste(sep="","top_ZFlrtM8.csv"),sep=";",col.names=NA)

ZFResults<-cbind(ZFCounts[,1:2],ZFlrtB5$table,ZFlrtD5$table,ZFlrtM8$table)
colnames(ZFResults)<-c("ENSEMBL   ID",   "Gene",   "logFC-B5",   "logCPM-B5","LR-B5","p-
B5","logFC-D5", "logCPM-D5","LR-D5","p-D5","logFC-M8", "logCPM-M8","LR-M8","p-M8")
head(ZFResults)
write.table(ZFResults,paste(sep="","ZFResults.csv"),sep=";",col.names=NA)

##Gene expression
expressionTable<-decideTests(ZFResults[,grepl("p",
colnames(ZFResults))],coefficients=ZFResults[,grepl("logFC",
colnames(ZFResults))],lfc=1.5,adjust.method="fdr")
colnames(expressionTable)<-c("B5","D5","M8")
head(expressionTable)
nrow(expressionTable)

ZFet<-cbind(ZFResults,expressionTable)
head(ZFet)
write.table(ZFet,paste(sep="","ZFet.csv"),sep=";",col.names=NA)

degTable<-ZFet[which(abs(ZFet[,15]) == 1 | abs(ZFet[,16]) == 1 | abs(ZFet[,17]) == 1),]
head(degTable)
nrow(degTable)
```

```
degTableX<-ZFet[which(abs(ZFet[,15]) == 1),]
write.table(degTableX,paste(sep="","degTableX.csv"),sep=";",col.names=NA)
windows()
plotSmear(ZFlrtB5,de.tags=rownames(degTableX),cex=0.5)
dev.print(tiff, paste(sep="","plotSmear_B5.tif"), height = 15, width = 15,  units = 'cm',
type="windows", res=300)

degTableY<-ZFet[which(abs(ZFet[,16]) == 1),]
write.table(degTableY,paste(sep="","degTableY.csv"),sep=";",col.names=NA)
windows()
plotSmear(ZFlrtD5,de.tags=rownames(degTableY),cex=0.5)
dev.print(tiff, paste(sep="","plotSmear_D5.tif"), height = 15, width = 15,  units = 'cm',
type="windows", res=300)

degTableZ<-ZFet[which(abs(ZFet[,17]) == 1),]
write.table(degTableZ,paste(sep="","degTableZ.csv"),sep=";",col.names=NA)
windows()
plotSmear(ZFlrtM8,de.tags=rownames(degTableZ),cex=0.5)
dev.print(tiff, paste(sep="","plotSmear_M8.tif"), height = 15, width = 15,  units = 'cm',
type="windows", res=300)

##Venn diagrams
windows()
vennDiagram(degTable[,15:17],
 include=c("up", "down"),
 counts.col=c("red","green"),
 circle.col=c("blue","red","yellow"),
 show.include=FALSE,
 cex=c(1.3,1.3,1.3),
 names=colnames(degTable)[15:17])
dev.print(tiff,
 paste(sep="","Venn.tif"),
 height = 15,
 width = 15,
 units = 'cm',
 type="windows",
 res=300)

##Up and down expressed gene tables
B5_upTable<-ZFet[which(ZFet[,15]==1 & ZFet[,16]==0 & ZFet[,17]==0),]
write.table(B5_upTable,paste(sep="","B5_upTable.csv"),sep=";",col.names=NA)
B5_downTable<-ZFet[which(ZFet[,15]==-1 & ZFet[,16]==0 & ZFet[,17]==0),]
write.table(B5_downTable,paste(sep="","B5_downTable.csv"),sep=";",col.names=NA)

D5_upTable<-ZFet[which(ZFet[,15]==0 & ZFet[,16]==1 & ZFet[,17]==0),]
write.table(D5_upTable,paste(sep="","D5_upTable.csv"),sep=";",col.names=NA)
D5_downTable<-ZFet[which(ZFet[,15]==0 & ZFet[,16]==-1 & ZFet[,17]==0),]
write.table(D5_downTable,paste(sep="","D5_downTable.csv"),sep=";",col.names=NA)
```

```
M8_upTable<-ZFet[which(ZFet[,15]==0 & ZFet[,16]==0 & ZFet[,17]==1),]
write.table(M8_upTable,paste(sep="","M8_upTable.csv"),sep=";",col.names=NA)
M8_downTable<-ZFet[which(ZFet[,15]==0 & ZFet[,16]==0 & ZFet[,17]==-1),]
write.table(M8_downTable,paste(sep="","M8_downTable.csv"),sep=";",col.names=NA)

B5D5_upTable<-ZFet[which(ZFet[,15]==1 & ZFet[,16]==1 & ZFet[,17]==0),]
write.table(B5D5_upTable,paste(sep="","B5D5_upTable.csv"),sep=";",col.names=NA)
B5D5_downTable<-ZFet[which(ZFet[,15]==-1 & ZFet[,16]==-1 & ZFet[,17]==0),]
write.table(B5D5_downTable,paste(sep="","B5D5_downTable.csv"),sep=";",col.names=NA)

B5M8_upTable<-ZFet[which(ZFet[,15]==1 & ZFet[,16]==0 & ZFet[,17]==1),]
write.table(B5M8_upTable,paste(sep="","B5M8_upTable.csv"),sep=";",col.names=NA)
B5M8_downTable<-ZFet[which(ZFet[,15]==-1 & ZFet[,16]==0 & ZFet[,17]==-1),]
write.table(B5M8_downTable,paste(sep="","B5M8_downTable.csv"),sep=";",col.names=NA)

D5M8_upTable<-ZFet[which(ZFet[,15]==0 & ZFet[,16]==1 & ZFet[,17]==1),]
write.table(D5M8_upTable,paste(sep="","D5M8_upTable.csv"),sep=";",col.names=NA)
D5M8_downTable<-ZFet[which(ZFet[,15]==0 & ZFet[,16]==-1 & ZFet[,17]==-1),]
write.table(D5M8_downTable,paste(sep="","D5M8_downTable.csv"),sep=";",col.names=NA)

B5D5M8_upTable<-ZFet[which(ZFet[,15]==1 & ZFet[,16]==1 & ZFet[,17]==1),]
write.table(B5D5M8_upTable,paste(sep="","B5D5M8_upTable.csv"),sep=";",col.names=NA)
B5D5M8_downTable<-ZFet[which(ZFet[,15]==-1 & ZFet[,16]==-1 & ZFet[,17]==-1),]
write.table(B5D5M8_downTable,paste(sep="","B5D5M8_downTable.csv"),sep=";",col.names=NA)
```

Gene ontology (GO) / gene enrichment (GE) and pathway analysis (R script):

```
##Load a R package
library(biomaRt)
library(stringr)
library(ggplot2)
library(cowplot)
library(org.Dr.eg.db)
library(multiGSEA)

##Create folders
dir.create("DEG/aux")
dir.create("GO")
dir.create("GO/aux")
dir.create("Fisher")
dir.create("Pathways")

##Directories
##Folders
pathDEG<-"DEG/"
pathDEGaux<-"DEG/aux/"
pathGO<-"GO/"
pathGOaux<-"GO/aux/"
pathFisher<-"Fisher/"
```

```
pathPathways<-"Pathways/"

##Objects
species<-c("Zebrafish")
treatment<-data.frame(Zebrafish = c("B5", "D5", "M8", "M8"),
                      Data = c("Total_", "Total_", "Total_", ""))
log10FDR<-expression(paste("-log"[10], "(adj. P-value)"))
GOCategory<-data.frame(Category = c("biological_process", "cellular_component",
"molecular_function"),
                       category = c("BP", "CC", "MF"))
GOBP<-c("cellular response to xenobiotic stimulus",
        "response to xenobiotic stimulus",
        "xenobiotic catabolic process",
        "xenobiotic detoxification by transmembrane export across the plasma membrane",
        "xenobiotic metabolic process",
        "signal transduction by p53 class mediator",
        "negative regulation of cell death",
        "negative regulation of extrinsic apoptotic signaling pathway via death domain
receptors",
        "regulation of neuron death",
        "apoptotic process",
        "execution phase of apoptosis",
        "extrinsic apoptotic signaling pathway in absence of ligand",
        "intrinsic apoptotic signaling pathway in response to DNA damage",
        "negative regulation of apoptotic process",
        "negative regulation of cysteine-type endopeptidase activity involved in apoptotic
process",
        "negative regulation of extrinsic apoptotic signaling pathway via death domain
receptors",
        "negative regulation of intrinsic apoptotic signaling pathway",
        "positive regulation of neutrophil apoptotic process",
        "regulation of apoptotic process",
        "regulation of glomerular visceral epithelial cell apoptotic process",
        "cell population proliferation",
        "chondrocyte proliferation",
        "growth plate cartilage chondrocyte proliferation",
        "myoblast proliferation involved in skeletal muscle regeneration",
        "negative regulation of alpha-beta T cell proliferation",
        "negative regulation of CD4-positive, alpha-beta T cell proliferation",
        "negative regulation of cell population proliferation",
        "negative regulation of smooth muscle cell proliferation",
        "positive regulation of cell population proliferation",
        "positive regulation of endothelial cell proliferation",
        "positive regulation of glial cell proliferation",
        "positive regulation of T cell proliferation",
        "regulation of cell population proliferation",
        "regulation of neuroblast proliferation",
        "T cell proliferation")
GOMF<-c("xenobiotic transmembrane transporter activity",
```

```
            "cysteine-type endopeptidase activity involved in apoptotic process",
            "cysteine-type endopeptidase activity involved in execution phase of apoptosis",
            "glucuronosyltransferase activity",
            "UDP-glycosyltransferase activity")
    GOCC<-c()

    ##Select the differentially-expressed genes
    degGenes<-function(pathDEG, pathDEGaux, species, treatment){
      Fet<-read.csv(paste(pathDEG, "ZFet.csv", sep = ""), sep=";", header=T)
      Fet$GeneName<-unlist(sapply(Fet$Gene, function(x) unlist(strsplit(x, "_symbol:", fixed
= TRUE))[2]))
      Fet$GeneName<-unlist(sapply(Fet$GeneName,     function(x)     unlist(strsplit(x,     "
description:", fixed = TRUE))[1]))
      Fet$EnsemblID<-unlist(sapply(Fet$ENSEMBL.ID, function(x) unlist(strsplit(x, ".", fixed
= TRUE))[1]))
      Fet<-Fet[,c(2, ncol(Fet), 3, ncol(Fet)-1, 4:(ncol(Fet)-2))]
      degTable<-Fet[which(abs(Fet[treatment[1,1]]) == 1 | abs(Fet[treatment[2,1]]) == 1 |
abs(Fet[treatment[3,1]]) == 1),]
      write.table(degTable, paste(pathDEGaux, species, "degTable.csv", sep = ""), sep = ";",
col.names = NA)
      save(degTable, file = paste(pathDEGaux, species, "degTable.RData", sep = ""))
      Ensembl(pathDEGaux, species, degTable)
    }

    ##Retrive the GO Terms associated with each Ensembl ID
    Ensembl<-function(pathDEGaux, species, degTable){
      GeneName<-unique(degTable$ENSEMBL.ID)
      GeneName<-unlist(sapply(GeneName,   function(x)   unlist(strsplit(x,   ".",   fixed   =
TRUE))[1]))
      print(GeneName[1:3])
      print(length(GeneName))
      GeneList<-getBM(
        filters="ensembl_gene_id",
        attributes  =  c("ensembl_gene_id",  "entrezgene_accession",  "go_id",  "name_1006",
"definition_1006", "go_linkage_type", "namespace_1003"),
        values=as.factor(GeneName),
        uniqueRows=TRUE,
        mart=geneSet
      )
      print(length(unique(GeneList[,1])))
      ##Which Ensembls IDs have different genes associated
      multipleGenes<-
unique(unique(GeneList[,c(1,2)])[which(duplicated(unique(GeneList[,c(1,2)])[,1])),][,1])
      save(GeneList,      multipleGenes,      file      =      paste(pathDEGaux,      species,
"EnsemblGeneList.RData", sep = ""))
      write.table(GeneList, paste(pathDEGaux, species, "EnsemblGeneList.csv", sep = ""), sep
= ";", col.names = NA)
    }
```

```
      ##Subset the tables according to the relative level of expression and present in the
tables
      subsetlogFC<-function(pathDEG, species, files, degTable, i){
        print(files)
        filename<-unlist(sapply(files, function(x) unlist(strsplit(x, ".", fixed = TRUE))[1]))
        aux<-str_count(files, "_")
        if(aux > 1){
          data<-unlist(sapply(filename, function(x) unlist(strsplit(x, "_", fixed = TRUE))[1]))
          treatment<-unlist(sapply(filename,  function(x)  unlist(strsplit(x,  "_",  fixed  =
TRUE))[2]))
          name<-paste(data, treatment, sep = "_")
        }
        else{
          data<-""
          treatment<-unlist(sapply(filename,  function(x)  unlist(strsplit(x,  "_",  fixed  =
TRUE))[1]))
          name<-treatment
        }
        relexp<-unlist(sapply(filename,  function(x)  tail(unlist(strsplit(x,  "_",  fixed  =
TRUE)), n = 1)))
        if(i %% 2)
          dir.create(paste(pathDEG, name, sep = ""))
        pathfiles<-paste(pathDEG, name, "/", sep = "")
        degAux<-read.csv(paste(pathDEG, "C/", files, sep = ""), sep=";", header=T)
        deg<-degTable[which(degTable$EnsemblID %in% degAux[,2]),]
        if(data == "Total" && relexp == "up")
          deg<-deg[which(deg[treatment] == 1),]
        else if(data == "Total" && relexp == "down")
          deg<-deg[which(deg[treatment] == -1),]
        else if(relexp == "up")
          deg<-deg[which(deg[treatment] == 1 & deg["B5"] == 0 & deg["D5"] == 0),]
        else
          deg<-deg[which(deg[treatment] == -1 & deg["B5"] == 0 & deg["D5"] == 0),]
        rownames(deg)<-NULL
        write.table(deg, paste(pathfiles, species, "_", filename, ".csv", sep = ""), sep = ";",
col.names = NA)
        save(deg, file = paste(pathfiles, species, "_", filename, ".RData", sep = ""))
      }

      ##Organize the Tables with GO Terms
      ##Add the name and category of GO:0051430 to the table
      ##Delete the GO Terms: "biological_process", "cellular_component", "molecular_function"
      ##Subset the GO Terms according to their category
      GOData<-function(pathGO, species, GOCategory, GeneList){
        for(i in nrow(GeneList):1){
          if(GeneList$go_id[i] == "")
            GeneList<-GeneList[-i,,drop = FALSE]
        }
```

```
        GeneList[which(GeneList$go_id == "GO:0051430" & GeneList$ensembl_gene_id ==
"ENSDARG00000115236"),c(4,7)]<-c("corticotropin-releasing hormone receptor 1 binding",
"molecular_function")
        GeneList<-GeneList[-which(GeneList$name_1006 %in% c("biological_process",
"cellular_component", "molecular_function")),,drop = FALSE]
        for(j in 1:nrow(GOCategory)){
          GO<-subset(GeneList, GeneList$namespace_1003 == GOCategory[j,1])
          print(nrow(GO))
          GO<-unique(GO[,c(1,3,4)])
          print(nrow(GO))
          assign(paste("GO", GOCategory[j,2], sep = ""), GO)
        }
        save(GeneList, GOBP, GOCC, GOMF, file = paste(pathGO, species, "GeneList.RData", sep =
""))
      }

      ##Calculating the percentage of genes related with a specific GO Term
      GOTerm<-function(pathGO, species, filename, relexp, GOCategory, deg, GOTable){
        GO<-unique(data.frame(GOTerm = GOTable$name_1006,
                              NumberORFs = 0))
        for(i in 1:nrow(deg)){
          GOaux<-GOTable[which(GOTable$ensembl_gene_id == deg$EnsemblID[i]),]
          if(!is.null(GOaux)){
            for(j in 1:nrow(GOaux)){
              GO[which(GO$GOTerm == GOaux[j,3]),2]<-GO[which(GO$GOTerm == GOaux[j,3]),2]+1
            }
          }
        }
        GO<-GO[order(-GO$NumberORFs),]
        GO<-data.frame(GO, GO$NumberORFs/nrow(deg)*100)
        colnames(GO)<-c("GOTerm", "NumberORFs", "Percentage")
        save(GO, file = paste(sep = "", pathGO, filename, "/", species, "_", GOCategory, "_",
filename, "_", relexp, ".RData"))
        write.table(GO, paste(sep = "", pathGO, filename, "/", species, "_", GOCategory, "_",
filename, "_", relexp, ".csv"), sep=";", col.names=NA)
        return(GO)
      }

      ##Preparing the data for plotting the Top10 GO Terms
      GOGraphData<-function(pathGOaux, species, filename, relexp, GO, GOCategory){
        pos<-which(GO$NumberORFs == 0)
        if(pos[1] < 10)
          GOsame<-pos[1]-1
        else
          GOsame<-which(GO$Percentage == GO$Percentage[10])
        GOTop10<-GO[1:GOsame[length(GOsame)],]
        GOGraph<-data.frame(GOTerm = GOTop10$GOTerm[1:GOsame[length(GOsame)]],
                            Numbers = GOTop10$Percentage[1:GOsame[length(GOsame)]],
                            group = GOCategory)
```

```
        GOGraph$group<-factor(gsub("_", "\\1 \\2", GOGraph$group))
        GOGraph$group<-factor(gsub("(^|[[:space:]])([[:alpha:]])", "\\1\\U\\2", GOGraph$group,
perl = TRUE))
        save(GOGraph, file = paste(pathGOaux, species, "_", "GOGraph", "_", GOCategory, "_",
filename, "_", relexp, ".RData", sep = ""))
        return(GOGraph)
      }

      ##Ploting the TOP10 GO Terms per treatment and also taking into consideration whether the
genes are up or down-regulated
      GOGraph<-function(pathGO, pathGOaux, species, filename, relexp, GOCategory,
legendposition, deg){
        load(paste(pathGO, species, "GeneList.RData", sep = ""))
        for(i in 1:nrow(GOCategory)){
          GO<-GOTerm(pathGO, species, filename, relexp, GOCategory$Category[i], deg,
get(paste("GO", GOCategory$category[i], sep = "")))
          GOGraphAux<-GOGraphData(pathGOaux, species, filename, relexp, GO,
GOCategory$Category[i])
          if(i == 1)
            GOGraph<-GOGraphAux
          else
            GOGraph<-rbind(GOGraph, GOGraphAux)
        }
        save(GOGraph, file = paste(pathGOaux, species, "_", filename, "_", relexp, "GOGraph",
".RData", sep = ""))
        ##Replace these two GO Terms by abreviations
        GOGraph$GOTerm<-gsub("oxidoreductase activity, acting on paired donors, with
incorporation or reduction of molecular oxygen, reduced flavin or flavoprotein as one donor,
and incorporation of one atom of oxygen", "oxidoreductase (...)", GOGraph$GOTerm)
        GOGraph$GOTerm<-gsub("oxidoreductase activity, acting on paired donors, with
incorporation or reduction of molecular oxygen", "oxidoreductase activity (...)",
GOGraph$GOTerm)
        ggplot(GOGraph, aes(reorder(GOTerm, Numbers), Numbers, fill = group))+
          geom_col()+
          facet_wrap(~group, nrow = 3, scales = "free_y")+
          coord_flip()+
          xlab("GO Terms")+
          ylab("Percentage of ORFs")+
          theme(panel.grid = element_blank(),
                panel.background = element_blank(),
                strip.background = element_blank(),
                strip.text = element_blank(),
                axis.text = element_text(colour = "black"),
                legend.position = "none")
      }

      ##Enrichment analysis
      ##Fisher analysis for the GO Terms
      ##The data in analysis is the TOP10 GO Terms together with GO Terms of Interest
```

```
      ##The p-value was adjusted by FDR method
      Fisher<-function(pathFisher, species, filename, totaldegup, totaldegdown, GOup, GOdown,
Terms, GOCategory, j){
        FisherAux<-merge(GOup, GOdown, by = "GOTerm", all = TRUE)
        rownames(FisherAux)<-FisherAux$GOTerm
        FisherAux<-FisherAux[,-c(1,3,5),drop=FALSE]
        colnames(FisherAux)<-c("up", "down")
        save(FisherAux, file = paste(sep = "", pathFisher, filename, "/", species, "_", filename,
"_", GOCategory, "FisherAux.RData"))
        FisherAux<-FisherAux[rownames(FisherAux) %in% Terms,]
        aux<-which(FisherAux$up == 0 & FisherAux$down == 0)
        if(!is.na(aux[1]))
          FisherAux<-FisherAux[-aux,, drop = FALSE]
        print(Terms)
        print(rownames(FisherAux))
        Fisher<-data.frame(matrix(data = NA, nrow = nrow(FisherAux), ncol = 5, dimnames =
list(NULL, c(GOCategory, "Upregulated", "Downregulated", "odds_ratio", "pvalue"))))
        print(Fisher)
        print(FisherAux)
        for(i in 1:nrow(Fisher)){
          contTable<-rbind(FisherAux[i,], c(totaldegup - FisherAux[i,"up"], totaldegdown -
FisherAux[i,"down"]))
          print(FisherAux[i,])
          print(contTable)
          fisherTest<-fisher.test(contTable)
          Fisher[i,]<-data.frame(rownames(FisherAux)[i],                    FisherAux[i,"up"],
FisherAux[i,"down"], fisherTest$estimate, fisherTest$p.value)
        }
        Fisher$FDRp<-p.adjust(Fisher$pvalue, method = "fdr")
        Fisher<-Fisher[order(Fisher$FDRp, -Fisher$odds_ratio),]
        save(Fisher, file=paste(sep = "", pathFisher, filename, "/", species, "_", filename,
"_", GOCategory, "Fisher.RData"))
        FisherFormatted(pathFisher, species, GOCategory, filename, Fisher)
        graph<-FisherGraph(species, GOCategory, filename, j, Fisher)
        return(graph)
      }

      ##Formatting the output table from the fisher analysis
      FisherFormatted<-function(pathFisher, species, GOCategory, filename, FisherFormatted){
        FisherFormatted$odds_ratio<-sprintf("%.3f",
as.numeric(format(FisherFormatted$odds_ratio, digits = 3)))
        FisherFormatted$pvalue<-format(FisherFormatted$pvalue, digits = 3)
        FisherFormatted$FDRp<-format(FisherFormatted$FDRp, digits = 3, scientific = TRUE)
        save(FisherFormatted, file = paste(sep = "", pathFisher, filename, "/", species, "_",
filename, "_", GOCategory, "FisherFormatted.RData"))
        write.table(FisherFormatted, paste(sep =  "", pathFisher, filename, "/", species, "_",
filename, "_", GOCategory, "FisherFormatted.csv"), sep=";", col.names=NA)
      }
```

```
##Bar plot with the results from the Fisher analysis
FisherGraph<-function(species, GOCategory, filename, i, Fisher){
  Fisher$odds_ratioGraph<-NA
  Fisher$odds_ratioGraph[which(Fisher$odds_ratio > 1)]<-c("Odds-ratio > 1")
  Fisher$odds_ratioGraph[which(Fisher$odds_ratio < 1)]<-c("Odds-ratio < 1")
  FisherGraphAux<-data.frame(Term = Fisher[,GOCategory],
                             Numbers = -log10(Fisher$FDRp),
                             group = Fisher$odds_ratioGraph)
  ##Replace these two GO Terms by abreviations
  FisherGraphAux$Term<-gsub("oxidoreductase activity, acting on paired donors, with incorporation or reduction of molecular oxygen, reduced flavin or flavoprotein as one donor, and incorporation of one atom of oxygen", "oxidoreductase (...)", FisherGraphAux$Term)
  FisherGraphAux$Term<-gsub("oxidoreductase activity, acting on paired donors, with incorporation or reduction of molecular oxygen", "oxidoreductase activity (...)", FisherGraphAux$Term)
  ggplot(FisherGraphAux, aes(reorder(Term, Numbers), Numbers, fill = group))+
    geom_col()+
    coord_flip()+
    xlab(gsub("(^|[[:space:]])([[:alpha:]])", "\\1\\U\\2", gsub("_", "\\1 \\2", GOCategory), perl = TRUE))+
    ylab(log10FDR)+
    scale_fill_manual(values = c("#fcb683", "#83d6fc"),
                      breaks = c("Odds-ratio > 1", "Odds-ratio < 1"))+
    geom_hline(yintercept = -log10(0.05), linetype = 2)+
    theme(panel.grid = element_blank(),
          panel.background = element_blank(),
          strip.background = element_blank(),
          strip.text = element_blank(),
          axis.text = element_text(colour = "black"),
          legend.position = "bottom",
          legend.title = element_blank(),
          legend.direction = "vertical",
          plot.title.position = "plot",
          plot.title = element_text(hjust = 0.8))
}

##Pathway Enrichment
PathwaysEnrichment<-function(pathDEG, pathPathways, treatment, species, omics, pathways, deg){
  filename<-paste(treatment$Data, treatment$Zebrafish, sep = "")
  dir.create(paste(pathPathways, filename, sep = ""))
  deg<-deg[,c("EnsemblID", paste("logFC.", treatment$Zebrafish, sep = ""), paste("p.", treatment$Zebrafish, sep = ""))]
  print(head(deg))
  omics$transcriptome<-rankFeatures(deg[,2], deg[,3])
  print(head(omics$transcriptome))
  names(omics$transcriptome)<-deg$EnsemblID
  ##For the analysis be reproducible, seed had to be specified
  ##This seed was specified according to github's example
```

```
        set.seed(42)
        enrichmentaux<-multiGSEA(pathways, omics)
        print(head(enrichmentaux))
        aux<-data.frame()
        for(i in 1:nrow(enrichmentaux$transcriptome)){
          aux[i,1]<-paste(enrichmentaux[["transcriptome"]][["leadingEdge"]][[i]], collapse = ",
")
        }
        ##Retrieve the enriched pathways, statistic results (p-value and adjusted p-value),
enrichment scores (ES and NES), size and leading edges
        ##The p-value is adjusted according to the BH method
        ##Size: total of genes from the dataset that are present in that specific pathway
        ##Leading edges: apparently correspond to the genes that are influencing/driving the
enrichment
        ##According to information present on biocondutor support site, if the enrichment is
positive (pathway up-regulated), the genes present in the leading edges are also up-regulated
and vice-versa
        enrichment<-data.frame(enrichmentaux$transcriptome[,c(1:3,5:7)], aux)
        colnames(enrichment)[7]<-"leadingEdge"
        enrichment<-enrichment[order(enrichment$padj,  enrichment$pval,  -enrichment$NES,  -
enrichment$ES),]
        save(omics, enrichmentaux, enrichment, file = paste(sep = "", pathPathways, filename,
"/", species, "_", filename, "_KEGG.RData"))
        write.table(enrichment, paste(sep =  "", pathPathways, filename, "/", species, "_",
filename, "_KEGG.csv"), sep=";", col.names=NA)
        write.table(enrichmentaux$transcriptome[,1:7], paste(sep =  "", pathPathways, filename,
"/", species, "_", filename, "_KEGG_aux.csv"), sep=";", col.names=NA)
      }

      ##R Console
      ##Converting the Ensembl IDs into Uniprot Accession
      geneSet = useMart(biomart="ensembl", dataset="drerio_gene_ensembl")
      degGenes(pathDEG, pathDEGaux, species, treatment)

      files<-list.files(path = "DEG/C/")
      load(paste(pathDEGaux, species, "degTable.RData", sep = ""))
      for(i in 1:length(files)){
        relexp<-subsetlogFC(pathDEG, species, files[i], degTable, i)
      }

      ##GO Terms
      load(paste(pathDEGaux, species, "EnsemblGeneList.RData", sep = ""))
      GOData(pathGO, species, GOCategory, GeneList)

      quartz()
      relexp<-c("up", "down")
      for(i in 1:nrow(treatment)){
        filename<-paste(treatment$Data[i], treatment$Zebrafish[i], sep = "")
        for(j in 1:length(relexp)){
```

```
          if(j %% 2)
            dir.create(paste(pathGO, filename, sep = ""))
          load(paste(pathDEG, filename, "/", species, "_", filename, "_", relexp[j], ".RData",
sep = ""))
          assign(paste(filename, relexp[j], sep = "_"), GOGraph(pathGO, pathGOaux, species,
filename, relexp[j], GOCategory, legendposition, deg))
        }
      }
      plot_grid(Total_B5_up, Total_B5_down, labels = "AUTO", label_fontface = "plain",
label_size = 12, vjust = 2, hjust = -3, label_fontfamily = "Arial")
      dev.print(tiff, paste(pathGO, "Total_B5/Total_B5_GOTerms.tif", sep = ""), height = 30,
width = 30, units = 'cm', res=600)
      plot_grid(Total_D5_up, Total_D5_down, labels = "AUTO", label_fontface = "plain",
label_size = 12, vjust = 2, hjust = -3, label_fontfamily = "Arial")
      dev.print(tiff, paste(pathGO, "Total_D5/Total_D5_GOTerms.tif", sep = ""), height = 30,
width = 30, units = 'cm', res=600)
      plot_grid(Total_M8_up, Total_M8_down, labels = "AUTO", label_fontface = "plain",
label_size = 12, vjust = 2, hjust = -3, label_fontfamily = "Arial")
      dev.print(tiff, paste(pathGO, "Total_M8/Total_M8_GOTerms.tif", sep = ""), height = 30,
width = 30, units = 'cm', res=600)
      plot_grid(M8_up, M8_down, labels = "AUTO", label_fontface = "plain", label_size = 12,
vjust = 2, hjust = -3, label_fontfamily = "Arial")
      dev.print(tiff, paste(pathGO, "M8/M8_GOTerms.tif", sep = ""), height = 30, width = 30,
units = 'cm', res=600)

      ##Fisher Analysis: GO Terms
      quartz()
      for(i in 1:nrow(treatment)){
        filename<-paste(treatment$Data[i], treatment$Zebrafish[i], sep = "")
        for(k in 1:nrow(GOCategory)){
          Terms<-get(paste("GO", GOCategory$category[k], sep = ""))
          for(j in 1:length(relexp)){
            if(j %% 2 & k == 1)
              dir.create(paste(pathFisher, filename, sep = ""))
            load(paste(sep = "", pathGO, filename, "/", species, "_", GOCategory$Category[k],
"_", filename, "_", relexp[j], ".RData"))
            load(paste(pathGOaux, species, "_", "GOGraph", "_", GOCategory$Category[k], "_",
filename, "_", relexp[j], ".RData", sep = ""))
            assign(paste("GO", relexp[j], sep =""), GO)
            Terms<-unique(c(Terms, GOGraph$GOTerm))
            load(paste(pathDEG, filename, "/", species, "_", filename, "_", relexp[j], ".RData",
sep = ""))
            assign(paste("deg", relexp[j], sep =""), deg)
          }
          assign(paste(filename, GOCategory$Category[k], sep ="_"), Fisher(pathFisher, species,
filename, nrow(degup), nrow(degdown), GOup, GOdown, Terms, GOCategory$Category[k], i))
        }
      }
```

```
      quartz()
      plot_grid(Total_B5_biological_process, scale = 0.98)
      dev.print(tiff, paste(pathFisher, "Total_B5/", "Total_B5_biological_process_Fisher.tif",
sep = ""), height = 30, width = 30,  units = 'cm', res=600)
      quartz()
      plot_grid(Total_B5_cellular_component)
      dev.print(tiff, paste(pathFisher, "Total_B5/", "Total_B5_cellular_component_Fisher.tif",
sep = ""), height = 30, width = 30,  units = 'cm', res=600)
      quartz()
      plot_grid(Total_B5_molecular_function)
      dev.print(tiff, paste(pathFisher, "Total_B5/", "Total_B5_molecular_function_Fisher.tif",
sep = ""), height = 30, width = 30,  units = 'cm', res=600)

      quartz()
      plot_grid(Total_D5_biological_process, scale = 0.98)
      dev.print(tiff, paste(pathFisher, "Total_D5/", "Total_D5_biological_process_Fisher.tif",
sep = ""), height = 30, width = 30,  units = 'cm', res=600)
      quartz()
      plot_grid(Total_D5_cellular_component)
      dev.print(tiff, paste(pathFisher, "Total_D5/", "Total_D5_cellular_component_Fisher.tif",
sep = ""), height = 30, width = 30,  units = 'cm', res=600)
      quartz()
      plot_grid(Total_D5_molecular_function)
      dev.print(tiff, paste(pathFisher, "Total_D5/", "Total_D5_molecular_function_Fisher.tif",
sep = ""), height = 30, width = 30,  units = 'cm', res=600)

      quartz()
      plot_grid(Total_M8_biological_process, scale = 0.98)
      dev.print(tiff, paste(pathFisher, "Total_M8/", "Total_M8_biological_process_Fisher.tif",
sep = ""), height = 30, width = 30,  units = 'cm', res=600)
      quartz()
      plot_grid(Total_M8_cellular_component)
      dev.print(tiff, paste(pathFisher, "Total_M8/", "Total_M8_cellular_component_Fisher.tif",
sep = ""), height = 30, width = 30,  units = 'cm', res=600)
      quartz()
      plot_grid(Total_M8_molecular_function)
      dev.print(tiff, paste(pathFisher, "Total_M8/", "Total_M8_molecular_function_Fisher.tif",
sep = ""), height = 30, width = 30,  units = 'cm', res=600)

      quartz()
      plot_grid(M8_biological_process, scale = 0.98)
      dev.print(tiff, paste(pathFisher, "M8/", "M8_biological_process_Fisher.tif", sep = ""),
height = 30, width = 30,  units = 'cm', res=600)
      quartz()
      plot_grid(M8_cellular_component)
      dev.print(tiff, paste(pathFisher, "M8/", "M8_cellular_component_Fisher.tif", sep = ""),
height = 30, width = 30,  units = 'cm', res=600)
      quartz()
      plot_grid(M8_molecular_function)
```

```
      dev.print(tiff, paste(pathFisher, "M8/", "M8_molecular_function_Fisher.tif", sep = ""),
height = 30, width = 30,  units = 'cm', res=600)

      ##Pathway Enrichment
      ##Retrieve the KEEG pathways from Danio rerio
      database<-c("kegg")
      omics<-initOmicsDataStructure(layer = c("transcriptome"))
      layers<-names(omics)
      pathways<-getMultiOmicsFeatures(dbs = database, layer = layers, returnTranscriptome =
"ENSEMBL", useLocal = FALSE, organism = "drerio")
      save(pathways, file = paste(pathPathways, "KEGG.RData", sep = ""))

      Fet<-read.csv(paste(pathDEG, "ZFet.csv", sep = ""), sep=";", header=T)
      Fet$EnsemblID<-unlist(sapply(Fet$ENSEMBL.ID, function(x) unlist(strsplit(x, ".", fixed =
TRUE))[1]))


      for(i in 1:nrow(treatment)){
        PathwaysEnrichment(pathDEG, pathPathways, treatment[i,], species, omics, pathways, Fet)
        print(omics)
      }
```

A.3 Results: model validation and RNAseq top 5 gene table

Coefficients	Estimate	Std. Error	z value	Pr(>|z|)	
(Intercept)	1.19E+00	1.07E-01	11.054	<2e-16	***
Exposure time (h)	-3.73E-02	2.43E-03	-15.329	<2e-16	***
[BaP]	-7.57E-03	3.00E-03	-2.525	0.0116	*
[DFC]	-3.58E-03	3.28E-04	-10.898	<2e-16	***
Exposure time (h) : [BaP]	6.94E-05	6.46E-05	1.074	0.2827	
Exposure time (h) : [DFC]	9.06E-05	4.71E-06	19.249	<2e-16	***
[BaP] : [DFC]	1.54E-05	8.36E-06	1.84	0.0658	.
Exposure time (h) : [BaP] : [DFC]	-1.96E-07	1.22E-07	-1.602	0.1091	

Signif. codes: (***) 0.001; (**) 0.01; (*) 0.05; (.) 0.1

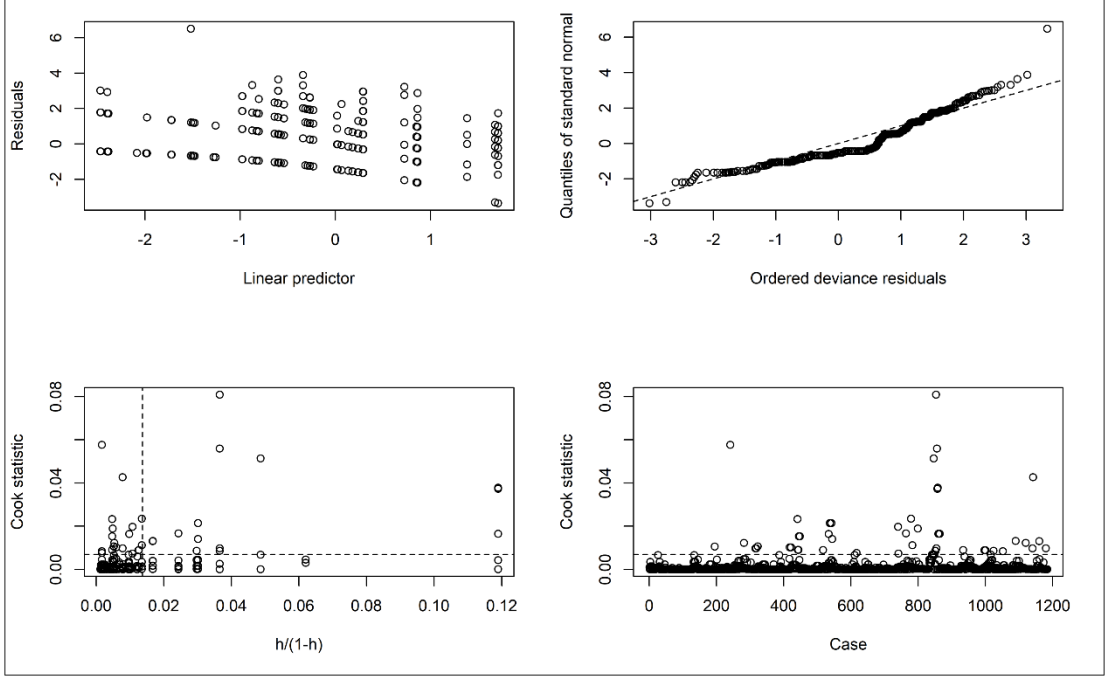

Figure A3.1. Mortality global model statistical analysis (model validation), using generalised linear models (GLM) through a Poisson regression with a log link taking variables as categorial predictors.

Coefficients	Estimate	Std. Error	z value	Pr(>|z|)	
(Intercept)	-1.74E+00	2.18E-01	-7.979	1.47E-15	***
Exposure time (h)	-1.95E-03	3.37E-03	-0.579	0.5623	
[BaP]	-6.39E-04	5.64E-03	-0.113	0.9098	
[DFC]	2.73E-03	3.36E-04	8.108	5.14E-16	***
Exposure time (h) : [BaP]	-4.20E-05	8.99E-05	-0.467	0.6403	
Exposure time (h) : [DFC]	1.36E-05	5.04E-06	2.702	0.0069	**
[BaP] : [DFC]	-2.63E-06	8.71E-06	-0.302	0.7624	
Exposure time (h) : [BaP] : [DFC]	8.91E-08	1.33E-07	0.672	0.5015	

Signif. codes: (***) 0.001; (**) 0.01; (*) 0.05; (.) 0.1

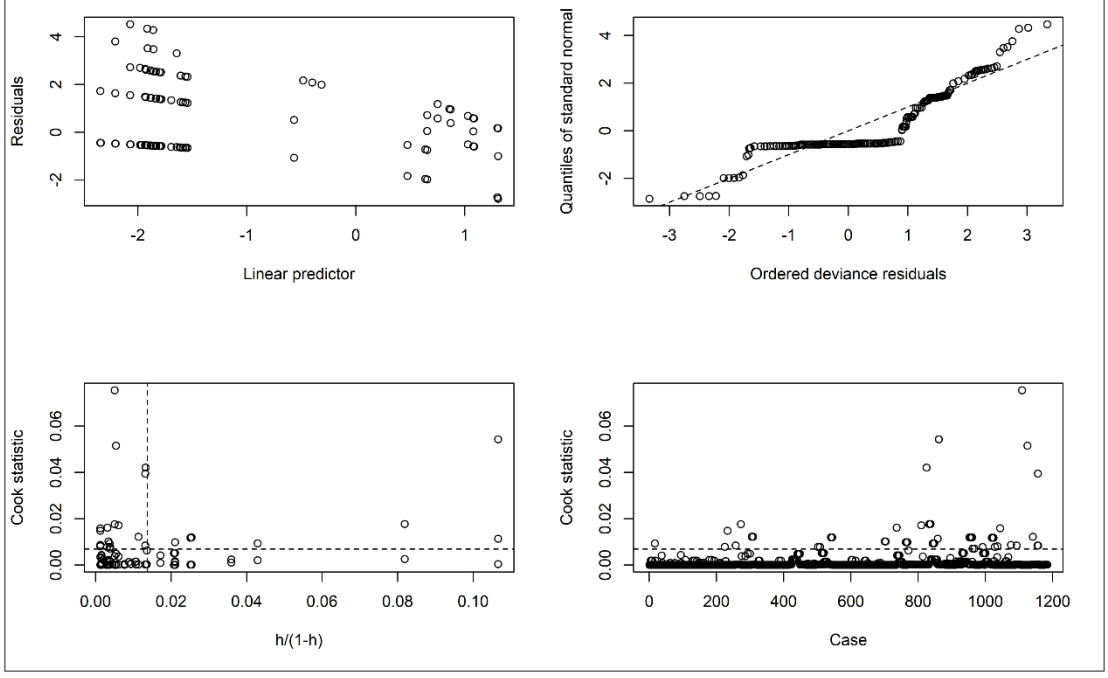

Figure A3.2. Development and pathological alterations global model statistical analysis (model validation), using generalised linear models (GLM) through a Poisson regression with a log link taking variables as categorial predictors.

Table A3.1. RNAseq top 5 genes overexpressed and underexpressed in zebrafish embryos exposed to B[*a*]P (0.4 µM), DFC (2.5 µM) and corresponding mixture.

	Accession	Gene	Gene name	NFC (logFC)	p-value	Remarks*
B[*a*]P Overexpression	ENSDARG00000034734.6	*med6*	mediator complex subunit 6	8.0696673	9.26E-07	Coactivator involved in the regulated transcription of nearly all RNA polymerase II-dependent genes
	ENSDARG00000019300.10	*ints7*	integrator complex subunit 7	7.9066723	7.74E-06	Complex involved in the small nuclear RNAs. DNA damage response signalling during the S phase. Essential during embryogenesis for eye development.
	ENSDARG00000112302.1	*pou3f1*	POU class 3 homeobox 1	7.6141121	5.03E-05	Involved in brain development and regulation of embryonic morphogenesis.
	ENSDARG00000098315.2	*cyp1a*	cytochrome P450, family 1, subfamily A	6.802180	1.70E-103	Metabolism of xenobiotics
	ENSDARG00000009438.8	*myog*	myogenin	6.1394187	1.52E-05	DNA-binding transcription activator activity. Involved in skeletal muscle tissue development and regeneration.
B[*a*]P Underexpression	ENSDARG00000117024.1	*rpe*	ribulose-5-phosphate-3-epimerase	-7.7245377	2.69E-08	Involved in metal ion binding activity and cilium morphogenesis.
	ENSDARG00000115689.1	*CU207215.1*	BTB (POZ) domain containing 10b	-6.8241841	4.99E-05	Activator of AKT family members. Prevent motor neuronal death and accelerate the growth of pancreatic beta cells.
	ENSDARG00000112962.1	*ppp1r3ca*	protein phosphatase 1, regulatory subunit 3Ca	-6.3437777	2.33E-05	Involved in glycogen biosynthetic process.
	ENSDARG00000100372.2	*alad*	aminolevulinate dehydratase	-6.2273385	8.68E-06	Involved in zinc ion binding activity and heme biosynthetic process.
	ENSDARG00000114758.1	*BX649452.1*	----------	-5.7320829	1.10E-05	----------
DFC Overexpression	ENSDARG00000112302.1	*pou3f1*	POU class 3 homeobox 1	10.2960270	2.91E-07	Involved in brain development. Regulate embryonic morphogenesis
	ENSDARG00000110479.1	*ptmaa*	prothymosin alpha a	10.0260869	1.79E-04	Mediate immune function by conferring resistance to certain opportunistic infections.
	ENSDARG00000116462.1	*btf3*	basic transcription factor 3	9.9336640	1.89E-04	General transcription factor that can form a stable complex with RNA polymerase II.
	ENSDARG00000111680.1	*ier5*	immediate early response 5	9.6349227	2.27E-04	Involved in heat shock response.
	ENSDARG00000110237.1	*rpl32*	ribosomal protein L32	9.5929483	2.33E-04	Structural constituent of ribosome involved in translation.

	Accession	Gene	Gene name	NFC (logFC)	p-value	Remarks*
DFC Underexpression	ENSDARG00000068716.7	*cuedc1a*	CUE domain containing 1a	-7.7450334	4.11E-03	Ubiquitin binding.
	ENSDARG00000114291.1	*zgc:174463*	E3 ubiquitin-protein ligase RBBP6	-7.2924118	2.32E-03	Ubiquitin protein ligase activity and zinc ion binding.
	ENSDARG00000114723.1	*ddb2*	damage-specific DNA binding protein 2	-7.1417709	6.32E-04	DNA repair (NER pathway) and protein ubiquitination.
	ENSDARG00000020866.10	*apoa4b.2*	apolipoprotein A-IV b, tandem duplicate 2	-7.0008580	2.08E-08	Lipid metabolism.
	ENSDARG00000036186.9	*mbpa*	myelin basic protein a	-6.8693724	4.63E-06	Structural constituent of myelin sheath
Mixture Overexpression	ENSDARG00000112302.1	*pou3f1*	POU class 3 homeobox 1	10.4347013	2.23E-07	Involved in brain development. Regulate embryonic morphogenesis
	ENSDARG00000055723.6	*hsp70l*	heat shock cognate 70-kd protein, like	9.0574293	1.32E-38	ATP binding. Stress response. Blood vessel development.
	ENSDARG00000110263.1	*rpl21*	ribosomal protein L21	8.8205604	4.52E-04	RNA binding. Structural constituent of ribosome involved in translation.
	ENSDARG00000029688.9	*hsp70.1*	heat shock cognate 70-kd protein, tandem duplicate 1	8.7121388	5.71E-34	ATP binding activity; misfolded protein binding activity; and protein folding chaperone. Stress response.
	ENSDARG00000110171.1	*BX248124.1*	----------	8.4693209	1.81E-07	----------
Mixture Underexpression	ENSDARG00000112408.1	*znf143b*	zinc finger protein 143b	-8.1252728	1.64E-03	Transcriptional activator.
	ENSDARG00000042620.8	*gstr*	glutathione S-transferase rho	-8.0617798	1.72E-03	Glutathione metabolic process in teleost fish.
	ENSDARG00000114220.1	*eif2b2*	eukaryotic translation initiation factor 2B, subunit 2 beta	-7.9865245	1.67E-03	Catalyses the exchange of eukaryotic initiation factor 2-bound GDP for GTP.
	ENSDARG00000068716.7	*cuedc1a*	CUE domain containing 1a	-7.7965090	3.60E-03	Ubiquitin binding.
	ENSDARG00000114723.1	*ddb2*	damage-specific DNA binding protein 2	-7.1417710	5.68E-04	DNA repair (NER pathway) and protein ubiquitination.

* From UniProt, ZFIN and Ensemble data bases

B

Appendix to Chapter 6

B.1 RGB split channel micrographs and composites

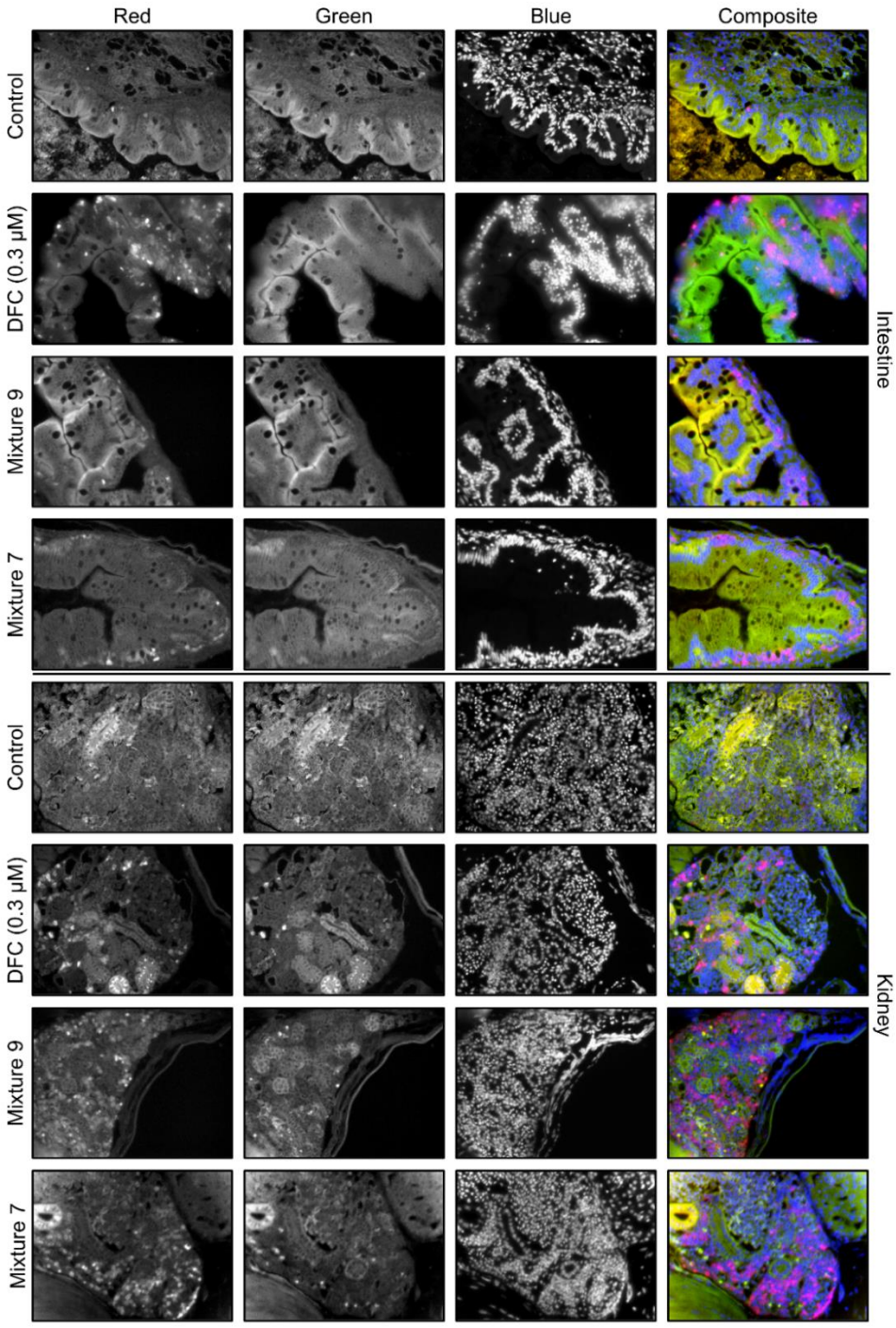

Figure B1.1. PCNA expression individual channels and RGB composite in intestine epithelium and kidney of F0 juvenile zebrafish (30 dpf).

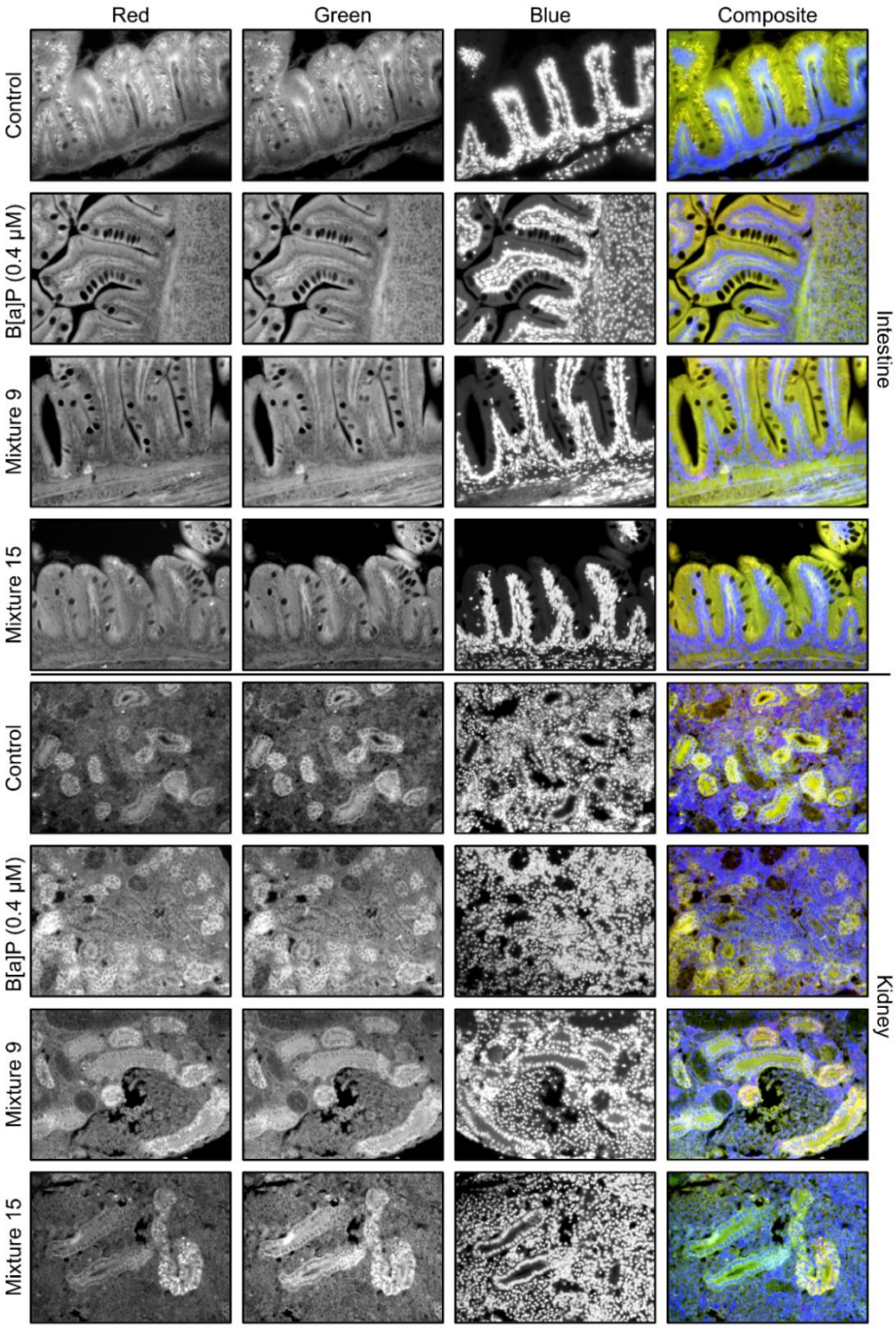

Figure B1.2. PCNA expression individual channels and RGB composite in intestine epithelium and kidney of F0 adult zebrafish (90 dpf).

.

2023

CARLA MARIA ALVES MARTINS

Carcinogenic toxicants and emerging pollutants. A comprehensive case-study on toxicant interactions in vivo and in vitro: from Molecular Toxicology to Environmental Risk Assessment